Continuous Metathesis Under Biphasic Liquid-Liquid Conditions Using Monolith-Supported Ionic Liquids

Von der Fakultät Chemie der Universität Stuttgart
zur Erlangung der Würde eines
Doktors der Naturwissenschaften (Dr. rer. nat.) genehmigte Abhandlung

vorgelegt von

Benjamin Autenrieth

aus Blaubeuren

Hauptberichter: Prof. Dr. Michael R. Buchmeiser
1. Mitberichter: Prof. Dr. Elias Klemm
2. Mitberichter: Prof. Dr. Sabine Ludwigs
Tag der mündlichen Prüfung: 15. Oktober 2013

Institut für Polymerchemie
der Universität Stuttgart
2013

II

Danksagung

„Das Schicksal mischt die Karten, wir spielen."

Arthur Schopenhauer (1788 – 1869)

Contents

Abbreviations and Symbols

Å	Angstrom
ATR	Attenuated total reflection
[BDMIM$^+$][BF$_4$$^-$]	1-Butyl-2,3-dimethylimidazolium tetrafluoroborate
CM	Cross metathesis
COE	*Cis*-cyclooctene
d	Doublet
DAFA	*N,N*-diallyl trifluoroacetamide
DCM	Dichloromethane
DEDAM	Diethyl diallyl malonate
DEDPM	Dipropargyl diethyl malonate
DME	1,2-Dimethoxyethane
DMF	*N,N*-Dimethylformamide
DMSO	Dimethylsulfoxide
ε_p	Microporosity
ε_t	Total porosity
ε_z	Intermicroglobular porosity
equiv.	Equivalents
EI	Electron ionization
ESI	Electrospray ionization
Et	Ethyl

Et$_2$O / DEE	Diethyl ether
Et$_3$N	Triethylamine
EtOAc	Ethyl acetate
EVE	Ethyl vinyl ether
FT-IR	Fourier transform infrared spectroscopy
g	Gram
GC-MS	Gas chromatography-mass spectrometry
GH	*Grubbs-Hoveyda* catalyst
GPC	Gel permeation chromatography
h	Hours
Hz	Hertz
ICP-OES	Inductively-coupled plasma optical emission spectroscopy
IL	Ionic liquid
IMesH$_2$	1,3-Dimesitylimidazolin-2-ylidene
ISEC	Inverse size exclusion chromatography
J	Coupling constant
k_i	Rate constant of initiation
k_p	Rate constant of propagation
M	Molar
m	Multiplet
m/z	mass/charge

M^+	Molecular ion
MALDI-TOF	Matrix-assisted laser desorption ionization time-of-flight
Me	Methyl
MeOH	Methanol
mg	Milligram
MHz	Megahertz
min	Minute
mL	Milliliter
mmol	Millimol
M_n	Number-average molecular weight
mol-%	Molar percentage
MS	Mass spectroscopy
M_w	Weight-average molecular weight
NBE	Norborn-2-ene
NHC	*N*-Heterocyclic carbene
NMR	Nuclear magnetic resonance
OTf	Trifluoromethanesulfonate
PCy_3	Tricyclohexylphosphine
PDI	Polydispersity index
Ph	Phenyl
ppm	Parts per million

Pr	Propyl
PrOH	Propanol
Py$^+$	Pyridinium
q	Quartet
RCM	Ring-closing metathesis
ROMP	Ring-opening metathesis polymerization
rt	Room temperature
s	Singlet
SEC	Size exclusion chromatography
SILP	Supported ionic-liquid phase
SM	Self-metathesis
SPS	Solvent purification system
t	Triplet
Tf$_2$N	Bis(trifluoromethanesulfonyl)imide
THF	Tetrahydrofuran
TMS	Tetramethylsilane
TON	Turn-over number
UV-Vis	Ultra violet-visible
wt.-%	Weight percentage
µmol	Micromol

Zusammenfassung

In der vorliegenden Arbeit wird die Entwicklung eines neuartigen, geträgerten Katalysesystems für kontinuierliche Olefinmetathese-Reaktionen vorgestellt. Das Konzept vereinbart Vorteile der heterogenen sowie der homogenen Katalyse und basiert auf der Kombination funktionalisierter, monolithischer Trägermaterialien mit neuartigen, ionischen Ruthenium-Alkylidenkomplexen.

Die Porenstruktur polymerer Monolithe lässt sich präzise und reproduzierbar einstellen. Durch geeignete Wahl der verwendeten Monomere und Quervernetzer, sowie deren Verhältnis zueinander und deren relativen Anteil an der Gesamtmasse des Polymerisationsansatzes können Monolithe mit hoher Formstabilität hergestellt werden. Diese ermöglichen einen großen Reaktantendurchsatz (d.h. es können hohe Flussraten angelegt werden), ohne dass sich dabei ein allzu hoher Gegendruck (p < 20 bar) einstellt. Die gewählte Herstellungsmethode bietet ein weiteres Argument dafür, weshalb polymere Monolithe geeignete Trägermaterialien für das im Folgenden vorgestellte Katalysekonzept darstellen. Monolithe können mittels Ring-öffnender Metathesepolymerisation (ROMP) synthetisiert werden. Unter Ausnutzung des *lebenden* Charakters dieser Polymerisationsart kann die monolithische Oberfläche auf einfache Weise funktionalisiert werden, was z.B. durch das Pfropfen ionischer Monomere erzielt werden kann. Monolithe eignen sich daher hervorragend als Trägermaterialien für kontinuierlich betriebene Flüssigphasen-Reaktionen. Die ionischen Gruppen erleichtern bzw. ermöglichen die Aufbringung und Fixierung ionischer Flüssigkeiten (engl. ionic liquids (ILs)) mit beliebig einstellbarer Filmdicke. Diese IL-Phase stellt die eigentliche stationäre Phase für die durchgeführten zweiphasigen flüssig-flüssig Reaktionen dar. Neu entwickelte, ionische Ruthenium-Alkylidenkomplexe werden in der ionischen Flüssigkeit gelöst und durch ionische Wechselwirkungen in dieser Phase immobilisiert. Die Substrate für die durchgeführten Olefinmetathesereaktionen werden in einem unpolaren, organischen Lösungsmittel aufgenommen und durch den, mit Katalysator beladenen Monolithen gepumpt. Diffusion der Edukte aus der mobilen Phase in die stationäre Phase ermöglicht dort die Umsetzung mit dem ionischen Katalysator. Diffusion der Produkte zurück in die mobile Phase garantiert dagegen deren Abtransport aus dem Monolithen. Neben dem augenscheinlichen Nutzen einer geringen

Katalysatorauswaschung und damit geringen Produktkontamination ermöglicht ein zweiphasiges flüssig-flüssig System die Verwendung einer großen Vielzahl an potentiell verfügbaren Substraten. Ein weiterer Vorteil liegt in der einfachen Entfernung der mobilen Phase und dem darin enthaltenen, inaktiven Katalysator, was durch Spülen des Monolithen mit Methanol erzielt werden kann. Durch einen einfachen Wiederbeladungsprozess ist das monolith-geträgerte Katalysatorsystem bereits nach kurzer Zeit für den erneuten Einsatz in kontinuierlich durchgeführten Metathesereaktionen verwendbar.

Kapitel 1: Theoretische Grundlagen

Kapitel 2: "Design of the Monolithic Support Material"

In diesem Kapitel wird auf die Entwicklung des bestgeeigneten monolithischen Trägermaterials eingegangen. Durch Variation des Verhältnisses und der Art der „Polymerisationsbestandteile": Monomer, Quervernetzer, Initiator und porogenen Lösungsmitteln, lässt sich die Porosität von Monolithen präzise einstellen. Die Porosität eines Trägermaterials ist entscheidend für seine Eignung in kontinuierlich durchgeführten, zweiphasigen flüssig-flüssig Prozessen. Im Hinblick auf das geplante Anwendungsgebiet ist es von enormer Wichtigkeit, dass der Monolith hohe Reaktantendurchsätze ermöglicht, dabei jedoch vertretbar geringe Gegendrücke erzeugt. Aus diesem Grunde wurden polymere Monolithe mit einem überwiegenden Anteil an Makroporen hergestellt. Trotz eines beachtlich hohen Leervolumens von > 70% weisen die Monolithe eine enorme Formstabilität auf. Dies wurde durch die Wahl des Monomers Norborn-2-en (NBE) und des Quervernetzers Tris(norborn-5-en-2-ylmethyloxy)methylsilan erzielt, beide Komponenten hatten einen Anteil von 15 Gewichts-% an der gesamten Polymerisationsmischung. Das makroporogene Lösungsmittel 2-Propanol hatte einen Anteil von 50 Gewichts-%, wohingegen der Anteil des mikroporogenen Lösungsmittels Toluol lediglich 20 Gewichts-% betrug. Es konnte gezeigt werden, dass diese Zusammensetzung den besten Kompromiss aus angelegter Flussrate und resultierendem Gegendruck ermöglicht.

Zahlreiche ionische Norbornenderivate wurden synthetisiert, von denen Norborn-5-en-2-ylmethyl-*N,N,N*-trimethylammoniumtetrafluoroborat ([NBE-CH$_2$-NMe$_3^+$][BF$_4^-$], **M2**) für die Funktionalisierung der monolithischen Oberfläche verwendet wurde.

Entscheidende Anforderungen, die an die ionische Flüssigkeit gestellt werden sind unter anderem eine vernachlässigbar geringe Mischbarkeit mit gebräuchlichen, unpolaren Lösungsmitteln sowie ein Schmelzpunkt der unterhalb der gewählten Reaktionstemperatur liegt. Für das hier vorgestellte Konzept wurde die ionische Flüssigkeit 1-Butyl-2,3-dimethylimidazoliumtetrafluoroborat ([BDMIM$^+$][BF$_4^-$]) gewählt, die zudem über ein nicht koordinierendes Anion verfügt. In diesem Kapitel wird erläutert, wie ein Film dieser ionischen Flüssigkeit mit variabler Dicke auf die monolithische Oberfläche aufgebracht werden kann. Schließlich wird die Aufmerksamkeit dem System IL/mobile Phase/Reaktant und dem relativen Verhältnis der verschiedenen Komponenten zugewandt. Als geeignetes Lösungsmittel um die mobile Phase zu bilden wurde Heptan gewählt. Heptan ist unpolar und mischt sich nicht mit [BDMIM$^+$][BF$_4^-$], es verfügt über einen ausreichend hohen Siedepunkt, ist wenig toxisch und löst sämtliche potentielle Reaktanten. Für eine Vielzahl an IL/Heptan/Reaktant-Systemen wurde bei verschiedenen Temperaturen die maximal mögliche Flussrate bestimmt, ab der die ionische Flüssigkeit ansatzweise, auf Grund hoher Scherkräfte, von der Monolithoberfläche abgelöst wurde. Die Summe all dieser Untersuchungen bereitet die Grundlage für die, in den folgenden Kapiteln beschriebenen, kontinuierlich durchgeführten Metathesereaktionen unter zwei-phasigen flüssig-flüssig Bedingungen.

Kapitel 3: "Continuous Biphasic Metathesis Using Monolith-Supported Ionic Liquids"

In diesem Kapitel wird die Synthese und Charakterisierung des neuartigen, dikationischen Ruthenium-Alkylidenkomplexes [Ru(DMF)$_3$(IMesH$_2$)(=CH-2-(2-PrO)-C$_6$H$_4$)$^{2+}$][(BF$_4^-$)$_2$] (**1**; IMesH$_2$=1,3-dimesitylimidazolin-2-yliden) präsentiert. Mit Hilfe dieses Katalysators wird erstmals die „Funktionstüchtigkeit" des vorgestellten Konzeptes nachgewiesen.

Der dikationische Ruthenium-Alkylidenkomplex [Ru(DMF)$_3$(IMesH$_2$)(=CH-2-(2-PrO)-C$_6$H$_4$)$^{2+}$][(BF$_4^-$)$_2$] wurde hergestellt und charakterisiert und in kontinuierlich betriebenen Metathesereaktionen eingesetzt bei denen die so genannte *supported ionic-liquid phase* (SILP) Technologie verwendet wurde. Als Trägermaterialien dienten polymere Monolithe die mittels Ring-öffnender Metathesepolymerisation hergestellt wurden. Als Monomer wurde Norborn-5-en verwendet, Tris(norborn-5-en-

2-ylmethyloxy) methylsilan diente als Quervernetzer, $[RuCl_2(PCy_3)_2(CHPh)]$ (Cy=cyclohexyl) als Initiator, 2-Propanol sowie Toluol bildeten das porogene Lösungsmittelgemisch. Die Oberfläche des Monolithen konnte durch Pfopfen des ionischen Monomers $[NBE-CH_2-NMe_3^+][BF_4^-]$ funktionalisiert werden. Das Monolith-geträgerte Katalysatorsystem wurde komplettiert durch anschließende Aufbringung eines dünnen Filmes der ionischen Flüssigkeit, $[BDMIM^+][BF_4^-]$, in der der ionische Katalysator **1** gelöst vorlag. Die für die Metathesereaktionen gewählten Substrate wurden in einer ebenfalls flüssigen, mit der ionischen Flüssigkeit nicht mischbaren, Transportphase aufgenommen. Indem die Reaktanten mittels der Transportphase durch das monolithische Trägersystem geführt wurden, konnten zahlreiche, kontinuierlich durchgeführte Metathesereaktionen in einem zweiphasigen flüssig-flüssig System realisiert werden.

In Lösung wurden mit dem Komplex $[Ru(DMF)_3(IMesH_2)(=CH-2-(2-PrO)-C_6H_4)^{2+}][(BF_4^-)_2]$ (**1**) sehr hohe Umsatzzahlen (engl. turnover numbers (TONs)) von bis zu 3700 für zahlreiche Ringschluss-Metathesereaktionen (engl. ring-closing metathesis (RCM)) erzielt. Näher betrachtet werden z.B. die RCM von *N,N*-Diallyltrifluoroacetamid, Diethyldiallylmalonat, Diethyldi(methallyl)malonat, *tert*-Butyl-*N,N*-diallylcarbamat, *N,N*-Diallylacetamid, Diphenyldiallylsilan und 1,7-Oktadien, sowie die Selbstmetathese von Methyloleat. Wurden diese Reaktionen unter zweiphasigen Bedingungen durchgeführt, in denen das System $[BDMIM^+][BF_4^-]$/Heptan gewählt wurde, so konnten die Umsätze noch weiter gesteigert werden. In kontinuierlich durchgeführten Metathesereaktionen unter *SILP*-Bedingungen wurden Umsatzzahlen bis zu 900 erzielt. Auf Grund seines ionischen Charakters wurde ein sehr geringes (<0.1%) Auswaschen des Ru-Komplexes **1** in die Transportphase detektiert. Nach Gebrauch konnte die ionische Flüssigkeit mit darin enthaltenem inaktivem Katalysator vollständig aus dem monolithischen Träger entfernt werden. Dies wurde durch Spülen mit Methanol erzielt. Durch einen einfachen Wiederbeladungsprozess mit $[BDMIM^+][BF_4^-]$/**1** kann der Monolith bereits nach kurzer Zeit als Trägermaterial für den Gebrauch in kontinuierlich durchgeführten Metathesereaktionen wieder verwendet werden.

Kapitel 4: "Reactivity of 1 in Ring-Opening Metathesis and Cyclopolymerization"

$[Ru(DMF)_3(IMesH_2)(=CH-2-(2-PrO)-C_6H_4)^{2+}][(BF_4^-)_2]$ (**1**) zeigt erstaunlich hohe Aktivität sowohl in Ring-öffnenden Metathesepolymerisationen als auch in Zyklopolymerisationsreaktionen von 1,6-Heptadiinen. Aus diesem Grunde wird der Untersuchung dieses Verhaltens ein eigenständiges Kapitel dieser Arbeit gewidmet.

In diesem Kapitel werden Untersuchungen über die Reaktivität des dikationischen Ruthenium-Alkylidenkomplexes $[Ru(DMF)_3(IMesH_2)(=CH-2-(2-PrO)-C_6H_4)^{2+}][(BF_4^-)_2]$ **1** in Ring-öffnenden Metathesepolymerisationen zahlreicher funktionalisierter Norborn-2-en-Derivaten sowie in Zyklopolymerisationsreaktionen verschiedener 1,6-Heptadiine erläutert. Auf Grund seines dikationischen Charakters verhält sich **1** stark elektrophil und besitzt eine hohe Reaktivität gegenüber Alkenen und 1,6-Heptadiinen. Grundsätzlich wurde bei diesen Reaktionen, abhängig davon ob Monomere mit oder ohne koordinierenden funktionellen Einheiten umgesetzt wurden, ein erheblicher Reaktivitätsunterschied festgestellt. In Gegenwart ionischer Monomere mit koordinierenden Anionen wie z.B. Br$^-$ oder I$^-$ wurde ein rascher Wandel des sich fortpflanzenden Rutheniumalkylidens von einer dikationischen hin zu einer neutralen Spezies beobachtet.

Kapitel 5: "Catalyst Optimization"

Die vorhergehenden Kapitel beleuchteten die Entwicklung und Realisierung eines Konzeptes für die kontinuierliche Durchführung von Olefinmetathesereaktionen unter zweiphasigen flüssig-flüssig Bedingungen. In diesem Zusammenhang wurde der dikationische Ruthenium-Alkylidenkomplex $[Ru(DMF)_3(IMesH_2)(=CH-2-(2-PrO)-C_6H_4)^{2+}][(BF_4^-)_2]$ (**1**) entwickelt, dessen Reaktivität allerdings bei der Verwendung von Substraten mit koordinierenden Einheiten gemindert wird. Dieser Effekt lässt sich durch eine Erhöhung der Reaktionstemperatur kompensieren und durch entsprechendes Vorgehen konnte gezeigt werden, dass sich das entwickelte System stabil gegenüber hohen Temperaturen verhält. Noch erstrebenswerter ist es jedoch, kontinuierlich ablaufende Metathesereaktionen bereits bei niedrigen Temperaturen durchführen zu können und dabei dennoch hohe Umsätze zu erzielen. Dieses Kapitel ist dementsprechend der Optimierung des Konzeptes durch die Entwicklung und Anwendung robusterer Metathesekatalysatoren gewidmet. Als Ansatzpunkt

wurde die Verschiebung der Ladung, weg vom Ruthenium-Zentrum, hin zu den Liganden, gewählt. Erzielt wurde dies, indem die Chlorid-Liganden des Ausgangskomplexes [RuCl$_2$(IMesH$_2$)(=CH-2-(2-PrO)-C$_6$H$_4$)] (**GH2**) durch Liganden mit ionischen Einheiten ersetzt wurden. Ein wesentlicher Vorteil in diesem Vorgehen besteht darin, dass die Liganden auch während des katalytischen Zyklus fest an das Zentralatom gebunden sind und dass sie, abhängig von ihrer Natur, eine Einflussnahme auf die Katalysatoraktivität ermöglichen. Anhand zahlreicher Beispiele wurde in der Vergangenheit gezeigt, dass stark elektronenziehende Liganden die Reaktivität von Ruthenium-Alkylidenkomplexen steigern. Initiatoren, die beispielsweise über perfluorierte Carboxylat- oder Pseudohalogenidliganden verfügen, weisen erhöhte Aktivitäten in Ringschluss-Metathesen auf und sind sogar in der Lage Zyklopolymerisationen von 1,6-Heptadiinen und 1,7-Oktadiinen zu induzieren. In diesem Kapitel wird daher die Herstellung von neuartigen Ruthenium-Alkylidenen aufgezeigt, bei denen ionische Carboxylatliganden verwendet werden. In diesem Zusammenhang wird die Synthese der beiden neuartigen, ionischen Ruthenium-Alkylidene [Ru[(4-CO$_2$)(1-CH$_3$)Py$^+$)]$_2$(IMesH$_2$)(=CH-2-(2-PrO)-C$_6$H$_4$)][OTf$^-$]$_2$ (**2**, IMesH$_2$=1,3-Dimesitylimidazolin-2-yliden, Py=Pyridin) und [RuCl[(4-CO$_2$)(1-CH$_3$)Py$^+$)](IMesH$_2$)(=CH-2-(2-PrO)-C$_6$H$_4$)][OTf$^-$] (**3**) beschrieben. Die Katalysatoren **2** und **3** wurden in zahlreichen Olefinmetathesereaktionen sowohl unter homogenen Bedingungen als auch in zweiphasigen flüssig-flüssig Systemen eingesetzt. Beide Katalysatoren lösen sich selektiv in der ionischen Flüssigkeit [BDMIM$^+$][BF$_4$$^-$], eine Eigenschaft, die bei der Verwendung des Zweiphasensystems [BDMIM$^+$][BF$_4$$^-$]/Heptan zu einer sehr geringen Austragung der Metallkomplexe in die organische Phase führte (<0.1% der ursprünglichen Menge an Katalysator). Die Komplexe **2** und **3** wiesen sowohl in homogenen Lösungen als auch unter zweiphasigen Bedingungen jeweils vergleichbar hohe Reaktivitäten auf. Die Katalysatoren **2** und **3** wurden darüber hinaus erfolgreich in den kontinuierlich, unter geträgerten flüssig-flüssig Bedingungen durchgeführten Metathesereaktionen von Methyloleat und 1,7-Oktadien eingesetzt. Mit Hilfe von ^{1}H NMR-Spektroskopie wurde die Disproportionierung des Monocarboxylato-monochloro-substituierten Ruthenium-Alkylidens **3** in Lösung nachgewiesen. Bei dieser Reaktion entstehen der Biscarboxylato-Komplex **3** sowie der neutrale Komplex [RuCl$_2$(=CH-2-(2-PrO)-C$_6$H$_4$)(IMesH$_2$)] (**GH2**).

Abstract

This work reveals the development of a novel, supported catalytic system for continuous olefin metathesis reactions. The concept enables to combine the advantages of both homogeneous as well as heterogeneous catalytic processes and is based on the combination of functionalized monolithic support materials and tailored, ionic ruthenium alkylidene complexes. The porosity of these monoliths can be adjusted with high precision and reproducibility. Adequate choice of the monomers and crosslinkers, their ratio towards each other, as well as their relative percentage in the total polymerization mixture enables the preparation of monoliths with convincing form stability. These monoliths allow for a high reactant throughput (this means high flow rates are applicable), hence without giving too high back pressures (< 20 bar). The monoliths` surface is functionalized by grafting an ionic monomer onto it, thereby taking advantage of the *living* character of the ROMP (ring-opening metathesis polymerization) reaction used for its preparation. For these reasons, ROMP-derived monoliths are outstandingly well-suited to be used as support materials in continuously operated biphasic liquid-liquid catalysis reactions. The ionic moieties facilitate/enable to attach and to fix films of ionic liquids with adjustable thickness. In fact, these films of ionic liquids represent the actual stationary phases for the performed metathesis reactions under biphasic liquid-liquid conditions. Novel ionic ruthenium alkylidene complexes were dissolved in the ionic liquid and are due to ionic interactions immobilized within this phase. The substrates intended to be used in metathesis reactions were first dissolved in a nonpolar, organic solvent and were then simply flushed through the monolith, which was loaded with catalyst immobilized in the ionic liquid. The metathesis reaction is rendered possible by diffusion of the reactants to the catalytically active Ru-complex immobilized in the stationary phase. Diffusion of the products back into the mobile phase guarantees for the transport of the desired compounds out of the monolithic support. Besides the benefit of low catalyst leaching, the fact, that a biphasic liquid-liquid system is used definitely widens the range of potentially accessible substrates. Moreover, the facile recycling of the monolithic support by flushing with, e.g., methanol, represents an additional advantage. The simple recharging process with

fresh catalyst dissolved in the ionic liquid allows restoring the catalytic system within a rather short period of time.

Chapter 1: "Brief Theoretical Survey"

Chapter 2: "Design of the Monolithic Support Material"

This chapter focuses on the development of a qualified monolithic support material. By varying the ratio and nature of the compounds used for monolith preparation, i.e. the monomer, crosslinker, initiator and porogenic solvents, its porosity can be adjusted precisely. The porosity of the support material is an essential factor relevant for influencing its performance in continuous biphasic liquid-liquid processes. Important features in view of the intended application are that the support material allows for a high reactant throughput, hence without giving too high back pressures. On this account, monoliths possessing a large fraction of macro pores were synthesized. Besides a noticeable void volume of > 70 vol.-%, the support material is showing considerably high shape persistence. This was accomplished by using norborn-2-ene as monomer and the crosslinker tris(norborn-5-ene-2-ylmethyloxy) methylsilane; both were used as 15 wt.-% fractions of the total polymerization mixture. The macroporogenic solvent 2-propanol accounted for 50 wt.-% whereas the microporogenic solvent toluene held for only 20 wt.-%. It was shown that this composition allowed for the best compromise between the applied flow rate and resulting back pressure.

Ionic NBE-based monomers were prepared, out of which norborn-5-en-2-ylmethyl-*N,N,N*-trimethylammonium tetrafluoroborate ([NBE-CH$_2$-NMe$_3^+$][BF$_4^-$], **M2**) was chosen to be used for the functionalization of the monolithic surface.

Important criteria the ionic liquid of choice had to fulfill are a negligible miscibility with common nonpolar, organic solvents as well as a liquid state of matter at reaction temperature. Therefore, 1-butyl-2,3-dimethylimidazolium tetrafluoroborate ([BDMIM$^+$][BF$_4^-$]) was chosen as it additionally possesses a non-coordinating counter ion. In this chapter, the method of how to prepare IL-films with adjustable thickness on the monolithic surface and the optimization of the procedure is reported. Finally, the focus was set on the combination IL/mobile phase/reactant. Heptane was found to be the solvent of choice as it is quite nonpolar, possesses an acceptable high boiling

point, has a low toxicity and is well-miscible with all the reactants considered to be used for metathesis under biphasic liquid-liquid conditions. The maximum flow rates, at which the IL-films were partly removed, were defined for various systems [BDMIM$^+$][BF$_4^-$]/heptane/reactant at different temperatures. The sum of all findings creates the basis on which the continuous metathesis reactions, carried out under biphasic conditions using monolith-supported ionic liquids, are founded.

Chapter 3: "Continuous Biphasic Metathesis Using Monolith-Supported Ionic Liquids"

In this chapter, the preparation and characterization of the novel dicationic ruthenium alkylidene complex [Ru(DMF)$_3$(IMesH$_2$)(=CH-2-(2-PrO)-C$_6$H$_4$)$^{2+}$][(BF$_4^-$)$_2$] (**1**; IMesH$_2$ = 1,3-dimesitylimidazolin-2-ylidene) is reported. By using this catalyst, the efficiency of the concept is verified for the first time.

1 was prepared and used in continuous metathesis reactions by exploiting supported ionic-liquid phase (SILP) technology. For these purposes, ROMP-derived monoliths were prepared from norborn-2-ene, tris(norborn-5-ene-2-ylmethyloxy)methylsilane, and [RuCl$_2$(PCy$_3$)$_2$(CHPh)] (Cy=cyclohexyl) in the presence of 2-propanol and toluene and surface grafted with [NBE-CH$_2$-NMe$_3^+$][BF$_4^-$]. Subsequent immobilization of the ionic liquid, 1-butyl-2,3-dimethylimidazolium tetrafluoroborate ([BDMIM$^+$][BF$_4^-$]), containing the ionic catalyst **1** created the SILP catalyst. The use of a second liquid transport phase, which contained the substrate and was immiscible with the IL, allowed for continuous metathesis reactions. High turnover numbers (TONs) of up to 3700 obtained in organic solvents for ring-closing metathesis (RCM) of, e. g., *N,N*-diallyltrifluoroacetamide, diethyl diallyl malonate, diethyl di(methallyl) malonate, *tert*-butyl-*N,N*-diallyl carbamate, *N,N*-diallyl acetamide, diphenyldiallylsilane, and 1,7-octadiene, as well as in the self-metathesis of methyl oleate, could be further increased by using biphasic conditions with [BDMIM$^+$][BF$_4^-$]/heptane. Under continuous SILP conditions, TONs up to 900 were observed. Due to the ionic character of the initiator, catalyst leaching into the transport phase was very low (<0.1% with respect to the initial amount of catalyst). Finally, the IL can, together with decomposed catalyst, be removed from the monolithic support by flushing with methanol. Upon reloading with [BDMIM$^+$][BF$_4^-$]/**1**, the recycled support material again qualified for utilization in continuous metathesis reactions.

Chapter 4: "Reactivity of 1 in Ring-Opening Metathesis and Cyclopolymerization"

The reactivity of the dicationic Ru-alkylidene complex **1** in the ring-opening metathesis polymerization of various functional norborn-2-enes as well as in the cyclopolymerization of different 1,6-heptadiynes is reported in this chapter. Due to its dicationic character, complex **1** is highly electrophilic and possesses high reactivity *versus* alkenes and 1,6-heptadiynes. Generally, a pronounced difference in reactivity between monomers bearing coordinating groups and those that lack such moieties is observed. In the presence of ionic monomers containing coordinating anions such as Br^- and I^-, a rapid change in the nature of the propagating alkylidene from a dicationic to a neutral one is observed.

Chapter 5: "Catalyst Optimization"

The previous chapters illustrate the development and realization of a concept for conducting continuous metathesis reactions under supported biphasic liquid-liquid conditions. However, the activity of the dicationic Ru-alkylidene **1** is reduced when using substrates bearing coordinating moieties. This effect can be compensated by increasing the reaction temperature. Performing continuous metathesis reactions with high yields at low temperatures certainly would be desirable. On that account this chapter deals with the optimization of the concept by developing more robust, ionic Ru-alkylidene complexes. Particular attention was turned to shift the charge toward the ligands. To optimize the previously introduced concept by using more robust catalysts, it was chosen to substitute the chloride ligands in the 2nd generation *Grubbs-Hoveyda* catalyst $[RuCl_2(IMesH_2)(=CH-2-(2-PrO)-C_6H_4)]$ (**GH2**) by ligands with ionic functionalities. These ligands will not demerge during the metathesis reaction and, depending on their nature, the reactivity of the catalyst can be adjusted. In general, the tendency is observed, that the reactivity of Ru-alkylidenes increases by attaching ligands that are more electron-withdrawing. For example, perfluorocarboxylate and several "pseudo-halide"-containing initiators display increased activity in RCM reactions and, yet, are capable to cyclopolymerize 1,6-heptadiynes or 1,7-octadiynes. In this chapter the preparation and use of novel Ru-alkylidenes possessing ionic carboxylate ligands is reported. The synthesis of the novel ionic Ru-alkylidenes $[Ru[(4-CO_2)(1-CH_3)Py^+)]_2(IMesH_2)(=CH-2-(2-PrO)-$

$C_6H_4)][OTf]_2$ (**2**, $IMesH_2$=1,3-dimesitylimidazolin-2-ylidene, Py=pyridine) and $[RuCl[(4-CO_2)(1-CH_3)Py^+)](IMesH_2)(=CH-2-(2-PrO)-C_6H_4)][OTf]$ (**3**) is reported. Catalysts **2** and **3** have been used in various metathesis reactions under both homogeneous and biphasic liquid-liquid conditions. The catalysts can selectively be dissolved in an ionic liquid phase. Using the biphasic system $[BDMIM^+][BF_4^-]$/heptane, leaching into the organic phase was very low (<0.1%). **2** and **3** showed comparable reactivity in organic solvents and under biphasic conditions. Catalysts **2** and **3** were also successfully used in the continuous metathesis of methyl oleate and 1,7-octadiene under supported liquid-liquid conditions. Dissolved in CH_2Cl_2, disproportionation of the mono-carboxylato-monochloro-substituted Ru-alkylidene **3** was traced by ^1H NMR analysis at 40°C, thereby demonstrating the formation of complex **3** and the neutral complex $[RuCl_2(=CH-2-(2-PrO)-C_6H_4)(IMesH_2)]$ (**GH2**).

Aim

Olefin-metathesis reactions have gained a strong position in organic synthesis and have found widespread application in the creation of carbon-carbon bonds. Especially for the synthesis of pharmaceutically active compounds it is, however, essential to reduce heavy metal contamination of the products to an unobjectionable low degree, a task, which is hard to accomplish *via* homogeneous catalysis and which entails a costly purification process. A multitude of examples exist where metathesis catalysts have been immobilized on different support materials. However, the heterogenization step often is quite complex and recycling of the support material is restricted or not possible.

The main goal of this PhD work was to develop a catalytic system for continuous metathesis-reactions under biphasic liquid-liquid conditions, based on porous ROMP-derived polymeric monoliths. In principle, the concept presented in this work shall enable to combine the advantages of both homogeneous as well as heterogeneous catalytic processes. Beside the primary objective to gain catalyst-free products, the concept shall enable continuous product formation using two liquid phases, i.e. one supported and a second continuous one, simply by cycling reactants through the monolithic support containing a suitable catalyst dissolved in an ionic liquid. The fact, that a biphasic liquid-liquid system shall be used definitely would widen the range of potentially accessible substrates. Moreover, it was desired to develop a process that allows for a facile recycling and recharging of the monolithic support material. This would represent an additional advantage over existing systems since it would allow restoring the catalytic system within a rather short period of time.

This work is structured in discrete chapters, which reflect important sub-steps with regard to reaching the defined aim.

The first objective was to design a suitable monolithic support material, which allows for creating a technically relevant and scalable setup. The monolith has to guarantee for a high reactant throughput (this means high flow rates are applicable), hence without giving too high back pressures. The monoliths' surface shall be functionalized by grafting ionic monomers onto it. These ionic moieties facilitate/enable the immobilization of films of ionic liquids with adjustable thickness. In fact, these films of

ionic liquids represent the actual stationary phases for the metathesis reactions under biphasic liquid-liquid conditions.

Consecutively, the focus was put on developing an ionic ruthenium alkylidene that dissolves selectively in an ionic liquid and is highly active in various metathesis reactions. Using this complex, the feasibility of the concept for performing continuous metathesis reactions under liquid-liquid conditions was to be investigated.

A further aim was to shed some more light on the reactivity of ionic Ru-alkylidenes in ring-opening metathesis polymerization reactions (ROMP) and, much more challenging, in cyclopolymerization reactions. On this account, the study of the performance of a dicationic Ru-alkylidene in these reactions is covered in chapter four.

Chapter five is dedicated to the optimization of the continuously operated catalytic system. This shall be accomplished by the design and use of novel, ionically tagged catalysts that are more robust to substrates with coordinating moieties and therefore allow for performing continuous metathesis reactions under biphasic conditions with high yields at low temperatures.

1. Brief Theoretical Survey

This chapter shall give a brief survey of the fundamental theoretical basis related to this PhD work. Main topics considered herein are: catalysis in general, olefin metathesis, polymeric monolithic materials and ionic liquids. This survey is by no means a comprehensive discussion of these quite broad scientific domains, rather than that it shall facilitate the comprehensibility of the research done in course of this PhD work.

1.1 Catalysis

The majority of the industrially most important chemical processes, as well as most of the biochemically relevant processes involve catalytic reactions[1]. The term catalysis is derived from the ancient Greek vocable *katálysis* ("to untie") and was introduced by *J. J. Berzelius* in 1836. A catalyzed reaction proceeds more rapidly than an uncatalyzed one running at the same temperature. A substance, called catalyst, that lowers the activation energy of a chemical reaction by offering an alternative pathway to the reaction products, is responsible for the increase in reaction rate[1]. Importantly, the catalyst influences solely the kinetics of a chemical reaction. It does not affect the chemical equilibrium. As a consequence, a catalyst is accelerating both, the forward and the reverse reaction. The crucial criterion for a substance being considered as a catalyst is that it will not be consumed during the reaction. Generally, during the reaction the catalyst reacts with substrate molecules to form an intermediate that decomposes to yield the final reaction products and to regenerate the catalyst. As the catalyst is able to form again the same type of intermediate, which after decomposition gives the same types of products, the reaction is called a catalytic cycle. Catalysis is a major research field involving many areas of chemistry, thereby resulting in a respectable number of *Nobel prizes*: *W. Ostwald* (1909), *P. Sabatier* (1912), *F. Haber* (1918), *I. Langmuir* (1932), *J. B. Sumner* (1946), *K. Ziegler* and *G. Natta* (1963), *J. W. Cornforth* (1975), *W. S. Knowles* and *R. Noyori* and *B. Sharpless* (2001), *Y. Chauvin*[2] and *R. H. Grubbs*[3] and *R. R. Schrock*[4] (2005), *G. Ertl* (2007), *R. F. Heck* and *E. Negishi* and *A. Suzuki* (2010).

1.1.1 Homogeneous Catalysis

In what is called homogeneous catalysis, the catalyst and the reactants are present in the same phase. Most often, homogeneously catalyzed reactions show a high degree of selectivity since defined catalytically active species are used, which allow for precise analysis and understanding of the reaction mechanism. The major drawback of homogeneous catalysis is the difficulty in removing catalyst residues from the reaction products. Important industrial applications for homogeneous catalysis are, e.g., the formation of acetaldehyde *via* the *Wacker* process, which refers to the organopalladium catalyzed oxidation of ethylene by oxygen in water. Acetic acid is yielded by organorhodium catalyzed carbonylation of methanol, this reaction being known as the *Monsanto* process. *BP plc* licenses the *Cativa* process, a process analogous to the *Monsanto* process catalyzing the carbonylation of methanol by iridium based complexes. Aldehydes with variable chain length are generally obtained *via hydroformylation* of olefins. Using either cobalt or rhodium based catalysts this fundamental, homogeneously catalyzed industrial process is applied in large quantities, e.g., by *BASF*, *ExxonMobil*, *Union Carbide* or *Shell*.

1.1.2 Heterogeneous Catalysis

In contrast to homogeneous catalysis, in heterogeneous reactions the catalyst and the reactants are present in different phases. The catalytic cycle involves the diffusion of reactants to the surface of the catalyst, the adsorption onto it and the conversion into products which then finally desorb from the surface and diffuse away. Heterogeneous catalytic processes take place only at the surface of the catalyst, consequently an increase in available catalyst surface area results in an increase in reaction rate. For that purpose, as well as for reducing costs, heterogeneous catalysts are commonly dispersed on highly porous support materials such as, e.g., zeolithes, alumina or activated carbon. Of advantage is the ease of removing heterogeneous catalysts from the product phase. An example for a large scale industrial process based on heterogeneous catalysis is, e.g., the synthesis of ammonia *via* the *Haber-Bosch* process. There, nitrogen and hydrogen are converted into ammonia by passing the gases over iron oxides dispersed on alumina at high pressures (~ 200 bars) and high temperatures (~450°C). The least expensive and

most common industrial route to yield hydrogen is *steam reforming* of natural gas. Hereby, methane and steam are reacted at temperatures between 800 and 1100°C in the presence of a nickel-based catalyst to yield carbon monoxide and hydrogen. Nitric acid is yielded *via* the *Ostwald* process, where in a key step nitric oxide results out of the reaction between ammonia and oxygen in the presence of platinum-rhodium gauze. Sulfuric acid is produced *via* the *contact process* by reacting sulfur dioxide and oxygen in the presence of a vanadium(V) oxide catalyst. Poly(propylene) is yielded *via Ziegler-Natta* polymerization of propylene; many variations exist but one example for an heterogeneous industrial application is the use of $TiCl_4$ supported on $MgCl_2$ in the presence of an activator such as $Al(C_2H_5)_3$.

1.2 Olefin Metathesis

Since the 1970s olefin metathesis is of continually growing importance to the synthesis of organic molecules and polymers and has become a powerful tool in inorganic, organic and polymer chemistry as well as in materials science [5-8]. Rudimentary, olefin metathesis can be considered as the synthesis of new C=C double bonds from existing C=C double bonds, the conversion being catalyzed by transition metal alkylidenes (Scheme 1) [9, 10]. The generally accepted and experimentally supported mechanism was proposed by *Y. Chauvin* and *P. J.-L. Hérisson* in 1971 and involves the formation of an intermediary metallacyclobutane from the reaction of a metal carbene and an olefin[10].
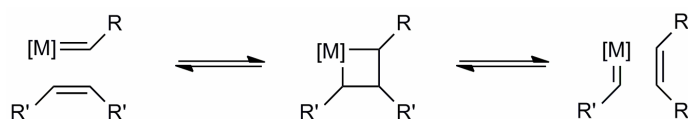
Scheme 1. The principle of olefin metathesis according to *Y. Chauvin*.

The "*Phillips Triolefin Process*" was the first major industrial process based on olefin metathesis and won great importance until the mid 1970s, denoting the conversion of propylene into ethylene and 2-butenes and vice versa (PTOP, Scheme 2). Due to the increased market demand for propylene the reversed reaction became more and more important. Nowadays this process is known as "*Olefins Conversion*

Technology" (OCT, Scheme 2) and runs with heterogeneous catalysts such as WO_3 on SiO_2.
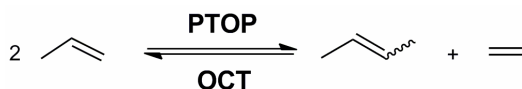
Scheme 2. "*Phillips Triolefin Process*" (PTOP) and "*Olefins Conversion Technology*" (OCT).

The total annual capacity of linear alpha- and internal olefins exceeds 1,200,000 tons. These important basic chemicals are yielded *via* the "*Shell Higher Olefin Process*" (SHOP) [11] and find applications as reactants for the preparation of, e.g., polymers, surfactants and fatty acids. The process first involves the oligomerization of ethylene, followed by isomerization of the resulting even-numbered alpha-olefins and an adjacent olefin metathesis step to get access to linear internal alkenes. α,ω-Diolefines are obtained using the "*FEAST*"-process (FEAST = Further Exploitation of Advanced Shell Technology) [12] *via* ethenolysis of cycloolefins such as cyclooctadiene. Today "*Oleometathesis*" is of growing importance since it might allow gaining useful functional and non-functional olefins from renewable resources such as plant oils.

Yet, most of the industrial metathesis processes are accomplished with poorly defined heterogeneous catalyst systems consisting of transition metal salts combined with main group alkylating agents[13]. Due to the harsh reaction conditions required, olefin metathesis is predominantly used in the large scale production of non-functionalized olefins. To make olefin metathesis attractive to advanced organic synthesis, great effort was put on the development of well defined, tailor-made transition metal alkylidenes. In course of target-oriented research, a wide assortment of different types of olefin metathesis reactions has been developed.

1.2.1 Types of Olefin Metathesis Reactions

The basic schemes of the most common metathesis reactions are illustrated in Figure 1. Dienes can be converted into cyclic olefins *via* the *ring-closing metathesis* (RCM) reaction, in which the release of low molecular weight olefins, such as, e.g., ethylene represents the driving force[14-16]. The opposite conversion in which cyclic

olefins are reacted with linear olefins to yield novel, linear olefinic products is known as *ring-opening metathesis* (ROM) reaction. Generally it is necessary to run RCM reactions at high dilution since these conversions involve equilibria. In contrast, when applying high concentrations, intermolecular reactions are favored. This may result in the formation of polymers *via* the *acyclic diene metathesis polymerization* (ADMET). For this process, the release of, e.g., ethylene represents the driving force, too. The conversion of cyclic olefins into polymers that possess repeating double bonds in their backbones is considered as *ring-opening metathesis polymerization* (ROMP) and proceeds *via* a chain growth process[17-19]. Since for this type of conversion the release of ring strain is the main driving force, strained cyclic olefins such as norbornene derivatives represent the most common monomers. Since 1976, metathesis derived poly(norbornene) is commercial available and is sold under the trade name Norsorex[®]. In general, the term *cross-metathesis* (CM) describes the conversion of linear olefinic reactants into the same number of olefinic products[20, 21]. The "OCT"-process as well as the "SHOP"-technology and the "FEAST"-process are prominent examples to illustrate the importance of olefin cross-metathesis in bulk and fine chemicals industry.

The synthesis of poly(acetylene) derivatives might be accomplished by polymerizing terminal alkynes *via* a metathesis-type process. The *1-alkyne polymerization* involves the intermediary formation of a metallacyclobutene, which, after reopening, produces a conjugated, growing polymer chain[22-24]. The *cyclopolymerization* of diynes such as 1,6-heptadiynes and 1,7-octadiynes[25-27] offers a very attractive alternative synthetic route to poly(acetylenes) [28, 29]. The thus prepared polymers possess cyclic repeat units. Depending on the nature of the initiator used, the cyclopolymerization of, e.g., 1,6-heptadiynes can be controlled in such a way, that conjugated polymers exhibiting predominantly only one repetitive unit are obtained[30-32]. For these particular monomers the repetitive unit would either consist of five-membered rings (1,3-(cyclopent-1-enylene)vinylens) or of six-membered rings (1,3-(cyclohexen-1-enylene)methylidenes), respectively[33-36] (see Chapter 4.2.2).
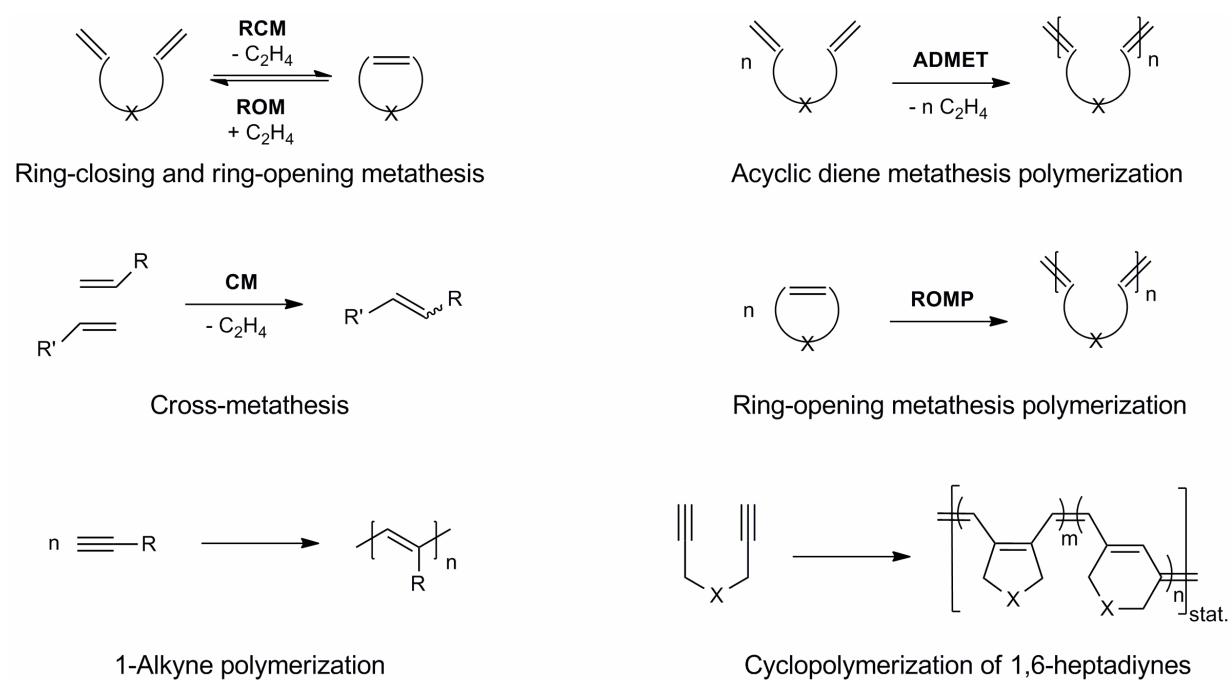
Figure 1. Types of olefin metathesis reactions.

1.2.2 Initiators

Today, there is a permanently growing number of well-defined metathesis catalysts available with all of them having their basic structural origin in the ruthenium based *Grubbs* type and the molybdenum based *Schrock* type catalysts[5]. Depending on the desired application, these basic complexes can be tuned in such a way that the number of possible modifications becomes arbitrarily large. Important representatives of both, *Grubbs* and *Schrock* type initiators are illustrated in Figure 2.
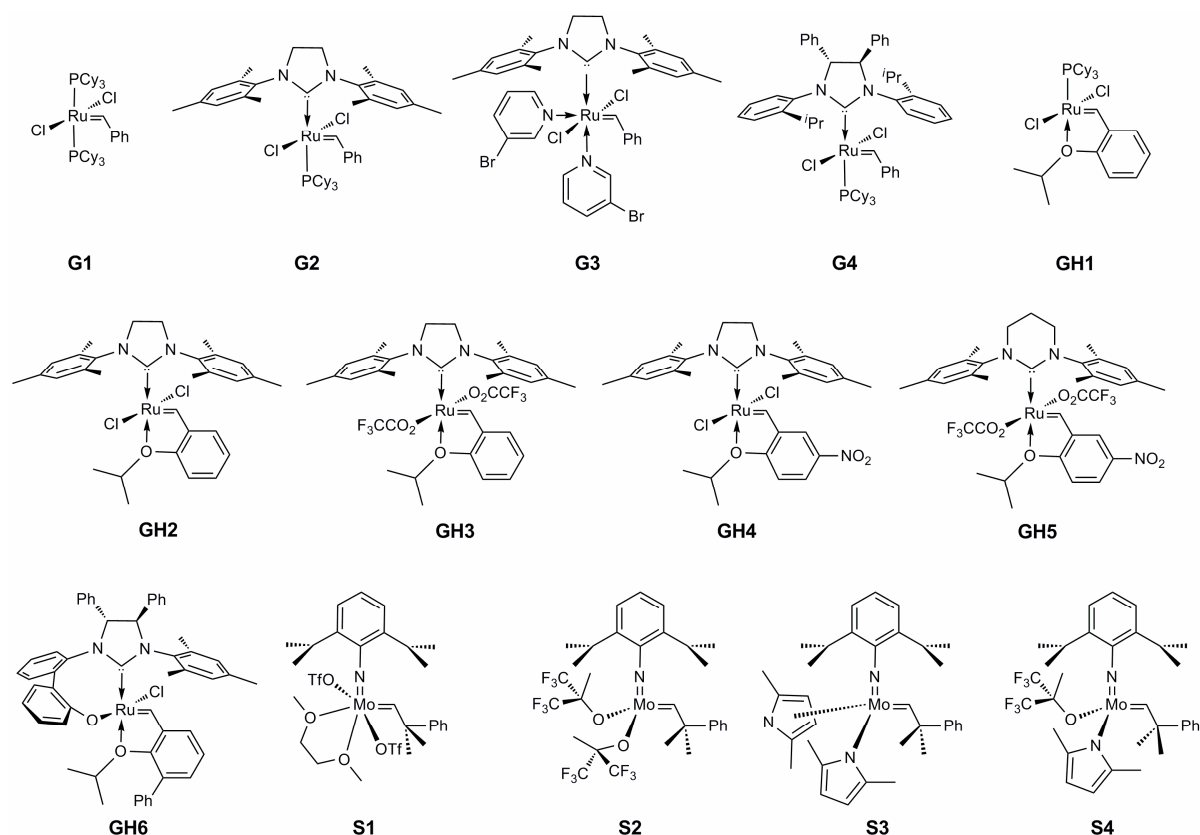
Figure 2. Important representatives of *Grubbs* and *Schrock* type catalysts.

In fact, all ruthenium-based initiators are alterations of the 1st generation *Grubbs* catalyst (**G1**) [37, 38], possessing two phosphines, and the 2nd generation *Grubbs* catalyst (**G2**) in which one of the phosphines is replaced by an N-heterocyclic carbene (NHC) [39-41]. The more electron donating NHC ligand promotes the release of the phosphine in the *trans* position, and thus is causing the enhanced initiation property and reactivity of **G2** compared to **G1**. The *Grubbs-Hoveyda* type catalysts, bearing a chelating 2-isopropoxybenzylidene ligand, are showing an increased stability which allows for chromatographical purification. Two so-called generations of these complexes are commercially available, as well (**GH1** and **GH2**) [42, 43]. The sixfold coordinated, octahedral complex [RuCl$_2$(3-Br-Py)$_2$(IMesH$_2$)(=CHC$_6$H$_5$)] (IMesH$_2$ = 1,3-dimesitylimidazolin-2-ylidene) is considered as the 3rd generation *Grubbs* catalyst (**G3**), once more showing an enhanced reactivity compared to the 2nd generation initiator and can be prepared in a simple synthetically transformation out of **G2** [44].

Modification of the anionic ligands severely affects the activity of the catalysts. Replacing the chlorides by more electron withdrawing ligands, such as, e.g.,

perfluorocarboxylates (**GH3**), provokes a more pronounced polarization of the Ru=C double bond, thus increasing the activity of a metathesis catalyst [35, 45-47]. These pseudo-halide based metathesis catalysts are officially named as *Buchmeiser-Grubbs-Hoveyda* type catalysts[48]. Introducing electron-withdrawing or electron-donating functionalities into the benzylidene moiety of a *Grubbs-Hoveyda* type catalyst offers the possibility to influence the initiation property of the complex (**GH4**) [49-51]. In 2004, a new family of metathesis catalysts based on tetrahydro-pyrimidin-2-ylidenes was introduced by the *Buchmeiser* group (**GH5**) [52, 53]. The use of asymmetric NHC-ligands even allows for the preparation of chiral *Grubbs*[54] and *Grubbs-Hoveyda*[55, 56] type catalysts (**G4** and **GH6**).

Though the highly active molybdenum based *Schrock* type catalysts are sensitive towards oxygen and many functional groups, they hold an outstanding position in olefin metathesis. As well, and particularly because of the high oxophilicity of molybdenum based complexes it is possible to attach an almost arbitrarily wide range of ligands such as, e.g., alkoxides, phenolates to the metal center[6]. The complex [Mo(N-2,6-^{i}Pr$_2$C$_6$H$_3$)(CHCMe$_2$Ph)(OTf)$_2$(DME)] (**S1**) represents a universal precursor, out of which all commonly used *Schrock*-type catalysts can be prepared[57-59]. Of great importance are the bisalkoxide type initiators (**S2**) [60, 61]. The activity generally increases by using more electron withdrawing alkoxides. The bispyrrolide complexes (**S3**) are important precursors for the preparation of either bisalkoxide or mono-alkoxide pyrrolide initiators (MAP-catalysts, **S4**). MAP-catalysts possess four different ligands arranged in a tetrahedral fashion, thus creating a stereogenic metal center. Varying the size of the alkoxide and the imido-substituent generally allows for conducting asymmetric metathesis reactions and cross-metathesis reactions in a stereoselective fashion[62-64].

1.2.3 Heterogenization of Metathesis Catalysts

In recent years, the development of sophisticated catalysts dramatically widened the range of application of olefin metathesis. However, most of the reaction systems are of homogeneous nature what is indispensably accompanied with a certain degree of liability. Probably the main problem in homogeneous catalysis is the difficulty in removing heavy metal impurities from the reaction products. Particularly for the synthesis of pharmaceutically active compounds, metal contamination above an

unobjectionable low degree (below 5 ppm) is not acceptable[65]. Since it is hard to accomplish a limit in the low ppm-level *via* homogeneous catalysis and since the process would entail a costly purification procedure, the economical application of expensive (chiral) metathesis catalysts is rather limited. Methods to decrease the remaining amount of catalyst are, e.g., the addition of activated carbon[66] or scavengers, such as DMSO,[67] isocyanide[68] or lead acetate[69], followed by column chromatography. However, by these methods the Ru level in the products merely can be reduced to 100 ppm in the best cases. Therefore, great effort was put on the immobilization of defined catalysts on suitable support materials, what appears to be the easiest and most convincing method to suppress metal contamination of the product phase[70-75]. Generally, metathesis catalysts can either be attached covalently to the surface of a support material or non-covalently by introducing functional moieties to the catalyst, which interact with functionalities present on the support. Considering *Grubbs*- or *Grubbs-Hoveyda* type complexes, generally all ligands can be used for a covalent attachment to a support material. Though frequently used, immobilization *via* the alkylidene moiety[76-83] will not be an issue in this work since this ligand demerges during the first metathesis cycle.

First to be considered is the attachment through neutral ligands such as phosphines and NHCs. In 1995, *R. H. Grubbs* published the synthesis and use of the first supported Ru based metathesis catalyst by immobilizing a 1st generation *Grubbs* type complex on the surface of a phosphine-containing styrene-divinylbenzene copolymer (**A** in Figure 3) [84]. In 2001, *F. Verpoort* reported the fixation of the catalyst **G1** (Figure 2) onto a phosphinated mesoporous matrix, giving acceptable activities in the ROMP of norbornene and the RCM of diethyl diallyl malonate (**B** in Figure 3) [85]. In 2000, *S. Blechert et al.* presented the first permanently bound 2nd-generation *Grubbs* catalyst, which was attached to crosslinked poly(styrene) *via* an ether-linked NHC ligand (**C** in Figure 3) [86]. Shortly after, *M. R. Buchmeiser* and co-workers presented the preparation and use of 2nd generation *Grubbs* catalysts, which were permanently bound to the surface of ROMP-derived monoliths *via* the NHC ligands (**D** in Figure 3) [87, 88]. The heterogenization of NHC-containing catalysts on silica was introduced by the same research group[89]. In 2009, the group of *R. H. Grubbs* published the syntheses of yet some further recyclable catalysts being attached to silica *via* the NHC ligands[90].

Attaching a metathesis catalyst to a support *via* its anionic ligands represents an alternative which, moreover, suppresses side reactions caused by the generation of free carbenes. In 2001, *J. C. Mol et al.* used a perfluorinated carboxylate linker to replace one of the chlorines in catalyst **G1** in order to permanently bind it to a poly(styrene) support (**E** in Figure 3) [91]. *M. R. Buchmeiser et al.* reported the development and use of a series of different monolith-supported ruthenium catalysts, showing both enhanced activity and improved stability (**F** in Figure 3) [47, 92-95]. For these systems, Ru-contaminations of the products below 1 ppm were detected and turn-over numbers were reported that almost reached those obtained for the corresponding homogeneous catalysts. In 2008, *P. A. Jacobs* published the immobilization of unmodified 2nd generation *Grubbs-Hoveyda* type catalyst (**GH2**, Figure 2) on silica[96]. The supported catalyst showed activity in various metathesis reactions. However, since no proof of the kind of interactions between support material and the metal complex could be provided (what hampered the identification of the metathetically active species), the system has to be considered a "black-box". In 2011, *B. Marciniec et al.* reported the immobilization and characterization of a siloxide based 2nd generation *Grubbs-Hoveyda* type catalyst $[Ru(OSiMe_2{}^tBu)_2$ $(IMesH_2)(=CH-2-(2-PrO)-C_6H_4)]$ ($IMesH_2$ = 1,3-dimesitylimidazolin-2-ylidene) on silica through covalent Ru-O-Si bonds and successfully applied the system to a few RCM, CM and ROMP reactions[97].
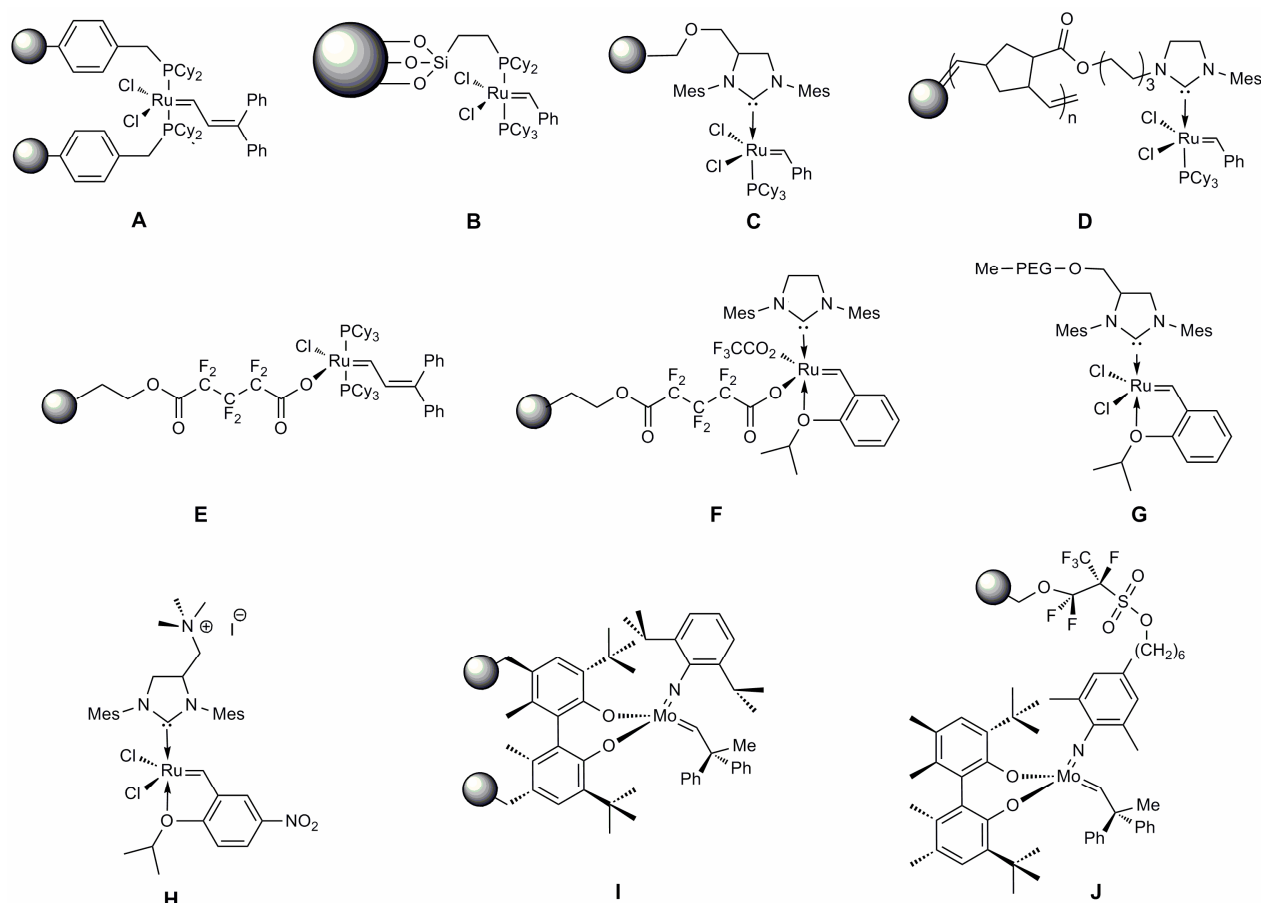
Figure 3. Examples for immobilized metathesis catalysts.

Generally, the activity of metathesis catalysts immobilized on solid support materials might be limited due to low catalyst loadings and certain diffusion limitations.

In 2005, *R. H. Grubbs* reported the development of catalysts attached to soluble supports such as, e.g., poly(ethylene glycol), an attempt to overcome diffusion related restrictions in activity (**G** in Figure 3) [98-100]. The tagged catalysts could be removed from the reaction mixture by extraction with water, and the final ruthenium contaminations of the products summed up to ~250 ppm. Very recently, *K. Grela et al.* published the syntheses of water soluble 2nd generation *Grubbs-Hoveyda* type catalysts bearing ionically tagged NHC ligands (**H** in Figure 3) [101-104]. Ruthenium contaminations of the products as low as 5 ppm were detected after both, either extensive extraction with water or filtration through silica.

The first example of a well defined, supported chiral *Schrock* type catalyst was reported by *A. H. Hoveyda* and *R. R. Schrock* in 2002 (**I** in Figure 3) [105]. The complex was anchored on a poly(styrene) support *via* an asymmetric biphenoxide ligand and showed convincing activity in enantioselective olefin metathesis reactions

combined with low catalyst leaching. *M. R. Buchmeiser et al.* used a ROMP-based approach to prepare monolith-supported chiral Schrock type catalysts which proved to be highly enantioselective in a series of asymmetric RCM reactions[106]. Furthermore, the *Buchmeiser* group pioneered in immobilizing *Schrock* catalysts through the arylimido ligand (**J** in Figure 3) [107]. This approach allows for a more precise tuning of the immobilized catalyst by varying the alkoxide ligands mainly responsible for its reactivity and selectivity[108, 109].

1.3 Polymeric Monolithic Support Materials

In this work, the term "monolith" generally refers to a continuous, cross-linked block of a polymeric material possessing a defined porous structure[110-115]. Until now, monolithic structures are predominantly attractive as media for high-performance liquid chromatography[116-119] (HPLC) and size exclusion chromatography[120]. In addition, they find applications as ion-exchange resins[121, 122] and support materials for continuous catalysis [73, 88, 92, 93, 123-127]. The most important parameters in order to characterize the porous structure of a monolith are illustrated in Figure 4.
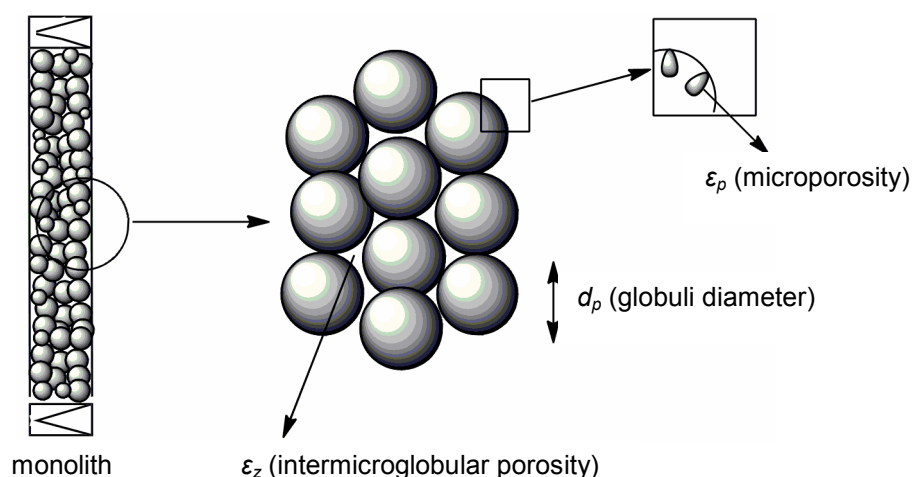
Figure 4. Characterization of the porosity of a monolith.

Independent on its nature, a monolith consists of interconnected structure-forming microglobules[128]. These microglobules are characterized by a certain diameter (d_p) and porosity, referred to as microporosity (ε_p). The void volume that is formed

between adjacent globules is considered as intermicroglobular porosity (ε_z). The total porosity (ε_t) is defined as the sum of ε_p and ε_z. The total pore volume (V_p) can be calculated from ε_t and is usually expressed in µL/g. These values, as well as the pore size distribution, can be determined *via* inverse size exclusion chromatography (ISEC) [129]. Since the measurement is performed in the solvated state, this method is the most qualified one to evaluate the porosity of a material that is supposed to be used in separation-science or continuous catalysis using liquid transport phases. To express it more descriptive: a monolith usually exhibits a fraction of *micropores* possessing diameters smaller than 2 nm and *mesopores* with diameters between 2 to 50 nm. *Micro-* and *mesopores* together contribute the most to the overall surface area of the material. In addition, *macropores* with diameters larger than 50 nm are essential for the performance of a monolith as they allow a liquid to flow through the device at a reasonable pressure[111, 130].

Nowadays, a multitude of monoliths based on either organic or inorganic polymers are available. Usually, inorganic, silica based monoliths are prepared *via* sol-gel techniques. Very briefly, the preparation of polymeric monoliths requires polymerizing a cross-linking monomer in the presence of two porogenic solvents. One, representing a thermodynamically good polymer solvent, is considered as microporogen, whereas the other one, representing a thermodynamically poorer solvent, is designed the macroporogen. In course of the polymerization, phase separation occurs, what can be described by the *Flory-Huggins* theory[131, 132]. The phase separation results in the formation of microglobuli. Dependent on the degree of cross-linking, these globuli are more or less well solvated and, in dependency of the accessibility of the propagating species, the microglobuli will continue growing more or less pronounced. Consequently, the reaction temperature, the polymerization time, the composition of the pore-forming solvent mixture and the content of crosslinking monomer, are the most effective parameters to adjust the pore sizes and the pore size distribution of a monolith.

The kinetics of the polymerization and thus the nucleation rate is affected by the reaction temperature[133, 134]. At high temperatures, predominantly the formation of a large number of small globules is observed, thus resulting in a larger surface area. This is because at higher temperatures the polymerization reaction proceeds very fast and a higher percentage of the growing polymer chains form individual

microglobuli rather than being captured by globules already present at that time. In contrast, low reaction temperatures slow down the polymerization rate. In this case, a substantial percentage of monomers will be transferred to existing nuclei which then will grow further. Consequently, a reduced total number of microglobuli possessing larger diameters will be formed, giving a smaller total surface area[133, 134]. The porogenic solvent influences the porous structure of the monolith by affecting the time at which a phase separation occurs [113, 115, 120, 124, 128, 134]. The solvent stabilizes the polymer chains in the reaction medium. Consequently, due to an earlier formation of nuclei, larger pores are obtained when more of a thermodynamically poor solvent is used, thus justifying the term macroporogen. By increasing the percentage of cross-linking monomer, the developing nuclei are more cross-linked as well, what negatively affects their swelling behaviour. Active polymerization centers are less accessible and as a consequence, the globules remain rather small in size. Since the final monolithic structure consists of a large number of small globules, a material possessing a very large surface area is yielded[134, 135].

To initiate the polymerization of organic monomers, different techniques can be applied. Conventional poly(acrylate)- or poly(styrene-*co*-divinylbenzene)-based monoliths are prepared *via* thermally initiated free radical polymerization[113, 114, 136]. Other approaches to induce radical polymerization for the preparation of monoliths use photolatent initiators or the power of electron beam. Using the latter method, *M. R. Buchmeiser et al.* prepared poly(ethyl methacrylate-*co*-trimethylpropane trimethacrylate)-based monoliths which allowed for fast separations of proteins. No additional initiator was required[118, 137-139].

Polycondensation is a relatively new contribution to the methods used for preparing monoliths[140-143]. Due to the step-growth nature of this polymerization technique, a repeated activation of the chain ends is required, thus allowing the growth of all polymer chains in the system independent on their sizes. Accessible materials are, e.g., poly(urethanes).

Yet another approach for preparing monoliths is the use of *living* or *controlled* polymerization techniques. These techniques are characterized by a fast and quantitative initiation and thus the creation of simultaneously growing polymer chains, what, in turn, raises the chance that the majority of chains grow with the same speed[113]. Applied to the preparation of monoliths, this implies that the nucleation and

phase separation process can be controlled to some enhanced extent, what might result in the formation of a more homogeneous structure. *Living* polymerization techniques applied to the preparation of monoliths are, e.g., nitroxide mediated polymerization[144, 145], atom transfer radical polymerization (ATRP) [146, 147] and ROMP.

ROMP derived monoliths, for the first time, have been introduced by *F. Sinner* and *M. R. Buchmeiser* in 2000[128, 148]. This approach offers the possibility to use a wide range of functional monomers what allows for preparing monoliths, tailor made for the particular scientific application[110]. The first setup entailed the copolymerization of norborn-2-ene (NBE) with a NBE based crosslinker such as $(NBE-CH_2O)_3SiCH_3$ in the presence of two porogenic solvents i.e. 2-propanol and toluene, initiated with $RuCl_2(PCy_3)_2(CHPh)$. Later the procedure was extended to the copolymerization of *cis*-cyclooctene (COE) with a COE-based crosslinker[149, 150]. While the NBE-based polymers exhibit a backbone structure with *tert*-allylic carbons, COE-based monoliths possess *sec*-allylic carbons, which have a higher oxidative stability. NBE-based structures, however, offer increased values for the intermicroglobular porosity ε_z, whereas the microporosity ε_p is reduced compared to their COE-based counterparts. This and the ease of preparing functionalized NBE derivatives makes NBE-based monoliths attractive for the use as support materials in continuous catalysis using liquid mobile phases. A further, striking feature of ROMP based monoliths is that, upon rod formation, the metathetically active metal alkylidenes predominantly are located on the surface of the material[110]. Taking advantage of the *living* character of this polymerization technique, this fact allows for a post-synthetic surface functionalization simply by introducing an additional, functional monomer into the monolith. Moreover, polymeric monoliths allow for high linear flow rates up to 20 mm/s at low counter pressures (<3 MPa) and at the same time allow for a fast mass transfer between the transport phase and the immobilized catalysts[73, 115].

1.4 Ionic liquids

An arbitrary, temperature based definition classifies ionic liquids (ILs) as salts with a melting temperature below the boiling point of water [151-154]. The very wide span of temperatures between melting point and boiling point represents an outstanding

characteristic of ionic liquids, which is not found in common molecular solvents. Although this feature is shown by molten salts as well, the liquidus range of ILs is located at much lower temperatures. Nowadays, most of the conventionally used ionic liquids are composed of organic cations and inorganic, mostly polyatomic anions. Low melting ionic liquids mainly consist of bulky and asymmetric cations, which prevent the simple formation of an ordered crystal structure. Examples for commonly used cations and anions are given in Figure 5[151].

a)

Imidazolium   Pyridinium   Ammonium   Phosphonium

b)

$Cl^{\ominus}$ $Br^{\ominus}$ $I^{\ominus}$ $BF_4^{\ominus}$ $PF_6^{\ominus}$ $CF_3SO_3^{\ominus}$

Halides   Tetrafluoroborate   Hexafluorophosphate   Trifluoromethanesulfonate

$AlCl_4^{\ominus}$ $N(CN)_2^{\ominus}$

Tetrachloroaluminate   Dicyanamide
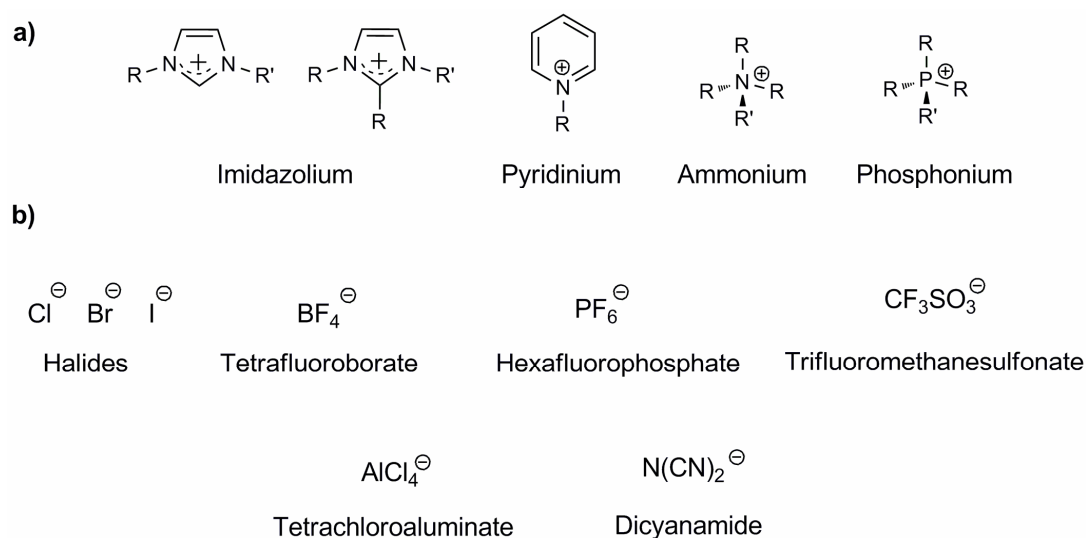
Figure 5. Commonly used **a)** cations and **b)** anions for ionic liquids.

Ethylammonium nitrate was described for the first time by *P. Walden* in 1914 and, with a melting point of 12°C, is considered as one of the earliest room temperature ionic liquids[155]. A U.S. patent from 1948 is describing the syntheses and possible applications of ionically conductive mixtures of 1-ethylpyridinium halides and $AlCl_3$[156]. In course of their research on molten salt electrolytes for thermal batteries, researchers at the *U.S. Air Force Academy* became aware of this patent and published the chemical and physical properties of the system 1-butylpyridinium chloride/$AlCl_3$ in 1978[157]. Henceforward, goal-oriented research on the development and characterization of novel ionic liquids constantly increased. The disadvantage of alkylpyridinum-based cations, which tend to easily being reduced in either a chemical or an electrochemical way, led to the successive development of dialkylimidazolium halogenoaluminate salts. An important feature of alkylpyridinium and alkylimidazolium halogenoaluminates is that their physical properties, such as, e.g.,

melting point and viscosity can be adjusted by varying the alkyl substituents and the halide/AlCl$_3$ ratio. In 1982 the ionic liquid system 1-ethyl-3-methylimidazolium chloride ([BMIM]Cl) + AlCl$_3$, showing a melting point below room temperature, was published[158] and proven to be a suited electrolyte for battery application, as well as a good solvent and catalyst for, e.g., *Friedel-Crafts* reactions. Chloroaluminate based ionic liquids, however, suffer from their sensitivity towards moisture. This was overcome by the introduction of IL systems based on dialkylimidazolium cations and water stable anions such as tetrafluoroborate, hexafluorophosphate, nitrate and sulfate by *M. J. Zaworotko* and *J. S. Wilkes* in 1992[159]. This particular development significantly widened the range of applications. Ten years later, *P. Wasserscheid* developed the syntheses of halogen-free, hydrolysis-stable ionic liquids, what gave this class of chemicals an even "greener" touch[151, 160]. Due to the large number of established and potential cations and anions (and consequently combinations thereof), it is believed that for most applications a suited ionic liquid can be designed. Ionic liquids exhibit very low vapor pressures, wide liquidus ranges, high viscosities, outstanding thermal stabilities[161] and, most important, adjustable solvating properties for various polar and non-polar compounds. Moreover, functionalized ILs may act as acids, bases or ligands in order to stabilize, e.g., organometallic compounds[152]. Ionic liquids are mainly used as powerful solvents and electrolytes, e.g., in battery applications[162]. Concomitantly, the number of reports concerning the use of ILs in *Heck*-, *Stille*-, *Negishi*- and *Suzuki*-coupling reactions is permanently growing[154, 163-178].

1.4.1 Supported Ionic Liquid Phase (SILP) Catalysis

Since researchers in various areas of chemistry became aware of the promising performance of ionic liquids used as solvents in catalytic reactions, this field of applications increased immensely. However, in case of fast chemical reactions, traditional biphasic ionic liquid/organic solvent systems suffer from limited mass transfer. Due to the high viscosity of the ionic liquids, this effect implies a certain limitation in reaction rate and merely the ionic liquid/catalyst solution within a rather narrow diffusion layer will participate in the reaction. This means that, for example, a considerably high percentage of expensive transition metal catalyst and ionic liquid simply are not utilized what turns the entire process uneconomic. Depositing a thin

layer of a catalyst containing ionic liquid on the inner surface of a highly porous support material may significantly reduce the influence of the mass transfer and would allow for more exhaustive use of the entire amount of catalyst. As a consequence, in the past decade concepts for *supported ionic liquid phase* (SILP) technology have been developed and the number of possible applications is increasing constantly[167, 172-177, 179-183]. In fact, the application of the SILP-approach to catalysis would preserve the advantages of both, homogeneous and heterogeneous catalysis, namely high reaction selectivity combined with low catalyst contamination of the products. In Figure 6, the SILP concept is illustrated schematically.
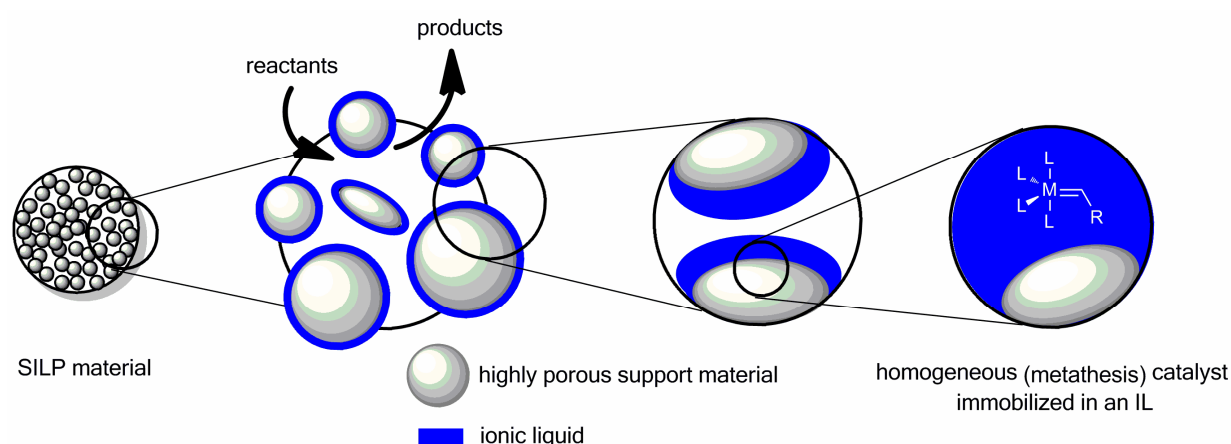
Figure 6. Schematic illustration of the SILP concept.

In principle, it is possible to immobilize ILs on support materials either by physisorption *via*, e.g., ionic interactions or by covalent bonding to the surface. Physisorption would allow for recycling the support material since the ionic liquid can be removed by flushing with polar solvents. This effect at the same time represents a somehow critical issue since the polarity of the reaction mixture has to be adjusted carefully. In recent years, the SILP-technology was successfully applied to metal-catalyzed hydroamination-, carbonylation-, hydrogenation- and *Heck* reactions. Moreover, the concept found its way into gas purification and separation processes. Very recently *P. Wasserscheid et al.* successfully applied the SILP-approach to continuous gas-phase metathesis reactions[184]. They conducted the cross-metathesis of propylene by dissolving commercial metathesis catalysts in an ionic liquid supported on silica and by using a gaseous transport phase. However, this smart approach is restricted to the metathesis of short-chain alkenes. For performing

continuous metathesis of higher, functional olefins, the use of a liquid transport phase is required.

1.5 References

[1]   C. Elschenbroich (Ed.), *Organometallics*, Wiley-VCH, Weinheim (Germany), **2006**.

[2]   Y. Chauvin, *Angew. Chem.* **2006**, *118*, 3824.

[3]   R. H. Grubbs, *Angew. Chem.* **2006**, *118*, 3845.

[4]   R. R. Schrock, *Angew. Chem.* **2006**, *118*, 3832.

[5]   R. H. Grubbs (Ed.), *Handbook of Metathesis*, Wiley-VCH, Weinheim (Germany), **2003**.

[6]   R. R. Schrock, *Chem. Rev.* **2009**, *109*, 3211.

[7]   Y. Vidavsky, A. Anaby, G. N. Lemcoff, *Dalton Trans.* **2012**, *41*, 32.

[8]   X. Wu, M. Tamm, *Beilstein J. Org. Chem.* **2011**, *7*, 82.

[9]   M. S. Sanford, M. Ulman, R. H. Grubbs, *J. Am. Chem. Soc.* **2001**, *123*, 749.

[10]   J.-L. Herisson, Y. Chauvin, *Makromol. Chem.* **1971**, *141*, 161.

[11]   W. Keim, *Chem. Ing. Technik* **1984**, *56*, 850.

[12]   P. Chaumont, C. S. John, *J. Mol. Catal.* **1988**, *46*, 317.

[13]   T. M. Trnka, R. H. Grubbs, *Acc. Chem. Res.* **2000**, *34*, 118.

[14]   M. A. Walters, *Progr. Heterocycl. Chem.* **2003**, *15*, 1.

[15]   S. J. Miller, H. E. Blachwell, R. H. Grubbs, *J. Am. Chem. Soc.* **1996**, *118*, 9606.

[16]   A. Fürstner, *Top. Catal.* **1998**, *4*, 285.

[17]   M. R. Buchmeiser, *Chem. Rev.* **2000**, *100*, 1565.

[18]   M. R. Buchmeiser, N. Atzl, G. K. Bonn, *J. Am. Chem. Soc.* **1997**, *119*, 8424.

[19]   T. L. Choi, R. H. Grubbs, *Angew. Chem. Int. Ed.* **2003**, *42*, 1743.

[20]   S. J. Connon, S. Blechert, *Angew. Chem. Int. Ed.* **2003**, *42*, 1900.

[21]   O. Arjona, A. G. Csaky, J. Plumet, *Synthesis* **2000**, *28*, 25.

[22]   R. Schlund, R. R. Schrock, W. E. Crowe, *J. Am. Chem. Soc.* **1989**, *111*, 8004.

[23]   M. R. Buchmeiser, R. R. Schrock, *Macromolecules* **1995**, *28*, 6642.

[24]   S. A. Krouse, R. R. Schrock, *Macromolecules* **1988**, *21*, 1885.

[25]   J. Unold, D. Wang, W. Frey, M. R. Buchmeiser, *Polym. Chem.* **2013**, *4,* 4129.

[26]   I. S. Lee, E.-H. Kang, T. L. Choi, *Chem. Sci.* **2012**, *3*, 761.

[27]   S. Naumann, J. Unold, W. Frey, M. R. Buchmeiser, *Macromolecules* **2011**, *44*, 8380.

[28]   M. R. Buchmeiser, *Adv. Polym. Sci.* **2005**, *176*, 89.

[29]   S.-K. Choi, Y.-S. Gal, S.-H. Jin, H. K. Kim, *Chem. Rev.* **2000**, *100*, 1645.

[30]   P. S. Kumar, K. Wurst, M. R. Buchmeiser, *J. Am. Chem. Soc.* **2009**, *131*, 387.

[31]   J. O. Krause, M. T. Zarka, U. Anders, R. Weberskirch, O. Nuyken, M. R. Buchmeiser, *Angew. Chem. Int. Ed.* **2003**, *42*, 5965.

[32]   M. R. Buchmeiser, J. O. Krause, D. Wang, U. Anders, R. Weberskirch, M. T. Zarka, O. Nuyken, C. Jäger, D. Haarer, *Macromol. Symp.* **2004**, *217*, 179.

[33]   U. Anders, O. Nuyken, M. R. Buchmeiser, K. Wurst, *Angew. Chem.* **2002**, *114*, 4226.

[34]   T. S. Halbach, J. O. Krause, O. Nuyken, M. R. Buchmeiser, *Macromol. Rapid Commun.* **2005**, *26*, 784.

[35]   J. O. Krause, O. Nuyken, M. R. Buchmeiser, *Chem. Eur. J.* **2004**, *10*, 2029.

[36]   H. H. Fox, R. R. Schrock, *Organometallics* **1992**, *11*, 2763.

[37]   P. Schwab, M. B. France, J. W. Ziller, R. H. Grubbs, *Angew. Chem. Int. Ed.* **1995**, *34*, 2039.

[38]   S. T. Nguyen, L. K. Johnson, R. H. Grubbs, J. W. Ziller, *J. Am. Chem. Soc.* **1992**, *114*, 3974.

[39]   T. Weskamp, W. C. Schattenmann, M. Spiegler, W. A. Herrmann, *Angew. Chem. Int. Ed.* **1998**, *37*, 2490.

[40]   U. Frenzel, T. Weskamp, F. J. Kohl, W. C. Schattenmann, O. Nuyken, W. A. Herrmann, *J. Organomet. Chem.* **2000**, *586*, 263.

[41]   T. Weskamp, F. J. Kohl, W. Hieringer, D. Gleich, W. A. Herrmann, *Angew. Chem. Int. Ed.* **1999**, *38*, 2416.

[42]   S. B. Garber, J. S. Kingsbury, B. L. Gray, A. H. Hoveyda, *J. Am. Chem. Soc.* **2000**, *122*, 8168.

[43]   J. S. Kingsbury, J. P. A. Harrity, P. J. Bonitatebus, A. H. Hoveyda, *J. Am. Chem. Soc.* **1999**, *121*, 791.

[44]   J. A. Love, J. P. Morgan, T. M. Trnka, R. H. Grubbs, *Angew. Chem. Int. Ed.* **2002**, *41*, 4035.

[45]   T. S. Halbach, S. Mix, D. Fischer, S. Maechling, J. O. Krause, C. Sievers, S. Blechert, O. Nuyken, M. R. Buchmeiser, *J. Org. Chem.* **2005**, *70*, 4687.

[46]   S. Naumov, M. R. Buchmeiser, *Organometallics* **2012**, *31*, 847.

[47]   J. O. Krause, O. Nuyken, K. Wurst, M. R. Buchmeiser, *Chem. Eur. J.* **2004**, *10*, 777.

[48]   B. Cornils, W. A. Herrmann, C.-H. Wang, H.-W. Zanthoff (Eds.), *Catalysis from A to Z*, Wiley-VCH, Weinheim (Germany), **2013**.

[49]   H. Wakamatsu, S. Blechert, *Angew. Chem. Int. Ed.* **2002**, *41*, 2403.

[50]   K. Grela, M. Kim, *Eur. J. Org. Chem.* **2003**, 963.

[51]   K. Grela, A. Michrowska, *Angew. Chem. Int. Ed.* **2002**, *41*, 4038.

[52]   P. S. Kumar, K. Wurst, M. R. Buchmeiser, *Organometallics* **2009**, *28*, 1785.

[53]   L. Yang, M. Mayr, K. Wurst, M. R. Buchmeiser, *Chem. Eur. J.* **2004**, *10*, 5761.

[54]   T. J. Seiders, D. W. Ward, R. H. Grubbs, *Org. Lett.* **2001**, *3*, 3225.

[55]   J. J. van Veldhuizen, S. B. Garber, J. S. Kingsbury, A. H. Hoveyda, *J. Am. Chem. Soc.* **2002**, *124*, 4954.

[56]   J. J. van Veldhuizen, D. G. Gillingham, S. B. Garber, O. Kataoka, A. H. Hoveyda, *J. Am. Chem. Soc.* **2003**, *125*, 12502.

[57]   J. B. Alexander, D. S. La, D. R. Cefalo, A. H. Hoveyda, R. R. Schrock, *J. Am. Chem. Soc.* **1998**, *120*, 4041.

[58]   G. C. Bazan, E. Khosravi, R. R. Schrock, W. J. Feast, V. C. Gibson, W. M. Davis, *J. Am. Chem. Soc.* **1990**, *112*, 8378.

[59]   R. R. Schrock, J. S. Murdzek, G. C. Bazan, J. Robbins, M. diMare, M. O'Reagan, *J. Am. Chem. Soc.* **1990**, *112*, 3875.

[60]   R. R. Schrock, Z. J. Tonzetich, A. G. Lichtscheidl, P. Müller, *Organometallics* **2008**, *27*, 3986.

[61]   R. R. Schrock, A. H. Hoveyda, *Angew. Chem. Int. Ed.* **2003**, *42*, 4592.

[62]   L. Ibrahem, M. Yu, R. R. Schrock, A. H. Hoveyda, *J. Am. Chem. Soc.* **2009**, *131*, 3844.

[63]   E. S. Sattely, S. J. Meek, S. J. Malcolmson, R. R. Schrock, A. H. Hoveyda, *J. Am. Chem. Soc.* **2009**, *131*, 943.

[64]   S. J. Malcolmson, S. J. Meek, E. S. Sattely, R. R. Schrock, A. H. Hoveyda, *Nature* **2008**, *456*, 933.

[65]   http://www.emea.europa.eu/pdfs/human/swp/444600en.pdf.

[66]   J. H. Cho, B. M. Kim, *Org. Lett.* **2003**, *5*, 531.

[67]   Y. M. Ahn, K. Yang, G. I. Georg, *Org. Lett.* **2001**, *3*, 1411.

[68]   B. R. Galan, K. P. Kalbarczyk, S. Szczepankiewicz, J. B. Keister, S. T. Diver, *Org. Lett.* **2007**, *9*, 1203.

[69]   L. A. Paquette, J. D. Schloss, I. Efremov, F. Fabris, F. Gallou, J. Mendez-Andino, J. Yang, *Org. Lett.* **2000**, *2*, 1259.

[70]   C. Coperet, J.-M. Basset, *Adv. Synth. Catal.* **22007**, *349*, 78.

[71]   M. R. Buchmeiser, *New J. Chem.* **2004**, *28*, 549.

[72]   D. E. Bergbreiter, J. Tian, C. Hongfa, *Chem. Rev.* **2009**, *109*, 530.

[73]   M. R. Buchmeiser, *Chem. Rev.* **2009**, *109*, 303.

[74]   E. B. Anderson, M. R. Buchmeiser, *ChemCatChem* **2012**, *4*, 30.

[75]   H. Clavier, K. Grela, A. Kirschning, M. Mauduit, S. P. Nolan, *Angew. Chem. Int. Ed.* **2007**, *46*, 6786.

[76]   Q. Yao, C. Zhang, *Angew. Chem.* **2003**, *115*, 3517.

[77]   G. Liu, H. He, J. Wang, *Adv. Synth. Catal.* **2009**, *351*, 1610.

[78]   C. Thurier, C. Fischmeister, C. Bruneau, H. Olivier-Bourbigou, P. H. Dixneuf, *J. Mol. Catal. A: Chem.* **2007**, *268*, 127.

[79]   H. Clavier, N. Audic, J.-C. Guillemin, M. Mauduit, *J. Organomet. Chem.* **2005**, *690*, 3585.

[80]   J. B. Binder, I. A. Guzei, R. T. Raines, *Adv. Synth. Catal.* **2007**, *349*, 395.

[81]   E. Borre, M. Rouen, I. Laurent, M. Magrez, F. Caijo, C. Crevisy, W. Solodenko, L. Toupet, R. Frankfurter, C. Vogt, A. Kirschning, M. Mauduit, *Chem. Eur. J.* **2012**, *18*, 16369.

[82]   S. W. Chen, J. H. Kim, K. Y. Ryu, W. W. Lee, J. Hong, *Tetrahedron* **2009**, *65*, 3397.

[83]   Q. Yao, M. Sheets, *J. Organomet. Chem.* **2005**, *690*, 3577.

[84]   S. T. Nguyen, R. H. Grubbs, *J. Organomet. Chem.* **1995**, *487*, 195.

[85]   K. Melis, D. De Vos, P. Jacobs, F. Verpoort, *J. Mol. Catal. A: Chem.* **2001**, *169*, 47.

[86]   S. C. Schürer, S. Gessler, N. Buschmann, S. Blechert, *Angew. Chem.* **2000**, *112*, 4062.

[87]   M. Mayr, D. Wang, R. Kröll, N. Schuler, S. Prühs, A. Fürstner, M. R. Buchmeiser, *Adv. Synth. Catal.* **2005**, *347*, 484.

[88]   M. Mayr, B. Mayr, M. R. Buchmeiser, *Angew. Chem. Int. Ed.* **2001**, *40*, 3839.

[89]   M. Mayr, M. R. Buchmeiser, K. Wurst, *Adv. Synth. Catal.* **2002**, *344*, 712.

[90]   D. P. Allen, M. M. van Wingerden, R. H. Grubbs, *Org. Lett.* **2009**, *11*, 1261.

[91]   P. Nieczypor, W. Buchowicz, W. J. N. Meester, F. P. J. T. Rutjes, J. C. Mol, *Tetrahedron Lett.* **2001**, *42*, 7103.

[92]   J. O. Krause, S. Lubbad, O. Nuyken, M. R. Buchmeiser, *Adv. Synth. Catal.* **2003**, *345*, 996.

[93]   J. O. Krause, S. Lubbad, O. Nuyken, M. R. Buchmeiser, *Macromol. Rapid Commun.* **2003**, *24*, 875.

[94]   T. S. Halbach, S. Mix, D. Fischer, S. Maechling, J. O. Krause, C. Sievers, S. Blechert, O. Nuyken, M. R. Buchmeiser, *J. Org. Chem.* **2005**, *70*, 4687.

[95]   L. Yang, M. Mayr, K. Wurst, M. R. Buchmeiser, *Chem. Eur. J.* **2004**, *10*, 5761.

[96]   B. van Berlo, K. Houthoofd, B. F. Sels, P. A. Jacobs, *Adv. Synth. Catal.* **2008**, *350*, 1949.

[97]   B. Marciniec, S. Rogalski, M. J. Potrzebowski, C. Pietraszuk, *ChemCatChem* **2011**, *3*, 904.

[98]   S. H. Hong, R. H. Grubbs, *J. Am. Chem. Soc.* **2006**, *128*, 3508.

[99]   J. P. Gallivan, J. P. Jordan, R. H. Grubbs, *Tetrahedron Lett.* **2005**, *46*, 2577.

[100]   S. H. Hong, R. H. Grubbs, *Org. Lett.* **2007**, *9*, 1955.

[101]   M. Kluciar, K. Grela, M. Mauduit, *Dalton Trans.* **2013**, *42*, 7354.

[102]   W. Kosnik, K. Grela, *Dalton Trans.* **2013**, *42*, 7463.

[103]   K. Skowerski, G. Szczepaniak, C. Wierzbicka, L. Gulajski, M. Bieniek, K. Grela, *Catal. Sci. Technol.* **2012**, *2*, 2424.

[104]   K. Skowerski, C. Wierzbicka, G. Szczepaniak, L. Gulajski, M. Bieniek, K. Grela, *Green Chem.* **2012**, *14*.

[105]   K. C. Hultzsch, J. A. Jernelius, A. H. Hoveyda, R. R. Schrock, *Angew. Chem.* **2002**, *114*, 609.

[106]   R. M. Kröll, N. Schuler, S. Lubbad, M. R. Buchmeiser, *Chem. Commun.* **2003**, 2742.

[107]   D. Wang, R. Kröll, M. Mayr, K. Wurst, M. R. Buchmeiser, *Adv. Synth. Catal.* **2006**, *348*, 1567.

[108]   R. R. Schrock, J.-K. Lee, R. O'Dell, J. H. Oskam, *Macromolecules* **1995**, *28*, 5933.

[109]   M. R. Buchmeiser, N. Schuler, G. Kaltenhauser, K.-H. Ongania, L. Lagoja, K. Wurst, H. Schottenberger, *Macromolecules* **1998**, *31*, 3175.

[110]   M. R. Buchmeiser, *Macromol. Rapid Commun.* **2001**, *22*, 1081

[111]   M. R. Buchmeiser (Ed.), *Polymeric Materials in Organic Synthesis and Catalysis*, Wiley-VCH, Weinheim (Germany), **2003**.

[112]   F. Svec, J. M. J. Frechet, *Science* **1996**, *273*, 205.

[113]   F. Svec, *J. Chromatogr. A* **2010**, *1217*, 902.

[114]   F. Svec, J. M. J. Frechet, *Anal. Chem.* **1992**, *64*, 820.

[115]   M. R. Buchmeiser, *Polymer* **2007**, *48*, 2187.

[116]   S. H. Lubbad, M. R. Buchmeiser, *J. Chromatogr. A* **2010**, *1217*, 3223.

[117]   S. H. Lubbad, M. R. Buchmeiser, *J. Sep. Sci* **2009**, *32*, 2521.

[118]   B. Schlemmer, R. Bandari, L. Rosenkranz, M. R. Buchmeiser, *J. Chromatogr. A* **2009**, *1216*, 1664.

[119]   G. Guiochon, *J. Chromatogr. A* **2007**, *1168*, 101.

[120]   S. H. Lubbad, M. R. Buchmeiser, *Macromol. Rapid Commun.* **2002**, *23*, 617.

[121]   J. Krenkova, A. Gargano, N. A. Lacher, J. M. Schneiderheinze, F. Svec, *J. Chromatogr. A* **2009**, *1216*, 6824.

[122]   C. Gatschelhofer, A. Mautner, F. Reiter, T. R. Pieper, M. R. Buchmeiser, F. Sinner, *J. Chromatogr. A* **2009**, *1216*, 2651.

[123]   R. Bandari, M. R. Buchmeiser, *Catal. Sci. Technol.* **2012**, *2*, 220.

[124]   S. H. Lubbad, B. Mayr, M. Mayr, M. R. Buchmeiser, *Macromol. Symp.* **2004**, *210*, 1.

[125]   M. Sudheendran, M. R. Buchmeiser, *Macromolecules* **2010**, *43*, 9601.

[126]   R. Bandari, T. Höche, A. Prager, K. Dirnberger, M. R. Buchmeiser, *Chem. Eur. J.* **2010**, *16*, 4650.

[127]   C. Elsner, C. Ernst, *J. Appl. Polym. Sci.* **2011**, *119*, 1450.

[128]   F. Sinner, M. R. Buchmeiser, *Macromolecules* **2000**, *33*, 5777.

[129]   I. Halasz, K. Martin, *Angew. Chem.* **1978**, *90*, 954.

[130]   J. Urban, P. Jandera, *J. Sep. Sci* **2008**, *31*, 2521.

[131]   M. L. Huggins, *J. Chem. Phys.* **1941**, *9*, 440.

[132]   P. J. Flory, *J. Chem. Phys.* **1941**, *9*, 660.

[133]   C. Viklund, F. Svec, J. M. J. Frechet, K. Irgum, *Chem. Mater.* **1996**, *8*, 7580.

[134]   F. Svec, J. M. J. Frechet, *Macromolecules* **1995**, *28*, 7580.

[135]   B. P. Santora, M. R. Gagne, K. G. Moloy, N. S. Radu, *Macromolecules* **2001**, *34*, 658.

[136]   S. Hjerten, J. L. Liao, R. Zhang, *J. Chromatogr.* **1989**, *473*, 273.

[137]   R. Bandari, W. Knolle, M. R. Buchmeiser, *J. Chromatogr. A* **2008**, *1191*, 268.

[138]   R. Bandari, W. Knolle, A. Prager-Duschke, M. R. Buchmeiser, *Macromol. Rapid Commun.* **2007**, *28*, 2090.

[139]   R. Bandari, C. Elsner, W. Knolle, C. Kühnel, U. Decker, M. R. Buchmeiser, *J. Sep. Sci.* **2007**, *30*, 2821.

[140]   J. Li, Z. Du, H. Li, C. Zhang, *Polymer* **2009**, *50*, 1526.

[141]   N. Tsujioka, N. Ishizuka, N. Tanaka, T. Kubo, K. Hosoya, *J. Polym. Sci. Polym. Chem.* **2008**, *46*, 3272.

[142]   N. Tsujioka, N. Hira, S. Aoki, N. Tanaka, K. Hosoya, *Macromolecules* **2005**, *38*, 9901.

[143]   X. F. Sun, Z. K. Chai, *J. Chromatogr. A* **2002**, *943*, 209.

[144]   K. Kanamori, K. Nakanishi, T. Hanada, *Adv. Mater.* **2006**, *18*, 2407.

[145]   M. D. Saban, M. K. Georges, R. N. Vereign, G. K. Hamer, P. M. Kazmaier, *Macromolecules* **1995**, *28*, 7032.

[146]   J. S. Wang, K. Matyjaszewski, *J. Am. Chem. Soc.* **1995**, *117*, 5614.

[147]   K. Kanamori, J. Hasegawa, K. Nakanishi, T. Hanada, *Macromolecules* **2008**, *41*, 7186.

[148]   F. Sinner, M. R. Buchmeiser, *Angew. Chem.* **2000**, *112*, 1491.

[149]   B. Schlemmer, C. Gatschelhofer, T. R. Pieper, F. Sinner, M. R. Buchmeiser, *J. Chromatogr. A* **2006**, *1132*, 124.

[150]   R. Bandari, A. Prager-Duschke, C. Kuhnel, U. Decker, B. Schlemmer, M. R. Buchmeiser, *Macromolecules* **2006**, *39*, 5222.

[151]   P. Wasserscheid, T. Welton (Eds.), *Ionic Liquids in Synthesis*, Wiley-VCH, Weinheim (Germany), **2003**.

[152]   P. Wasserscheid, T. Welton (Eds.), *Ionic Liquids in Synthesis, Vol. 2: Transition Metal Catalysis in Ionic Liquids, 2nd ed.*, Wiley-VCH, Weinheim (Germany), **2007**.

[153]   P. Wasserscheid, *Chemie unserer Zeit* **2003**, *37*, 52.

[154]   P. Wasserscheid, W. Keim, *Angew. Chem.* **2000**, *112*, 3926.

[155]   P. Walden, *Bull. Acad. Imper. Sci. St. Petersbourg* **1904**, *8*, 405.

[156]   F. Hurley, U.S. Patent 4, 446, 331, **1948**.

[157]   R. J. Gale, B. Gilbert, R. A. Osteryoung, *Inorg. Chem.* **1978**, *17*, 2728.

[158]   J. S. Wilkes, J. A. Levisky, R. Wilson, C. L. Hussey, *Inorg. Chem.* **1982**, *21*, 1263.

[159]   J. S. Wilkes, M. J. Zaworotko, *Chem. Commun.* **1992**, 965.

[160]   P. Wasserscheid, R. van Hal, A. Bösmann, *Green Chem.* **2002**, *4*, 400.

[161]   M. Kosmulski, J. Gustafsson, J. B. Rosenholm, *Thermochimi. Acta* **2004**, *412*, 47.

[162]   M. Armand, F. Endres, D. R. MacFarlane, H. Ohno, Scorsati, *Nature Mater.* **2009**, *8*, 621.

[163]   D. Zhao, Z. Fei, T. J. Geldbach, R. Scopelliti, P. J. Dyson, *J. Am. Chem. Soc.* **2004**, *126*, 15876.

[164]   X. Li, D. Zhao, Z. Fei, L. Wang, *Science in China: B* **2006**, *35*, 181.

[165]   A. Bösmann, G. Francio, E. Janssen, M. Solinas, W. Leitner, P. Wasserscheid, *Angew. Chem.* **2001**, *113*, 2769.

[166]   C. C. Brasse, U. Englert, A. Salzer, H. Waffenschmidt, P. Wasserscheid, *Organometallics* **2000**, *19*, 3818.

[167]   M. Haumann, K. Dentler, J. Joni, A. Riisager, P. Wasserscheid, *Adv. Synth. Catal.* **2007**, *349*, 425.

[168]   D. S. McGuiness, W. Mueller, P. Wasserscheid, K. J. Cavell, B. W. Skelton, A. H. White, U. Englert, *Organometallics* **2002**, *21*, 175.

[169]   W. Miao, Chan. T. H., *Acc. Chem. Res.* **2006**, *39*, 897.

[170]   V. I. Parvulescu, C. Hardacre, *Chem. Rev.* **2007**, *107*, 2615.

[171]   M. Picquet, I. Tkatchenko, I. Tommasi, P. Wasserscheid, J. Zimmermann, *Adv. Synth. Catal.* **2003**, *345*, 959.

[172]   A. Riisager, K. M. Eriksen, P. Wasserscheid, R. Fehrmann, *Catal. Lett.* **2003**, *90*, 149.

[173]   A. Riisager, R. Fehrmann, S. Flicker, R. van Hal, M. Haumann, P. Wasserscheid, *Angew. Chem.* **2005**, *117*, 826.

[174]   A. Riisager, R. Fehrmann, M. Haumann, P. Wasserscheid, *Eur. J. Inorg. Chem.* **2006**, 695.

[175]   A. Riisager, R. Fehrmann, M. Haumann, P. Wasserscheid, *Top. Catal.* **2006**, *40*, 91.

[176]   A. Riisager, B. Jorgensen, P. Wasserscheid, R. Fehrmann, *Chem. Commun.* **2006**, 994.

[177]   A. Riisager, P. Wasserscheid, R. van Hal, R. Fehrmann, *J. Catal.* **2003**, *219*, 452.

[178]   R. Sheldon, *Chem. Commun.* **2001**, 2399.

[179]   M. A. Gelesky, S. S. X. Chiaro, F. A. Pavan, J. H. Z. dos Santos, J. Dupont, *Dalton Trans.* **2007**, 5549.

[180]   P. Lozano, E. Garcia-Verdugo, R. Piamtonkam, N. Karbass, T. De Diego, M. I. Burguete, S. V. Luis, J. L. Iborra, *Adv. Synth. Catal.* **2007**, *349*, 1077.

[181]   C. P. Mehnert, *Chem. Eur. J.* **2004**, *11*, 50.

[182]   C. P. Mehnert, R. A. Cook, N. C. Dispenziere, M. Afeworki, *J. Am. Chem. Soc.* **2002**, *124*, 12932.

[183]   C. P. Mehnert, E. J. Mozeleskip, R. A. Cooka, *Chem. Commun.* **2002**, 3010.

[184]   J. Scholz, S. Loekman, N. Szesni, W. Hierienger, A. Goerlinger, M. Haumann, P. Wasserscheid, *Adv. Synth. Catal.* **2011**, *353*, 2701.

2. Design of the Monolithic Support Material
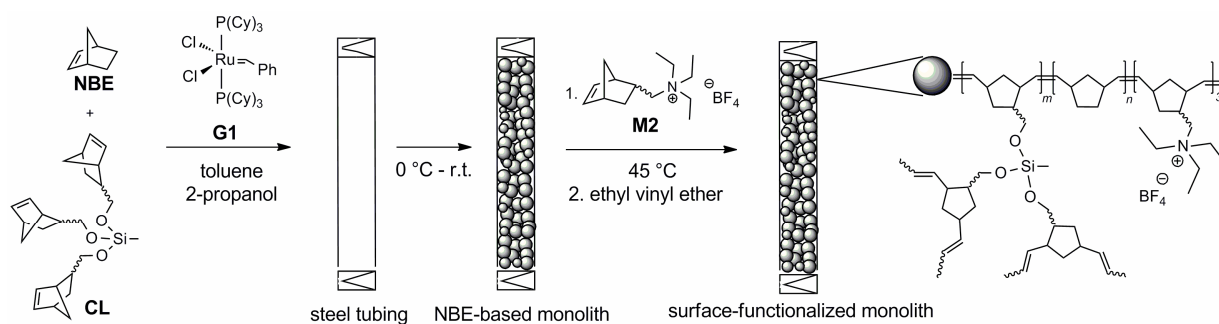
Monolithic support material
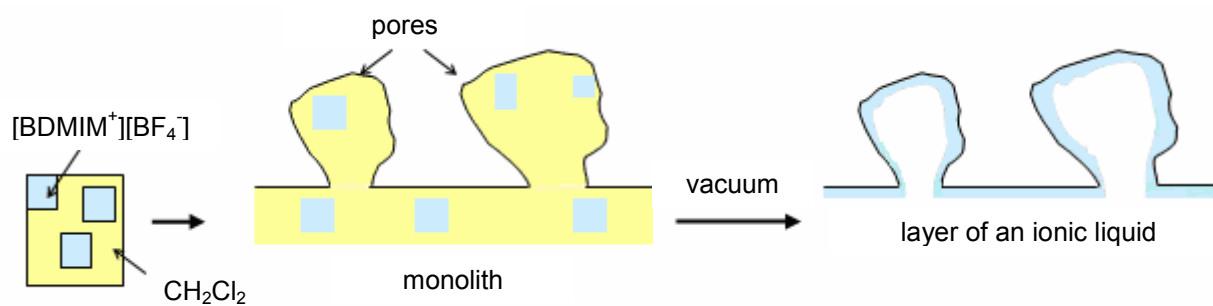
Layer of an ionic-liquid on a monolithic surface

2.1 Introduction

A highly qualified support material is of crucial importance for the success of continuous catalysis performed under biphasic liquid-liquid conditions. Thereby, the materials' porosity is an essential factor, since it should allow for a high reactant throughput without giving rise to immoderately high back pressures, but at the same time it should not negatively affect the supports strength of shape. In addition, the chosen material must offer the possibility to immobilize a suited liquid stationary phase upon its surface, it should be chemically inert and it has to withstand reaction temperatures up to 150°C without fading in its performance. Preferably, the preparation of the support material can be accomplished in a simple, reproducible process. Probably one of the most important features is a low expense regarding the chosen basic materials and the fabrication of the desired support, thereof. Ideally, the support can be recharged and reused in a facile and fast fashion, without being removed out of its jacket. Polymeric, ROMP-derived monoliths fulfill all these requirements[1-7]. On that account, these devices are chosen to serve as support materials in this particular project. By varying the ratio and nature of the compounds used for monolith preparation, namely the monomer, crosslinker, initiator and porogenic solvents, its porosity can be adjusted precisely[4, 8-10]. This allows for adjusting the ideal compromise between the applied flow rates and resulting back pressures. The monoliths` surface can be functionalized easily by grafting an ionic monomer onto it, thereby taking advantage of the *living* character of the ROMP reaction used for its preparation [11-13]. The ionic moieties facilitate/enable to attach and to fix films of ionic liquids with adjustable thickness. In fact, these films of ionic liquids represent the actual stationary phases for the performed metathesis reactions under biphasic liquid-liquid conditions. Due to their negligible vapor pressures and their excellent dissolving power toward polar compounds, ionic liquids represent qualified reaction media [6, 14-19]. Important criteria the ionic liquid of choice has to fulfill, are a negligible miscibility with common nonpolar, organic solvents as well as a liquid state of matter at reaction temperature. The various combination possibilities between available cations and anions almost guarantee for finding a suited ionic liquid[20]. Importantly, the possibility that components of the ionic liquid react later with the utilized ruthenium-catalyst, has to be excluded. The ILs' duty is to selectively

dissolve the metal-complexes without negatively influencing their activity. In the following, the development of a qualified support material is described in detail.

2.2 Results and Discussion

2.2.1 Preparation of Monoliths

The procedure of how to prepare ROMP-derived monoliths has been well established in studies previously accomplished in the *Buchmeiser* research group [21, 22]. Various monomers and crosslinkers have been investigated and their performance with respect to monolith formation has been examined. Detailed research revealed that norborn-2-ene (NBE)-based monoliths, formed *via* the copolymerization of NBE and the crosslinker (**CL**) tris(norborn-5-ene-2-ylmethyloxy) methylsilane ((NBE-CH$_2$O)$_3$SiCH$_3$), are possessing both a defined and stable porous structure as well as a certain degree of flexibility. In terms of initiation efficiency and control over propagation, the complex [RuCl$_2$(PCy$_3$)$_2$(=CHC$_6$H$_5$)] (**G1**) is showing a balanced activity in the ROMP of both substrates and, therefore, represents the initiator of choice. 2-Propanol and toluene serve as porogenic solvents, 2-propanol thereby acting as macroporogen and toluene possessing micropore-forming properties [1]. For this project, a support material whose porous structure is mainly built up of macropores and which nonetheless is showing a high shape persistence is desired. Monoliths have been prepared by varying the ratio between the two monomers norborn-2-ene and (NBE-CH$_2$O)$_3$SiCH$_3$ and the porogenic solvents 2-propanol and toluene (Table 1), in order to obtain support materials differing in their porous constitutions and thus possessing dissimilar flow-through characteristics. In either case, phase-separation and globule-growth were allowed to happen for 30 min at 0°C and additional 30 min at room temperature, before terminating the ROMP-reaction by flushing with ethyl vinyl ether. All monoliths were prepared inside stainless steel columns (100 x 4.6 mm, V$_{column}$ = 1.66 mL) and have been characterized by means of inverse size exclusion chromatography (ISEC). The method is based on several assumptions, but it reveals an appropriate way to reveal differences in porosity between the monoliths[23]. One fundamental requirement for ISEC is that the polymer does not interact with the surface of the monolith and that its elution time, under defined conditions, solely depends on its hydrodynamic radius[24].

Table 1. Physicochemical data for ROMP-derived monoliths (V_{column} = 1.66 mL).

| #	**Polymerization mixture [wt.-%]**					**Structural data**					
	NBE	CL	2-PrOH	toluene	**G1**	$V_{z, calc.}$ mL	$V_{z, exp.}$ mL	ε_p vol.-%	ε_z vol.-%	ε_t vol.-%	$\overline{\Phi}_m$ Å[a]
A	12.5	12.5	52.5	22.5	0.4	1.25	1.36	4	80	85	1240
B	15	15	50	20	0.4	1.16	1.25	5	75	80	1160
C	20	20	46	14	0.4	1.00	1.08	14	55	69	850
D	25	25	40	10	0.4	0.83	0.93	26	31	57	480

[a] Average pore diameter.

The void volumes $V_{z, exp.}$, determined by ISEC, are approximately 10% larger than the calculated ones. This finding is in accordance with data reported in the literature and is explained by volume contraction during polymerization causing shrinkage of 5 – 10% [1, 25]. As intended, the structures are built up mainly of macropores for most monoliths listed in Table 1, which was achieved by using a three- to fourfold excess of 2-propanol with respect to toluene. With increasing solids content, that is the percentage of monomers related to the total mass of the polymerization mixture, the void-volume decreases as expected. The microporosity (ε_p) is increasing when raising the monomer content, whereas the intermicroglobular porosity (ε_z) is decreasing notably. The total porosity (ε_t), which is defined as the sum of ε_p and ε_z, consequently decreases as well. With increasing solids content, the average pore diameters of the monoliths decrease. When considering the structural data of, e.g., monolith **A**, the large void volume of 90% with regard to the total column volume is mainly caused by the interstitial porosity (ε_z = 80%) and should guarantee for low back-pressures. The same is true for monolith **B**, whereas the total porosity of monolith **D** is mainly caused by micropores. Monoliths **A** - **C** were designed to possess almost exclusively macropores, thus favoring diffusion and allowing for high reagent throughput. In contrast to most silica-based materials, which also have a large fraction of micro- and mesopores, this particular feature makes polymeric

monoliths ideal support materials for the intended continuous metathesis reactions under biphasic conditions. Following, all monoliths have been examined in flow-through experiments, whereat the resulting back-pressures at different flow-rates were recorded.

2.2.1.1 Flow-through Characteristics of Monoliths *A – D*

To find the most qualified support material, the resulting back-pressures were recorded when flushing heptane through monoliths **A** – **D** at different flow-rates. Heptane was chosen as solvent, since it is strongly nonpolar and might thereby be used for continuous catalysis under biphasic liquid-liquid conditions. The experiments were conducted at three different temperatures (room temperature, 45°C, 100°C) to simulate a wide range of reaction conditions. To perform the measurements, monoliths were connected to an HPLC-pump, which allowed to adjust the flow-rate and to monitor the resulting back-pressures. In order to heat the columns and the solvent tubing, an HPLC-column oven was used. The results are graphically illustrated in Figure 7.
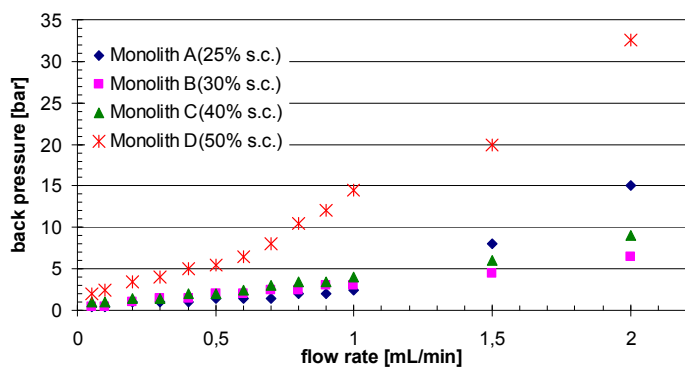
1a. Heptane at room-temperature.
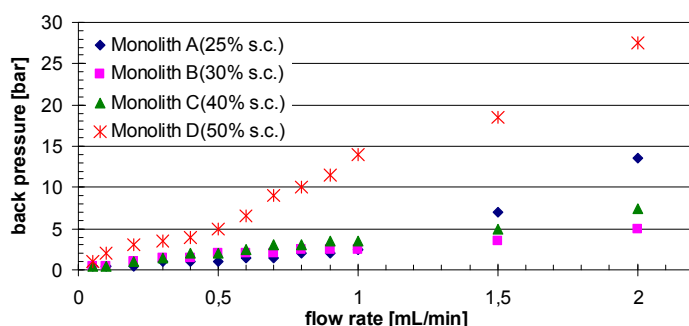
1b. Heptane at 45°C.
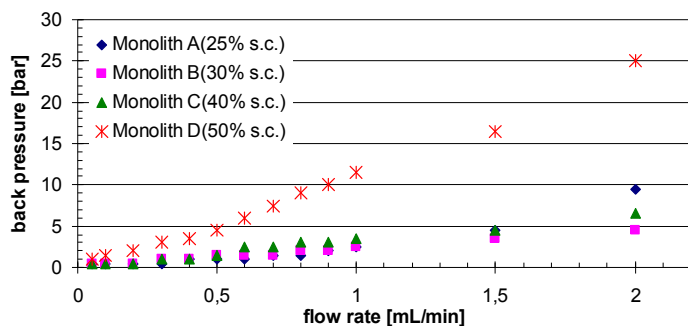
1c. Heptane at 100°C.

Figure 7. Resulting back pressures when flushing heptane through monoliths **A** – **D** at different temperatures.

The composition of monolith **D** was obviously not well qualified, since high back-pressures resulted already at low flow-rates. The solids content of 50% for this device was simply too high and its structure, to a large extent, was dominated by micropores. Decreasing solids content and thus an increasing void-volume leads to reduced back-pressures. Consequently, for monolith **A**, the lowest back-pressures were recorded. However, at flow-rates above 1.5 mL/min, the back-pressures increased considerably for this device. Thereupon, again, low flow-rates starting from 0.05 mL/min were applied, however backpressures as low as recorded for the first cycle could not be obtained anymore. When removing the monolith out of is jacket, it was found that its texture was rather flexible than rigid. Probably the support material was compressed at high flow-rates and its porous structure was enduringly damaged. A void volume of 90% obviously did not allow for the formation of a stable structure. Monolith **B**, possessing a void volume of 80%, was giving low back-pressures at all flow-rates. The same was true for monolith **C** ($V_{Z, exp.}$ = 70%), although the obtained back-pressures were slightly higher than for monolith **B**. The back pressures decrease with increasing temperature, caused by the concomitantly decreasing viscosity of the solvent. For all temperatures it was proven, that monoliths possessing enlarged void-volumes provoke lower back pressures. In an additional experiment, the time required for flushing 2 mL solvent through the monoliths **A** - **C** at 45°C was measured three times for different flow-rates and the average values are given in Table 2.

Table 2. Time required for flushing 2 mL heptane through monoliths **A** - **C** at room-temperature.

Monolith / ε_t [vol.-%]	Flow-rate [mL/min]	Time [min] [a]
A / 90	1.0	3.33
A	0.5	6.67
A	0.1	39.85
B / 80	1.0	2.85
B	0.5	5.76
B	0.1	34.34
C / 70	1.0	2.42
C	0.5	5.06
C	0.1	27.32

[a] Value given is the average of three independent measurements.

For monoliths **A** – **C**, the back-pressures increased almost linearly with increasing flow-rates up to 1.0 mL/min. As expected, a reduced period of time was required for flushing a certain volume of solvent through the monolithic support materials with decreasing void-volumes, since all of the monoliths did not give rise to exceedingly high back pressures. In summary, monoliths **B** and **C** showed the best stability and they allowed for high flow rates, what directly corresponds to a high reactant throughput, without creating unacceptable high back-pressures. For further modifications, such as surface-functionalization and immobilization of the ionic-liquid layer, monolith **B** was chosen. Due to the large void-volume of 80% this particular support material offers sufficient space to graft a functional monomer onto the surface without tremendously affecting its permeability. The preparation of ionic NBE-

derivatives as well as the preparation of surface-functionalized support materials is outlined in the next chapter.

2.2.1.2 Surface Functionalization

In order to effectively immobilize an ionic liquid onto the surface of a monolithic support material, its surface needs to be functionalized with polar/charged moieties. In addition to capillary actions, the IL is then retained by ionic interactions as well. The monoliths' surface can be functionalized by grafting an ionic monomer onto it, thereby taking advantage of the *living* character of the ROMP reaction used for its preparation[11, 12]. On that account, NBE-derivatives, bearing either imidazolium or ammonium moieties, have been designed (Scheme 3). Importantly, the ionic monomers need to possess non-coordinating counter ions, in order to avoid injury of the Ru-complexes. For this reason tetrafluoroborate was chosen as the anion.
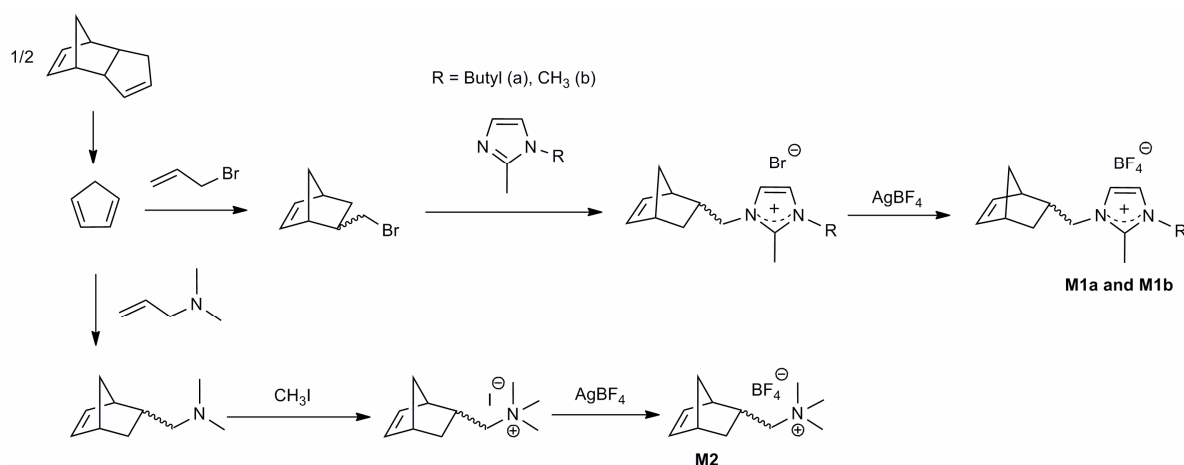
Scheme 3. Synthesis of ionic NBE-based monomers; for **M1a** R = butyl, **M1b** R = CH_3.

In order to simulate the post synthetic surface functionalization, the tailor-made monomers **M1a**, **M1b** and **M2** were first subjected to homopolymerization induced by the 1st generation *Grubbs* type catalyst [$RuCl_2(PCy_3)_2(=CHC_6H_5)$] (**G1**). 50 equivalents of all monomers could be polymerized within less than 12 h at 40°C. In a next step, copolymerizations were conducted, thereby using the same monomer ratio as it was used for the preparation of monolith **B**. Norborn-2-ene and (NBE-CH$_2$O)$_3$ SiCH$_3$ were copolymerized for 30 min at 0°C, then 30 equivalents of the functional

monomer were added and the temperature was raised to 40°C. Conversions are illustrated in Figure 8.
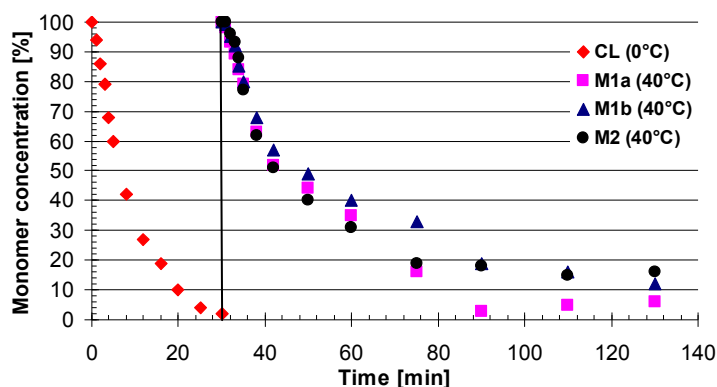
Figure 8. Copolymerizations between NBE, $(NBE-CH_2O)_3SiCH_3$ (CL) and monomers **M1a**, **M1b**, **M2**. Monomers were added after 30 min in order to simulate surface grafting.

In summary, it can be stated, that all monomers **M1a**, **M1b** and **M2** are potentially suited for post synthetic surface-functionalization. In imidazolium units, the cationic charge is delocalized to some degree. In contrast, the ammonium functionality provided by monomer **M2** should enforce the ionic interactions between an ionic liquid, an ionic catalyst and the monoliths surface. For this reason, the ammonium monomer $[NBE-CH_2-NMe_3^+][BF_4^-]$ was chosen for surface-functionalization of the monolithic support material. The process is illustrated in Scheme 4. Again, with the surface-functionalized support, the flow-through experiments outlined above have been carried out. The grafting did not significantly influence the support materials` performance when applying a solvent flow up to 2.0 mL/min.
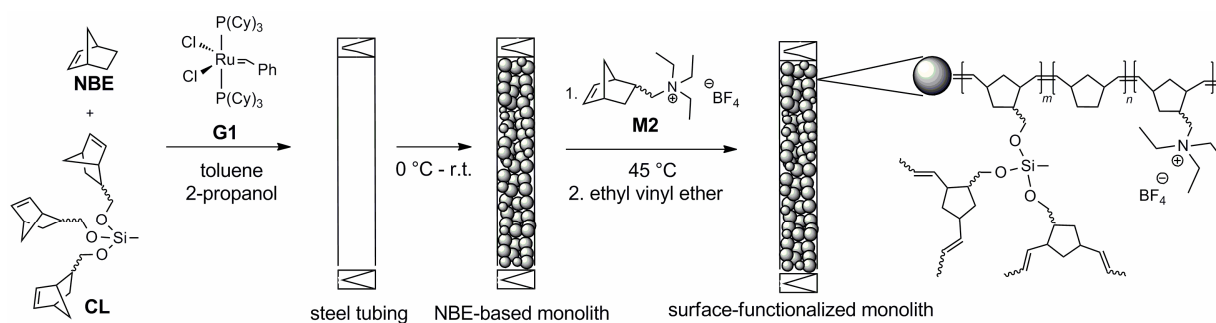
Scheme 4. Preparation of a surface-functionalized monolithic support. p=3.

2.2.2 Immobilization of Ionic Liquids (ILs)

2.2.2.1 Ionic Liquids

For further applications in continuous metathesis reactions it is required to develop a system in which the ionic catalyst used is selectively soluble in the ionic liquid phase but not in the solvent/reactant phase. Therefore, the IL needs to show a negligible miscibility with common nonpolar, organic solvents as well as a liquid state of matter at reaction temperature. That means that the melting point of the IL has to be below 40°C. The reactants should possess good solubility in both phases and at best, the products preferentially dissolve in the mobile phase. To avoid affecting the Ru-catalysts' activity, neither the anion nor the cation of the IL should show coordinating ability. For this reason, halide as well as pseudo-halide (e.g., trifluoroacetate) containing ILs have been excluded *a priori.* The imidazolium-based compounds exhibit a methyl group in 2-position (type B in Figure 9) in order to prevent deprotonation and coordination to the ruthenium. The basic structures of some ILs are shown in Figure 9. The miscibility of ionic liquids with diethyl ether, *tert*-butyl methyl ether, pentane, heptane and THF was examined.

R = alkyl   X = BF$_4$, PF$_6$, OTf, Tf$_2$N
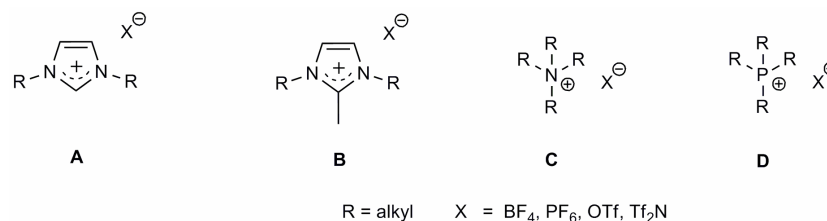
Figure 9. Basic structures of ionic liquids.

All ammonium-based ILs (type C in Figure 9) considered indeed did not mix with the chosen organic solvents, however, the melting points of these compounds by far exceed a tolerable limit. Melting points can be reduced by introducing longer alkyl-chains. Thus, tributylmethylammonium methyl sulfate possesses a melting point of ~60°C. However, an increase in the length of the alkyl-chains, leads to a reduction in polarity of the compound. This is true for phosphonium-based ionic liquids as well (type D in Figure 9). The melting point of tetrabutylphosphonium tetrafluoroborate is located above 100°C. In turn, trihexyl-tetradecylphosphonium tetrafluoroborate, is showing a liquid state of matter at room temperature. Unfortunately, the low melting point is induced by long alkyl-chains, which additionally decrease the polarity of the

compound to an extent, which makes it soluble even in heptan. The imidazolium-based compounds [BMIM$^+$], possessing a proton in 2-position (type A in Figure 9) were not considered since deprotonation and coordination to the ruthenium can occur[18, 26]. Trimethylimidazolium [TriMIM$^+$]-based compounds, such as trimethyl-imidazolium methyl sulfate or the ethyl sulfate derivative, exhibit a methyl group in 2-position, but their melting points are above 100°C. The ionic liquids of the type [BDMIM$^+$][X$^-$] ([X$^-$], e.g., BF$_4^-$, PF$_6^-$, OTf$^-$), in contrast, wherein the butyl-moiety is inducing a reduction of the melting points, suggest to be a promising choice, albeit they display lower polarity than their [BMIM$^+$] analogues. Depending on the nature of its counter ion, these ILs possess melting points around T$_m$~38°C. This is advantageous since they precisely can be weighted in a solid state and convert into a liquid at reaction temperature, thereby showing a viscosity that is high enough to withstand the shear forces induced at elevated flow rates.

For further experiments, IL 1-butyl-2,3-dimethylimidazolium tetrafluoroborate [BDMIM$^+$][BF$_4^-$] was chosen, also because it is slightly less viscous and more polar than the PF$_6^-$-derivative, which for example is showing a reduced solubility in methanol. The bis(trifluoromethanesulfonyl)imide-analog [BDMIM$^+$][Tf$_2$N$^-$] is showing decreased solubility in methanol, is comparably non-polar and high in price. This is also true for the triflate-derivative [BDMIM$^+$][TfO$^-$]. [BDMIM$^+$][BF$_4^-$] does not mix with diethyl ether, *tert*-butyl methyl ether, pentane and heptane. THF dissolves the IL to some extent. For the following experiments, heptane was chosen as the liquid mobile phase since it allows reducing the polarity that is eventually induced by the employed reactants. Pentane was excluded due to its low boiling point, hexane was not considered due to its toxicity[27, 28].

2.2.2.2 Preparation of IL Films

At this stage of the work, all components required for the preparation of a monolith-supported ionic liquid phase had been defined, i.e. the composition of the monolith, the monomer suited for surface-functionalization, the type of the ionic liquid as well as the mobile phase. Next, the technique of how to introduce IL-layers into the monolith had to be developed.

2.2.2.2.1 Introducing Neat IL

In first experiments, neat $[BDMIM^+][BF_4^-]$ was injected into monoliths functionalized with monomer **M2**. The ionic liquid possesses a melting point of T_m = 38°C. Consequently, heating was required during injection. In doing so the accessible void volume of the support was completely filled with IL. The process is illustrated in Figure 10.
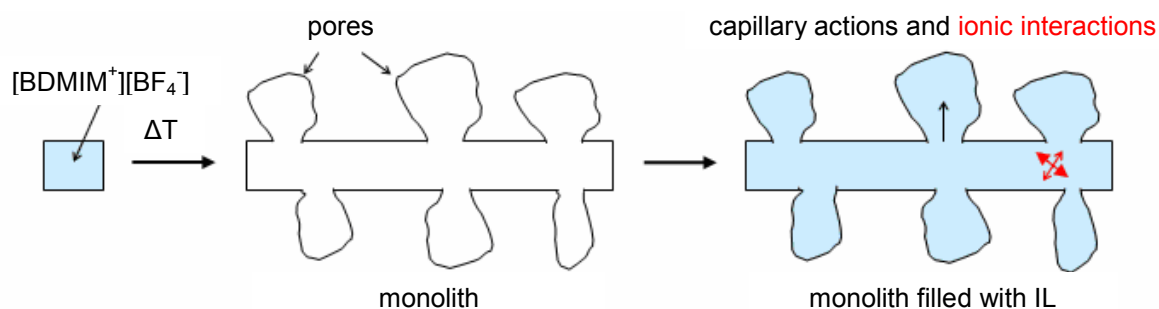
Figure 10. Injection of neat IL.

The idea was to remove excess of ionic liquid simply by flushing with neat heptane. Afterwards, reactants, dissolved in heptane, shall be transported through the support and *via* diffusion will reach the catalytically active centers within the ionic liquid phase. However, only a small fraction of the initial amount of $[BDMIM^+][BF_4^-]$ could be removed by flushing with heptane at temperatures the IL possesses a liquid state of matter. In addition to capillary actions, the stationary phase is retained due to intermolecular ionic interactions. These strong interactions are inducing a certain resistance what allowed for flushing only at flow-rates greater than 0.3 mL/min. As expected, no flushing was possible at room temperature at all, the column was clogged by the solid IL. Using the described method for immobilizing $[BDMIM^+][BF_4^-]$, the macropores of the support material seem to be completely filled with the IL. As a consequence, the diffusion path is enlarged, what might negatively influence the catalytic activity of the system. For compensation, a higher concentration of the catalyst would be required. The considerably large amounts of the ionic liquid as well as of the Ru-catalyst would raise the costs required for setting up and operating a system for continuous catalysis using monolith-supported ionic liquids. On that account, a procedure was needed for depositing *thin* IL-layers with adjustable thickness.

2.2.2.2.2 Introducing Dissolved IL - Adjustable Film Thickness

To reduce the amount of IL and thus the layer thickness, a solution of $[BDMIM^+][BF_4^-]$ in CH_2Cl_2 was injected as is shown in Figure 11.
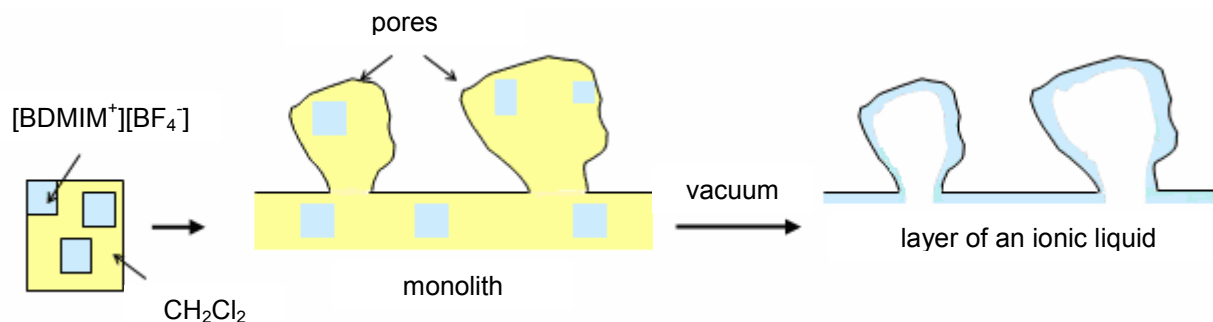

Figure 11. Preparation of IL layers with adjustable thickness on monolithic surfaces.

This way, injection was possible at room temperature. After filling the monolith with a solution of IL in CH_2Cl_2, the column can simply be subjected to vacuum in order to remove the solvent. In detail, the volume of the steel-column used was 1.66 mL and the interstitial porosity ε_z of the monolith was found to be 80%, what corresponds to a volume of 1.25 mL. To adjust the thickness of the ionic liquid layer, a variable amount of $[BDMIM^+][BF_4^-]$ was dissolved in dichloromethane (1.25 mL). The solution was then inserted into the monolith, afterwards the solvent was removed *in vacuo*. Flushing the monolith with heptane was now possible at room temperature. To verify whether the IL was distributed all over the length of the support, the monolith was removed out of the jacket, cut into pieces of equal weight and extracted with $CDCl_3$. NMR measurements revealed a homogeneous distribution of the IL over the entire monolith. Using this method, the amount of IL could be reduced by more than 90%.

2.2.2.3 Influence of Immobilized Ionic Liquid on Flow-through Performance

Now, that an adequate method for preparing IL layers with adjustable thickness on monolithic surfaces was found, the question arised as to which extent the thickness of the ionic liquid layer would influence the flow-through performance of the support material under reaction conditions. In addition, it was to be defined up to which flow rate the IL remains immobilized, before being detached due to high shear forces. For this purpose, ionic liquid layers with different thickness were prepared on the surface

of the support material. Comparable to the procedure described above, heptane was flushed through the monolith at 45°C and at 100°C thereby applying different flow-rates. The resulting back-pressures (Figure 12) were recorded and any possible detachment of the ionic liquid was determined by NMR-analysis. At different flow rates, the time required for flushing a volume of 2 mL heptane through the support was measured. Each measurement was performed three times and the average values are summarized in Table 3.
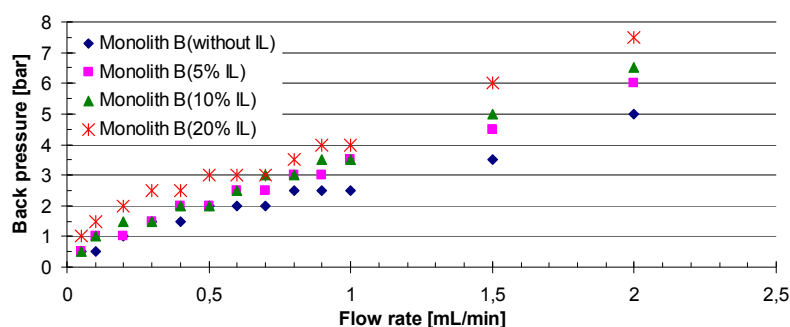

Figure 12a. 45°C.
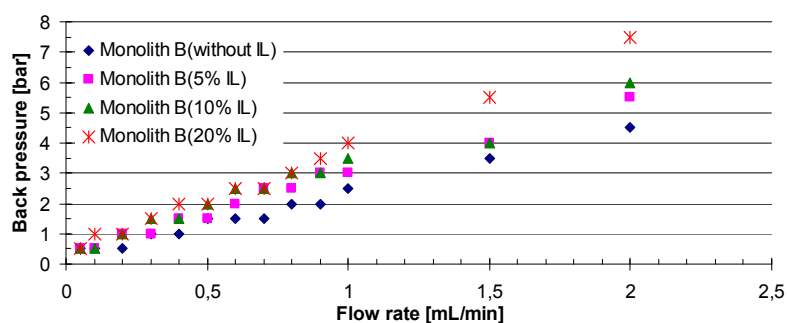
Figure 12b. 100°C.

Figure 12. Resulting back pressures when flushing heptane through monolith **B**, loaded with variable amounts of [BDMIM$^+$][BF$_4^-$] (given in vol.-% of the void volume determined by ISEC), at different temperatures.

Table 3. Time required for flushing 2 mL of heptane through monolith **B**, loaded with variable amounts of [BDMIM$^+$][BF$_4$$^-$] (given in vol.-% of the void volume determined by ISEC), at 45°C and at 100°C using different flow-rates.

Flow rate [mL/min]	5% of void-volume (~0.06 mL) filled with IL (~80 mg)			20% of void-volume (~0.12 mL) filled with IL (~320 mg)		
	Time [min]	Detachment of IL[a]		Time [min]	Detachment of IL	
		45°C	100°C		45°C	100°C
0.05	18.83	-	-	19.20	-	-
0.1	10.66	-	-	9.72	-	-
0.2	4.50	-	-	4.57	-	-
0.3	3.83	-	-	3.50	-	-
0.4	2.66	-	-	2.58	-	-
0.5	2.16	-	-	1.88	-	-
1.0	1.23	-	-	1.02	-	+
2	0.78	-	-	0.67	-	+

[a] -: no detachment observed; +: detachment observed (determined by NMR).

For IL-layers filling up to 20% of the monoliths' void volume, at both temperatures (45°C and 100°C), no removal of ionic liquid was observed at flow-rates up to 1 mL/min and the resulting back pressures increased only slightly compared to the unfunctionalized support. Merely at high temperature, the stationary phase detached to some degree when flow-rates >1mL/min were applied to monoliths with an IL-loading of 20%. Fortunately, the immobilized stationary phase does not considerably damp down the flow-through characteristics of the monolith. As it is shown in Table 3, the time required for transporting a certain volume of mobile phase through the support, is nearly halved when doubling the flow rate.

2.2.2.4 Removal of the IL-Layer – Recycling of the Support Material

Without any doubt, metathesis catalysts are not immortal, every catalyst will lose its activity after a certain period of time. Both 1st and 2nd generation *Grubbs* type catalysts undergo thermal decomposition as well as decomposition in the presence of functional groups[29-31]. Particularly those functionalities that coordinate strongly to the Ru center, e.g., DMSO, CH_3CN, CH_3OH are inapplicable[30, 32, 33]. The thermal decomposition of ruthenium catalysts was studied by examining the decomposition of the ruthenium methylidenes $[RuCl_2(PCy_3)_2=CH_2]$ and $[RuCl_2(PCy_3)(IMesH_2)=CH_2]$ which both decompose in a unimolecular process[31]. Kinetics data for the methylidene decomposition reveal a first order reaction resulting in the formation of a mixture of ruthenium species. No ethylene was observed as would be the expected product of methylidene dimerization. In addition it was found that the rate of decomposition is related to the rate of initiation. Most probably, all organometallic compounds and ionic by-products, generated during the decomposition of an ionic metathesis catalyst, will be retained within the highly polar IL-phase. For being able to further conduct metathesis reactions, it is required to replace the decomposed catalyst by some fresh one. In case of the concept proposed in this work, the regeneration of the support and its recharging can simply be accomplished by flushing with a polar solvent, e.g., methanol, in order to completely remove the ionic liquid. It was shown by means of ^1H NMR measurements, that no residual IL remained within the support after flushing with methanol. Afterwards, a fresh IL-layer could be deposited, which again withstood high flow rates at elevated temperatures.

2.2.3 Distribution Coefficients

At this point, the ionic liquid $[BDMIM^+][BF_4^-]$ has been defined to represent the stationary phase in the supported biphasic liquid-liquid system and heptane was selected as the appropriate mobile phase (Chapter 2.2.2.1).

An important point is to define up to which percentage a particular reactant dissolves in both phases, since this feature infuences the efficiency of the catalyzed reaction. Therefore, for the substrates 1,7-octadiene, diethyl diallyl malonate (DEDAM) and *N,N*-diallyl trifluoroacetamide (DAFA) the distribution coefficients $K_{solvent/IL}$ were determined for the solvent system heptane/$[BDMIM^+][BF_4^-]$ at 40 and 80°C,

respectively. The distribution coefficient for a particular substrate in a biphasic system is defined as the ratio of the concentration of the compound in both phases, herein:

$$K_{heptane/IL} = \frac{c\,(substrate\,in\,heptane)}{c\,(substrate\,in\,IL)}$$. In addition, for DAFA, the distribution coefficient

$$K_{dodecane/IL} = \frac{c\,(substrate\,in\,dodecane)}{c\,(substrate\,in\,IL)}$$ was determined for dodecane/[BDMIM$^+$][BF$_4^-$]

at 40 and 80°C as well. For the quite unpolar substrates 1,7-octadiene and methyl oleate, the solubility of these compounds in [BDMIM$^+$][BF$_4^-$] was quantified by determining the distribution coefficients $K_{substrate/IL}$ using the neat reactants. The distribution coefficients for different solvent systems at different temperatures are given in Table 4.

Table 4. Distribution coefficients $K_{solvent/IL}$ of 1,7-octadiene (1,7-OD), DEDAM and DAFA in [BDMIM$^+$][BF$_4^-$]/heptane and [BDMIM$^+$][BF$_4^-$]/dodecane as well as $K_{substrate/IL}$ of 1,7-OD and methyl oleate in substrate/[BDMIM$^+$][BF$_4^-$] at different temperatures.

Substrate	T/°C	Solvent	$K_{solvent/IL}$[*]
1,7-OD	40	heptane	9
1,7-OD	80	heptane	10
1,7-OD	40	---	14
1,7-OD	80	---	13
DEDAM	40	heptane	1.2
DEDAM	80	heptane	0.8
DAFA	40	heptane	0.2
DAFA	80	heptane	0.2
DAFA	40	dodecane	0.1
DAFA	80	dodecane	0.2
methyl oleate	40	---	39
methyl oleate	80	---	34

[*] Values are the average of four independent measurements for each substrate.

Conditions for $K_{solvent/IL}$: 200 mg IL, 200 mg heptane, 50 mg substrate. For $K_{substrate/IL}$:

200 mg IL, 200 mg substrate, 50 mg dodecane. Values were determined *via* GC-MS analysis. Dodecane served as standard for the measurements in heptane and dicyclopentadiene in case when dodecane was used as solvent itself.

All biphasic systems were stirred with 600 rpm at the indicated temperature for 1 h and distribution ratios then were determined by means of GC measurements (Chapter 6.2, Experimental section). 1,7-Octadiene dissolves tenfold better in the unpolar mobile phase heptane than in the ionic liquid [BDMIM$^+$][BF$_4^-$]. In view of the low polarity of this particular substrate, this finding is not surprising though illustrating that merely a small fraction will be available for reacting with an ionic catalyst immobilized in the ionic liquid phase. This observation not necessarily implies some disqualifying consequences, since the experimental setup introduced above allows for cycling the reaction mixture trough the support as often as desired. Quite in contrast, the low polarity of the substrate will suppress dissolution of the stationary phase and allows for using neat 1,7-octadiene in the reaction system. The polarity of methyl oleate is even lower than the one of 1,7-octadiene and a distribution coefficient $K_{substrate/IL}$ of 39 at 40°C implies that a rather limited amount of substrate is present in the stationary IL phase at this temperature. Showing a value of ~ 1 for $K_{solvent/IL}$, diethyl diallyl malonate (DEDAM) is equally good soluble in both phases at 40°C as well as at 80°C. For *N,N*-diallyl trifluoroacetamide (DAFA) the distribution coefficient $K_{solvent/IL}$ was determined to be 0.2, expressing a fivefold enhanced tendency to dissolve in [BDMIM$^+$][BF$_4^-$] rather than in heptane or dodecane. Consequently, in order to reduce the polarity of the reaction mixture and to avoid dissolving of the staionary phase, both DEDAM and DAFA may be subjected to the supported catalyst only when dissolved in an unpolar mobil phase such as heptane. For all substrates examined, a raise in temperature from 40°C to 80°C did not significantly alter the distribution coefficients and consequently, reaction mixtures possessing the same composition may be used at different temperatures within this range.

2.3 Conclusions

A qualified monolithic support material was designed for the immobilization of ionic liquid phases and for the subsequent use as a support material in continuous catalysis under biphasic liquid-liquid conditions. Therefore, monoliths possessing a large fraction of macropores were synthesized. Besides a noticeable void volume of 80% the support material showed a considerably high shape persistence. This was accomplished by using NBE as monomer and the crosslinker (NBE-CH$_2$O)$_3$ SiCH$_3$, both were used as 15 wt.-% fractions of the total polymerization mixture. The monolithic surface was functionalized by post-synthetical grafting of the ionic monomer [NBE-CH$_2$-NMe$_3^+$][BF$_4^-$] (**M2**). The ionic liquid [BDMIM$^+$][BF$_4^-$] was found to exhibit good qualities to serve as the stationary phase, when heptane was chosen as the mobile phase. A technique was developed, which allowed for depositing IL-layers with adjustable thickness on the support materials' surface. Due to capillary actions and ionic interactions, these IL-layers were found to remain immobilized, even when applying high flow rates of the mobile phase at elevated temperatures. A method for the facile recycling of the monolithic support by flushing with, e.g., methanol, was developed and represents an additional advantage. The simple recharging process with fresh catalyst dissolved in the ionic liquid allows restoring the catalytic system within a rather short period of time. The hereby introduced support material, in combination with a suited ionic catalyst, represents the *SILP*-catalyst for use in continuous metathesis. In the following chapters its adaptability will be proven.

2.4 References

[1]   M. R. Buchmeiser, *Polymer* **2007**, *48*, 2187.

[2]   E. B. Anderson, M. R. Buchmeiser, *ChemCatChem* **2012**, *4*, 30.

[3]   M. R. Buchmeiser, *Macromol. Rapid Commun.* **2001**, *22*, 1081.

[4]   M. R. Buchmeiser, *Chem. Rev.* **2009**, *109*, 303.

[5]   M. R. Buchmeiser (Ed.), *Polymeric Materials in Organic Synthesis and Catalysis*, Wiley-VCH, Weinheim (Germany), **2003**.

[6]   P. Wasserscheid, T. Welton (Eds.), *Ionic Liquids in Synthesis, Vol. 2: Transition Metal Catalysis in Ionic Liquids, 2nd ed.*, Wiley-VCH, Weinheim (Germany), **2007**.

[7]   F. Svec, J. M. J. Frechet, *Science* **1996**, *273*, 205.

[8]   F. Sinner, M. R. Buchmeiser, *Angew. Chem.* **2000**, *112*, 1491.

[9]   F. Sinner, M. R. Buchmeiser, *Macromolecules* **2000**, *33*, 5777.

[10]   F. Svec, *J. Chromatogr. A* **2010**, *1217*, 902.

[11]   K. Matyjaszewski, *Macromolecules* **1993**, *26*, 1787.

[12]   C. W. Bielawski, R. H. Grubbs, *Prog. Polym. Sci.* **2007**, *32*, 1.

[13]   M. Szwarc, *Nature* **1956**, *178*, 1168.

[14]   J. Scholz, S. Loekman, N. Szesni, W. Hierienger, A. Goerlinger, M. Haumann, P. Wasserscheid, *Adv. Synth. Catal.* **2011**, *353*, 2701.

[15]   P. Sledz, K. Grela, *Chem. Soc. Rev.* **2008**, *37*, 2433.

[16]   H. Olivier-Bourbigou, L. Magna, D. Morvan, *Applied Catalysis A: General* **2010**, *373*, 1.

[17]   V. I. Parvulescu, C. Hardacre, *Chem. Rev.* **2007**, *107*, 2615.

[18]   Y. S. Vygodskii, A. S. Shaplov, E. I. Lozinskaya, O. A. Filippov, E. A. Shubina, R. Bandari, M. R. Buchmeiser, *Macromolecules* **2006**, *39*, 7821.

[19]   T. Welton, *Chem. Rev.* **1999**, *99*, 2071.

[20]   P. Wasserscheid, *Chemie unserer Zeit* **2003**, *37*, 52.

[21]   S. H. Lubbad, M. R. Buchmeiser, *Macromol. Rapid. Commun* **2002**, *27*, 617.

[22]   S. H. Lubbad, B. Mayr, M. Mayr, M. R. Buchmeiser, *Macromol. Symp.* **2004**, *210*, 1.

[23]   I. Halasz, Martin, K., *Angew. Chem.* **1978**, *90*, 954.

[24]   Z. Grubisic, P. Rempp, H. Benoit, *J. Polym. Sci.: Polym. Lett.* **1976**, *5*, 753.

[25]   S. H. Lubbad, M. R. Buchmeiser, *Macromol. Rapid Commun.* **2003**, *24*, 580.

[26]   P. A. Thomas, B. B. Marvey, E. E. Ebenso, *Int. J. Mol. Sci.* **2011**, *12*, 3989.

[27]   U.S. Department of Health and Human Services, *Toxicological profile for n-hexane*, Atlanta, **1999**.

[28]   G. J. Hathaway, N. H. Proctor, J. P. Hughes, M. Fischmann, *Proctor and Hughes' chemical hazards of the workplace*, Wiley-VCH, Weinheim, **2004**.

[29]   R. H. Grubbs (Ed.), *Handbook of Metathesis*, Wiley-VCH, Weinheim (Germany), **2003**.

[30]   T. M. Trnka, *Ph.D. thesis,* California Institute of Technology, **2003**.

[31]   M. Ulman, R. H. Grubbs, *J. Org. Chem.* **1999**, *64*, 7202.

[32]   S. T. Nguyen, R. H. Grubbs, J. W. Ziller, *J. Am. Chem. Soc.* **1993**, *115*, 9858.

[33]   S. T. Nguyen, L. K. Johnson, R. H. Grubbs, J. W. Ziller, *J. Am. Chem. Soc.* **1994**, *114*, 3974.

3. Continuous Biphasic Metathesis Using Monolith-Supported Ionic Liquids

loaded monolithic support $Y^+ X^- = [BDMIM^+][BF_4^-]$
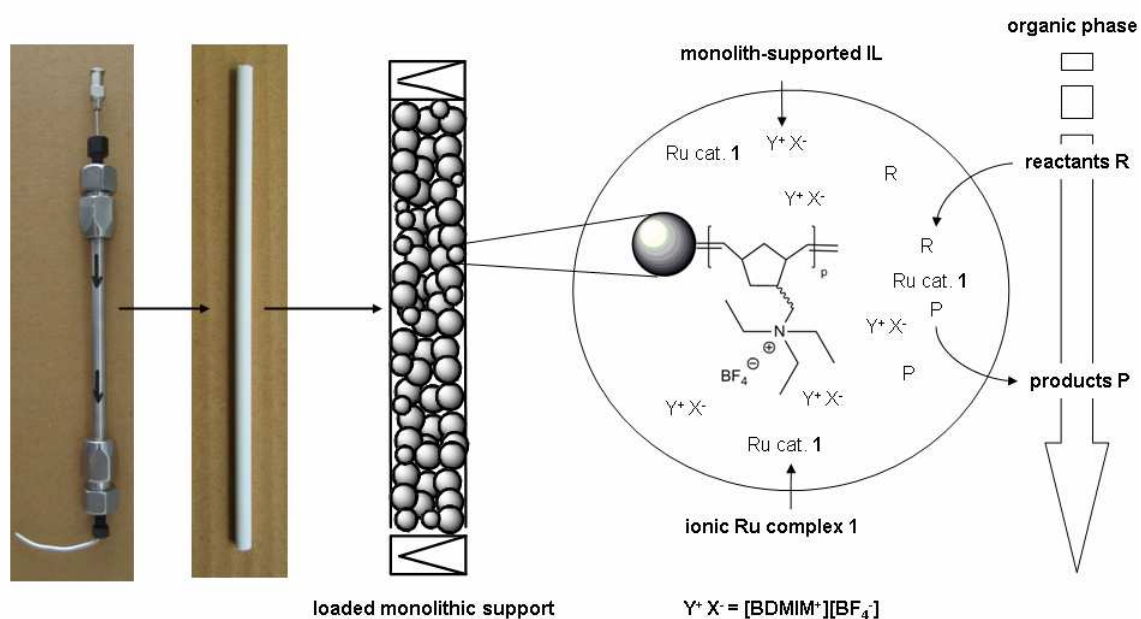
The material covered in this chapter has appeared in:

B. Autenrieth, W. Frey, M. R. Buchmeiser, *Chem. Eur. J.*, **2012**, *18*, 14069 – 14078.

3.1 Introduction

In this chapter, the efficiency of the concept for conducting continuous metathesis reactions under supported liquid-liquid conditions has been verified for the first time. Almost 100 years after the discovery of ionic liquids (ILs) [1, 2] by *P. Walden*[3], the interest in this class of compounds has dramatically increased and within comparably short time ILs made their way from a physico-chemical curiosity into numerous chemical, technical and industrial applications,[4] for example, as solvents for catalytic reactions[5-25] (including asymmetric ones[26]) and for polymerizations,[27-41] as coatings and mobile phases in liquid chromatography and electromigration techniques,[42-46] as low-vapor pressure solvents for head-space GC analysis,[47] as coatings for GC columns,[48] as well as electrolytes in fuel[49] and solar cells.[50] In addition, applications in biocatalysis[51-53] have to be mentioned. The first reports on the use of molten salts used as supported ionic liquid phases (SILPs) for use in heterogeneous catalysis were published in 1988 by *R. Datta et al.*[54] as well as by *D. P. Eyman et al.*.[55] Following this concept, *P. Wasserscheid* et al., *C. P. Mehnert et al.*, *J. Dupont et al.* and others have published a series of applications of SILPs since then.[15, 17, 19-25, 56-60] Using simple adsorption and capillary forces, they immobilized various ILs on silica- and zeolithe-type supports using capillary forces and used them as supported solvents for catalytic reactions, e.g., for hydroformylations, hydrogenations, methanol carbonylation but also for enzyme-triggered biocatalysis. Recently, *J. Le Bideau et al.* confirmed by ^{1}H-MAS-NMR experiments that the dynamics of ILs immobilized within the confines of siliceous materials experienced only a minor slow down.[61] In fact, the confinement preserved the IL's properties while *reducing* their crystallization temperature compared to the pristine ILs. Thus, supported ILs can in fact be compared to unsupported ones in terms of diffusion coefficients, which in turn guarantees for fast reactions kinetics of the catalytic reactions within monolith-supported ILs.

More recently, *P. Wasserscheid et al.* reported on metathesis reactions in supported ILs using gaseous reactants as the second (transport) phase[62]. Such an approach allows for using "standard" metathesis catalysts within the IL. However, both the metathesis of higher (functional) olefins and metathesis-based polymerizations require the use of a second *liquid* transport phase that is immiscible with the IL. In order to prevent catalyst leaching into this second phase, tailored catalysts need to

be developed that *selectively* dissolve in the IL. Equally important, in order to allow for continuous reaction conditions, any substrate and product must have sufficient solubility in both phases in order to allow for substantial turn-over numbers (TONs) and to prevent product accumulation within the IL. Herein, a novel dicationic metathesis catalyst dissolved within a polymeric monolith-supported IL phase that allows for the first continuous metathesis reactions using two liquid phases is reported. Scheme 5 illustrates the fundamental concept. Beside the primary objective to gain catalyst-free products, this concept enables continuous product formation, simply by cycling liquid reactants or solutions thereof through the support. Most important, the entire concept is not limited to gaseous substrates such as ethene, propene or butenes. Consequently, no high pressures need to be applied. Finally, the possibility of recycling of the monolithic support has been addressed.
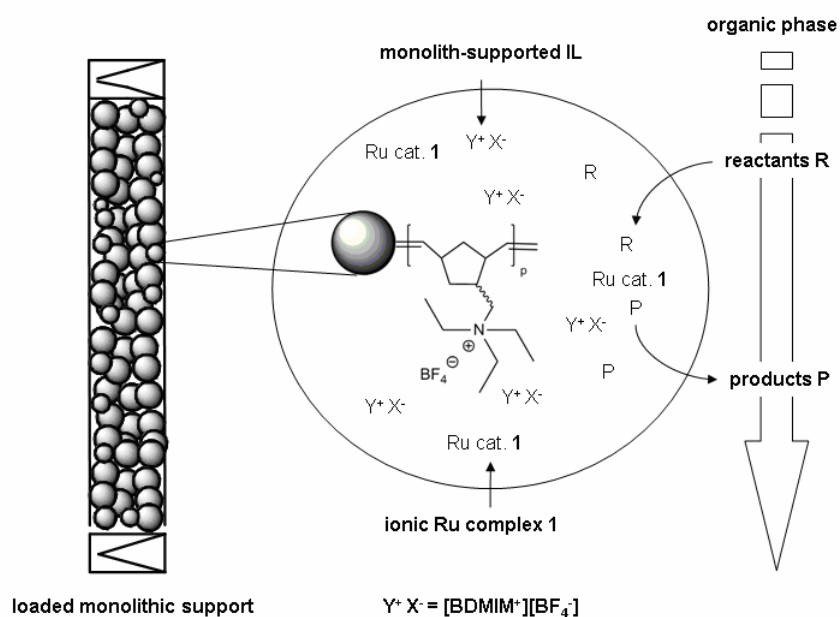

Scheme 5. Continuous metathesis under biphasic conditions by using monolith-supported ILs. $Y^+ X^- = [BDMIM^+][BF_4^-]$.

3.2 Results and Discussion

3.2.1 Synthesis and Structure determination of $[Ru(DMF)_3(IMesH_2)(=CH-2-(2-PrO)-C_6H_4)^{2+}][(BF_4^-)_2]$ (**1**)

As outlined above, the primary objective was to create a supported metathesis catalyst based on SILP-technology that allows for running metathesis reactions under biphasic conditions *using two immiscible liquid phases*. For that purpose, an ionic, Ru-alkylidene complex for metathesis reactions in ionic liquids had to be created. Since pseudohalide-derivatives of *Grubbs-* and *Grubbs-Hoveyda* (GH) catalysts are known to possess high activity resulting from the high polarization of the Ru-alkylidene moiety,[63-71] such electron-deficient cationic catalysts may well be expected to display high activity, too. Such an ionic metathesis catalyst would *selectively* dissolve in the IL but not in the second liquid transport phase, e.g., heptane. For this reason, the ionic catalyst $[Ru(DMF)_3(IMesH_2)(=CH-2-(2-PrO)-C_6H_4)^{2+}][(BF_4^-)_2]$ (**1**, $IMesH_2$=1,3-dimesitylimidazolin-2-ylidene) was prepared in 95% isolated yield by adding three equivalents of *N,N*-dimethylformamide (DMF) and two equivalents of $AgBF_4$ to the 2nd-generation *Grubbs-Hoveyda* (**GH2**) catalyst $[RuCl_2(IMesH_2)(=CH-2-(2-PrO)-C_6H_4)]$ (Scheme 6).
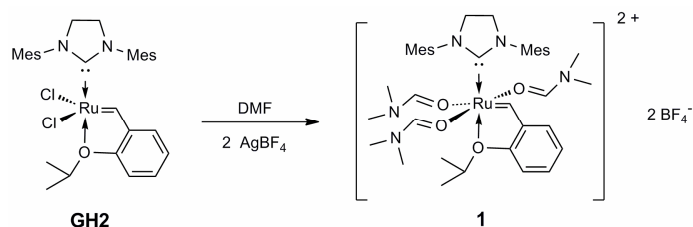
Scheme 6. Synthesis of the dicationic Ru complex **1**.

Complex **1** crystallizes in the monoclinic space group *P2₁/n*, *a* = 2192.6(2) pm, *b* = 1756.0(6) pm, *c* = 2327.4(2) pm, *β* = 92.485°, *Z* = 8 (Figure 13, CCDC-900128 contains the supplementary crystallographic data for complex **1** and can be obtained from "The Cambridge Crystallographic Data Centre" *via* www.ccdc.cam.ac.uk/data_request/cif.). Selected bond lengths and angles are given in Table 5.
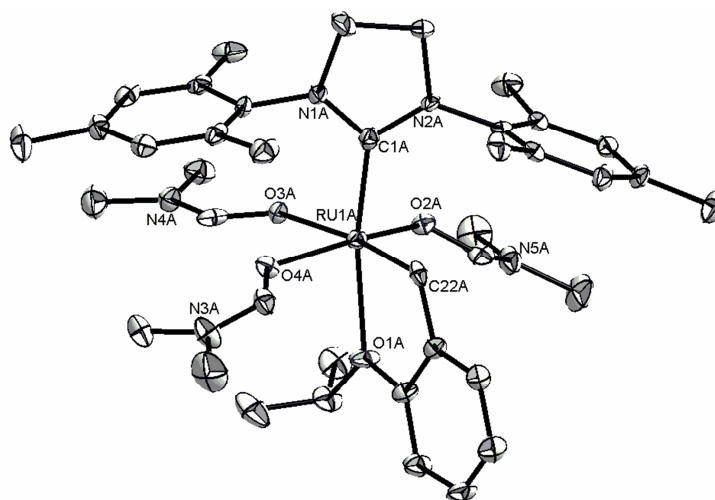
Figure 13. X-ray structure of **1**. Counteranions (BF_4^-) and hydrogen atoms have been omitted for clarity. Ellipsoids are given at the 50% probability level.

Table 5. Selected bond lengths [pm] and angles [°] for **1**.

Ru1A-C22A	185.0(4)
Ru1A-C1A	201.1(4)
Ru1A-O1A	232.5(3)
Ru1A-O2A	203.7(3)
Ru1A-O3A	222.5(3)
Ru1A-O4A	205.6(3)
C22A-Ru1A-C1A	93.30(16)
C22A-Ru1A-O1A	77.50(13)
C22A-Ru1A-O2A	101.39(13)
C22A-Ru1A-O4A	94.12(13)
C22A-Ru1A-O3A	172.22(14)
C1A-Ru1A-O2A	91.70(14)
C1A-Ru1A-O4A	100.64(14)
C1A-Ru1A-O3A	94.27(12)
C1A-Ru1A-O1A	169.26(13)
O2A-Ru1A-O4A	159.59(10)
O2A-Ru1A-O3A	80.22(10)
O2A-Ru1A-O1A	84.81(10)
O3A-Ru1A-O1A	95.15(90)
O4A-Ru1A-O3A	82.69(10)
O4A-Ru1A-O1A	85.70(10)

Complex **1** is a d^6 low-spin complex having a distorted octahedral ligand sphere with the NHC- and the 2-PrO-ligand in the apical positions. The Ru(1A)-O(1A) distance in **1** is significantly longer than the one in the parent **GH2**-complex (232.5(3) pm *vs.* 226.13 pm[72]). The Ru(1A)-O(2A) and Ru(1A)-O(4A) distances of the two DMF ligands located trans to each other are virtually identical (203.7(3) *vs.* 205.6(3) pm). In contrast, the Ru(1A)-O(3A) distance of the DMF ligand located *trans* to the benzylidene ligand is significantly longer (Ru(1A)-O(3A) = 222.5(3) pm). Interestingly, the Ru(1A)-C(1A) distance is also longer than in the parent Grubbs-Hoveyda catalyst (201.1(4) *vs.* 198.1(5) pm)[72] while the Ru-alkylidene bond is somewhat shorter in **1** compared to the parent complex (182.5(5) *vs.* 185.0(4) pm)[72]. While some monocationic Ru-alkylidenes have been reported,[73-75] it is worth mentioning that complex **1** is one of the very rare examples of a dicationic Ru(II)-alkylidene[76] and, to the best of knowledge, the first example of a metathetically highly active one.

3.2.2 Metathesis Reactions in Organic Solvents (CH$_2$Cl$_2$, C$_2$H$_4$Cl$_2$, Toluene)

Before the attention was turned to reactions in ionic liquids, the general reactivity of **1** in various metathesis reactions was investigated. Ring-closing metathesis (RCM) reactions in CH$_2$Cl$_2$ at T=40°C with substrates that contain coordinating, i.e. oxygen- or nitrogen-containing groups, i.e. diethyl diallylmalonate (DEDAM), diethyl dimethallyl malonate, *tert*-butyl-*N,N*-diallyl carbamate, diallyldiphenylsilane or *N,N*-diallylacetamide (Table 6) resulted in low TONs (≤50) and conversion (≤5%). However, with the electron-poor substrate *N,N*-diallyl trifluoroacetamide (DAFA), high TONs up to 3500 were obtained, exceeding by far those obtained with the parent GH-catalyst under identical conditions (TON=730).

**Table 6.** Selected substrates for metathesis reactions in organic solvents promoted by catalyst **1**.

Substrate	1 [mol%]	Solvent	T [°C]	t	TON
DEDAM	0.05	CH_2Cl_2	40	1 h	50
		$C_2H_4Cl_2$	80	1 h	560
		toluene	100	15 min	1300
tert-butyl-*N,N*-diallyl carbamate	0.1	CH_2Cl_2	40	1 h	10
		$C_2H_4Cl_2$	80	0.5 h	40
		toluene	100	0.5 h	320
1,7-octadiene	0.05	CH_2Cl_2	40	1 h	100
		$C_2H_4Cl_2$	80	15 min	500
		toluene	100	15 min	1200
DAFA	0.02	CH_2Cl_2	40	15 min	3500
		$C_2H_4Cl_2$	80	5 min	3500
		toluene	100	2 min	3700
N,N-diallylacetamide	0.05	CH_2Cl_2	40	4 h	10
		$C_2H_4Cl_2$	80	4 h	30
		toluene	100	1 h	240
diallyldiphenylsilane	0.2	CH_2Cl_2	40	4 h	5
		toluene	100	4 h	130
diethyl di(methallyl)malonate	1.4	CH_2Cl_2	40	12 h	0
		toluene	100	0.5 h	6
methyl oleate	0.05	CH_2Cl_2	40	12 h	100
		$C_2H_4Cl_2$	80	4 h	530
		toluene	100	4 h	780

Clearly, even weakly coordinating groups such as esters and amides coordinate to the dicationic center, thereby impeding the coordination of the alkene. This is further illustrated by comparing the RCM results of DAFA to those of the analogous, non-fluorinated derivative, i.e. *N,N*-diallylacetamide, obtained at T=40°C. In these reactions, TONs of 3500 *vs.* 10 were observed (Table 6). To promote the dissociation of any coordinating moieties from the cationic Ru-center, all reactions were again run at elevated temperature. This way, the activity of **1** increased tremendously for all substrates (Table 6). Thus, in case reactions were run in toluene at 100°C, TONs up to 1300 and 1200, respectively, were obtained in the RCM reactions of diethyl diallyl malonate and 1,7-octadiene. These values are worth to be highlighted since **1**

possesses a poor solubility in toluene and, consequently, reactions are mostly heterogeneous. Likewise, in case of *N,N*-diallylacetamide, *tert*-butyl-*N,N*-diallyl carbamate and diallyldiphenylsilane, an increase in temperature resulted in an increasing TON reaching values between 130 and 320.

The reaction temperature has also a great influence on the selectivity of the RCM of 1,7-octadiene. When conducted at T=40°C, the formation of purple, conjugated isomerization products was observed and consequently the yield in cyclohexene was low. However, at T=80°C, no isomerization products were observed and cyclohexene was the only product detected by means of GC-MS and NMR. This suggests the absence of any active Ru-hydride species at elevated temperature. Since DAFA does not coordinate to the Ru-center *via* the amide-bond, the high TON observed at T=40°C could not be significantly increased, however the reaction rate increased. While at T=40°C a TON of 3500 was achieved within 15 min, a TON of 3700 was accomplished at T=100°C in less than 2 minutes. Notably, the reactivity *vs.* diethyl di(methallyl)malonate remained low under all conditions.

Reaction temperature also greatly influences the self-metathesis of methyl oleate (Scheme 7). At T=40°C, the reaction proceeds slowly with low yields (~ 5% of primary metathesis products, TON=100). Running the reaction at T=100°C resulted in TONs of 780. Moreover, again only the desired *primary* metathesis products were obtained (Scheme 7 and Figure S1, Appendix), again suggesting the absence of (stable) Ru-hydrides. In contrast, predominantly alkenes with different chain lengths, resulting from secondary cross-metathesis reactions were observed with the **GH2**-catalyst (Figure S2, Appendix).
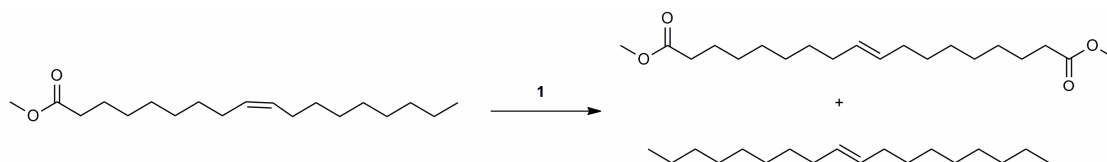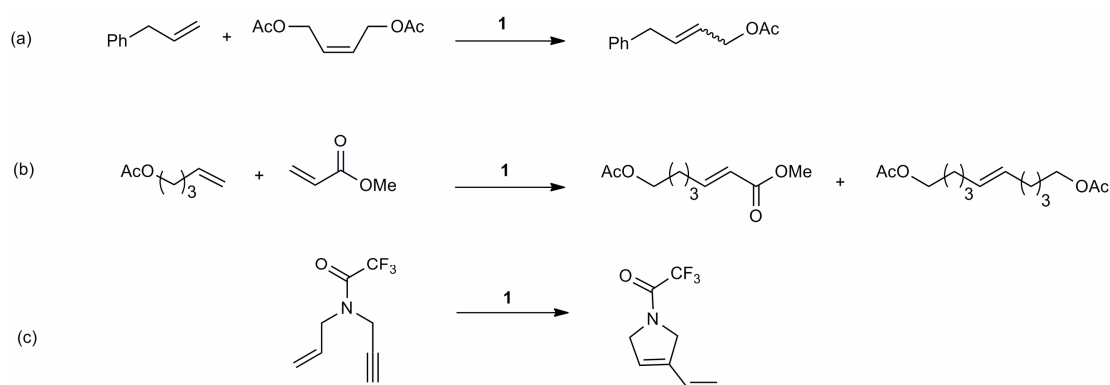

Scheme 7. Self-metathesis of methyl oleate catalyzed by **1**.

3.2.3 Cross-Metathesis (CM) and Ene-yne Metathesis Reactions

In the CM reaction between allylbenzene and *cis*-1,4-acetoxy-2-butene (Scheme 8a) no conversion was observed at T=40°C. However, at T=100°C, product formation was quantitative within 1 h using a catalyst loading of 0.2 mol-% in toluene. The

inactivity of **1** at 40°C was also noticed for the CM reaction between 5-hexenyl acetate and methyl acrylate (Scheme 8b). In turn, at 100°C, 70% conversion was achieved within 1 h using a catalyst loading of 0.2 mol-%. Finally, **1** was applied to the ene-yne metathesis of *N*-allyl-*N*-propargyl trifluoroacetamide (Scheme 8c). Using a catalyst loading of 0.5 mol-% a TON of 60 was obtained in CH_2Cl_2 at 35°C. Interestingly, at elevated temperature, merely red colored, polymeric products formed *via* 1-alkyne polymerization were obtained as evidenced by the absence of any alkyne groups in the IR (Figure S17, Appendix).

Scheme 8. CM reactions between allylbenzene and cis-1,4-acetoxy-2-butene (a) and between 5-hexenyl acetate and methyl acrylate (b). Ene-yne metathesis of N-allyl-N-propargyl trifluoroacetamide (c).

3.2.4 Metathesis Reactions Under Biphasic Conditions (Organic Solvent/ Ionic Liquid)

The RCM of DAFA, DEDAM and 1,7-octadiene as well as the self-metathesis of methyl oleate were carried out under biphasic conditions using [BDMIM$^+$][BF$_4^-$] as IL phase and either neat reactants or heptane as the second liquid phase (Table 7). Generally, the choice of the IL turned out to be a crucial feature concerning ruthenium-alkylidene promoted metathesis reactions [34, 77, 78]. The anion in the ionic liquid [BDMIM$^+$][BF$_4^-$] is non-coordinating and additionally identical to the counter ion in complex **1**. This prevents ligand scrambling, an often observed feature of Ru-alkylidenes in ionic solvents with different counter ion[34]. Furthermore, possessing a melting point of 37°C, [BDMIM$^+$][BF$_4^-$] is liquid at a reaction temperature of 40°C. However, the most important property of [BDMIM$^+$][BF$_4^-$] is its very poor miscibility with common non-polar organic solvents such as toluene, diethyl ether or heptane.

However, all substrates investigated displayed sufficient solubility in the IL as illustrated by their distribution coefficients $K_{heptane/IL}$ (Table 4, Chapter 2), which were 0.2 (DAFA), 1.2 (DEDAM) and 9 (1,7-octadiene), respectively. Despite the comparably small amount of IL and the large amount of polar substrate, which both favor transfer of the catalyst into the non-polar phase, a low catalyst leaching of ≤0.1% into the product phase was observed for most reactions. For comparison, leaching of the **GH2**-catalyst under otherwise identical conditions into the heptane phase was up to 25 times higher. Running the reaction in the IL, the TONs for the RCM of DAFA could be further increased up to 3600 by increasing the temperature, though on the expense of a slightly higher metal leaching (2.4%, 4.8 ppm Ru). In the RCM of DEDAM, TONs up to 1600 were obtained, again exceeding those observed in an organic solvent (Table 6). Due to the low polarity of the 1,7-octadiene and its immiscibility with the IL, its RCM was performed without the use of another liquid transport phase. There, an increase in reaction temperature from 80-100°C led to an increase in the TON from 800 to 1600 without noticeable affecting catalyst leaching. As observed in organic solvents, only the formation of cyclohexene and no isomerization products were observed. Admittedly, Ru-leaching was also low with the parent **GH2**-catalyst giving TONs up to 2400. However, with this catalyst, the IL phase was purple in color suggesting the formation of conjugated isomerization products. In the self-metathesis of methyl oleate (Scheme 7) catalyzed by **1**, an increase in temperature resulted in an increase in TONs from 95 to 1000. Reaction monitoring *via* GC-MS revealed the selective formation of the two desired cross-metathesis products as well as isomerization of the *Z*-double bond in the substrate molecule (Figure S1, Appendix). This isomerization reaction is the predominant reaction at low temperature, forming a less reactive *E*-double bond that gives raise to low TONs. At higher temperature, self-metathesis predominates. Despite high TONs, the use of the **GH2**-catalyst yielded a multitude of products (more than 30!) *via* subsequent isomerization- and secondary metathesis processes (see gas-chromatogram in Figure S2, Appendix).

Table 7. Metathesis reactions under biphasic conditions ([BDMIM$^+$][BF$_4^-$])/heptane).

Substrate	Catalyst ([mol %])	T [°C]	TON[a]	Ru leaching [%][b]	Ru contamination [ppm]
DAFA[c]	**1** (0.02)	40	3300	0.09	0.2
		80	3600	2.4	4.8
DAFA	**GH2** (0.02)	40	600	3.1	6.2
		80	1300	8.6	17.2
DEDAM[d]	**1** (0.02)	80	1400	0.02	0.04
		100	1650	0.03	0.06
DEDAM	**GH2** (0.02)	80	1500	0.03	0.06
		100	1900	0.2	0.4
1,7-octadiene[e]	**1** (0.02)	80	810	0.1	0.2
		100	1660	0.1	0.2
1,7-octadiene	**GH2** (0.02)	80	2300	0.1	0.2
		100	2410	0.5	1.0
methyl oleate[f]	**1** (0.05)	40	95	0.07	0.4
		80	800	0.11	0.6
		110	1000	0.6	3.0
methyl oleate	**GH2** (0.05)	40	2000	0.2	1.0
		80	2000	0.5	2.5
		110	2000	1.4	7.0

[a] Determined by GC-MS after 12 h. [b] % of initial Ru (catalyst) loading. [c] Heptane as second liquid phase; IL (0.2 g), heptane (2.0 g), DAFA (0.8 g). [d] Heptane as second liquid phase; IL (0.2 g), heptane (3.0 g), DEDAM (1.25 g). [e] Neat; IL (0.04 g), 1,7-octadiene (0.4 g). [f] Neat; IL (0.05 g), methyl oleate (0.5 g).

3.2.5 Preparation and Characterization of Monolithic Supports

Polymeric monoliths represent versatile supports for heterogeneous catalysis. They allow for high linear flow rates up to 20 mm/s at low counter pressure (<2 MPa) and guarantee for a fast mass transfer between the transport phase and the immobilized catalysts.[79] Monoliths were prepared by copolymerization of norborn-2-ene (NBE) with the cross-linker (CL) tris(norborn-2-enylmethylenoxy)methylsilane ((NBE-CH$_2$O)$_3$ SiCH$_3$) in the presence of the two porogenic solvents 2-propanol and toluene (Scheme 9). [RuCl$_2$(PCy$_3$)$_2$(CHC$_6$H$_5$)] (**G1**, Cy=cylohexyl) was chosen as initiator,

since it possesses a balanced activity for both NBE and the CL[80, 81]. Next, charged groups had to be introduced to the monoliths' inner surface. These should help retaining the ILs that are otherwise only physically adsorbed to the monoliths' surface. Taking advantage of the "*living*" character of the ring-opening metathesis polymerization- (ROMP) based protocol[82], surface functionalization was accomplished *in-situ* by simply passing a solution of the ionic monomer [NBE-CH$_2$-NMe$_3$$^+$][BF$_4$$^-$] (**M2**) through the monolith right after its synthesis[83-85]. Finally, the *living* Ru-alkylidenes were completely removed *via* treatment with ethyl vinyl ether as proved by means of inductively-coupled plasma optical emission spectroscopy (ICP-OES) measurements, which indicated a residual Ru-content of the monolith of 38 ppm. Elemental analysis confirmed the effective grafting of **M2** with an average degree of oligomerization of three. Such low degrees of oligomerization on the one hand guarantee for the binding of the IL and, on the other hand, do not give raise to higher back-pressures.
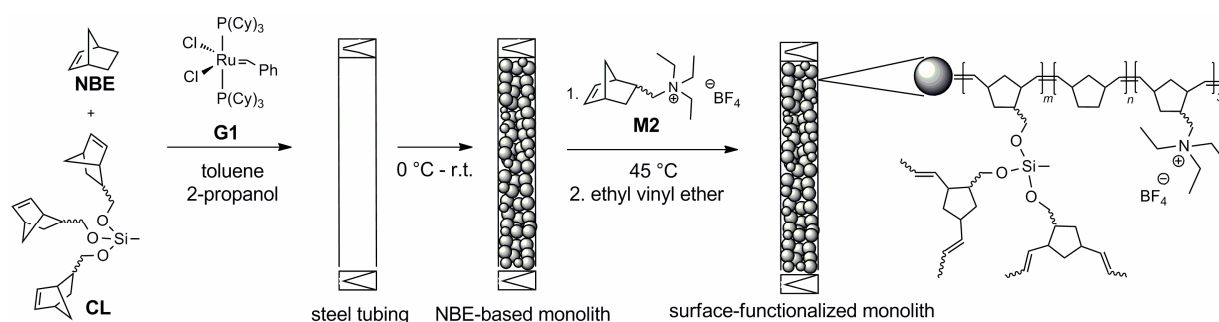
Scheme 9. Preparation of a surface-functionalized monolithic support. p=3.

In general, a monolith consists of interconnected structure-forming microglobules. Important parameters are the diameter (d_p) and the microporosity (ε_p) of the microglobules as well as the intermicroglobular porosity (ε_z). The total porosity (ε_t) is defined as the sum of ε_p and ε_z. These values as well as the pore size distribution (Figure S18, Appendix) were determined *via* inverse size exclusion chromatography (ISEC)[86]. The corresponding values for the surface-functionalized monolith are summarized in Table 8.

Table 8. Composition and structural data of the monolithic support (V_{column}=1.66 mL) after ROMP-based grafting of **M2**.

ε_p [vol %]	ε_z [vol %]	ε_t [vol %]	V_z [mL]	$\overline{\Phi}_m$ [a] [Å]
5	75	80	1.25	1160

[a] Average pore diameter.

As can be seen, the large void volume of 80% with regard to the total column volume guarantees for low back-pressures and is mainly caused by the interstitial porosity (ε_z=75%). In clear words, the monolith was designed to possess almost exclusively macropores, thus favoring diffusion and allowing for high reagent throughput. In contrast to most silica-based materials, which also have a large fraction of micro- and mesopores, this particular feature makes polymeric monoliths ideal support materials for the intended continuous metathesis reactions under biphasic conditions.

3.2.6 Continuous Metathesis Under Biphasic Conditions Using Monolith-Supported ILs

Layers of [BDMIM$^+$][BF$_4^-$] on the monoliths' surface containing **1** were prepared by simply injecting a solution of the IL and **1** in CH$_2$Cl$_2$. Then, the solvent was completely removed *in vacuo*. A homogeneous distribution of the IL over the entire support was confirmed by cutting a monolith into pieces of equal weight, which were then extracted with CDCl$_3$ and subjected to ^{1}H-NMR analysis. With the help of NMR-analysis it could also be shown that the IL can be removed quantitatively by flushing the column with methanol. Finally, NMR analysis helped confirming that at flow rates between 0.05 mL/min and 2.00 mL/min no [BDMIM$^+$][BF$_4^-$] was removed from the monolith when heptane was used as mobile phase and up to 20 vol.-% of the void volume of the monolith were filled with the IL.

3.2.6.1 RCM of N,N-Diallyl Trifluoroacetamide, DEDAM and 1,7-Octadiene Under Biphasic Conditions Using Monolith-Supported ILs

Since catalyst **1** showed a very high activity in the RCM of DAFA in both CH$_2$Cl$_2$ and [BDMIM$^+$][BF$_4^-$] at T=40°C, this reaction was chosen to demonstrate the soundness and viability of the concept of running metathesis reactions under biphasic conditions

using monolith-supported [BDMIM$^+$][BF$_4^-$]/**1**. Due to the high polarity of DAFA, the optimization of the reaction conditions, i.e. the adjustment of the thickness of the IL-layer and the identification of the optimum concentrations became notably challenging. For comparison, all experiments were additionally carried out with the **GH2**-catalyst under likewise identical conditions. Conversions were determined by means of GC-MS, leaching of **1** into the heptane-phase was quantified by ICP-OES. Under all conditions, monolith-supported [BDMIM$^+$][BF$_4^-$]/**1** outrivaled the monolith-supported [BDMIM$^+$][BF$_4^-$]/**GH2**-catalyst (Table S1, Appendix). Metal leaching into the heptane phase was lower by a factor of 4-10 for [BDMIM$^+$][BF$_4^-$]/**1** compared to [BDMIM$^+$][BF$_4^-$]/**GH2**-catalyst and allowed for TONs up to 900. Generally, leaching could be reduced *via* dilution of the mobile phase with heptane, thereby decreasing the polarity of the transport phase. However, this was associated with a decrease in TONs. TONs could be increased by reducing the thickness of the immobilized IL layer, however on the expense of an increasing catalyst leaching. The lower TONs that were obtained in comparison to the biphasic solution experiments may be attributed to the reduced contact times and the fact, that mixing of the two phases proceeds more effectively under mechanical stirring than on a monolith. However, the fact that halving the flow rate did not increase the TONs (Table S1, Appendix), most probably is attributed to catalyst deactivation processes. As outlined in chapter 1.2.1, the release of ethylene represents the driving force in case terminal dienes are used in RCM reactions. Particularly in closed reaction systems where the release of the gas is not given, ethylene can act as a substrate in metathesis reactions, too. Definitely, in reactions performed inside a polymeric monolith the fast ethylene removal is somewhat hindered. In addition, as was shown by P. Wasserscheid, that the use of an ionic liquid as the reaction phase might lead to further accumulation of ethylene inside the system and to the formation of ruthenacyclobutanes [62]. Also, the ruthenium methylidenes resulting from the metathesis reaction between Ru alkylidenes and ethylene are known to be responsible for a large percentage of catalyst decompositon [87]. The quite reactive and somewhat unstable methylidene spezies tend to decompose in an unimolecular fashion [87, 88]. This consideration might serve as an explanation for the lower TONs observed in RCM reactions performed under continuous monolith supported conditions. Supporting this hypothesis, increasing the temperature to T=60°C led to a higher product fraction in the eluting phase within the first minutes of the reaction. However, because the

enhanced reaction rate goes along with an increased formation of ethylene, deactivation occurred faster compared to reactions performed at 40°C and the overall TON did not change significantly. Plots of conversion *vs.* time of DAFA at different reaction conditions are shown in Figure S19 and Figure S20 (Appendix). These show the typical deactivation of a metathesis catalyst over time and clearly demonstrate the advantages of the SILP-approach presented here over traditional immobilization strategies.

As observed for reactions in organic solvents, DEDAM and 1,7-octadiene reacted with catalyst **1** under SILP conditions only at elevated temperature (T=80°C) resulting in TONs of 650 and 770 and a Ru-leaching of 0.2 and 0.05%. While 1,7-octadiene could be passed through the monolith neat, heptane was used as the second liquid transport phase in the RCM of DEDAM in order to establish a biphasic reaction mixture.

3.2.6.2 Self-Metathesis of Methyl Oleate Under Biphasic Conditions Using Monolith-Supported ILs

Since the self-metathesis of methyl oleate requires prolonged reaction times even at 80°C, it was required to cycle the methyl oleate phase, i.e. to pass it through the monolith several times at a flow rate of 0.1 mL/min. After each run, conversion was checked by GC-MS, then the reaction mixture was again flushed through the monolithic support. This procedure was repeated three times, then catalyst leaching was checked by ICP-OES (Table 9). A total TON of 800 was obtained within 45 min at T=80°C with the highest conversion occurring within the first cycle. Notably, again only the primary metathesis products formed suggesting the absence of any active Ru-hydride species. This TON is in view of the low solubility of methyl oleate in the IL ($K_{\text{methyl oleate/IL}}$=34 at T=80°C, Table 4, Chapter 2) remarkable and underlines the high reactivity of **1**. It is worth mentioning that the TON obtained in this continuously performed experiment is as high as the one obtained in biphasic unsupported reactions at the same temperature. Since in this particular reaction no ethylene is generated, catalyst deactivation processes seem to be much less pronounced, supporting the explanation given in the previous chapter 3.2.6.1.

Table 9. Self-metathesis of methyl oleate.

Cycle	Integral conversion[a] [%]
1 (after 15 min)	45
2 (after 28 min)	56
3 (after 45 min)	63
total Ru leaching	0.6% (4.5 ppm)

[a] Primary metathesis products; catalyst **1** (4.5 mg), [BDMIM$^+$][BF$_4^-$] (90 mg), methyl oleate (1.8 g, 1300 equiv.), T=80°C, flow rate: 0.1 mL min^{-1}.

3.3 Conclusions

The synthesis of a novel, dicationic Ru-alkylidene complex **1** [Ru(DMF)$_3$(IMesH$_2$)(=CH-2-(2-PrO)-C$_6$H$_4$)$^{2+}$][(BF$_4^-$)$_2$] is described. The catalyst can be selectively dissolved in an IL in the presence of a second organic phase and possesses high activity towards dienes lacking coordinating moieties. At elevated temperatures, **1** shows also high activity in RCM, CM and self-metathesis reactions. For RCM and self-metathesis reactions under supported biphasic conditions, surface-functionalized ROMP-derived monoliths were prepared and used for the immobilization of [BDMIM$^+$][BF$_4^-$] containing catalyst **1**. High TONs and an exceptionally low catalyst leaching (≤ 0.01%) were observed. Importantly, the concept also enables continuous product formation, simply by cycling reactants through a monolithic support containing a suitable catalyst dissolved in an IL. The fact that a biphasic liquid-liquid system is used definitely widens the range of potentially accessible substrates. In contrast to any other surface-immobilized catalyst, the facile recycling of the monolithic support by flushing with, e.g., methanol, represents an additional advantage over existing systems.

3.4 References

[1]   C. A. Angell, N. Byrne, J.-P. Belieres, *Acc. Chem. Res.* **2007**, *40*, 1228.

[2]   T. Welton, *Chem. Rev.* **1999**, *99*, 2071.

[3]   P. Walden, *Bull. Acad. Imper. Sci. St. Petersbourg* **1904**, *8*, 405.

[4]   N. V. Plechkova, S. K. R., *Chem. Soc. Rev.* **2008**, *37*, 123.

[5]   V. I. Pârvulescu, C. Hardacre, *Chem. Rev.* **2007**, *107*, 2615.

[6]   W. Miao, T. H. Chan, *Acc. Chem. Res.* **2006**, *39*, 897.

[7]   P. Wasserscheid, *Chemie unserer Zeit* **2003**, *37*, 52.

[8]   P. Wasserscheid, W. Keim, *Angew. Chem.* **2000**, *112*, 3927.

[9]   R. Sheldon, *Chem. Commun.* **2001**, 2399.

[10]   C. C. Brasse, U. Englert, A. Salzer, H. Waffenschmidt, P. Wasserscheid, *Organometallics* **2000**, *19*, 3818.

[11]   P. Wasserscheid, H. Waffenschmidt, *J. Molec. Catal A: Chem.* **2000**, *164*, 61.

[12]   A. Bösmann, G. Franciò , E. Janssen, M. Solinas, W. Leitner, P. Wasserscheid, *Angew. Chem.* **2001**, *113*, 2769.

[13]   D. S. McGuinness, W. Mueller, P. Wasserscheid, K. J. Cavell, B. W. Skelton, A. H. White, U. Englert, *Organometallics* **2002**, *21*, 175.

[14]   M. Picquet, I. Tkatchenko, I. Tommasi, P. Wasserscheid, J. Zimmermann, *Adv. Synth. Catal.* **2003**, *345*, 959.

[15]   A. Riisager, R. Fehrmann, M. Haumann, P. Wasserscheid, *Eur. J. Inorg. Chem.* **2006**, 695.

[16]   P. Wasserscheid, T. Welton (Eds.), *Ionic Liquids in Synthesis*, Wiley-VCH, Weinheim, **2003**.

[17]   A. Riisager, R. Fehrmann, S. Flicker, R. van Hal, M. Haumann, P. Wasserscheid, *Angew. Chem.* **2005**, *117*, 826.

[18]   P. Wasserscheid, P. Schulz, in *Ionic Liquids in Synthesis 2*, 2nd ed. (Eds.: P. Wasserscheid, T. Welton), Wiley-VCH Verlag, Weinheim, **2008**, pp. 369.

[19]   A. Riisager, R. Fehrmann, P. Wasserscheid, R. van Hal, *ACS Symposium Series (Ionic Liquids IIIB: Fundamentals, Progress, Challenges, and Opportunities)* **2005**, *902*, 334.

[20]   P. Wasserscheid, *J. Ind. Eng. Chem.* **2007**, *13*, 325.

[21]   M. Haumann, K. Dentler, J. Joni, A. Riisager, P. Wasserscheid, *Adv. Synth. Catal.* **2007**, *349*, 425.

[22]   A. Riisager, P. Wasserscheid, R. van Hal, R. Fehrmann, *J. Catal.* **2003**, *219*, 452.

[23]   A. Riisager, B. Jørgensen, P. Wasserscheid, R. Fehrmann, *Chem. Commun.* **2006**, 994.

[24]   A. Riisager, K. M. Eriksen, P. Wasserscheid, R. Fehrmann, *Catal. Lett.* **2003**, *90*, 149.

[25]   A. Riisager, R. Fehrmann, M. Haumann, P. Wasserscheid, *Topics in Catal.* **2006**, *40*, 91.

[26]   K. Bica, P. Gaertner, *Eur. J. Org. Chem.* **2008**, 3235.

[27]   L. Liao, L. Liu, C. Zhang, S. Gong, *Macromol. Rapid Commun.* **2006**, *24*, 2060.

[28]   Y. S. Vygodskii, E. I. Lozinskaya, A. S. Shaplov, *Macromol. Chem. Macromol. Symp.* **2002**, *3*, 676.

[29]   Y. S. Vygodskii, E. I. Lozinskaya, A. S. Shaplov, K. A. Lyssenko, M. Y. Antipin, Y. G. Urman, *Polymer* **2004**, *145*, 5031.

[30]   Y. S. Vygodskii, O. A. Mel'nik, E. I. Lozinskaya, A. S. Shaplov, *Polym. Sci. Ser. A* **2004**, *46*, 347.

[31]   Y. S. Vygodskii, E. I. Lozinskaya, A. S. Shaplov, *Polym. Sci. Ser. A* **2001**, *43*, 236.

[32]   Y. S. Vygodskii, E. I. Lozinskaya, A. S. Shaplov, K. A. Lyssenko, M. Y. Antipin, Y. G. Urman, *Polymer* **2001**, *45*, 5031.

[33]   E. I. Lozinskaya, A. S. Shaplov, Y. S. Vygodskii, *Eur. Polym. J.* **2004**, *40*, 2065.

[34]   Y. S. Vygodskii, A. S. Shaplov, E. I. Lozinskaya, O. A. Filippov, E. A. Shubina, R. Bandari, M. R. Buchmeiser, *Macromolecules* **2006**, *39*, 7821.

[35]   Y. S. Vygodskii, A. S. Shaplov, E. I. Lozinskaya, K. A. Lyssenko, D. G. Golovanov, I. A. Malyshkina, N. D. Gavrilova, M. R. Buchmeiser, *Macromol. Chem. Phys.* **2007**, *209*, 40.

[36]   Y. S. Vygodskii, A. S. Shaplov, E. I. Lozinskaya, P. S. Vlasov, I. A. Malyshkina, N. D. Gavrilova, P. S. Kumar, M. R. Buchmeiser, *Macromolecules* **2008**, *41*, 1919.

[37]   C. Guerrero-Sanchez, R. Hoogenboom, U. S. Schubert, *Chem. Commun.* **2006**, 3797.

[38]   V. Strehmel, A. Laschewsky, H. Wetzel, E. Görnitz, *Macromolecules* **2006**, *39*, 923.

[39]   M. A. Klingshirn, G. A. Broker, J. D. Holbrey, K. H. Shaughnessy, R. D. Rogers, *Chem. Commun.* **2002**, 1394.

[40]   T. Biedron, P. Kubisa, *Macromol. Rapid Commun.* **2001**, *22*, 1237.

[41]   P. Kubisa, *Progr. Polym. Sci.* **2004**, *29*, 3.

[42]   B. Buszewski, S. Studzińska, *Chromatographia* **2008**, *68*, 1.

[43]   F. Zhao, Y. Meng, J. L. Anderson, *J. Chromatogr. A* **2008**, *1208*, 1.

[44]   H. Qiu, Q. Zhang, L. Chen, X. Liu, S. Jiang, *J. Sep. Sci.* **2008**, *31*, 2791.

[45]   H. Qiu, Q. Jiang, Z. Wei, X. Wang, X. Liu, S. Jiang, *J. Chromatogr. A.* **2007**, *1163*, 63.

[46]   G. A. Baker, S. N. Baker, S. Pandey, F. V. Bright, *Analyst* **2005**, *130*, 800.

[47]   M. Andre, J. Loidl, G. Laus, H. Schottenberger, G. Bentivoglio, K. Wurst, K.-H. Ongania, *Anal. Chem.* **2005**, *77*, 702.

[48]   J. L. Anderson, D. W. Armstrong, G. T. Wei, *Anal. Chem.* **2006**, *78*, 2892.

[49]   S. S. Sekhon, B. S. Lalia, J.-S. Park, C.-S. Kim, K. Yamada, *J. Mater. Chem.* **2006**, *16*, 2256.

[50]   Z. Fei, D. Kuang, D. Zhao, F. Klein, W. H. Ang, S. M. Zakeeruddin, M. Grätzel, P. J. Dyson, *Inorg. Chem.* **2006**, *45*, 10407.

[51]   C. Baudequin, J. Baudoux, J. Levillain, D. Cahard, A.-C. Gaumont, J.-C. Plaquevent, *Tetrahedron Assym.* **2003**, *14*, 3081.

[52]   C. E. Song, *Chem. Commun.* **2004**, 1033.

[53]   M. T. Reetz, W. Wiesenhöfer, G. Franciòa, W. Leitner, *Chem. Commun.* **2002**, 992.

[54]   V. Rao, R. Datta, *J. Catal.* **1988**, *114*, 377.

[55]   X. Wu, Y. A. Letuchy, D. P. Eyman, *J. Catal.* **1996**, *161*, 164.

[56]   C. P. Mehnert, R. A. Cook, N. C. Dispenziere, M. Afeworki, *J. Am. Chem. Soc.* **2002**, *124*, 12932.

[57]   C. P. Mehnert, E. J. Mozeleskib, R. A. Cooka, *Chem. Commun.* **2002**, 3010.

[58]   C. P. Mehnert, *Chem. Eur. J.* **2004**, 50.

[59]   P. Lozano, E. García-Verdugo, R. Piamtongkam, N. Karbass, T. De Diego, M. I. Burguete, S. V. Luis, J. L. Iborra, *Adv. Synth. Catal.* **2007**, *349*, 1077.

[60]   M. A. Gelesky, S. S. X. Chiaro, F. A. Pavan, J. H. Z. dos Santos, J. Dupont, *Dalton Trans.* **2007**, 5549.

[61]   J. Le Bideau, P. Gaveau, S. Bellayer, M.-A. Néouze, A. Vioux, *Phys. Chem. Chem. Phys.* **2007**, *9*, 5419.

[62]   J. Scholz, S. Loekman, N. Szesni, W. Hierienger, A. Goerlinger, M. Haumann, P. Wasserscheid, *Adv. Synth. Catal.* **2011**, *353*, 2701.

[63]   S. Naumov, M. R. Buchmeiser, *Organometallics* **2012**, *31*, 847.

[64]   M. R. Buchmeiser, I. Ahmad, V. Gurram, P. S. Kumar, *Macromolecules* **2011**, *44*, 4098.

[65]   J. O. Krause, S. H. Lubbad, O. Nuyken, M. R. Buchmeiser, *Macromol. Rapid Commun.* **2003**, *24*, 875.

[66]   J. O. Krause, O. Nuyken, M. R. Buchmeiser, *Chem. Eur. J.* **2004**, *10*, 2029.

[67]   J. O. Krause, K. Wurst, O. Nuyken, M. R. Buchmeiser, *Chem. Eur. J.* **2004**, *10*, 777.

[68]   J. O. Krause, M. T. Zarka, U. Anders, R. Weberskirch, O. Nuyken, M. R. Buchmeiser, *Angew. Chem.* **2003**, *115*, 6147.

[69]   P. S. Kumar, M. R. Buchmeiser, *Organometallics* **2009**, *28*, 1785.

[70]   P. S. Kumar, K. Wurst, M. R. Buchmeiser, *J. Am. Chem. Soc.* **2009**, *131*, 387.

[71]   P. S. Kumar, K. Wurst, M. R. Buchmeiser, *Chem. Asian J.* **2009**, *4*, 1275.

[72]   S. B. Garber, J. S. Kingsbury, B. L. Gray, A. H. Hoveyda, *J. Am. Chem. Soc.* **2000**, *122*, 8168

[73]   C. S. Yi, D. W. Lee, Y. Chen, *Organometallics* **1999**, *18*, 2043.

[74]   O. Songis, A. M. Z. Slawin, C. S. J. Cazin, *Chem. Commun.* **2012**, *48*, 1266.

[75]   M. S. Sanford, L. M. Henling, R. H. Grubbs, *Organometallics* **1998**, *17*, 5384.

[76]   S. Gatard, S. Kahlal, D. Méry, S. Nlate, E. Cloutet, J.-Y. Saillard, D. Astruc, *Organometallics* **2004**, *23*, 1313.

[77]   Rogier C. Buijsman, Elizabeth van Vuuren, J. G. Sterrenburg, *Org. Lett.* **2001**, *3*, 3785

[78]   P. Sledz, M. Mauduit, K. Grela, *Chem. Soc. Rev.* **2008**, *37*, 2433

[79]   E. B. Anderson, M. R. Buchmeiser, *ChemCatChem* **2012**, *4*, 30.

[80]   S. Lubbad, M. R. Buchmeiser, *Macromol. Rapid Commun.* **2002**, *23*, 617.

[81]   S. Lubbad, B. Mayr, M. Mayr, M. R. Buchmeiser, *Macromol. Symp.* **2004**, *210*, 1.

[82]   M. Okubo, M. Shiozaki, M. Tsujihiro, Y.Tsukuda, *Colloid Polym. Sci,* **1991**, *269*, 222.

[83]   R. Bandari, W. Knolle, A. Prager-Duschke, M. R. Buchmeiser, *Macromol. Rapid Commun.* **2007**, *28*, 2090.

[84]   M. R. Buchmeiser, F. Sinner, M. Mupa, K. Wurst, *Macromolecules* **2000**, *33*, 32.

[85]   S. Lubbad, M. R. Buchmeiser, *Macromol. Rapid Commun.* **2003**, *24*, 580.

[86]   I. Halasz, K. Martin, *Angew. Chem.* **1978**, *90*, 954.

[87]   R. H. Grubbs (Ed.), *Handbook of Metathesis*, Wiley-VCH, Weinheim (Germany), **2003**.

[88]   P. W. N. M. van Leeuwen, J. C. Chadwick (Eds.), *Homogeneous Catalysts- Activity, Stability, Deactivation*, Wiley-VCH, Weinheim (Germany), **2011**.

4. Reactivity of 1 in Ring-Opening Metathesis and
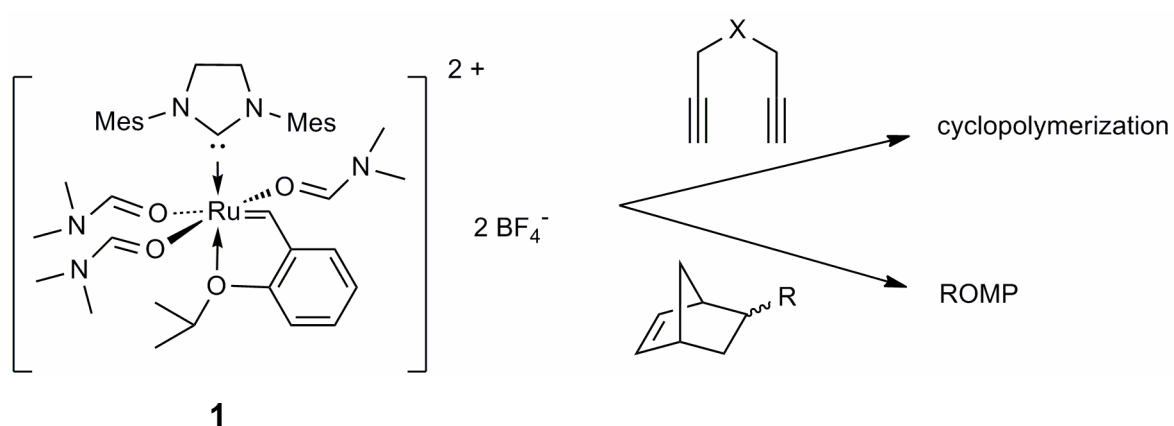
Cyclopolymerization

The material covered in this chapter has appeared in:

The article has been highlighted in *Materials Views*, Nov. 22, **2012** by Stefan Spiegel

4.1 Introduction

In the previous chapter the synthesis of the dicationic Ru-alkylidene complex [Ru(DMF)$_3$(IMesH$_2$)(=CH-2-(2-PrO)-C$_6$H$_4$)$^{2+}$][(BF$_4^-$)$_2$]   (**1**,   IMesH$_2$=1,3-dimesityl-imidazolin-2-ylidene, Figure 14) and its use in cross-metathesis reactions in ionic liquids under continuous biphasic liquid-liquid conditions was reported.[1] There, due to its dicationic character, **1** can be immobilized within a polar liquid phase, e.g., an ionic liquid, whereas the reactants diffuse to the catalytic centers out of a second, non-polar, liquid transport phase. In **1**, the Ru=C double bond is strongly polarized compared to neutral Ru-alkylidene complexes. Evidence for that is the observed shift of the alkylidene-signal in the ^{1}H-NMR spectrum from δ=16.58 ppm (CD$_2$Cl$_2$) for the parent 2nd-generation Grubbs-Hoveyda initiator (**GH2**) to δ=19.28 ppm (CD$_2$Cl$_2$) in **1**, also indicating a strong agostic interaction between the alkylidene-proton and the ruthenium. Such pronounced downfield shifts in the ^{1}H-NMR for the alkylidene proton are also observed for several "pseudohalide"-derivatives of *Grubbs-* or *Grubbs-Hoveyda*-type initiators (Table S2, Appendix)[2-8] where a strong polarization of the Ru-alkylidene has been suggested by DFT calculations.[9]
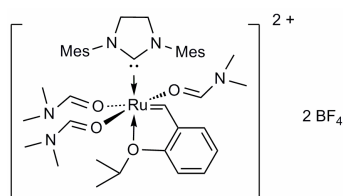

Figure 14. Structure of [Ru(DMF)$_3$(IMesH$_2$)(=CH-2-(2-PrO)-C$_6$H$_4$)$^{2+}$][(BF$_4^-$)$_2$] (**1**).

Here, the reactivity of **1**, which in fact is a rare example of dicationic Ru-alkylidenes, in ring-opening metathesis polymerization (ROMP) is reported. However, in view of the strong propensity of the above-mentioned pseudo-halide derivatives of *Grubbs-* and *Grubbs-Hoveyda* type initiators to cyclopolymerize 1,6-heptadiynes, of particularly interest was the use of **1** in the cyclopolymerization of 1,6-heptadiynes bearing either electron-withdrawing or electron-donating functionalities.

4.2 Results and Discussion

4.2.1 Ring-opening Metathesis Polymerization (ROMP) of Norborn-2-enes

In order to screen the activity of **1** in ROMP and to investigate its tolerance towards functional groups, **1** was reacted with different norborn-2-ene-(NBE)-based monomers (Figure 15).
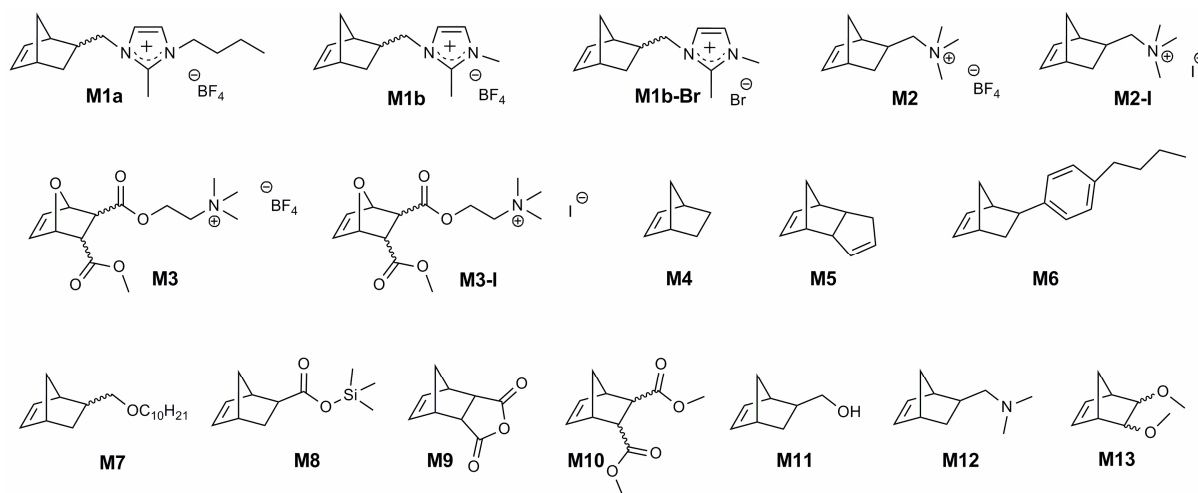

Figure 15. NBE-based monomers **M1** – **M13** used for ROMP-reactions.

With the exception of the dimethyl ester derivative **M10** and monomers **M11** - **M13**, which required elevated reaction temperature, all NBE-derivatives underwent immediate polymerization at room temperature. Polymerization results are summarized in Table 10. In terms of stereoselectivity in ROMP initiated by **1**, most polymers displayed a *trans*-content of roughly 60-75%, which is in line with the *trans*-content of polymers obtained with most other Ru-alkylidenes. Exceptions are poly-**M4** and the 2,3-disubstituted polymers poly-**M9**, poly-**M10** and poly-**M13**, which possessed a *trans*-content <56%.

Table 10. Summary of the polymerization results for monomers **M1**-**M13**.

#	Monomer	1 [mol-%]	T [°C]	t [h]	Yield [a] [%]	$\overline{M}_{n\,(calc.)}$ [g/mol]	$\overline{M}_{n\,(exp.)}$ [g/mol]	PDI	*cis/trans*[b]
1	**M1a**[d]	0.5	20	5	70	66000	132000	1.07	36/64
2	**M1b**[d]	0.5	20	5	100	58000	194000	1.04	27/73
3	**M2**[d]	0.5	20	5	100	51000	173000	1.1	33/67
4	**M2-I**[d]	0.5	20	5	89	59000	165000	1.4	35/65
5	**M3**[d]	0.5	20	5	95	74000	155000	1.2	29/71
6	**M3-I**[d]	0.5	20	5	100	82000	197000	1.4	28/72
7	**M4**	0.02	20	0.17	90	450000	457000	1.3	48/52
8	**M5**	0.1	20	1	100	132000	i[c]	-	-
9	**M6**	0.5	20	1	93	45000	39500	2.6	33/67
10	**M7**	0.5	20	1	88	53000	131000	2.3	38/62
11	**M8**	0.5	20	5	90	42000	31000	2.2	35/65
12	**M9**	0.5	20	5	86	33000	i	i	44/56[e]
13	**M10**	0.5	80	12	38	42000	9500	1.8	74/26
14	**M11**	0.5	80	12	27	25000	i	-	-
15	**M12**	0.5	80	12	16	30000	i	-	-
16	**M13**	0.5	80	12	25	36000	8600	2.4	55/45

[a]isolated yields; [b]determined by the ratio of the olefinic-protons in the ^{1}H-NMR spectrum (Figure S21, Appendix). [c]cross-linked polymer. [d]poly-**M1a** – poly-**M3-I** were measured in DMF, all polymers were aggregated; [e]Soluble fraction. i=insoluble.

As can be deduced from Table 10, some of the experimentally determined $\overline{M}_n$ values exceeded the theoretical ones by a factor of 2. To shed light on that issue, plots of monomer conversion and ln(c_0/c_t) *versus* time for monomers **M6**, **M9** and **M1b** (Figures S22 and S23, Appendix) were recorded. The ROMP of 200 equivalents of the electron rich monomer **M6**, which does not contain any coordinating functional moieties, is quantitatively completed within 25 minutes. *Vice versa*, in the ROMP of

M9 and **M1b**, more than 3 hours are required to achieve quantitative conversion. None of the plots of $\ln(c_0/c_t)$ *vs.* time for **M6**, **M9** and **M1b** revealed a *living* polymerization process. The presence of functional groups such as esters (**M10**) can slow down insertion kinetics, most presumably *via* coordination to the highly electrophilic Ru-center. *Vice versa*, the cationic monomers **M1a, M1b, M1b-Br, M2, M2-I, M3, M3-I** might suffer from electrostatic repulsion by dicationic **1**. This is reflected by the comparably high ratios of the rate constant of polymerization, k_p, over the rate constant of initiation, k_i, of these monomers (Table 11).

Table 11. Selected k_p/k_i values for the reaction of **M1a**, **M1b**, **M2**, **M6**, **M9** and **M10** with **1**.

Monomer	T [°C]	k_p/k_i
M1a	20	40
M1b	20	50
M2	20	70
M6	20	2
M9	20	2
M10	80	40

The ROMP of **M1a**, **M1b** and **M2** proceeded with quantitative yield at room temperature, albeit not in a *living* manner. The experimentally determined $\overline{M}_n$ values of the corresponding polymers were significantly higher than the theoretical ones, but accurate GPC-data could not be obtained due to polymer aggregation in solution (Figures S24 and S25, Appendix). Multiple peaks were visible in DLS spectra indicating the formation of aggregates in DMF polymer solutions. These aggregates form due to inter-chain interactions such as ionic aggregation,[10] and GPC of aggregated polymers leads to determination of the aggregate size rather than a single polymer chain.[11] Measuring samples at 40 *versus* 20 °C did not significantly decrease the formation of these aggregates. Adding safe quantities of additives for GPC instrument measurements, such as LiBr, have been shown to break aggregates in DMF solution for GPC analysis.[10, 12-14] However, the addition of LiBr up to 0.5 M

did not sufficiently screen the charged groups on these polymers as aggregates were still visible in DLS. Therefore, GPC molecular weights were not accurate for these polymers.

During the ROMP of the ionic monomers **M1b-Br** and **M2-I**, it was found that the alkylidene signal of the parent complex vanished completely. In the case of **M1b-Br** (Figure S26, Appendix), a new sharp signal at δ=16.40 ppm formed and suggests the formation of $[RuBr_2(IMesH_2)(=CH-2-(2-PrO)-C_6H_4)]$.[15] When reacting the iodide salt **M2-I** (Figure S27, Appendix), a sharp signal at δ=15.67 ppm was observed, which is in agreement with the reported shift for $[RuI_2(IMesH_2)(=CH-2-(2-PrO)-C_6H_4)]$.[15] These findings give evidence for the formation of the *neutral* alkylidene species $[RuX_2(IMesH_2)(=CH-2-(2-PrO)-C_6H_4)]$ (X=Br, I) when subjecting the dicationic complex **1** to the polymerization of monomers containing coordinating anions. Notably, by removing the newly formed Ru-alkylidenes from the polymer chains by addition of 2(2-PrO)-styrene (Scheme 10), the corresponding neutral Ru-complexes could in fact be isolated and unambiguously could be identified.
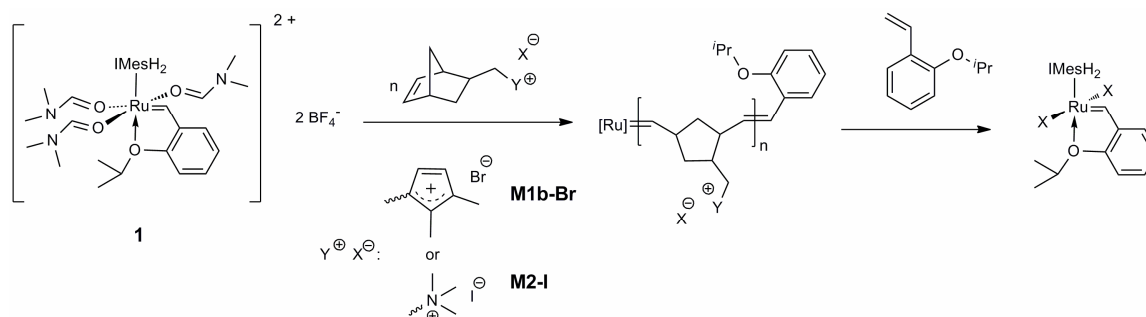

Scheme 10. Trapping of the propagating alkylidene species formed during the ROMP of **M1b-Br** and **M2-I**. The final neutral complexes $[Ru(X)_2(IMesH_2)(=CH-2-(2-PrO)-C_6H_4)]$ (X=Br, I) are formed by nucleophilic attack of Br$^-$ or I$^-$ to the dicationic Ru-center.

Vice versa, in the polymerization of **M2** containing the BF_4^- counter ion, the cationic character of the catalyst is preserved (Figure S28, Appendix). The high ROMP-activity of the dicationic species becomes evident by comparing the reaction kinetics for monomers **M1b** and **M2** (containing BF_4^-) to those of their halide containing analogs **M1b-Br** and **M2-I** (Figures S29 and S30, Appendix). Although **M1b** and **M2** are polymerized in a controlled manner, polymerization rates continuously decrease after 2 minutes with the halide containing monomers **M1b-Br** and **M2-I** and polymerizations cease around 70-80% conversion.

4.2.2 Cyclopolymerization of 1,6-Heptadiynes

The controlled or even *living* cyclopolymerization of 1,6-heptadiynes can proceed *via* α- or β-addition (Scheme 11) and has long been the domain of well-defined, tailor-made molybdenum-based *Schrock*-type initiators.[16-27] However, with the advent of *Grubbs*- and *Grubbs-Hoveyda* type initiators in which both chlorides had been replaced by electron-withdrawing ligands such as perfluorocarboxylates, nitrates or by pseudo-halides such as isocyanates and isothiocyanates,[4, 5, 7, 8, 28-34] this type of polymerizations became possible with the above-mentioned tailor-made Ru-alkylidenes, even allowing polymerizations to be carried out in aqueous solvents.[2, 5, 6, 9, 28, 35-40]
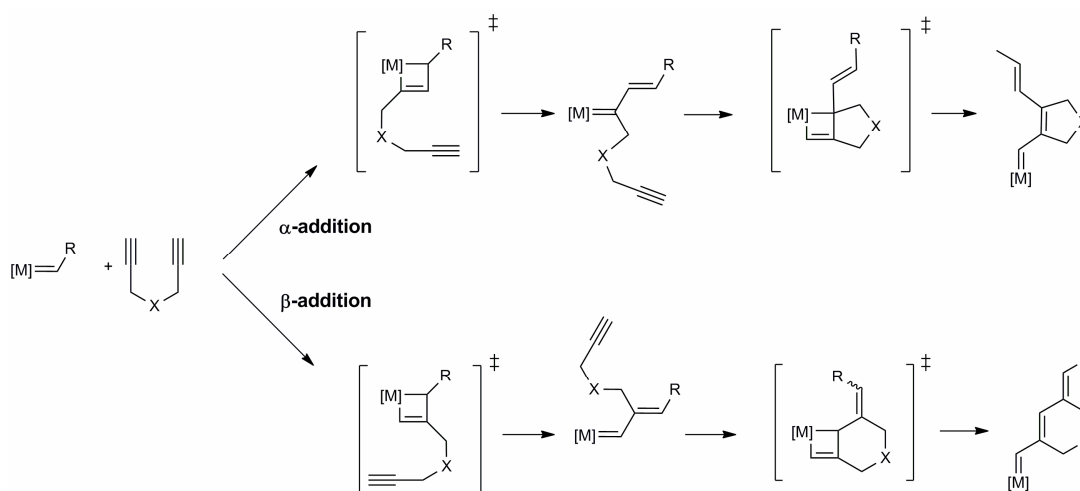
Scheme 11. The two possible reaction pathways (α- and β-insertion) leading to the formation of five- and six-membered repeat units. X=e.g., CH_2, NR, $C(COOEt)_2$.

Recently, this chemistry was extended to 1,7-octadiynes.[41] *Choi et al.* demonstrated that 1,6-heptadiynes and 1,7-octadiynes can be cyclopolymerized by "standard" *Grubbs*-initiators using a coordinating solvent such as THF.[42] In view of the significantly downfield shifted signals for both the alkylidene proton and carbon (Table S2, Appendix), **1** should display an even stronger polarization of the Ru-alkylidene than the above-mentioned perfluorocarboxylate and "pseudo-halide"-containing initiators. Accordingly, **1** was used in the cyclopolymerization of a variety of 1,6-heptadiynes (Figure 16).
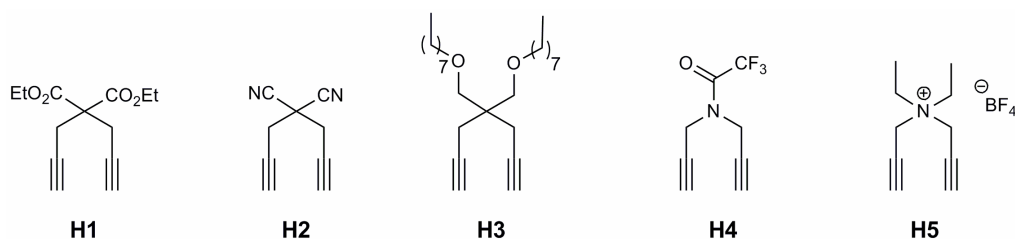
Figure 16. 1,6-Heptadiynes **H1** – **H5** used in cyclopolymerization.

After polymerizing 20 equivalents of **H1** at T=20°C, an $\overline{M}_n$ of 3200 g mol^{-1} and a PDI of 1.4 were found by GPC-analysis ($\overline{M}_{n\ (calc.)}$= 4800 g mol^{-1}, Table 12). Doubling the monomer:initiator ratio resulted in an $\overline{M}_n$ of 11600 g mol^{-1} and a PDI of 1.4 ($\overline{M}_{n\ (calc.)}$=9600 g mol^{-1}). At this temperature, a k_p/k_i[43] value of 3 (CD$_2$Cl$_2$) was found, which accounts for the good agreement between the theoretical and experimentally determined $\overline{M}_n$ values. To further confirm the controlled nature of the polymerization, a poly-**H1** sample prepared by polymerizing 5 equivalents of **H1** [44] at 20°C and terminating the reaction with ethyl vinyl ether was subjected to MALDI-TOF measurements (Figure S31, Appendix). All oligomers contained the two expected end groups, i.e. the initiator-derived =CH-2-(2-PrO)-C$_6$H$_4$ and the capping agent-derived =CH$_2$ moiety. ^{13}C-NMR spectroscopy revealed that poly-**H1**, prepared by the action of **1** was virtually solely based on five-membered repeat units (Figure 17). Seven signals, which also fit the chemical shifts of the model compound 1,1-di(ethoxycarbonyl)cyclopent-3-ene[20, 21] were observed and rule out the formation of either 6-membered repeat units (10 signals) or a mixture of 5- or 6-membered repeat units (>10 signals). Initiator **1** thus displays the same regioselectivity in insertion, i.e. the high α-insertion propensity (Scheme 11) than the previously reported perfluorocarboxylate or pseudo-halide-containing initiators.[9, 28, 34]
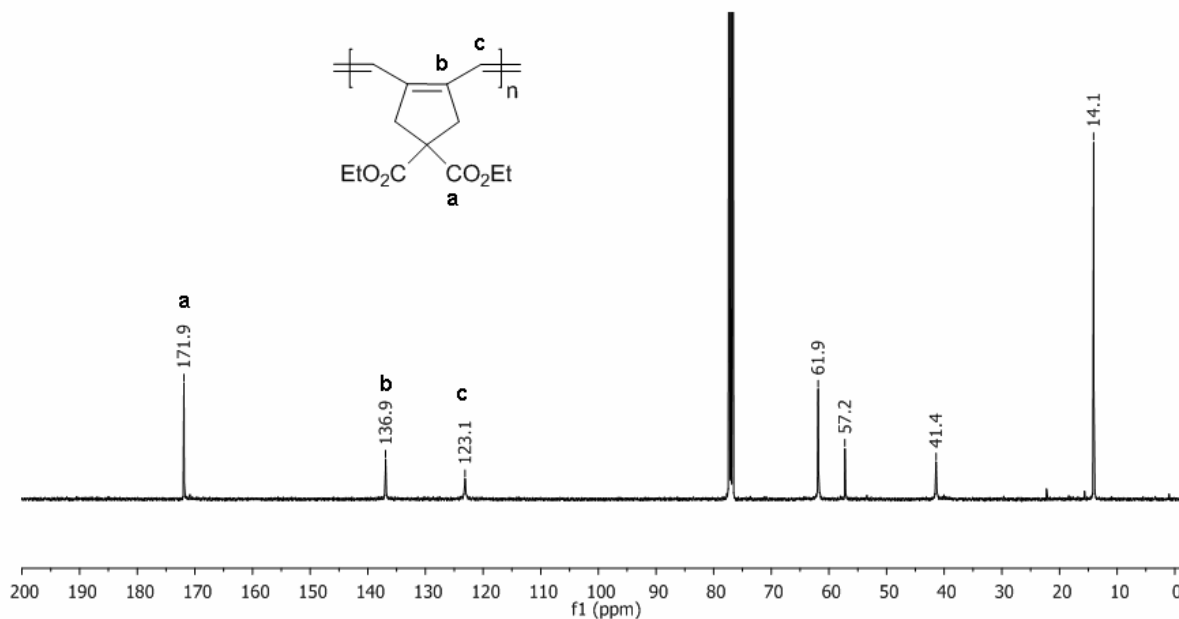
Figure 17. ^{13}C-NMR of poly-**H1** prepared by the action of **1** (CDCl$_3$).

The cyclopolymerization of the electron-poor dipropargyl malodinitrile (**H2**)[45] was carried out at 35°C and yielded an insoluble, purple polymer, which precipitates from the reaction mixture at an early stage in the polymerization. A low final conversion of only 30% was achieved within only a few minutes. Plots of $\ln(c_0/c_t)$ *versus* reaction time (Figure S32, Appendix) revealed, that the polymerization of **H2** initiated by **1** followed roughly 1st-order kinetics until maximum conversion (ca 30%) was achieved. The value for $k_{p,38°C(average)}$ was 4×10^{-3} s^{-1}. In the polymerization of 4,4-bis(octyl-oxymethyl)-1,6-heptadiyne (**H3**, Figure S33, Appendix)[46], a conversion of 94% was obtained at 20°C. Maximum conversion was again obtained within only a few minutes for the polymerization of monomer **H3**. Again, ^{13}C-NMR spectroscopy revealed that poly-**H3**, prepared by the action of **1**, essentially possessed solely five-membered repeat units (Figure S34, Appendix). Similar to **H1**, the value for k_p/k_i for the polymerization of **H3** was 3 (CD$_2$Cl$_2$) and again accounts for the good agreement between the theoretical and experimentally determined $\overline{M}_n$-values (Table 12). The cyclopolymerization of the electron-poor monomer *N,N*-dipropargyl trifluoroacetamide (**H4**) allowed for a final conversion of 77% within a few minutes (Figure S32, Appendix). A ruby-colored polymer was obtained whose IR-spectrum (Figure S45, Appendix) did not display any signals for remaining triple bonds. This suggests that cyclopolymerization predominated over any cross-linking reactions. The rate constant

73

of polymerization for **H4**, $k_{p,\ 38°C\ (average)}$ was 3×10^{-5} s^{-1} and thus roughly 100 times smaller than the one for **H2**, which is not surprising in view of the electron deficient character of the monomer. Finally, polymerization of ionic **H5** yielded a bright red solid in 93% isolated yield. Again, the IR-spectrum of poly-**H5** revealed the absence of any triple bonds suggesting that cyclopolymerization dominates over cross-linking (Figure S36, Appendix). Both poly-**H4** and poly-**H5** were heavily aggregated in solution as evidenced by DLS-measurements (Figures S37-38, Appendix). This aggregate formation could not be suppressed with the addition of salt or changes in the measurement temperature and prevented any conclusive GPC and NMR measurements.

Table 12. Results from GPC-measurements for cyclopolymerization-derived polymers prepared by the action of **1**.

No.	Monomer / equiv.[a]	Solvent / T [°C]	$\overline{M}_{n\ (calc.)}$ [g mol^{-1}]	$\overline{M}_{n\ (exp.)}$ [b] [g mol^{-1}]	PDI	Yield [c] [%]
1	**H1** / 20	CH$_2$Cl$_2$ / 20	4800	3200	1.4	98
2	**H1** / 40	CH$_2$Cl$_2$ / 20	9600	11600	1.4	93
3	**H1** / 40	CH$_2$Cl$_2$ / 35	9600	8900	1.7	87
4	**H3** / 70	CH$_2$Cl$_2$ / 20	26000	21000	1.9	78
5	**H3** / 30	CH$_2$Cl$_2$ / 20	11000	9600	1.8	94
6	**H4** / 100	CH$_2$Cl$_2$ / 35	19000	125000	1.07 [d]	77
7	**H4** / 100	CH$_2$Cl$_2$ / 35	24000	185000	1.03 [d]	93

[a]With respect to initiator; [b]For poly-**H1** and poly-**H3**, GPC was run in CHCl$_3$ using UV-detection; [c]Isolated yields; [d]GPC was performed in DMF, both samples were heavily aggregated as determined with DLS-measurements.

4.3 Conclusions

Due to its highly electrophilic character, **1** is an active initiator for the ROMP of substituted norborn-2-enes and the cyclopolymerization of 1,6-heptadiynes, even at low temperature and particularly for monomers containing electron-rich carbon-carbon-multiple bonds. The ROMP of NBE-based monomers proceeds quickly and with high yield even at room temperature. For monomers lacking coordinating moieties, polymerization proceeds in a controlled yet not in a *living* manner. For monomers possessing potentially coordinating functional groups such as ether or ester moieties, an increase in reaction temperature resulted in increased reaction rates. Higher polymer yields were obtained, albeit in conjunction with a loss of control. In the presence of coordinating anions such as Br$^-$ or I$^-$, for example, during the ROMP of the ionic monomers **M1b-Br** and **M2-I**, the parent dicationic complex $[Ru(DMF)_3(IMesH_2)(=CH-2-(2-PrO)-C_6H_4)^{2+}][(BF_4^-)_2]$ was converted into the corresponding neutral complexes $[Ru(X)_2(IMesH_2)(=CH-2-(2-PrO)-C_6H_4)]$ (X=Br, I). This change in active species led to changes in the polymerization kinetics. Finally, the unprecedented capability of dicationic Ru-based alkylidene complexes for cyclopolymerizing 1,6-heptadiynes was discovered. These cyclopolymerizations proceeded smoothly even at lower temperature. For monomers lacking coordinating moieties (**H4**, **H5**) the reactions proceed in a highly controlled though not perfectly *living* manner as supported by linear plots of $\ln(c_0/c_t)$ *versus* time and MALDI-TOF measurements. The latter clearly demonstrated the presence of both the initiator- and capping agent-derived end group in the final polymer and thus suggested the absence of chain-transfer or back-biting reactions, at least at low conversion. An increase in reaction temperature resulted in increased reaction rates as well as in higher polymer yields for cyclopolymerization reactions but accompanied with a significant loss of control. $[Ru(DMF)_3(IMesH_2)(=CH-2-(2-PrO)-C_6H_4)^{2+}][(BF_4^-)_2]$ essentially displays the same regioselectivity in insertion (i.e., the high α-insertion propensity) compared with results from the previously reported "pseudo-halide"-containing initiators and thereby enriches the existing portfolio of cyclopolymerization-active Ru-alkylidenes.

4.4 References

[1]   B. Autenrieth, W. Frey, M. R. Buchmeiser, *Chem. Eur. J.* **2012**, *18*, 14069.

[2]   J. O. Krause, M. T. Zarka, U. Anders, R. Weberskirch, O. Nuyken, M. R. Buchmeiser, *Angew. Chem.* **2003**, *115*, 6147.; *Angew. Chem. Int. Ed.* **2003**, *42*, 5965.

[3]   J. O. Krause, M. Mayr, S. Lubbad, O. Nuyken, M. R. Buchmeiser, *e-Polymers-conference papers section* **2003**, *P_007*.

[4]   J. O. Krause, K. Wurst, O. Nuyken, M. R. Buchmeiser, *Chem. Eur. J.* **2004**, *10*, 777.

[5]   J. O. Krause, O. Nuyken, M. R. Buchmeiser, *Chem. Eur. J.* **2004**, *10*, 2029.

[6]   J. O. Krause, D. Wang, U. Anders, R. Weberskirch, M. T. Zarka, O. Nuyken, C. Jäger, D. Haarer, M. R. Buchmeiser, *Macromol. Symp.* **2004**, *217*, 179.

[7]   P. S. Kumar, M. R. Buchmeiser, *Organometallics* **2009**, *28*, 1785.

[8]   P. S. Kumar, K. Wurst, M. R. Buchmeiser, *Chem. Asian J.* **2009**, *4*, 1275.

[9]   S. Naumov, M. R. Buchmeiser, *Organometallics* **2012**, *31*, 847.

[10]   E. Žagar, M. Žigon, *Polymer* **2000**, *41*, 3513.

[11]   I. Teraoka (Ed.), *Polymer Solutions: An Introduction to Physical Properties,* John Wiley & Sons, Inc., Hoboken (New Jersey), **2002**.

[12]   G. Volet, J. Lesec, *J. Liq. Chromatogr. Relat.Technol.* **1994**, *17*, 559.

[13]   N. Manabe, K. Kawamura, T. Toyoda, H. Minami, M. Ishikawa, S. Mori, *J. Appl. Polym. Sci.* **1998**, *68*, 1801.

[14]   B. Trathnig, *Size-exclusion Chromatography of Polymers,* In: Encyclopedia of Analytical Chemistry,* Ed.: R. A. Meyers, John Wiley & Sons Ltd., Chichester (England), **2000**.

[15]   J. Wappel, C. A. Urbina-Blanco, M. Abbas, J. H. Albering, R. Saf, S. P. Nolan, C. Slugovc, *Beilstein J. Org. Chem.* **2010**, *6*, 1091.

[16]   H. H. Fox, R. R. Schrock, *Organometallics* **1992**, *11*, 2763.

[17]   H. H. Fox, M. O. Wolf, R. O'Dell, B. L. Lin, R. R. Schrock, M. S. Wrighton, *J. Am. Chem. Soc.* **1994**, *116*, 2827.

[18]   F. J. Schattenmann, R. R. Schrock, W. M. Davis, *J. Am. Chem. Soc.* **1996**, *118*, 3295.

[19]   R. R. Schrock, Z. J. Tonzetich, A. G. Lichtscheidl, P. Müller, F. J. Schattenmann, *Organometallics* **2008**, *27*, 3986.

[20]   U. Anders, O. Nuyken, K. Wurst, M. R. Buchmeiser, *Angew. Chem.* **2002**, *114*, 4226.; *Angew. Chem. Int. Ed.* **2002**, *41*, 4044.

[21]   U. Anders, O. Nuyken, K. Wurst, M. R. Buchmeiser, *Macromolecules* **2002**, *35*, 9029.

[22]   U. Anders, M. Wagner, O. Nuyken, M. R. Buchmeiser, *Macromolecules* **2003**, *36*, 2668.

[23]   U. Anders, O. Nuyken, M. R. Buchmeiser, *J. Molec. Catal. A: Chem.* **2004**, *213*, 89.

[24]   U. Anders, J. O. Krause, D. Wang, O. Nuyken, M. R. Buchmeiser, *Des. Monomers Polym.* **2004**, *7*, 151.

[25]   M. R. Buchmeiser, *Adv. Polym. Sci.* **2005**, *176*, 89.

[26]   M. R. Buchmeiser, *Novel Cyclopolymerization Derived Conjugated Polyenes: Smart Materials for Electronics and Sensors* In: NATO Science for Peace and Security Series A. Chemistry and Biology*, Eds.:* E. Khosravi, Y. Yagci, Y. Savelyev, Klywer, Dordrecht (Netherlands), **2009**.

[27]   M. G. Mayershofer, O. Nuyken, M. R. Buchmeiser, *Macromolecules* **2006**, *39*, 2452.

[28]   P. S. Kumar, K. Wurst, M. R. Buchmeiser, *J. Am. Chem. Soc.* **2009**, *131*, 387.

[29]   L. Yang, M. Mayr, K. Wurst, M. R. Buchmeiser, *Chem. Eur. J.* **2004**, *10*, 5761.

[30]   T. S. Halbach, S. Mix, D. Fischer, S. Maechling, J. O. Krause, C. Sievers, S. Blechert, O. Nuyken, M. R. Buchmeiser, *J. Org. Chem.* **2005**, *70*, 4687.

[31]   J. O. Krause, S. Lubbad, O. Nuyken, M. R. Buchmeiser, *Adv. Synth. Catal.* **2003**, *345*, 996.

[32]   J. O. Krause, S. Lubbad, M. Mayr, O. Nuyken, M. R. Buchmeiser, *Polym. Prepr. (Am. Chem. Soc., Div. Polym. Chem.)* **2003**, *44*, 790.

[33]   M. R. Buchmeiser, I. Ahmad, V. Gurram, P. S. Kumar, *Macromolecules* **2011**, *44*, 4098.

[34]   E. B. Anderson, M. R. Buchmeiser, *Synlett* **2011**, *23*, 185.

[35]   M. R. Buchmeiser, C. Schmidt, D. Wang, *Macromol. Chem. Phys.* **2011**, *212*, 1999.

[36]   T. S. Halbach, J. O. Krause, O. Nuyken, M. R. Buchmeiser, *Macromol. Rapid Commun.* **2005**, *26*, 784.

[37]   T. S. Halbach, J. O. Krause, O. Nuyken, M. R. Buchmeiser, *Polym. Prepr. (Am. Chem. Soc., Div. Polym. Chem.)* **2005**, *46*, 615.

[38]   M. Mayershofer, O. Nuyken, M. R. Buchmeiser, *Macromolecules* **2006**, *39*, 3484.

[39]   C. Schmidt, M. R. Buchmeiser, *Macromol. Symp.* **2007**, *254*, 370.

[40]   Y. S. Vygodskii, A. S. Shaplov, E. I. Lozinskaya, P. S. Vlasov, I. A. Malyshkina, N. D. Gavrilova, P. S. Kumar, M. R. Buchmeiser, *Macromolecules* **2008**, *41*, 1919.

[41]   S. Naumann, J. Unold, W. Frey, M. R. Buchmeiser, *Macromolecules* **2011**, *44*, 8380.

[42]   I. S. Lee, E.-H. Kang, T. L. Choi, *Chem. Sci.* **2012**, *3*, 761.

[43]   G. C. Bazan, E. Khosravi, R. R. Schrock, W. J. Feast, V. C. Gibson, M. B. O´Regan, J. K. Thomas, W. M. Davis, *J. Am. Chem. Soc.* **1990**, *112*, 8378.

[44]   G. Eglinton, A. R. Galbraith, *J. Chem. Soc.* **1959**, 889.

[45]   E. Diez-Barra, A. de la Hoz, A. Moreno, P. Sanchez-Verdu, *J. Chem. Soc. Perkin Trans 1: Org. Bio-Org. Chem.* **1991**, 2589.

[46]   S. Mavila, M. Horecha, A. Kiriy, S. A. Gevorgyan, F. C. Krebs, M. R. Buchmeiser, *Polymer Chem.* **2012**, *4*, 1590.

5. Catalyst Optimization

2   **3**

The material covered in this chapter has appeared in:

5.1 Introduction

The previous chapters illustrated the development and realization of a concept for conducting continuous metathesis reactions under supported biphasic liquid-liquid conditions. In Chapter 3, the development of the dicationic Ru-alkylidene $[Ru(DMF)_3(IMesH_2)(=CH-2-(2-PrO)-C_6H_4)^{2+}][(BF_4^-)_2]$ (for a general structure of Ru-alkylidenes bearing the ionic charge at the metal center see structure A in Figure 18) was reported, with which the feasibility of the concept was verified [1]. Thereby, the decisive factor has been the compounds' tendency to immobilize *selectively* within an ionic liquid phase, a task that cannot be accomplished with neutral Ru-alkylidene complexes [2, 3]. Due to its electrophilic character, this catalyst showed high reactivity towards electron-rich carbon-carbon multiple bonds, however coordinating moieties, e.g., ester groups, coordinated to the Ru-center as well [4]. This in turn led to a decrease in reactivity, what then again could be compensated by increasing the reaction temperature. The main reason for the sensitivity of catalysts of the type A towards coordinating moieties is that the positive charge is located directly at the Ru center (Figure 18) [5, 6]. However, performing continuous metathesis reactions under biphasic conditions with high yields at low temperatures is certainly desirable. On that account, this chapter deals with the development of ionically tagged Ru-alkylidene complexes that meet these requirements.
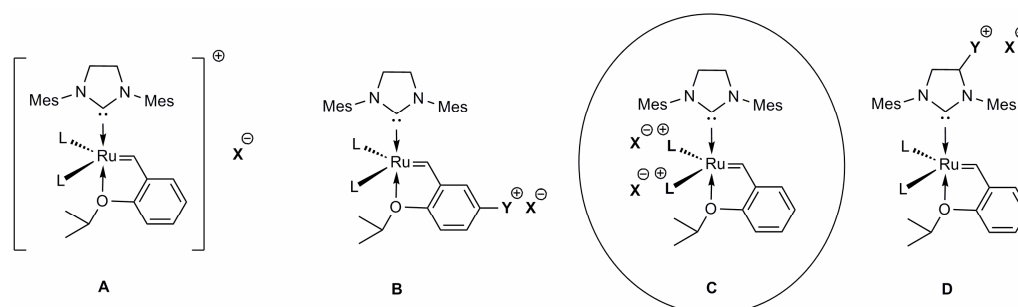
Figure 18. Possibilities for introducing an ionic charge to *Grubbs-Hoveyda* type Ru-alkylidene complexes. A: Ionic Ru center. B: Ionically tagged benzylidene ligand. C: Ligands with ionic functionalities. D: Ionically tagged NHC ligand.

There are few Ru-alkylidene complexes, which exhibit ionically tagged alkylidene-moieties (Type B, Figure 18) [7-16]. Irrespective of their activity, the loss of the alkylidene ligand during the first catalytic cycle and the poor "boomerang" effect of the corresponding styrene derivative[17] represent a serious drawback, particularly

under biphasic conditions, where the intermediary formed neutral Ru-alkylidene would immediately be transferred to the second organic phase. Under biphasic liquid-liquid conditions such a complex would completely lose its charge and thus its tendency to selectively immobilize within a (supported) ionic liquid phase. Despite these obvious disadvantages, there are reports in which complexes with ionic alkylidene ligands were used for metathesis reactions under biphasic conditions, though Ru-leaching was high or has not been quantified at all [7-16]. Therefore, the focus was on creating active metathesis catalysts with a permanent ionic charge by introducing charged ligands. One way to introduce an ionic charge to a Ru-alkylidene complex is the use of ionically tagged NHC ligands (Type D, Figure 18) [18-22]. To optimize the previously introduced concept by preparing more robust catalysts, herein, both chloride ligands in the parent 2nd-generation *Grubbs-Hoveyda* catalyst $[RuCl_2(IMesH_2)(=CH-2-(2-PrO)-C_6H_4)]$ (**GH2**) were substituted by ligands with ionic functionalities (Figure 18, Type C). These ligands will not demerge during the metathesis reaction and, depending on their electronic nature, the reactivity of the catalyst can be further adjusted, the more, since derivatives of *Grubbs-* and *Grubbs-Hoveyda* (**GH**) catalysts possessing electron withdrawing ligands, e.g., perfluorocarboxylates or pseudo-halides are known to show high activity resulting from the high polarization of the Ru-alkylidene moiety [23-28]. In the following, the preparation of the novel ionic Ru-alkylidenes $[Ru[(4-CO_2)(1-CH_3)Py^+)]_2(IMesH_2)(=CH-2-(2-PrO)-C_6H_4)][OTf^-]_2$ (**2**) and $[RuCl[(4-CO_2)(1-CH_3)Py^+)](IMesH_2)(=CH-2-(2-PrO)-C_6H_4)][OTf^-]$ (**3**) possessing ionic carboxylate ligands and their use in various metathesis reactions under both homogeneous and biphasic conditions, including supported liquid phase ones, is reported.

5.2 Results and Discussion

5.2.1 Catalyst Preparation

As outlined above, the primary objective was to create an ionically tagged, Ru-alkylidene complex for metathesis reactions under biphasic conditions, which would retain the ionic charge throughout the entire metathesis reaction and be active at lower temperature towards substrates bearing coordinating functionalities than $[Ru(DMF)_3(IMesH_2)(=CH-2-(2-PrO)-C_6H_4)^{2+}][(BF_4^-)_2]$.[1, 4] Such an ionically tagged metathesis catalyst would *selectively* dissolve in an ionic liquid but not in the second

liquid transport phase, e.g., heptane, which should allow for low metal contamination of the products. For this purpose, the bis-ionically tagged catalyst $[Ru[(4-CO_2)(1-CH_3)Py^+)]_2(IMesH_2)(=CH-2-(2-PrO)-C_6H_4)][OTf]_2$ (**2**), was prepared in 82% isolated yield and was obtained as a red solid by adding two equivalents of $[(1-CH_3)(4-CO_2K)Py^+][BF_4^-]$ to the modified *Grubbs-Hoveyda* type catalyst $[Ru(CF_3SO_3)_2(IMesH_2)(=CH-2-(2-PrO)-C_6H_4)]$ [24] (Scheme 12). Typically, silver salts were used to replace the chlorides in the Grubbs-Hoveyda type complex $[RuCl_2(IMesH_2)(=CH-2-(2-PrO)-C_6H_4)]$ (**GH2**) by the desired ligands. Since the very poor solubility of the pyridinium salt used in the synthesis described herein did not allow for the preparation of highly pure silver salts, the corresponding potassium salts were used to substitute the more weakly bound triflate ligands in the complex $[Ru(CF_3SO_3)_2(IMesH_2)(=CH-2-(2-PrO)-C_6H_4)]$ [24] instead (Scheme 12).
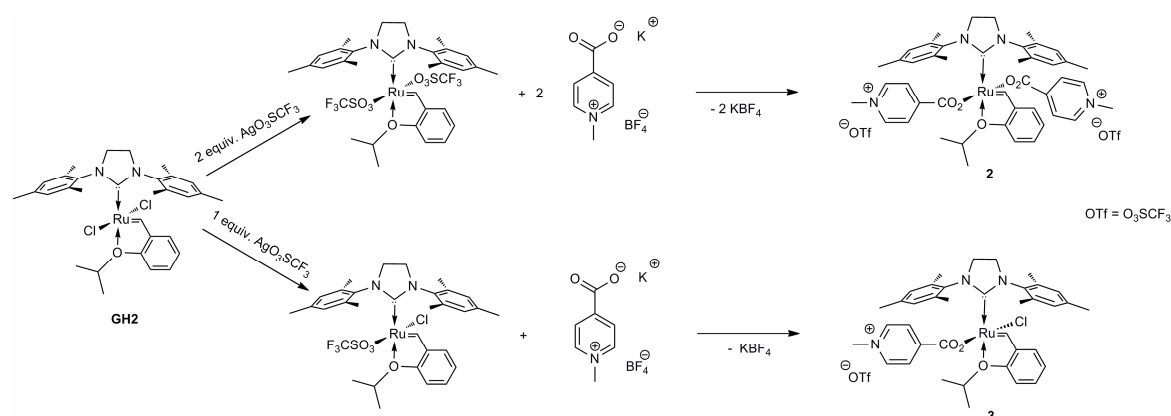
Scheme 12. Syntheses of the ionic Ru complexes **2** and **3**.

In an analogous manner, the ionic monocarboxylato-monochloro-Ru-alkylidene $[RuCl[(4-CO_2)(1-CH_3)Py^+)](=CH-2-(2-PrO)-C_6H_4)(IMesH_2)][OTf]$ (**3**) was prepared in 89% isolated yield by adding one equivalent of $[(1-CH_3)(4-CO_2K)Py^+][BF_4^-]$ to $[RuCl(CF_3SO_3)(IMesH_2)(=CH-2-(2-PrO)-C_6H_4)]$ (Scheme 12). In fact, catalyst **3** can be expected to be more active than the bis-ionic Ru-alkylidene **2**. Thus, compared to the pyridinium-carboxylate ligand, the chloride is more electron-withdrawing and should therefore lead to a more polarized Ru=C bond than in **2**. The absence of a signal for BF_4^- in the ^{19}F NMR spectrum implies its substitution by the triflate (OTf⁻, $CF_3SO_3^-$)-ligand, which now acts as the counter ion. In fact, solely the signal for OTf⁻ was observed while BF_4^- was detected in the precipitate of KBF_4 that formed during the reaction in CH_2Cl_2. After removal of the potassium tetrafluoroborate, the product was precipitated in diethyl ether. The fact, that complex **3** was obtained as a pure

compound is remarkable since monocarboxylato-monochloro-Ru-alkylidenes are known to undergo fast ligand-scrambling, and thereby disproportionate into the corresponding bis-carboxylate and bis-chloride species (Scheme 13)[24, 29, 30]. In fact, the disproportionation rate of **3**, which can be obtained in a pure form, is quite low at ambient temperature. Thus, after 24 hours in solution, only 8% of the bis-carboxylate complex **2** and the **GH2** complex could be detected by NMR spectroscopy. However, at 40°C, a temperature typical for many metathesis reactions, the disproportionation proceeds more rapidly (Figure 19).
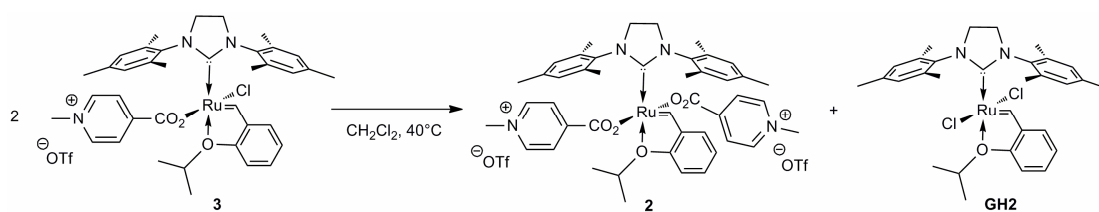
Scheme 13. Disproportionation reaction of the mono-carboxylate complex **3** in CH_2Cl_2.
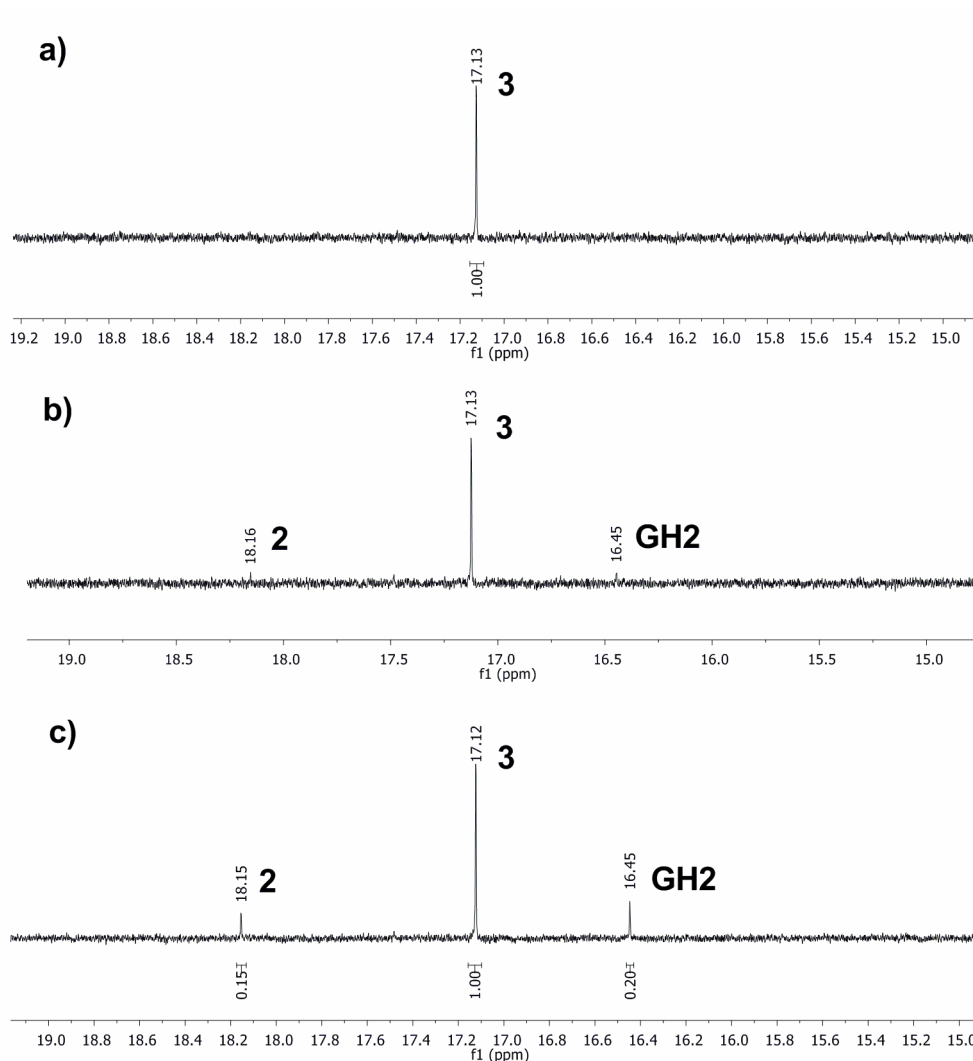
Figure 19. Disproportionation of **3** at 40°C in CD$_2$Cl$_2$. a): Complex **3** after 1 h in CD$_2$Cl$_2$ at 40°C. b): Complex **3** after 2 h in CD$_2$Cl$_2$ at 40°C. c): Complex **3** after 24 h in CD$_2$Cl$_2$ at 40°C.

As can be followed by ^{1}H NMR analysis, disproportionation was first detected after 2 h at 40°C. Besides the signal for the alkylidene proton of **3** at δ=17.13 ppm (CD$_2$Cl$_2$), the signals for the alkylidene protons of **2** at δ=18.16 ppm and of **GH2** at δ=16.45 ppm appeared (Figure 19). After 8 h in solution at 40°C, the bis-carboxylate complex **2** and bis-chloride complex **GH2** amounted to 38%, an equilibrium concentration, which did not change any further (Figure 20). At 80°C, the disproportionation reaction proceeded more rapidly, and 40% of the initial amount of complex **3** disproportionated within 30 minutes. While the ratio between **2** and **GH2** was about 1 : 1 at lower temperature, it decreased to 1 : 5 at 80°C suggesting significant decomposition of **2** at this temperature (Figure S48, Appendix).

83
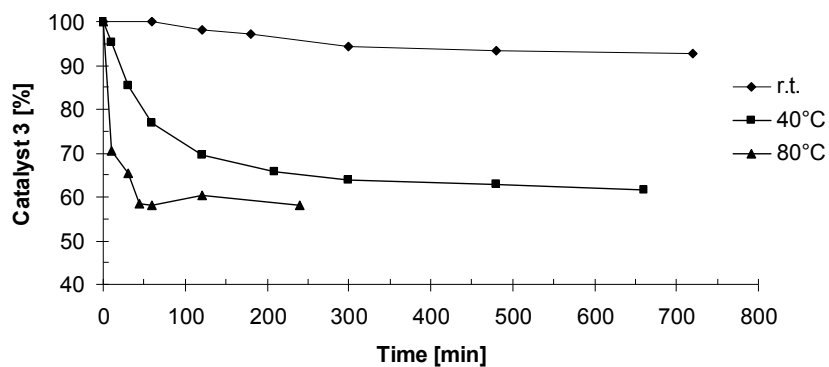
Figure 20. Disproportionation of catalyst **3** in solution at different temperatures.

5.2.2 Homogeneous Metathesis Reactions Using **2** and **3** in Organic Solvents

In order to screen activities and to compare their performance to the one of $[Ru(DMF)_3(IMesH_2)(=CH-2-(2-PrO)-C_6H_4)^{2+}][(BF_4^-)_2]$, initiators **2** and **3** were subjected to ring-closing metathesis (RCM) reactions of various dienes in CH_2Cl_2 at T=40°C, as well as in $C_2H_4Cl_2$ at T=70°C. 1,7-Octadiene, diethyl diallyl malonate (DEDAM), diethyl dimethallyl malonate, *tert*-butyl-*N,N*-diallyl carbamate, *N,N*-diallylacetamide and *N,N*-diallyltrifluoroacetamide (DAFA) served as substrates. In addition, the self-metathesis reaction of methyl oleate was examined (Table 13).

Table 13. Metathesis reactions in organic solvents promoted by catalysts **2** and **3**.

Substrate	Catalyst [mol.-%]	Solvent	T [°C]	TON[a]
DEDAM	**2** [0.1]	CH_2Cl_2	40	380
		$C_2H_4Cl_2$	70	400
	3 [0.05]	CH_2Cl_2	40	> 2000
tert-butyl-*N,N*-diallyl carbamate	**2** [0.1]	CH_2Cl_2	40	150
		$C_2H_4Cl_2$	70	200
	3 [0.05]	CH_2Cl_2	40	1000
1,7-octadiene	**2** [0.1]	CH_2Cl_2	40	500
		$C_2H_4Cl_2$	70	550
	3 [0.05]	CH_2Cl_2	40	> 2000
DAFA	**2** [0.1]	CH_2Cl_2	40	400
		$C_2H_4Cl_2$	70	550
	3 [0.05]	CH_2Cl_2	40	1300
N,N-diallylacetamide	**2** [0.1]	CH_2Cl_2	40	300
		$C_2H_4Cl_2$	70	360
	3 [0.1]	CH_2Cl_2	40	300
diethyl di(methallyl) malonate	**2** [1.0]	CH_2Cl_2	40	30
		$C_2H_4Cl_2$	70	30
	3 [1.0]	CH_2Cl_2	40	60
methyl oleate	**2** [0.05]	CH_2Cl_2	40	700
		$C_2H_4Cl_2$	70	850
		Toluene	100	800
	3 [0.05]	CH_2Cl_2	40	1300

[a] Conversion was determined by GC-MS

The reaction kinetics for the RCM of 1,7-octadiene and *N,N*-diallyl trifluoroacetamide promoted by **2** at 40°C and 70°C, respectively, are given in Figure S49 in the Appendix. In the RCM of 1,7-octadiene, a maximum turn-over number (TON) of roughly 500 was obtained at both temperatures. As expected, the reaction rate was significantly higher at 70°C. The same was observed in the RCM of DAFA, where

final TONs of 400 and 550, respectively, were found. For all substrates listed in Table 13 the maximum TON did not increase tremendously when increasing the temperature, though the reactions proceed more rapidly. These findings indicate that complex **2** exhibits, *a priori*, a certain reactivity towards diverse olefins, which is primarily not limited by decomposition at elevated temperature. The fact, that **2** is in contrast to $[Ru(DMF)_3(IMesH_2)(=CH-2-(2-PrO)-C_6H_4)^{2+}][(BF_4^-)_2]^{[1]}$ already active at low temperatures suggests that reactivity is not affected by substrates with coordinating moieties. Notably, **3** allows for substantial TONs of 60 in the RCM of diethyl di(methallyl) malonate.

In the self-metathesis of methyl oleate, a final TON of 700 was obtained at 40°C. In this reaction, alongside the *E*-isomer, only the primary metathesis products were observed. When conducting the reaction at 70°C, conversion slightly increased, however, again, the *E*-isomer remained. Since methyl oleate isomerizes already at room temperature,[1] this process competes with the metathesis reaction. At higher temperature, self-metathesis predominates. Conducting the reaction at 100°C gave a TON of 800, when considering exclusively the formation of primary metathesis products. The reaction proceeded faster than at 70°C, however, at this temperature selectivity decreased, i.e., products resulting from secondary metathesis processes were observed, too. These compounds amounted to about 10% of the total product fraction.

For most reactions, much higher conversions were obtained when using the mono-carboxylato-chloro complex **3** instead of **2**, which is attributed to a stronger polarization of the Ru-alkylidene[27]. As outlined above, this complex slowly disproportionates when dissolved in CH_2Cl_2, thereby generating the neutral complex $[RuCl_2(IMesH_2)(=CH-2-(2-PrO)-C_6H_4)]$ (**GH2**) (Scheme 13, Figure 19). Therefore it is not possible to claim, without restrictions, that the high conversions are *solely* caused by the defined species **3**. In fact, the difficulty, that the active species at reaction conditions might not be identical to the one initially used may generally arise for all *Grubbs-Hoveyda* type initiators bearing mixed anionic ligands and caution should be taken in interpreting the results [30, 31]. However, in view of a reaction time of 3 hours and the slow propensity of **3** to disproportionate (*vide supra*), the TONs observed for **3** at 40°C can, at least to a major extent, be attributed to **3** and not to the **GH2**-complex, which forms only slowly upon disproportionation.

5.2.3 Metathesis Reactions Under Biphasic Conditions (Organic Solvent/ Ionic Liquid) Using Catalysts **2** and **3**

The RCM of DAFA, DEDAM, 1,7-octadiene and *tert*-butyl *N,N*-diallyl carbamate as well as the self-metathesis of methyl oleate were carried out under biphasic conditions using [BDMIM$^+$][BF$_4^-$] as ionic liquid phase and either neat reactants or heptane as the second liquid phase (Table 14). Despite the comparably small amount of ionic liquid and the large amount of polar substrate, which both favor the transfer of catalyst into the non-polar phase, a low catalyst leaching of ≤ 0.4% into the product phase was observed for all reactions when using the bis-ionically tagged complex **2**. This leaching translates into Ru-contaminations < 2.5 ppm in the products. Notably, for reactions with low conversions the Ru-leaching was below the detection limit of inductively-coupled plasma-optical emission spectroscopy (ICP-OES) and is therefore reported as 0%. The TONs observed for **2** under biphasic conditions were in the same range than those determined for reactions in solution. In the RCM of DEDAM, TONs up to 700 were obtained, exceeding those observed in an organic solvent (Table 13). Due to the low polarity of 1,7-octadiene and its immiscibility with the IL, its RCM was performed without the use of another liquid transport phase. Catalyst leaching for this reaction was negligibly low (0.03%) and a TON of 500 was obtained, which is within the same range than as observed in CH$_2$Cl$_2$ at 40°C. Only the formation of cyclohexene and no isomerization products were observed at this temperature.

In the self-metathesis of methyl oleate catalyzed by **2**, a TON of 560 was obtained in case the reaction was performed under biphasic conditions. Again, for this reaction the TON was similar to the one determined in solution. As observed in solution, reaction monitoring *via* GC-MS again revealed the selective formation of the two desired cross-metathesis products as well as isomerization of the *Z*-double bond in the substrate molecule.

Table 14. Metathesis reactions under biphasic conditions ([BDMIM$^+$][BF$_4^-$])/heptane) using **2** and **3**. T=40°C.

Substrate	Catalyst [mol-%]	TON[a]	Ru leaching [%][b]	Ru contamination [ppm]
DAFA[c]	**2** [0.1]	400	0.04	0.4
	3 [0.05]	1300	0.17	0.9
DEDAM[d]	**2** [0.1]	700	0.13	1.3
	3 [0.05]	1800	0.27	1.4
1,7-octadiene[e]	**2** [0.1]	500	0.03	0.3
	3 [0.05]	> 2000	0.12	0.6
tert-butyl *N,N*-diallycarbamate	**2** [0.2]	100	0	0
	3 [0.1]	500	0.24	2.4
methyl oleate[f]	**2** [0.05]	560	0.22	1.1
	3 [0.05]	940	0.35	1.8

[a] Determined by GC-MS after 12 h. [b] % of initial Ru (catalyst) loading. [c] Heptane as second liquid phase; IL (0.1 g), heptane (2.0 g), DAFA (0.2 g). [d] Heptane as second liquid phase; IL (0.1 g), heptane (2.0 g), DEDAM (0.25 g). [e] Neat; IL (0.1 g), 1,7-octadiene (0.1 g). [f] Neat; IL (0.1 g), methyl oleate (0.5 g).

Again, much higher conversion was achieved in case the mono-ionic initiator **3** was used for reactions under biphasic conditions (Table 14). Ru leaching was low (≤ 0.35%), and TONs were again comparable to the ones obtained in solution for that particular catalyst.

5.2.4 RCM of 1,7-Octadiene and Self-Metathesis of Methyl Oleate Promoted by **2** and **3** Under Biphasic Conditions Using Monolith-Supported Ionic Liquids

Since catalysts **2** and **3** displayed about the same reactivity in homogeneous as well as in biphasic metathesis, the self-metathesis of methyl oleate as well as the RCM of 1,7-octadiene were carried out in a continuous manner. In Chapter 3, a method to perform continuous metathesis under biphasic liquid-liquid conditions using a

monolith-supported ionic liquid phase (SILP) was introduced, which was herein applied to the bis-ionic catalyst **2** as well as to the mono-ionic complex **3**. For these purposes, ROMP-derived polymeric monoliths were prepared and surface-grafted with norborn-5-en-2-ylmethyl-*N,N,N*-trimethylammonium tetrafluoroborate (**M2**). The ionic liquid, i.e. [BDMIM$^+$][BF$_4^-$], containing, e.g., catalyst **2** was then immobilized on the monoliths' surface. Importantly, the concept enables continuous product formation, simply by cycling reactants through a monolithic support containing a suitable catalyst dissolved in an IL. The fact that a *biphasic liquid-liquid* system is used definitely widens the range of potentially accessible substrates. Due to their low polarity, both methyl oleate and 1,7-octadiene were used as neat reactants. Reactions were performed at a temperature of 40°C as well as at 80°C when catalyst **2** was used (Table 15). Reactions catalyzed by complex **3** were performed at 40°C. For the self-metathesis of methyl oleate, at 40°C a TON of 500, comparable to the one obtained under biphasic conditions, was observed for catalyst **2** (Table 14). Catalyst leaching was only 0.08% of the initial amount of initiator. Since the reaction proceeded slowly at this temperature it was required to cycle the reactant through the supported catalyst, what in turn demonstrated its stability during a prolonged period of time. An increase in temperature to 80°C accelerated the reaction; maximum conversion was already obtained after 60 min, concomitantly, ruthenium leaching slightly increased to 0.24%. The same trend was observed in the RCM of 1,7-octadiene, an increase in reaction temperature from 40°C to 80°C resulted in a fivefold shorter reaction time when using the dicationic complex **2**. Catalyst contamination of the product phase was low in this case, too (0.2%). Importantly, despite ethylene is generated during the RCM of 1,7-octadiene, TONs comparable to those observed in unsupported reactions were obtained. Probably this is because bis-cationic catalyst **2** is a relatively inactive catalyst, giving relatively slow reaction rates what in turn goes along with a comparably slow formation of ethylene.

Again for reactions under supported biphasic conditions (Table 15), much higher conversion was achieved in case the mono-ionic initiator **3** was used, as was observed for reactions in organic solvents (Table 13) and under biphasic conditions (Table 14). For the self-metathesis of methyl oleate TONs were comparable to the ones obtained under biphasic conditions for that particular catalyst and the Ru leaching was low ($\leq$ 0.43%). Maximum conversion was obtained within only 100 min for the self-metathesis of methyl oleate and within 35 min in case of the RCM of 1,7-

octadiene. Considering the RCM of 1,7-octadiene, the drop in TON is more pronounced in case of catalyst **3**. Whereas a TON of > 2000 was observed in biphasic unsupported reactions, in continuous monolith supported reactions just 1450 turnovers were obtained. This in turn can be explained by the relatively high activity of mono-ionic catalyst **3**, giving relatively high reaction rates what in turn goes along with a fast formation of relatively large amounts of ethylene. The reactions were performed at 40°C in order to minimize the influence of the disproportionation reaction which is more pronounced at elevated temperatures.

No isomerization reactions were observed and both catalysts yielded solely products resulting from primary metathesis under supported biphasic conditions, as well.

Table 15. Metathesis reactions under continuous monolith-supported liquid-liquid conditions using **2** and **3**.

Substrate	Flow-rate [mL/min]	Catalyst [mol-%]	T [°C]	t [min][a]	TON	Ru leaching [%][b]	Ru contamination [ppm]
methyl oleate	0.1	**2** [0.1]	40	240	500	0.08	0.8
	0.1	**2** [0.1]	80	60	600	0.24	2.4
	0.1	**3** [0.1]	40	100	800	0.22	2.2
1,7-octadiene	0.1	**2** [0.1]	40	100	550	0.11	1.1
	0.1	**2** [0.1]	80	20	550	0.20	2.0
	0.1	**3** [0.05]	40	35	1450	0.43	2.2

[a] Time to maximum TON, cyclization of the substrates was required. The volume of the column used was 1.66 mL[1]. The total porosity of the monolith was 80%. 3 mg of catalysts **2** and **3** have been dissolved in 100 mg [BDMIM$^+$][BF$_4^-$], respectively. [b] based on the initial amount of catalyst.

5.3 Conclusions

The novel ionic Ru-alkylidene complexes, $[Ru[(4-CO_2)(1-CH_3)Py^+)]_2(IMesH_2)(=CH-2-(2-PrO)-C_6H_4)][OTf^-]_2$ (**2**) and $[RuCl[(4-CO_2)(1-CH_3)Py^+)](IMesH_2)(=CH-2-(2-PrO)-C_6H_4)][OTf^-]$ (**3**), were synthesized from $[Ru(CF_3SO_3)_2(IMesH_2)(=CH-2-(2-PrO)-C_6H_4)]$ and $[RuCl(CF_3SO_3)(IMesH_2)(=CH-2-(2-PrO)-C_6H_4)]$, respectively, and were used in various RCM-reactions in solution as well as under biphasic liquid-liquid conditions. Catalysts **2** and **3** were also used in the continuous metathesis of methyl oleate and 1,7-octadiene under supported liquid-liquid conditions. Both catalysts could successfully be immobilized within an ionic liquid phase, as illustrated by the low Ru-leaching ($\leq 0.4\%$). Compared to the dicationic complex $[Ru(DMF)_3(IMesH_2)(=CH-2-(2-PrO)-C_6H_4)^{2+}]$ $[(BF_4^-)_2]$, which required elevated reaction temperatures to be active, **2** and **3** are metathesis active for a variety of substrates at low temperatures. Clearly, the use of ionic ligands preserves the catalytic activity for substrates with coordinating functionalities. At the same time it also guarantees for an effective and permanent immobilization within a polar stationary phase, i.e. an ionic liquid. **2** and **3** showed comparable reactivity when performing the reactions either in solution or under biphasic conditions. An increase in temperature considerably accelerates the reaction, yet it is not leading to significantly higher TONs. Complex **3**, possessing one chloride and one ionic carboxylate ligand, is showing an increased activity compared to complex **2**. In solution, the disproportionation reaction of this compound was traced by means of ^{1}H NMR at elevated temperature, whereby the bis-ionic species **2** and the neutral complex $[RuCl_2(IMesH_2)(=CH-2-(2-PrO)-C_6H_4)]$ (**GH2**) formed. This finding illustrates an intermolecular anionic ligand exchange with *Grubbs-Hoveyda* type initiators bearing mixed anionic ligands.

5.4 References

[1]   B. Autenrieth, W. Frey, M. R. Buchmeiser, *Chem. Eur. J.* **2012**, *18*, 14069.

[2]   J. H. Kim, B. Y. Park, S.-W. Chen, S.-g. Lee, *Eur. J. Org. Chem.* **2009**, 2239.

[3]   R. C. Buijsman, E. van Vuuren, J. G. Sterrenburg, *Org. Lett.* **2001**, *3*, 3785.

[4]   B. Autenrieth, E. B. Anderson, D. Wang, M. R. Buchmeiser, *Macromol. Chem. Phys.* **2013**, *214*, 33.

[5]   O. Songis, A. M. Slawin, C. S. Cazin, *Chem. Comm.* **2012**, *48*, 1266.

[6]   M. S. Sanford, L. M. Henling, R. H. Grubbs, *Organometallics* **1998**, *17*, 5384.

[7]   Q. Yao, M. Sheets, *J. Organomet. Chem.* **2005**, *690*, 3577.

[8]   J. B. Binder, I. A. Guzei, R. T. Raines, *Adv. Synth. Catal.* **2007**, *349*, 395.

[9]   E. Borre, M. Rouen, I. Laurent, M. Magrez, F. Caijo, C. Crevisy, W. Solodenko, L. Toupet, R. Frankfurter, C. Vogt, A. Kirschning, M. Mauduit, *Chem. Eur. J.* **2012**, *18*, 16369.

[10]   S. W. Chen, J. H. Kim, K. Y. Ryu, W. W. Lee, J. Hong, *Tetrahedron* **2009**, *65*, 3397.

[11]   H. Clavier, N. Audic, J.-C. Guillemin, M. Mauduit, *J. Organomet. Chem.* **2005**, *690*, 3585.

[12]   C. Thurier, C. Fischmeister, C. Bruneau, H. Olivier-Bourbigou, P. H. Dixneuf, *J. Mol. Catal. A: Chem.* **2007**, *268*, 127.

[13]   Q. Yao, Y. Zhang, *Angew. Chem.* **2003**, *115*, 3517.

[14]   G. Liu, H. He, J. Wang, *Adv. Synth. Catal.* **2009**, *351*, 1610.

[15]   X. Ding, X. Lv, B. Hui, Z. Chen, M. Xiao, B. Guo, W. Tang, *Tetrahedron Lett.* **2006**, *47*, 2921.

[16]   N. Audic, H. Clavier, M. Mauduit, J.-C. Guillemin, *J. Am. Chem. Soc.* **2003**, *125*, 9248.

[17]   T. Vorfalt, K.-J. Wannowius, H. Plenio, *Angew. Chem.* **2010**, *122*, 5665.

[18]   M. Kluciar, K. Grela, M. Mauduit, *Dalton Trans.* **2013**, *42*, 7354.

[19]   W. Kosnik, K. Grela, *Dalton Trans.* **2013**, *42*, 7463.

[20]   D. M. Lynn, B. Mohr, R. H. Grubbs, L. M. Henling, M. W. Day, *J. Am. Chem. Soc.* **2000**, *122*, 6601.

[21]   K. Skowerski, G. Szczepaniak, C. Wierzbicka, L. Gulajski, M. Bieniek, K. Grela, *Catal. Sci. Technol.* **2012**, *2*, 2424.

[22]   K. Skowerski, C. Wierzbicka, G. Szczepaniak, L. Gulajski, M. Bieniek, K. Grela, *Green Chem.* **2012**, *14*.

[23]   J. O. Krause, M. T. Zarka, U. Anders, R. Weberskirch, O. Nuyken, M. R. Buchmeiser, *Angew. Chem.* **200**3, *115*, 6147.

[24]   J. O. Krause, O. Nuyken, K. Wurst, M. R. Buchmeiser, *Chem. Eur. J.* **2004**, *10*, 777.

[25]   J. O. Krause, O. Nuyken, M. R. Buchmeiser, *Chem. Eur. J.* **2004**, *10*, 2029.

[26]   T. S. Halbach, S. Mix, D. Fischer, S. Maechling, J. O. Krause, C. Sievers, S. Blechert, O. Nuyken, M. R. Buchmeiser, *J. Org. Chem.* **2005**, *70*, 4687.

[27]   S. Naumov, M. R. Buchmeiser, *Organometallics* **2012**, *31*, 847.

[28]   B. F. Straub, *Adv. Synth. Catal.* **2007**, *349*, 204.

[29]   M. R. Buchmeiser, *Chem. Rev.* **2009**, *109*, 303.

[30]   K. Tanaka, V. P. Böhm, D. Chadwick, M. Roeper, D. C. Braddock, *Organometallics* **2006**, *25*, 5696.

[31]   G. Occhipinti, F. R. Hansen, K. W. Törnroos, V. R. Jensen, *J. Am. Chem. Soc.* **2013**, *135*, 3331.

6. Experimental and Spectroscopic Data

6.1 General

Chemicals and Solvents

Unless noted otherwise, all preparations were performed in a LabMaster 130 glove box (MBraun; Garching, Germany) or by standard *Schlenk* techniques under a N_2 atmosphere. DMF was purchased from Sigma Aldrich (Munich, Germany) and passed through a pad of alumina prior to use. Starting materials were purchased from Aldrich, TCI Europe (Zwijndrecht, Belgium), and ABCR (Karlsruhe, Germany) and used without further purification. $CDCl_3$ and CD_2Cl_2 were distilled from CaH_2 and stored over molecular sieves (4Å). CH_2Cl_2, THF, diethyl ether, toluene and pentane were purchased from J. T. Baker (Devender, Netherlands) and were dried by using an MBraun SPS-800 solvent purification system with alumina drying columns.

Nuclear Magnetic Resonance Spectroscopy (NMR)

NMR spectra were recorded on a Bruker Avance III 400 spectrometer or a Bruker DRX 250 spectrometer in the indicated solvent at 25°C and data are listed in parts per million downfield from tetramethylsilane (TMS) as an internal standard.

Gas-Chromatography Mass-Spetroscopy (GC-MS)

GC-MS data were obtained by using an Agilent Technologies 5975C inert MSD with triple-axis detector, an 7693 autosampler, and a 7890A GC system equipped with a SPB-5 fused silica column (34.13 m x 0.25 mm x 0.25 µm film thickness). The injection temperature was set to 150°C. The column temperature ramped from 45 to 250°C within 8 min, and was then held for further 5 min. The column flow was 1.05 mL min^{-1}.

UV-Visible Spectroscopy

UV/Vis measurements were carried out in $CHCl_3$ or DMF on a Perkin Elmer Lambda 2.

Infrared Spectroscopy

IR spectra were measured on a Bruker IFS 28 using ATR technology in NaCl cuvettes or as KBr pellets.

Size Exclusion Chromatography (SEC)

SEC measurements were carried out on a system consisting of a Waters 515 HPLC pump, a Waters 2707 autosampler, PolyPore columns (300 x 7.5 mm, Agilent technologies, Böblingen, Germany), a Waters 2489 UV/vis- and a Waters 2414 refractive index detector. For calibration, polystyrene standards with $800 < \overline{M}_n < 2\ 000\ 000$ g/mol were used. The flow rate was set to 1 mL min^{-1}. Narrow polystyrene (PS) standards were purchased from Polymer Standard Service (PSS, Mainz, Germany). When using DMF as solvent, poly(methyl methacrylate) (PMMA) standards were used, which were purchased from PSS as well. Prior to measurements, polymer solutions were filtered through Millipore 0.20 µm filters.

Inverse Size Exclusion Chromatography (ISEC)

For ISEC measurements, a G1314B UV detector (Agilent 1200 series) and a G1310A isopump (Agilent 1200 series) equipped with an Agilent instant pilot G4208A and a manual sample injection system were used. Polystyrene (PS) standards ($800 < \overline{M}_n < 2\ 000\ 000$ g mol^{-1}) used for ISEC were purchased from Polymer Standard Service (Mainz, Germany).

Elemental Analysis

Elemental analysis was done in a Carlo Erba elemental analyzer (1106) at the Institute of Organic Chemistry, University of Stuttgart, Germany.

Matrix-Assisted Laser Desorption Ionization Time-of-Flight (MALDI-TOF)

Positive ion MALDI-TOF measurements were performed on a Bruker Autoflex III device with smart beam. Measurements were carried out in the reflector mode. Samples were prepared from THF/CHCl$_3$ (5:3) solution by mixing dithranol (10 mg/mL), the polymer sample (5 mg/mL), and sodium trifluoromethane sulfonate (17 mg/mL) in a ratio of 20:5:2.

Dynamic Light Scattering (DLS)

Dynamic light scattering (DLS) was conducted on a ZEN3600 Zetasizer Nano-ZS (Malvern Instruments GmbH). A glass cuvette was used to analyze 1 mg/mL polymer solutions at 20 and 40 ºC. The equilibration time between runs was 3 min, and 3 runs were made with an average of 15 measurements each and a 1 s delay between each measurement.

Inductively Coupled Plasma Optical Emission Spectrometry (ICP-OES)

The Ru content was measured by ICP-OES (ion line at λ=240.272 nm, background lines at λ_1= 240.254 nm and λ_2= 240.295 nm) using a Spectro Arcos device (Ametek GmbH; Meerbusch, Germany). Standardization was carried out with Ru standards containing 0.1, 0.5, 1.0, 2.5, and 5 ppm of Ru. The Ru content of both the support and the product fraction was determined by dissolving samples (100 mg) in aqua regia.

6.2 "Design of the Monolithic Support Material"

Norborn-5-en-2-ylmethyl-(3-butyl-2-methylimidazolium)tetrafluoroborate M1a

Norborn-5-en-2-ylmethyl-(3-butyl-2-methylimidazolium)bromide **M1a-Br**: Exo, endo-5-norbornen-2-yl-methyl bromide was prepared by Diels-Alder cycloaddition between freshly cracked cyclopentadiene (66.0 g, 1.0 mol) and allyl bromide (121.0 g, 1.0 mmol). The reaction proceeded at 180°C for 16 h in a steel autoclave. The substance was purified by distillation under reduced pressure (45°C, 0.5 mbar) and yielded as a colorless liquid.

A solution of 1-*n*-butyl-2-methylimidazole (4.69 g, 25.0 mmol) in THF (10 mL) was added to a solution of *exo,endo*-norborn-5-en-2-ylmethyl bromide (3.72 g, 20.0 mmol, in 15 mL THF). The reaction mixture was heated to 70°C and was kept at this temperature for 48 h under N_2. After removing the solvent *in vacuo*, a brownish, highly viscous liquid was obtained. For purification, the residue was dissolved in CH_2Cl_2 and reprecipitated in diethyl ether for several times. Norborn-5-en-2-ylmethyl-(3-butyl-2-methylimidazolium)bromide was yielded as a yellowish, waxy solid (4.33 g, 13.3 mmol, 67%). ^{1}H NMR (400.13 MHz, $CDCl_3$): δ = 7.52 - 7.43 (m, 2 H), 6.27 - 6.10 (m, 2 H), 4.39 – 3.96 (m, 4 H), 2.83 – 2.70 (m, 2 H), 1.90 – 1.85 (m, 4H), 1.35 – 1.32 (m, 5 H), 0.94 – 0.90 ppm (m, 3 H). ^{13}C-NMR (100.61, $CDCl_3$): δ = 143.4, 138.0, 136.0, 122.4, 122.0, 53.2, 50.2, 49.3, 44.6, 42.8, 39.7, 32.2, 30.5, 20.1, 14.0, 11.6 ppm. IR (film): $\bar{\nu}$ = 3423 (b), 3053 (s), 2958 (vs), 2868 (s), 1616 (m), 1579 (m), 1527 (s), 1456 (s), 1425 (m), 1377 (m), 1339 (m), 1261 (b), 717 (s), 669 cm^{-1} (m).

Norborn-5-en-2-ylmethyl-(3-butyl-2-methylimidazolium)tetrafluoroborate **M1a**: Under exclusion of light, an aqueous solution of **M1a-Br** (2 g, 6.2 mmol,) was added dropwise to a solution of silver tetrafluoroborate (1.19 g, 6.2 mmol) in water at 50°C. The reaction mixture was stirred for 1 h, then the yellow precipitate of silver bromide was filtered off and the solvent was removed *in vacuo*. Compound **M1a** was obtained as a beige colored waxy solid (1.57 g, 4.7 mmol, 77%). ^{1}H NMR (400.13 MHz, $CDCl_3$): δ = 7.62 - 7.53 (m, 2 H), 6.49 - 6.33 (m, 2 H), 4.65 - 4.16 (m, 4 H), 3.03 - 2.88 (m, 2 H), 2.00 - 1.96 (m, 4H), 1.48 - 1.40 (m, 5 H), 0.82 - 0.77 ppm (m, 3 H). ^{13}C NMR (100.61 MHz, $CDCl_3$): δ = 146.2, 138.8, 136.8, 123.1, 122.7, 55.1, 51.1, 48.6, 45.2, 41.2, 40.3, 33.0, 29.7, 20.6, 15.1, 12.4 ppm; ^{19}F NMR (376.50 MHz, $CDCl_3$): δ =

-150.2 ppm; IR (film): $\bar{\nu}$ = 3176 (m), 3141 (s), 3056 (m), 2960 (vs), 2870 (s), 1583 (s), 1527 (s), 1444 (s), 1369 (m), 1340 (m), 1265 (vs), 1036 (vs), 731 (vs), 523 cm^{-1} (s); MS (ESI): 245.20 [$C_{16}H_{25}N_2$].

Norborn-5-en-2-ylmethyl-(2,3-dimethylimidazolium)tetrafluoroborate M1b

Norborn-5-en-2-ylmethyl-(2,3-dimethylimidazolium)bromide **M1b-Br**: The same synthetic procedure as described for the synthesis of **M1a** was used, thereby substituting 1-*n*-butyl-2-methylimidazole by 1,2-dimethylimidazole (2.42 g, 25.0 mmol). Purification by repeated precipitation from diethyl ether yielded **M1b-Br** as a white solid (5.18 g, 18.3 mmol, 92%).

^{1}H NMR (400.13 MHz, CDCl$_3$): δ = 7.70 – 7.42 (m, 2 H), 6.33 - 6.15 (m, 2 H), 4.25 – 4.21 (m, 1 H), 4.04 (s, 3 H), 3.88 – 3.84 (m, 2 H), 2.93 – 2.87 (m, 1 H), 2.81 (s, 3 H), 2.58 – 2.56 (m, 1 H), 1.99 – 1.95 (m, 1 H), 1.48 – 1.34 ppm (m, 3 H); ^{13}C-NMR (100.61, CDCl$_3$): δ = 143.5, 137.3, 135.4, 123.1, 120.8, 52.6, 49.5, 43.9, 42.2, 39.0, 36.2, 29.9, 11.0 ppm; IR (KBr): $\bar{\nu}$ = 3446 (b), 3053 (m), 2960 (m), 2864 (m), 2354 (m), 1684 (m), 1587 (s), 1535 (s), 1458 (m), 1418 (m), 1335 (m), 1246 (s), 1146 (m), 1113 (m), 930 (m), 779 (s), 714 (s), 652 cm^{-1} (m); MS (ESI): *m/z* = 203.15 for [$C_{13}H_{19}N_2$].

Norborn-5-en-2-ylmethyl-(2,3-dimethylimidazolium)tetrafluoroborate **M1b**: The exchange of the anion was performed in a way equal to the preparation of **M1a** and **M1b** was yielded in form of a waxy, colorless solid (1.68 g, 5.8 mmol, 94%). ^{1}H NMR (400.13 MHz, CDCl$_3$): *δ* = 7.81 – 7.61 (m, 2 H), 6.42 - 6.29 (m, 2 H), 4.45 – 4.38 (m, 1 H), 4.11 (s, 3 H), 4.02 – 3.96 (m, 2 H), 3.05 – 2.99 (m, 1 H), 2.74 (s, 3 H), 2.38 – 2.32 (m, 1 H), 1.88 – 1.85 (m, 1 H), 1.46 – 1.30 ppm (m, 3 H); ^{13}C NMR (100.61 MHz, CDCl$_3$): *δ* = 145.2, 136.9, 134.1, 123.6, 122.2, 53.8, 50.6, 44.3, 43.1, 39.8, 35.7, 31.9, 13.1 ppm; ^{19}F NMR (376.50 MHz, CDCl$_3$): *δ* = -150.2 ppm; IR (KBr): $\bar{\nu}$ = 3421 (b), 3149 (m), 3053 (m), 2958 (m), 2870 (m), 2343 (m), 1589 (m), 1539 (m), 1429 (m), 1336 (m), 1246 (m), 1039 (vb), 837 (m), 750 (s), 714 (s), 652 (m), 519 cm^{-1} (s); MS (ESI): *m/z* = 203.15 for [$C_{13}H_{19}N_2$].

Norborn-5-en-2-ylmethyl-*N,N,N*-trimethylammonium tetrafluoroborate M2

*(exo,endo-Norborn-5-en-2-ylmethyl) dimethylamine: (exo,endo-*Norborn-2-en-5-yl-methyl) dimethylamine was prepared by Diels-Alder cycloaddition between freshly cracked cyclopentadiene (14.1 g, 214 mmol) and dimethylallylamine (18.20 g, 214 mmol). Hydroquinone (10 mg) was added and the reaction proceeded at 200 °C for 48 h in a steel autoclave. Fractionated distillation (40 °C, 0.1 mbar) yielded (*exo,endo*-norborn-2-en-5-ylmethyl)dimethylamine as a colorless, oily liquid (21.34 g, 141 mmol, 66%). ^{1}H NMR (250.13 MHz, CDCl$_3$): δ = 5.90 - 6.13 (2 x m, 2 H; -CH=CH-), 2.80 -2.72 (m, 2 H;), 2.19 - 2.17 (m, 6 H; -*N*-(CH$_3$)$_2$), 2.05 - 1.97 (m, 1 H), 1.87 - 1.77 (m, 2 H), 1.17 - 1.43 (m, 3 H), 0.54 - 0.47 ppm (2 x m, 1 H); ^{13}C NMR (62.5 MHz, CDCl$_3$): δ = 136.5, 132.2, 65.9, 64.3, 49.2, 46.7, 44.5, 42.1, 36.7, 30.9 ppm; IR (film): $\bar{\nu}$ = 3067 (m), 2965 (s), 2860 (m), 2814 (m), 2768 (s), 2360 (m), 1441 (s), 1375 (m), 1223 (m), 1033 (s), 838 (s), 718 cm^{-1} (s); GC-MS (EI, 70 eV): *m/z* calculated for C$_{10}$H$_{17}$N: 151.14; found: 151.1, t_R=6.05 min.

*Norborn-5-en-2-ylmethyl-N,N,N-trimethylammonium iodide **M2-I***: (*exo,endo*-Norborn-2-en-5-ylmethyl)dimethylamine (1.00 g, 6.6 mmol) was dissolved in CH$_2$Cl$_2$ (10 mL) and cooled to 0°C. A solution of methyl iodide (1.22 g, 8.6 mmol) in CH$_2$Cl$_2$ (3 mL) was slowly added and the mixture was stirred for 2 h. After solvent removal, compound **2a** was obtained as a white solid (1.71 g, 5.9 mmol, 91%). The product was purified by washing with diethyl ether and dried *in vacuo*. ^{1}H NMR (250 MHz, DMSO): δ = 6.27 - 6.00 (2 x m, 2 H; -CH=CH-), 3.25 - 3.14 (m, 2 H), 3.07 - 3.05 (m, 9 H; -*N*-(CH$_3$)$_3$), 3.00 - 2.83 (m, 3 H), 2.13 - 2.03 (m, 1 H), 1.52 - 1.26 (m, 3 H), 0.77 - 0.70 ppm (2 x m, 1 H); ^{13}C NMR (62.5 MHz, DMSO): δ = 139.4, 132.3, 71.1, 53.4, 49.9, 46.9, 42.9, 34.3, 33.5 ppm; IR (KBr): $\bar{\nu}$ =3425 (b), 3053 (s), 2995 (m), 2962 (m), 2866 (s), 2595 (m), 2341 (m), 1477 (vs), 1336 (s), 1252 (m), 1144 (m), 1078 (m), 972 (s), 912 (s), 829 (s), 715 cm^{-1} (vs).

*Norborn-5-en-2-ylmethyl-N,N,N-trimethylammonium tetrafluoroborate **M2***: Under exclusion of light, an aqueous solution of **M2-I** (0.50 g, 1.76 mmol,) was added dropwise to a solution of silver tetrafluoroborate (0.38 g, 1.90 mmol) in water at 50°C. The reaction mixture was stirred for 1 h, then the yellow precipitate of silver iodide was filtered off and the solvent was removed *in vacuo*. Compound **2** was obtained as a colorless solid (0.40 g, 1.58 mmol, 90%). ^{1}H NMR (400.13 MHz, D$_2$O): δ = 6.33 - 6.06 (2 x m, 2 H; -CH=CH-), 3.56 - 3.43 (m, 1 H), 3.33 - 3.28 (m, 1 H), 3.14 - 3.12 (m, 9 H; -*N*-(CH$_3$)$_3$), 2.97 - 2.85 (m, 3 H), 2.13 - 2.20 (m, 1 H), 1.59 - 1.29 (m, 3 H), 0.85 -

0.80 ppm (m, 1 H;); ^{13}C NMR (100.61 MHz, D$_2$O): δ = 139.8, 138.2, 136.5, 131.6, 73.3, 72.0, 53.8, 49.4, 47.7, 46.7, 45.6, 42.8, 42.3, 34.3, 33.5 ppm; ^{19}F NMR (376.50 MHz, D$_2$O): δ = -150.2 ppm; IR (KBr): $\bar{\nu}$ = 3423 (b), 3060 (m), 2972 (s), 2875 (m), 1622 (m), 1487 (s), 1423 (m), 1340 (m), 1268 (m), 1051 (vs), 970 (m), 904 (s), 825 (m), 769 (m), 721 (vs), 521 cm^{-1} (s); MS (ESI): 166.16 [C$_{11}$H$_{20}$N].

Polymerization of Monomers M1a, M1b and M2

The monomers were dissolved in dichloromethane (2 mL) and polymerized at 40°C for 12 h using 2 mol-% [RuCl$_2$(PCy$_3$)$_2$(=CHC$_6$H$_5$)]. The reaction was terminated by adding excess ethyl vinyl ether, whereupon the polymers as well as unreacted ionic monomers precipitated. The precipitate was washed with diethyl ether and dried *in vacuo*. ^{1}H NMR spectra recorded in DMSO-d$_6$, revealed complete conversion.

Copolymerization of NBE, (NBE-CH$_2$O)$_3$SiCH$_3$ and the Monomers M1a, M1b, M2

In order to simulate surface grafting, norborn-2-ene (100 mg, 1.06 mmol) and (NBE-CH$_2$O)$_3$SiCH$_3$ (100 mg, 0.25 mmol) were copolymerized at 0°C for 30 min using [RuCl$_2$(PCy$_3$)$_2$(=CHC$_6$H$_5$)] (**G1**, 1.0 mg, 1.2 µmol) as initiator and CDCl$_3$ as solvent. Samples were taken and diluted with ethyl vinyl ether in order to examine conversion *via* GC-MS. Twenty equivalents of the ionic monomers then were added and the reaction temperature was raised to 40°C. Conversion from that time on was monitored *via* NMR-analysis.

Preparation of Surface-Functionalized Monoliths

Monoliths were prepared in 125 x 4.4 mm I.D. stainless-steel tubings, according to a well-established procedure [1, 2]. The polymerization mixture composed of NBE (15 wt.-%), the CL (NBE-CH$_2$O)$_3$SiCH$_3$[2] (15 wt.-%), the porogenic solvents toluene (20 wt.-%) and 2-propanol (50 wt.-%), as well as the initiator [RuCl$_2$(PCy$_3$)$_2$(=CHC$_6$H$_5$)] (**G1**, 0.4 wt.-%). The steel column was placed vertically, one end closed, in an ice bath. Polymerization proceeded at 0°C for 30 min, then the temperature was raised to 20°C for another 30 min.

For the grafting of monomer **M2** to the surface of the monoliths, the column was provided with adapters and flushed with CH$_2$Cl$_2$ for 2 h at a flow rate of 0.1 mL min^{-1}. The monomer (10 equiv. with respect to the initiator) was dissolved in CH$_2$Cl$_2$ (1.2 mL) and introduced into the monolith. The loaded monolith was sealed and kept at 45

°C for 12 h. To remove the initiator, the column was flushed with a 1:1 mixture of ethyl vinyl ether and CH_2Cl_2 for 2 h at a flow rate of 0.1 mL min^{-1}. After this, flushing was continued with pure CH_2Cl_2 for a further 2 h at a flow rate of 0.1 mL min^{-1}.

Determination of the Distribution Coefficients ($K_{\text{solvent/IL}}$)

For 1,7-octadiene, DEDAM, and DAFA, the distribution coefficients, $K_{\text{heptane}/\text{IL}} = \dfrac{c\,(substrate\ in\ heptane)}{c\,(substrate\ in\ IL)}$, were determined for the solvent system heptane/[BDMIM$^+$][BF$_4^-$] at 40 and 80°C, respectively. In addition, for DAFA, $K_{\text{dodecane}/\text{IL}} = \dfrac{c\,(substrate\ in\ dodecane)}{c\,(substrate\ in\ IL)}$ was determined for dodecane/[BDMIM$^+$][BF$_4^-$] at 40 and 80°C as well. Four measurements were performed for each substrate/solvent/temperature system to yield an average distribution coefficient with sufficient validity. Substrate (50 mg; 1,7-octadiene, DEDAM, DAFA) and an internal standard (15 mg) were dissolved in solvent (200 mg) and added to [BDMIM$^+$][BF$_4^-$] (200 mg). Dodecane was used as an internal standard when heptane was the organic solvent and dicyclopentadiene served as the nonpolar reference for the determination in dodecane. The biphasic system was stirred with 600 rpm at the indicated temperature for 1 h. Then a sample was removed from the organic phase and examined by means of GC measurements. The immiscibility of the internal standards with the IL was checked by ^{1}H NMR spectroscopy. Comparing the integral areas for the substrate signal and the signal caused by the internal standard, before and after mixing, allowed the distribution coefficient to be calculated.

$K_{\text{substrate/IL}}$ for Neat 1,7-Octadiene and Methyl Oleate in [BDMIM$^+$][BF$_4^-$]

Substrate (200 mg) and dodecane (50 mg) as the internal standard were added to [BDMIM$^+$][BF$_4^-$] (200 mg). The biphasic system was stirred at 600 rpm at the indicated temperature for 1 h. Then a sample was removed from the organic phase and analyzed by GC-MS. The ratio of the integral areas for the substrate signal and the signal caused by the internal standard, before and after mixing, corresponded directly to the distribution coefficient.

6.3 *"Continuous Biphasic Metathesis Using Monolith-Supported Ionic Liquids"*

[Ru(DMF)$_3$(IMesH$_2$)(=CH-2-(2-PrO)-C$_6$H$_4$)$^{2+}$][(BF$_4^-$)$_2$] (1)

Under exclusion of light, AgBF$_4$ (130 mg, 670 µmol) was dissolved in DMF (100 mg, 1.37 mmol) and CH$_2$Cl$_2$ (5 mL). Then a solution of the **GH2**-catalyst (200 mg, 320 µmol) in CH$_2$Cl$_2$ was slowly added. The immediate formation of AgCl was observed and stirring was continued for 1 h. After filtering off the precipitate and passing the solution through a short pad of Celite, the solvent was removed in vacuo. A light green solid was obtained (290 mg, 305 µmol, 95%). Green crystals suitable for X-ray analysis were obtained by layering THF over a concentrated solution of **1** in CH$_2$Cl$_2$ at 20 °C. ^{1}H NMR (400.13 MHz, CD$_2$Cl$_2$): δ=19.28 (s, 1 H), 7.94 (s, 1 H), 7.88 - 7.84 (m, 2 H), 7.28 (t, J = 7.3 Hz, 1 H), 7.06 (d, J = 8.5 Hz, 1 H), 6.96 (s, 4 H), 5.64 (s, 2 H), 4.99 - 4.93 (m, 1 H), 4.08 (s, 3.95), 3.16 - 3.10 (m, 6 H), 2.60 (d, J = 8.0 Hz, 12 H), 2.37 (s, 12 H), 2.30 (s, 6 H), 1.03 ppm (d, J = 6.4 Hz, 6 H); ^{13}C NMR (100.61 MHz, CD$_2$Cl$_2$): δ = 317.7, 166.0, 154.1, 145.7, 139.4, 137.0, 136.2, 134.4, 129.7, 125.0, 124.8, 114.9, 77.3, 53.0, 39.1, 33.2, 21.7, 21.0, 18.5 ppm; ^{19}F NMR (376.50 MHz, CD$_2$Cl$_2$): δ = - 152.6 ppm; IR (KBr): $\bar{v}$ = 3438 (b), 3047 (m), 2916 (s), 2856 (m), 2729 (m), 1668 (vs), 1591 (s), 1477 (s), 1383 (s), 1282 (m), 1259 (vs), 1215 (m), 1039 (vs), 930 (s), 858 (m), 750 (s), 701 (m), 680 (m), 658 (m), 579 (s), 521 (s), 422 cm^{-1} (s); elemental analysis calculated (%) for C$_{40}$H$_{59}$B$_2$F$_8$N$_5$O$_4$Ru (M_r= 950.61 g mol^{-1}): C 50.49, H 6.26, N 7.27; found: C 50.58, H 6.21, N 7.13.

N,N-Diallylacetamide

Over a period of 1 h, diallylamine (15.0 g, 154 mmol) was added to ice cold acetic anhydride (26.8 g, 263 mmol) under vigorous stirring. Then the temperature was raised to 100 °C and stirring was continued for a further 2 h. Fractionated distillation yielded *N,N*-diallylacetamide (70°C, 0.1 mbar) as a colorless liquid (18.3 g, 131 mmol, 85%). ^{1}H NMR (400.13 MHz, CDCl$_3$): δ = 5.76 - 5.65 (m, 2 H), 5.16 - 5.04 (m, 4 H), 3.87 (dd, J = 5.8 Hz, 4 H), 2.04 ppm (s, 3 H); ^{13}C NMR (100.61MHz, CDCl$_3$): δ = 170.5, 132.8, 116.7, 48.7, 21.2 ppm; IR (film): $\bar{v}$ =3473 (b), 3078 (s), 2991 (m), 2979 (s), 2912 (m), 2354 (m), 1718 (m), 1633 (vs), 1448 (m), 1407 (vs), 1261 (s), 1241 (vs), 1192 (s), 1008 (m), 982 (s), 918 (s), 773 (m), 687 (s), 600 (s), 557 cm^{-1}

(m); GC-MS (EI, 70 eV): *m/z* calculated for $C_8H_{13}NO$: 139.10; found: 139.1, t_R=6.268 min.

N-Allyl-N-propargyltrifluoroacetamide

N-Allyl-N-propargylamine: This compound was prepared according to a procedure reported in the literature[3]. A solution of allylamine (7.660 g, 134 mmol) in 2 M aqueous NaOH (50 mL) was warmed to 40 °C. Propargyl chloride (5 g, 67 mmol) was then added dropwise over a period of 3 h. Stirring was continued for a further 3 h, then the reaction mixture was allowed to cool to ambient temperature. The mixture was extracted with diethyl ether (3 x 30 mL) and the combined organic phases were washed with brine (2 x 50 mL). After drying over $MgSO_4$, the solvent was removed. *N*-Allyl-*N*-propargylamine was isolated by column chromatography (silica, pentane / diethyl ether gradient) as a colorless liquid (2.3 g, 24 mmol, 36%). ^{1}H NMR (400.13 MHz, $CDCl_3$): *δ* = 5.76 - 5.66 (m, 1 H), 5.29 - 5.21 (m, 2 H), 4.17 - 4.10 (m, 4 H), 2.32 - 2.26 ppm (m, 1 H); ^{13}C NMR (100.61 MHz, $CDCl_3$): *δ* = 134.6, 118.5, 78.5, 73.0, 56.0, 41.5 ppm; GC-MS (EI, 70 eV): *m/z* calculated for C_6H_9N: 95.14; found: 95.1, t_R = 3.258 min.

Alongside the desired product, the dialkylated species *N*-allyl-*N,N*-dipropargylamine was isolated (1.83 g, 14 mmol, 21%). ^{1}H NMR (400.13 MHz, $CDCl_3$): *δ* = 5.86 - 5.76 (m, 1 H), 5.22 (d, *J* = 11.1 Hz, 2 H), 3.41 (s, 4 H), 3.14 (d, *J* = 6.7 Hz, 2 H), 2.21 ppm (s, 2 H); ^{13}C NMR (100.61 MHz, $CDCl_3$): *δ* = 134.6, 118.5, 78.5, 73.0, 56.0, 41.5 ppm; GC-MS (EI, 70 eV): *m/z* calculated for $C_9H_{11}N$: 133.09; found: 133.1, t_R = 5.141 min.

N-Allyl-N-propargyl trifluoroacetamide: A mixture of *N*-allyl-*N*-propargylamine (1.00 g, 11 mmol) and triethylamine (1.34 g, 13 mmol) in CH_2Cl_2 (18 mL) was cooled to 0°C. Trifluoroacetic anhydride (2.66 g, 13 mmol) in CH_2Cl_2 (5 mL) was added dropwise over a period of 30 min. The reaction mixture then was warmed to 30 °C and stirring was continued for 15 h. A saturated aqueous solution of $NaHCO_3$ (30 mL) was added and the mixture was then extracted with CH_2Cl_2 (2 x 30 mL). The organic phase was washed with water (30 mL) and then dried over $MgSO_4$. After solvent removal, the residue was subjected to column chromatography (silica, diethyl ether) to yield the target compound as a colorless liquid (1.71 g, 8.9 mmol, 81%). ^{1}H NMR (400.13 MHz, $CDCl_3$): *δ* = 5.91 - 5.80 (m, 1 H), 5.22 - 5.09 (m, 2 H), 3.40 (d, *J* = 4.5 Hz, 2 H),

3.31 (d, J = 5.3 Hz, 2 H), 2.21 - 2.19 ppm (m, 1 H); ^{13}C NMR (100.61 MHz, CDCl$_3$): δ = 135.9, 116.6, 81.9, 71.3, 50.8, 37.2 ppm; ^{19}F NMR (376.50 MHz, CDCl$_3$): δ = - 75.7 ppm; IR (film): $\bar{\nu}$ = 3292 (vs), 3083 (m), 2985 (m), 2923 (m), 2343 (m), 2123 (m), 1691 (vs), 1419 (vs), 1353 (s), 1277 (s), 1205 (vs), 1141 (vs), 1003 (s), 937 (s), 756 s), 698 cm^{-1} (s); GC-MS (EI, 70 eV): m/z calculated for C$_8$H$_8$F$_3$NO: 191.06; found: 190.1, t_R=4.964.

Immobilization of [BDMIM$^+$][BF$_4$] and the Catalyst 1 on the Surface of the Monoliths

Complex **1** (2.5 mg, 2.6 µmol) and [BDMIM$^+$][BF$_4$] (100 mg) were mixed and dissolved in CH$_2$Cl$_2$ (1.2 mL). The solution was then introduced into the monolith. Vacuum was applied for 3 h at 40°C to remove the solvent. Prior to use, the support was flushed with heptane for 1 h at 40°C by applying a flow rate of 0.1 mL min^{-1}.

Metathesis Under Biphasic Conditions

Complex **1** (2.5 mg, 2.6 µmol) was dissolved in [BDMIM$^+$][BF$_4$] (200 mg) and the solution was heated to 40°C. Then a solution of the substrate (0.6 - 13 mmol) in heptane (2 mL) was added and the biphasic system was stirred vigorously (600 rpm) for 12 h. Reactions were quenched by adding ethyl vinyl ether (1 mL). After removing the nonpolar phase, the IL phase was extracted extensively with diethyl ether. The organic phases were combined and subjected to GC-MS analysis to determine conversion.

Metathesis Under Biphasic Conditions Using Monolith-Supported ILs

Metathesis reactions under SILP conditions were performed in air. The loaded monolithic support was placed inside a Merck L-5025 column thermostat and warmed to the indicated temperature (Table S1 in the Appendix). By using a syringe pump (WPT, Aladdin-1000), the substrate (*N,N*-diallyl trifluoroacetamide and DEDAM dissolved in heptane; 1,7-octadiene and methyl oleate as neat reactants) was flushed through the monolith at a flow rate of 0.1 mL min^{-1}. The eluent was collected and subjected to GC-MS analysis to determine conversion. Used SILP phases were removed by subsequent flushing with methanol (5 mL) and CH$_2$Cl$_2$ (5 mL). The cleaned monolithic supports were again charged and used for catalysis.

X-Ray Measurements and Structural Determination of 1

Data were collected on a Bruker Kappa Apex 2 duo diffractometer at 100 K. The structure was solved by using direct methods with refinement by full-matrix least-squares on F^2, with the program system SHELXL 97 in connection with a multiscan absorption correction. All non-hydrogen atoms were refined anisotropically.

CCDC-900128 contains the supplementary crystallographic data for complex **1**. These data can be obtained free of charge from The Cambridge Crystallographic Data Centre *via* www.ccdc.cam.ac.uk/data_request/cif.

Inverse Size Exclusion Chromatography (ISEC)

Functionalized monoliths were characterized by ISEC measurements in terms of inter-microglobular porosity (ε_z), microporosity (ε_p), and total porosity (ε_t). A volume of 10 µL per sample of individual PS standard (0.25 mg mL^{-1}) dissolved in the mobile phase (CHCl$_3$) was injected into the column at a flow rate of 0.6 mL min^{-1}. The total accessible porosity was determined by injecting a 10 µL sample of toluene. A wavelength of 254 nm was applied to record the chromatograms. Retention times and volumes corresponding to each injection were determined from the peak maximum. Each retention volume was corrected for the extra-column volume of the equipment. For calculations it was assumed that the hydrodynamic radii of the PS standards in CHCl$_3$ did not differ significantly from those reported in CH$_2$Cl$_2$ [4].

6.4 "Reactivity of 1 in Ring-Opening Metathesis and Cyclopolymerization"

Diethyl dipropargyl malonate (**H1**) [5], dipropargyl malodinitrile (**H2**) [6], 4,4-bis(octyloxymethyl)-1,6-heptadiyne (**H3**) [7], *exo, endo*-norborn-2-en-5-ylmethyl trimethylammonium tetrafluoroborate (**M2**), *exo, endo*-norborn-2-en-5-ylmethyl trimethylammonium iodide (**M2-I**) [8], and the initiator [Ru(DMF)$_3$(IMesH$_2$)(=CH-2-(2-PrO)-C$_6$H$_4$)$^{2+}$][(BF$_4^-$)$_2$] (**1**) [8] were prepared as described earlier.

General Method for ROMP

ROMP-derived polymers listed in Table 10 (Chapter 4.2.1) were prepared as follows: **1** (1.0 mg, 1.05 x10^{-6} mol), dissolved in CH$_2$Cl$_2$ (0.5 mL), was added to a solution containing the correspondent equivalents of monomer (Table 10) in CH$_2$Cl$_2$ or 1,2-dichloroethane (3 mL). The mixture was stirred for 0.5 - 12 h at the indicated temperature. Then, ethyl vinyl ether was added and stirring was continued for another 30 min. A major part of the solvent was removed *in vacuo*; then the polymer was precipitated from methanol. The ionic polymers poly-**M1a,** poly-**M1b**, poly-**M2**, poly-**M2-I**, poly-**M3**, poly-**M3-I** precipitated during the reaction. Isolated yields are given in Table 10.

For the investigation of the reaction kinetics of the ROMP-reactions, the initiator:substrate ratio was set to 1:200 and reactions were conducted either at 20 or at 80°C using CH$_2$Cl$_2$ or 1,2-dichloroethane as solvent. The procedure for non-ionic monomers was the same as described for the determination of the cyclopolymerization kinetics (*vide infra*). ROMP kinetics of the ionic monomers **M1b**, **M1b-Br**, **M2** and **M2-I** were evaluated by ^{1}H-NMR-analysis in DMSO-d$_6$ using benzene as internal standard.

Trapping of the Propagating Alkylidenes Formed During ROMP

*Polymerization of exo, endo-norborn-2-en-5-ylmethyltrimethylammonium iodide (**M2-I**) and Isolation of [RuI$_2$(IMesH$_2$)(=CH-2-(2-PrO)-C$_6$H$_4$)] (IMesH$_2$=1,3-dimesityl-imidazolin-2-ylidene)*: **M2-I** (93.0 mg, 3.15 x10^{-4} mol, 20 equiv.) was dissolved in CH$_2$Cl$_2$ (4 mL). At 20°C, a solution of **1** (15.0 mg, 1.58 x10^{-5} mol) in CH$_2$Cl$_2$ (0.5 mL) was added and the mixture was stirred for 15 min. Then, 2-(2-propoxy)styrene (10.2

mg, 6.32 x10^{-5} mol, 4 equiv.), dissolved in CH_2Cl_2 (1 mL), was added. Stirring was continued for another 15 min, then diethyl ether (3 mL) was added. The precipitated polymer was filtered off and the green solution was flashed over a pad of alumina. After removing all volatiles *in vacuo*, the residue was redissolved in CH_2Cl_2 (0.5 mL) and precipitated from *n*-hexane. This procedure was repeated twice and the thus obtained green powder was dried *in vacuo* (9.0 mg, 1.11 x10^{-5} mol, 70%). ^{1}H -NMR (400.13 MHz, $CDCl_3$): 15.67 (s, 1 H), 7.55-7.50 (m, 1 H), 7.08 (bs, 2 H), 7.00 (bs, 2 H), 6.96 (d, *J*=7.4 Hz, 1 H), 6.85-6.81 (m, 2 H), 5.03 (sept, 1 H), 4.14 (s, 4 H), 2.68 (s, 6 H), 2.52 (s, 6 H), 2.44 (s, 3 H), 2.33 (s, 3 H), 1.45 ppm (d, *J*=6.2 Hz, 6 H). ^{13}C-NMR (100.61 MHz, $CDCl_3$): 298.6, 214.1, 153.0, 145.2, 139.0, 138.8, 138.6, 138.0, 137.6, 134.6, 130.4, 129.7, 129.6, 123.2, 121.9, 113.4, 75.7, 52.7, 51.0, 23.3, 21.7, 21.1, 21.0, 20.1 ppm. Analytical data were identical to those reported for this compound.[9]

Polymerization of exo, endo-norborn-2-en-5-ylmethyl-2,3-dimethylimidazolium bromide **(M1b-Br)** *and Isolation of [RuBr$_2$(IMesH$_2$)(=CH-2-(2-PrO)-C$_6$H$_4$)]* *(IMesH$_2$=1,3-dimesitylimidazolin-2-ylidene)*: The same procedure was used as described for the polymerization of **M2-I**. *Exo, endo*-norborn-2-en-5-ylmethyl-2,3-dimethyl imidazolium bromide (**M1b-Br**, 89.0 mg, 3.15 x10^{-4} mol, 20 equiv.) was used as the monomer. 2-(2-propoxy)styrene was used to cleave the ruthenium-alkylidene from the polymer chain end, and the isolated yield of [RuBr$_2$(IMesH$_2$)(=CH-2-(2-PrO)-C$_6$H$_4$)] was 9 mg (1.26 x10^{-5} mol, 80%). ^{1}H -NMR (400.13 MHz, $CDCl_3$): 16.40 (s, 1 H), 7.53-7.48 (m, 1 H), 7.06 (bs, 4 H), 6.96-6.93 (m, 1 H), 6.85-6.79 (m, 2 H), 4.95 (septet, 1 H), 4.17 (s, 4 H), 2.52 (bd, 18 H), 1.34 ppm (d, *J*=6.9 Hz, 6 H). ^{13}C-NMR (100.61 MHz, $CDCl_3$): 299.9, 212.4, 152.4, 145.6, 139.6, 138.8, 129.9, 129.3, 122.7, 122.2, 113.1, 75.3, 52.3, 21.3, 21.2, 21.0 ppm. Analytical data were identical to those reported for this compound.[9]

Cyclopolymerizations

Cyclopolymerization-derived polymers listed in Table 12 (Chapter 4.2.2) were prepared as follows: **1** (2.0 mg, 2.11 x10^{-6} mol), dissolved in CH_2Cl_2 (0.5 mL), was added to a solution containing the correspondent equivalents of monomer (Table 12) in CH_2Cl_2 (3 mL). The mixture was stirred for 6 h at the indicated temperature. Then, ethyl vinyl ether was added and stirring was continued for another 30 min. A major part of the solvent was removed *in vacuo*. Then the polymer was precipitated from

methanol or acetone. Poly-**H4** and the ionic polymer poly-**H5** precipitated during the reaction. Isolated yields are given in Table 12.

For all cyclopolymerization kinetics, the initiator:substrate ratio was set to 1:80. **1** (5.0 mg, dissolved in CH_2Cl_2 (0.5 mL), and was added to the monomer solution [**H1** (9.5 mg, 4.21×10^{-4} mol), **H2** (65.0 mg, 4.21×10^{-4} mol), **H3** (158.6 mg, 4.21×10^{-4} mol), **H4** (79.6 mg, 4.22×10^{-4} mol), **H5** (99.8 mg, 4.21×10^{-4} mol); each in 3 mL of CH_2Cl_2]. The reaction temperature varied between 0 and 35°C. Dodecane (0.1 mL) was added as internal standard (for **H1** – **H4**) and samples were taken from the reaction mixture and diluted with ethyl vinyl ether / acetone (1:5). Conversion was determined *via* GC-MS analysis. For the polymerization of **H5**, samples were subjected to ^{1}H NMR analysis. Spectra were recorded using DMSO-d_6 as the solvent and benzene as an internal standard.

Determination of the k_p/k_i Values [10]

For the determination of k_p/k_i values, the ratio of **1**:monomer was set to 1:5. **1** (5.0 mg, 5.26×10^{-6} mol), dissolved in CD_2Cl_2 (0.3 mL), was added to a solution of monomer in 0.3 mL of CD_2Cl_2. The mixture was stirred for 5 min at the indicated temperature (20 or 38°C) and was then subjected to ^{1}H NMR analysis.

N,N-Dipropargyl Trifluoroacetamide (H4)

N,N-Dipropargyl trifluoroacetamide was synthesized as described in the literature[3]. K_2CO_3 (14.7 g, 106 mmol) and tetrabutylammonium bromide (0.85 g, 2.6 mmol) were added to a solution of trifluoroacetamide (3.00 g, 26.5 mmol) and propargyl bromide (12.6 g, 106 mmol) in acetonitrile (60 mL). The mixture was stirred for 24 h at 70°C. After cooling to room temperature, the inorganic solid was filtered off and extracted with CH_2Cl_2. All organic phases were combined and the solvents were removed *in vacuo* to yield crude product, which was finally purified by column chromatography (silica, diethyl ether / pentane (1:1)). Yield: 2.71 g, 14 mmol, 54%. ^{1}H-NMR (400.13 MHz, CDCl$_3$): δ = 4.36 (2 x d, *J*=2.9, Hz 4 H), 2.34 ppm (2 x t, *J*=2.5 Hz, 2 H). ^{13}C-NMR (100.61 MHz, CDCl$_3$): δ = 156.0 (q, *J*=37.0 Hz), 116.0 (q, *J*=286.8 Hz), 76.1, 75.9, 74.0, 73.8, 35.0 ppm. ^{19}F-NMR (376.50 MHz, CDCl$_3$): δ = - 69.3 ppm. IR (film, cm^{-1}): $\bar{v}$ = 3286 (vs), 2981 (m), 2919 (m), 2127 (s), 1689 (vs), 1510 (s), 1442 (vs), 1357 (s), 1278 (s), 1201 (vs), 1138 (vs), 1012 (vs), 956 (s), 757 (s), 638 (vs), 567

(m); GC-MS (EI, 70 eV): m/z calculated for $C_8H_6F_3NO$, 189.04; found 189.0, t_R = 4.878 min.

6.5 "Catalyst Optimization"

The initiators [RuCl(CF$_3$SO$_3$)(=CH-2-(2-PrO)-C$_6$H$_4$)(IMesH$_2$)] and [Ru(CF$_3$SO$_3$)$_2$(=CH-2-(2-PrO)-C$_6$H$_4$)(IMesH$_2$)] were prepared as described in the literature [11].

[(1-CH$_3$)(4-CO$_2$K)Py$^+$][BF$_4^-$]

To an aqueous solution of 4-carboxy-1-methylpyridinium chloride (500 mg, 2.88 mmol), KOH (162 mg, 2.88 mmol) was added and the mixture was stirred for 15 minutes at room temperature. Then, an aqueous solution of AgBF$_4$ (561 mg, 2.88 mmol) was added dropwise and stirring was continued for another 2 h. The white precipitate of AgCl was filtered off and the solvent was removed *in vacuo*. The salt obtained was treated with anhydrous THF in order to remove traces of water and was then dried *in vacuo*. Yield: 725 mg (2.76 mmol, 96%). ^{1}H NMR (400.13 MHz, D$_2$O): δ = 8.84 (d, J = 6.5 Hz, 2 H), 8.24 (d, J = 6.5 Hz, 2 H), 4.41 ppm (s, 3 H); ^{13}C NMR (100.61 MHz, D$_2$O): δ = 169.0, 152.2, 145.7, 126.5, 47.9 ppm; ^{19}F NMR (376.50 MHz, D$_2$O): δ = -150.5 ppm; IR (KBr): $\bar{v}$ = 3444 (b), 3106 (m), 3037 (s), 1633 (s), 1602 (m), 1560 (s), 1456 (m), 1360 (s), 1285 (m), 1182 (m), 1030 (m), 899 (m), 879 (m), 858 (s), 783 (vs), 687 (s), 613 (s), 521 (s), 459 (m) cm^{-1}.

[Ru[(4-CO$_2$)(1-CH$_3$)Py$^+$)]$_2$(=CH-2-(2-PrO)-C$_6$H$_4$)(IMesH$_2$)][OTf$^-$]$_2$ (2)

A solution of [Ru(CF$_3$SO$_3$)$_2$(IMesH$_2$)(=CH-2-(2-PrO)-C$_6$H$_4$)] (200 mg, 0.23 mmol) in CH$_2$Cl$_2$ (5 mL) was added to a suspension of [(1-CH$_3$)(4-CO$_2$K)Py$^+$][BF$_4^-$] (129 mg, 0.49 mmol) in CH$_2$Cl$_2$ (10 mL). A color change to dark red was observed and stirring was continued for 2 h at room temperature. The mixture was then passed through a pad of celite and the solvent was removed *in vacuo*. The target compound was obtained as a dark red solid (216 mg, 0.19 mmol, 82%). ^{1}H NMR (400.13 MHz, CD$_2$Cl$_2$): δ = 18.23 (s, 1 H), 8.80 (d, J = 6.5 Hz, 4 H), 8.01 (d, J = 6.7 Hz, 4 H), 7.52 (d, J = 5.9 Hz, 1 H), 7.46 (t, J = 8.7 Hz, 1 H), 7.12 (t, J = 7.3 Hz, 1 H), 6.83 (s, 4 H), 6.73 (d, J = 8.3 Hz, 1 H), 4.66 - 4.56 (m, 1 H), 4.47 (s, 6 H), 4.00 (s, 4 H), 2.32 (s, 12 H), 2.14 (s, 6 H), 0.94 ppm (d, J = 6.2 Hz, 6 H); ^{13}C NMR (100.61 MHz, CD$_2$Cl$_2$): δ = 309.7, 202.2, 166.0, 154.9, 147.1, 145.9, 143.5, 138.8, 137.8, 136.9, 130.8, 130.1, 127.6, 123.9, 123.6, 123.0, 119.8, 112.8, 75.3, 52.8, 49.2, 21.5, 21.1, 18.7 ppm; ^{19}F NMR (376.50 MHz, CD$_2$Cl$_2$): δ = -78.9 ppm; IR (KBr): $\bar{v}$ = 3452 (b), 3107 (m), 3046

(m), 2960 (m), 2913 (m), 2850 (m), 1946 (m), 1722 (m), 1637 (s), 1571 (m), 1479 (m), 1398 (m), 1301 (m), 1257 (s), 1138 (m), 1091 (m), 1026 (s), 926 (m), 852 (m), 795 (m), 769 (m), 681 (m), 638 (vs), 571 (s), 515 (s), 467 (m), 420 (m) cm^{-1}; elemental analysis calculated (%) for $C_{47}H_{53}F_6N_4O_{11}RuS_2$ (M_r = 1129.13 g mol^{-1}): C 50.00, H 4.73, N 4.98; found: C 49.98, H 4.75, N 5.16.

[RuCl[(4-CO$_2$)(1-CH$_3$)Py$^+$)](IMesH$_2$)(=CH-2-(2-PrO)-C$_6$H$_4$)][OTf] (3)

A solution of [RuCl(CF$_3$SO$_3$)(IMesH$_2$)(=CH-2-(2-PrO)-C$_6$H$_4$)] (200 mg, 0.27 mmol) in CH$_2$Cl$_2$ (5 mL) was quickly added to a suspension of [(1-CH$_3$)(4-CO$_2$K)Py$^+$][BF$_4^-$] (71 mg, 0.27 mmol) in CH$_2$Cl$_2$ (15 mL). A color change from green to red was observed and stirring was continued for 1 h at room temperature. The precipitate was removed by filtering the reaction mixture through a pad of celite. After solvent removal, [RuCl[(4-CO$_2$)(1-CH$_3$)Py$^+$)](IMesH$_2$)(=CH-2-(2-PrO)-C$_6$H$_4$)][OTf] was obtained as a red powder, which was redissolved in CH$_2$Cl$_2$ (3 mL) and precipitated in diethyl ether (15 mL). Yield: 210 mg, 0.24 mmol, 89%. ^{1}H NMR (400.13 MHz, CD$_2$Cl$_2$): δ = 17.18 (s, 1 H), 8.79 (d, J = 6.5 Hz, 2 H), 8.02 (d, J = 6.7 Hz, 2 H), 7.47 – 7.42 (m, 1 H), 7.24 (s, 2 H), 7.07 (s, 2 H), 7.06 – 7.02 (m, 1 H), 6.99 – 6.93 (m, 1 H), 6.73 (d, J = 8.3 Hz, 1 H), 4.78 - 4.69 (m, 1 H), 4.47 (s, 3 H), 4.16 – 4.08 (m, 4 H), 2.55 (s, 6 H), 2.49 (s, 6 H), 2.12 (s, 6 H), 1.30 (d, J = 6.1 Hz, 3 H), 0.91 ppm (d, J = 6.1 Hz, 3 H); ^{13}C NMR (100.61 MHz, CD$_2$Cl$_2$): δ = 304.4, 208.7, 162.6, 151.9, 147.1, 144.6, 142.8, 138.7, 138.0, 136.5, 134.6, 130.3, 129.1, 128.9, 128.6, 126.5, 126.3, 121.8, 121.5, 112.3, 111.5, 73.9, 50.7, 47.9, 29.3, 20.1, 20.0, 18.1, 17.6 ppm; ^{19}F NMR (376.50 MHz, CD$_2$Cl$_2$): δ = -79.0 ppm; IR (KBr): $\bar{v}$ = 3417 (vb), 2955 (m), 29113 (m), 2846 (m), 2353 (vs), 1643 (vs), 1574 (m), 1471 (s), 1381 (m), 1319 (m), 1265 (vs), 1149 (s), 1097 (m), 1026 (s), 926 (m), 845 (m), 791 (m), 665 (m), 633 (s), 571 (m) cm^{-1}; elemental analysis calculated (%) for $C_{39}H_{45}F_3N_3O_6RuS$ (M_r = 877.37 g mol^{-1}): C 53.39, H 5.17, N 4.79; found: C 53.59, H 5.17, N 4.77.

Metathesis Under Biphasic Conditions

2 (2.5 mg, 2.2 µmol) was dissolved in [BDMIM$^+$][BF$_4^-$] (200 mg) and the solution was heated to 40°C. Then a solution of the substrate (0.1 – 4.4 mmol) in heptane (2 mL) was added and the biphasic system was stirred vigorously (600 rpm) for 12 h. Reactions were quenched by adding ethyl vinyl ether (1 mL). After removing the non-polar phase, the ionic-liquid phase was extracted extensively with diethyl ether (3 x 1

mL; stirring for 20 min with 600 rpm). The organic phases were combined and subjected to GC-MS analysis in order to determine conversion.

Metathesis Under Biphasic Conditions Using Monolith-Supported Ionic Liquids

Metathesis reactions under SILP-conditions were performed under air, comparable to the method described in Chapter 6.3 [8]. The loaded monolithic support was placed inside a Merck L-5025 column thermostat and warmed to 45°C. Using a syringe pump (WPT, Aladdin-1000), the substrate (1,7-octadiene and methyl oleate as neat reactants) was flushed through the monolith at a flow rate of 0.1 mL/min. The eluent was collected and subjected to GC-MS analysis in order to determine conversion. Used SILP-phases were removed by subsequent flushing with methanol (5 mL) and CH_2Cl_2 (5 mL). The thus cleaned monolithic support was again charged and used for catalysis.

6.6 References

[1]   S. H. Lubbad, B. Mayr, M. Mayr, M. R. Buchmeiser, *Macromol. Symp.* **2004**, *210*, 1.

[2]   S. H. Lubbad, M. R. Buchmeiser, *Macromol. Rapid. Commun* **2002**, *27*, 617.

[3]   J. K. Stille, Y. Becker, *J. Org. Chem.* **1980**, *45*, 2139.

[4]   I. Halasz, K. Martin, *Angew. Chem.* **1978**, *90*, 954.

[5]   G. Eglington, A. R. Galbraith, *J. Chem. Soc.* **1959**, 889.

[6]   E. Diez-Barra, A. de la Hoz, A. Moreno, P. Sanchez-Verdu, *J. Chem. Soc. Perkin Trans I: Org. Bio-Org. Chem.* **1991**, 2589.

[7]   M. Sudheendran, M. Horecha, A. Kiriy, S. A. Gevorgyan, F. C. Krebs, M. R. Buchmeiser, *Polym. Chem.* **2013**, *4*, 1590.

[8]   B. Autenrieth, W. Frey, M. R. Buchmeiser, *Chem. Eur. J.* **2012**, *18*, 14069.

[9]   J. Wappel, C. A. Urbina-Blanco, M. Abbas, J. H. Albering, R. Saf, S. P. Nolan, C. Slugovc, *Beilstein J. Org. Chem.* **2010**, *6*, 1091.

[10]   G. C. Bazan, E. Khosravi, R. R. Schrock, W. J. Feast, V. C. Gibson, W. M. Davis, *J. Am. Chem. Soc.* **1990**, *112*, 8378.

[11]   J. O. Krause, O. Nuyken, M. R. Buchmeiser, *Chem. Eur. J.* **2004**, *10*, 777.

7. Appendix

7.1 "Continuous Biphasic Metathesis Using Monolith-Supported Ionic Liquids"

Table S1. RCM of DAFA under monolith-supported biphasic conditions.

Catalyst [mg]	IL [mg]	Heptane [g]	Flow rate [mL/min]	T [°C]	TON*	Ru leaching [%]	Ru contamination [ppm]
1 [2.5]	160	3	0.1	40	800	0.3	1.8
GH2 [1.7]	160	3	0.1	40	700	1.6	9.4
1 [2.5]	160	3	0.1	60	700	0.7	4.1
1 [2.5]	160	7	0.1	40	550	0.09	0.5
GH2 [1.7]	160	7	0.1	40	400	1.0	5.9
1 [2.5]	100	7	0.1	40	900	0.5	2.9
GH2 [1.7]	100	7	0.1	40	750	1.8	10.6
1 [2.5]	100	7 (dodecane)	0.1	40	450	0.06	0.4
1 [2.5]	100	7 (dodecane)	0.1	80	290	0.21	1.2
1 [2.5]	100	7	0.05	40	700	0.34	2.0
1 [2.5]	100	7	0.05	60	500	0.46	2.7
1 [2.5]	160	7	0.5	40	300	0.1	0.6
GH2 [1.7]	160	7	0.5	40	260	1	5.9

*The reaction mixture contained 850 mg of DAFA (1700 equiv. with respect to **1**) and was passed through the monolith only once. **GH2** = $RuCl_2(IMesH_2)(=CH-2-(2-PrO)-C_6H_4)$].
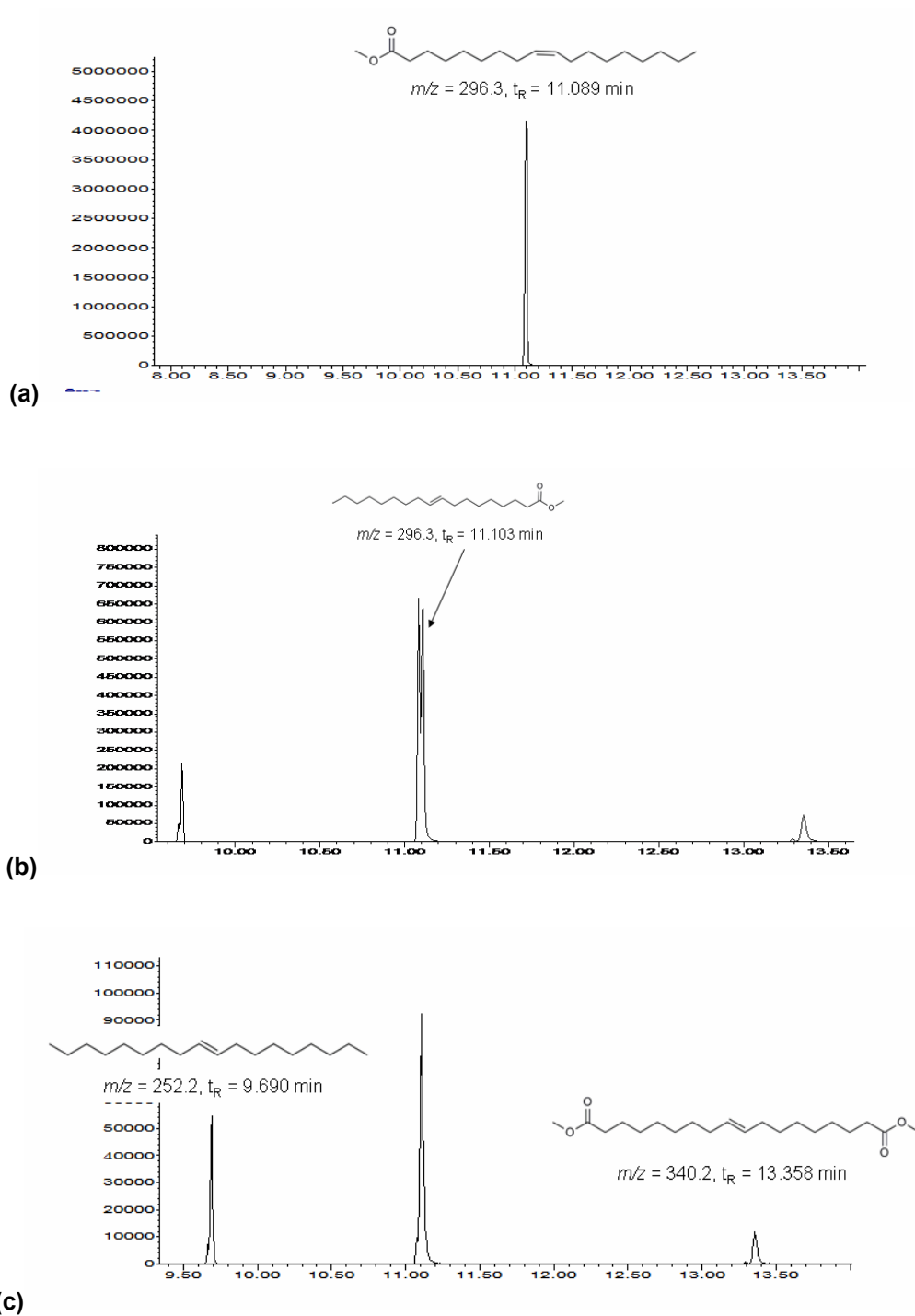
Figure S1. Gas-chromatograms for the self-metathesis of methyl oleate catalyzed by **1**. (a) Methyl oleate prior to metathesis, (b) isomerization process during reaction, (c) primary metathesis products and *E*-isomer.
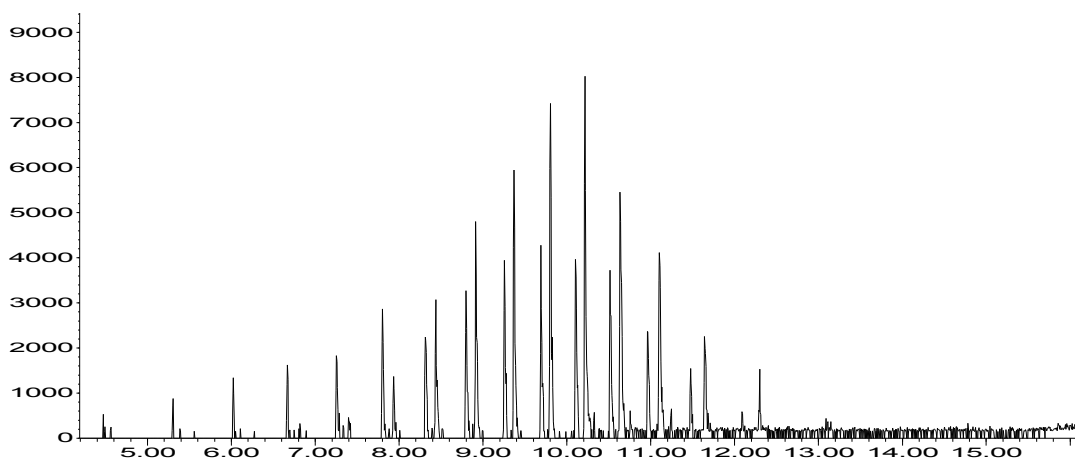
Figure S2. Gas-chromatogram for the self-metathesis of methyl oleate catalyzed by [RuCl$_2$(IMesH$_2$)(=CH-2-(2-PrO)-C$_6$H$_4$)] (**GH2**) - formation of a multitude of products.

m/z = 165.0, t$_R$ = 5.015

m/z = 193.0, t$_R$ = 4.958
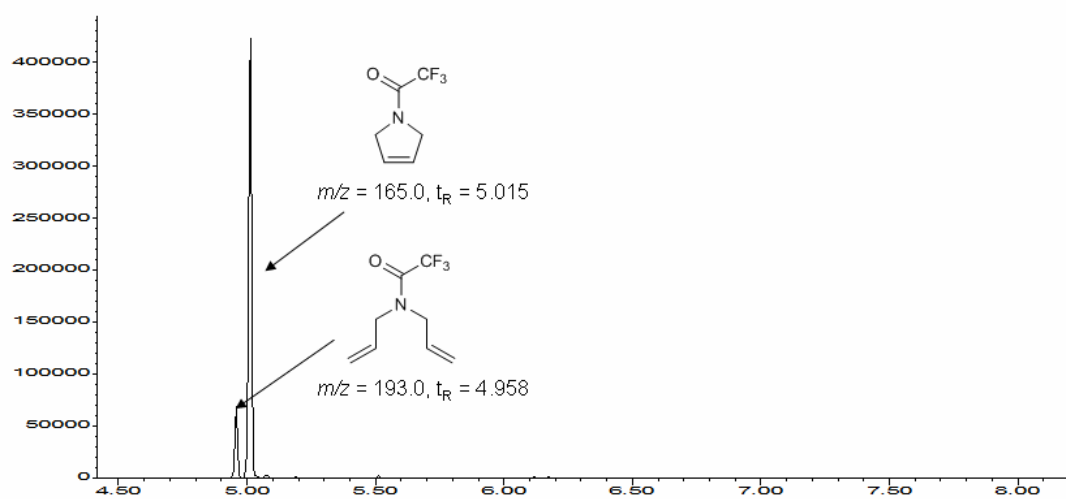
Figure S3. Gas-chromatogram for the RCM of *N,N*-diallyl trifluoroacetamide.

m/z = 212.1, t$_R$ = 7.584

m/z = 240.1, t$_R$ = 7.876
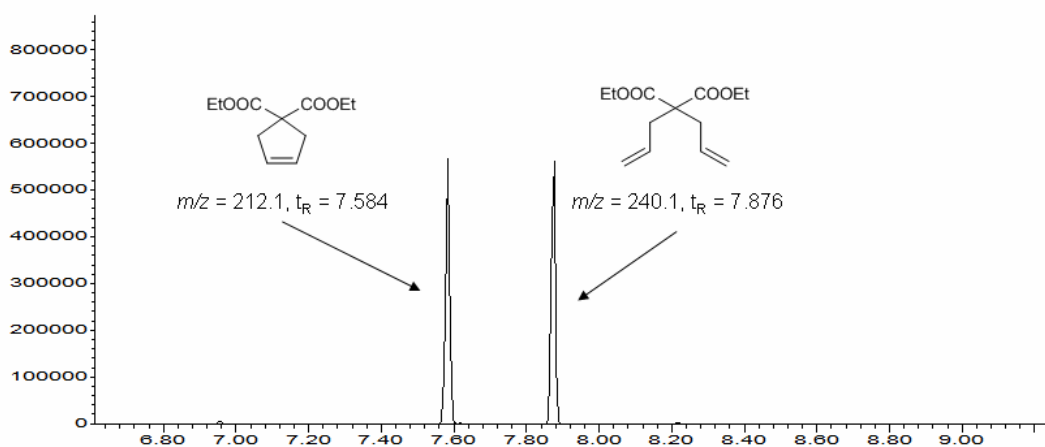
Figure S4. Gas-chromatogram for the RCM of diethyl diallyl malonate.
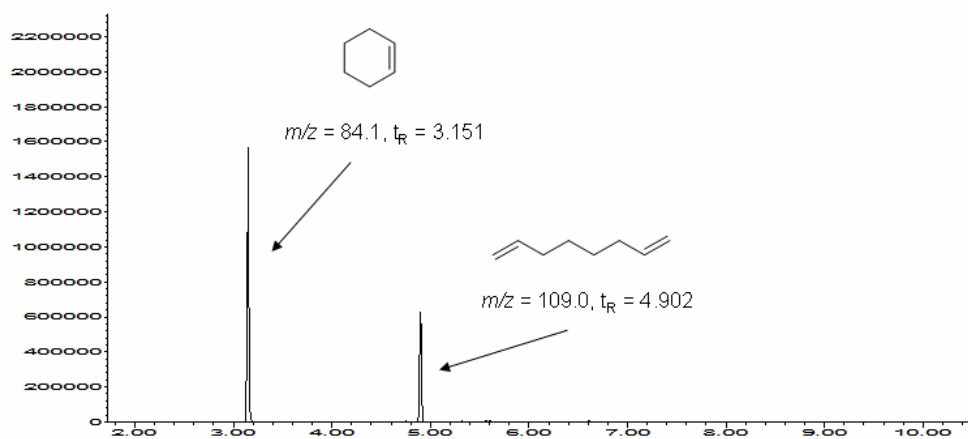
Figure S5. Gas-chromatogram for the RCM of 1,7-octadiene.
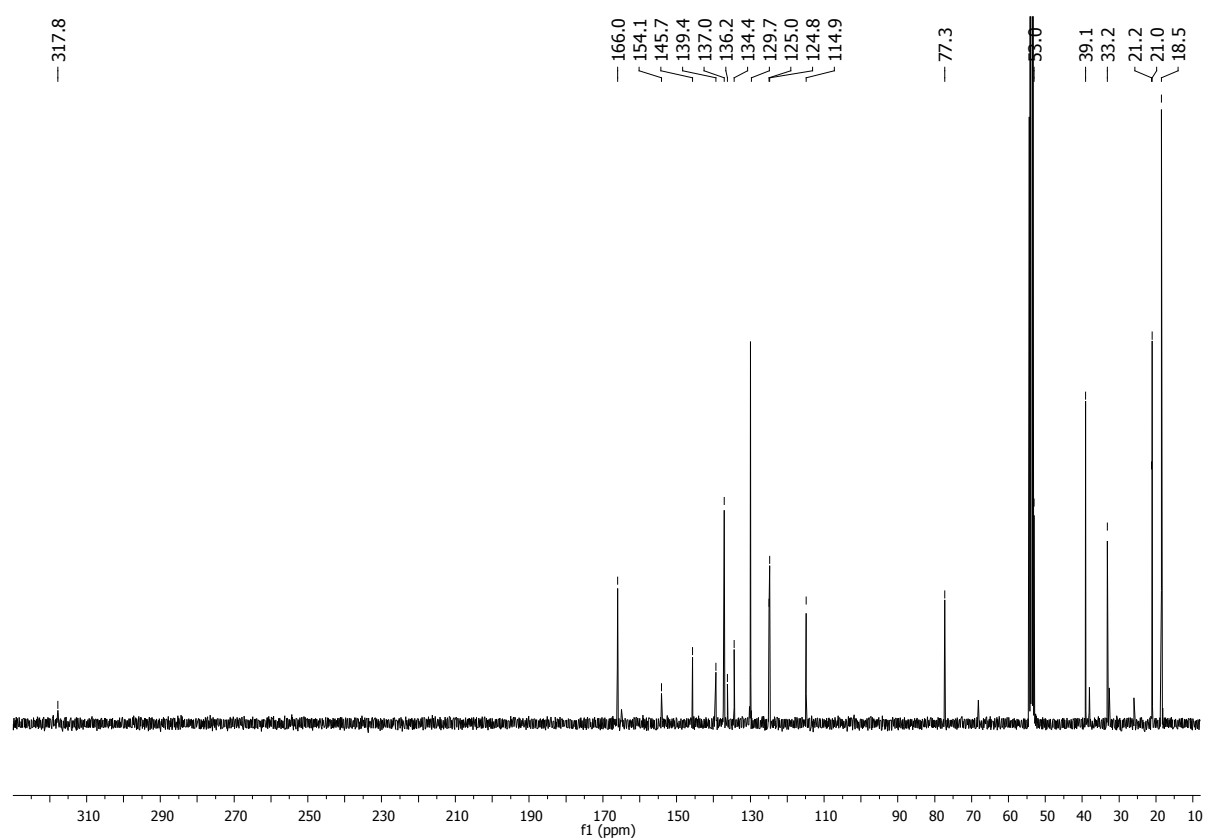
Figure S6. ^{13}C-NMR (CD$_2$Cl$_2$) for [Ru(DMF)$_3$(IMesH$_2$)(=CH-2-(2-PrO)-C$_6$H$_4$)$^{2+}$] [(BF$_4^-$)$_2$] **1**.

115

19.28

7.94
7.85
7.28
7.06
6.96

5.64

4.96

4.08

3.13
2.60
2.37
2.30

1.03

0.91

0.95
1.91
0.96
1.06
3.73

1.86

1.00

3.95

6.28
11.47
11.47
5.69

5.70

Figure S7. ^{1}H-NMR (CD$_2$Cl$_2$) for [Ru(DMF)$_3$(IMesH$_2$)(=CH-2-(2-PrO)-C$_6$H$_4$)$^{2+}$] [(BF$_4^-$)$_2$] **1**.

139.8
138.2
136.5
131.6

73.3
72.0

53.8
49.4
47.7
46.7
45.6
42.8
42.3

34.3
33.5

Figure S8. ^{13}C-NMR (D$_2$O) for *exo, endo*-norborn-2-en-5-ylmethyl-trimethylammonium tetrafluoroborate (**M2**).

116
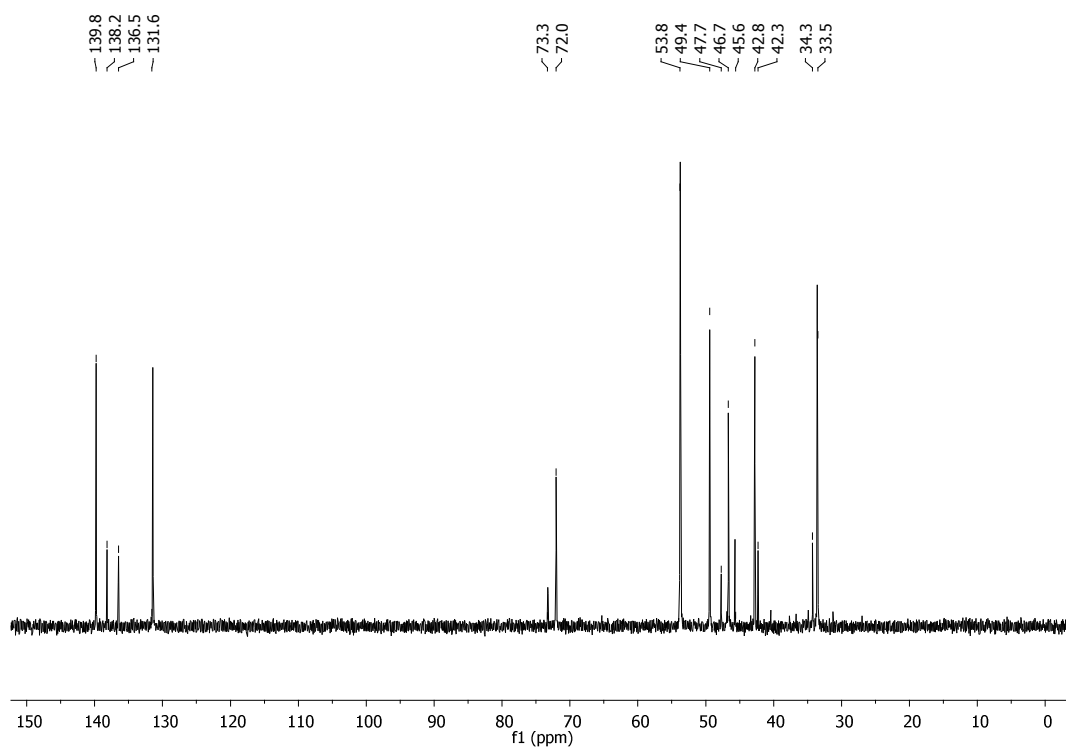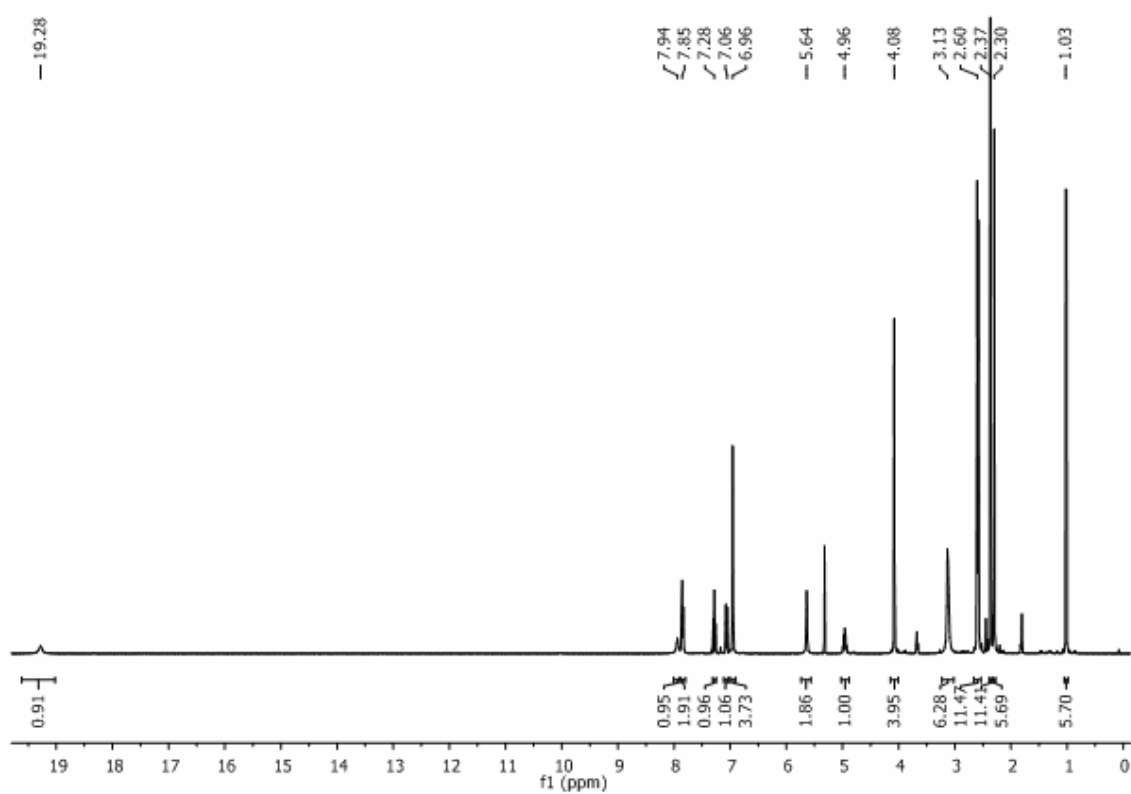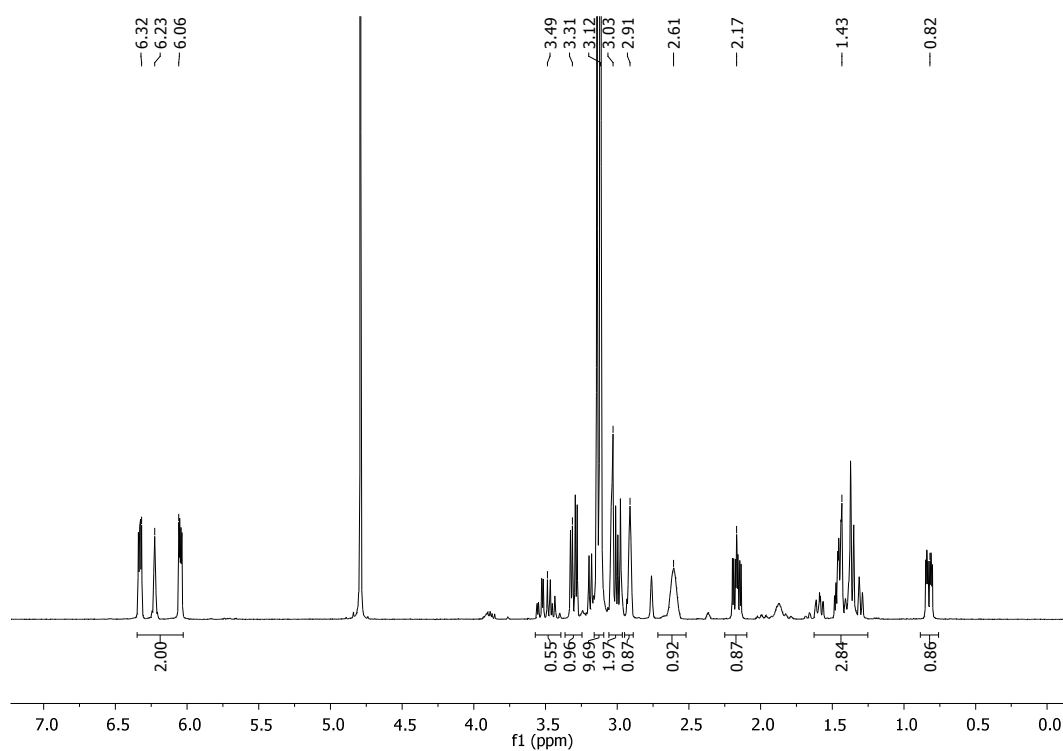
Figure S9. ^{1}H-NMR (D$_2$O) for *exo, endo*-norborn-2-en-5-ylmethyl-trimethylammonium tetrafluoroborate (**M2**).
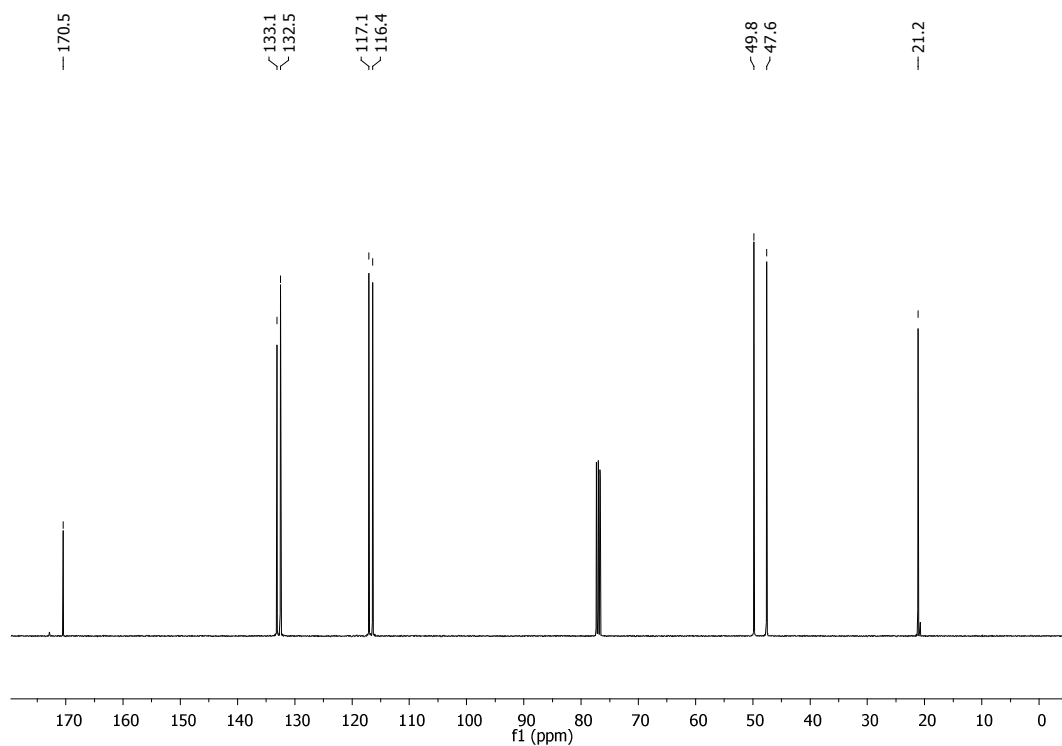
Figure S10. ^{13}C-NMR (CDCl$_3$) for *N,N*-diallylacetamide.

117
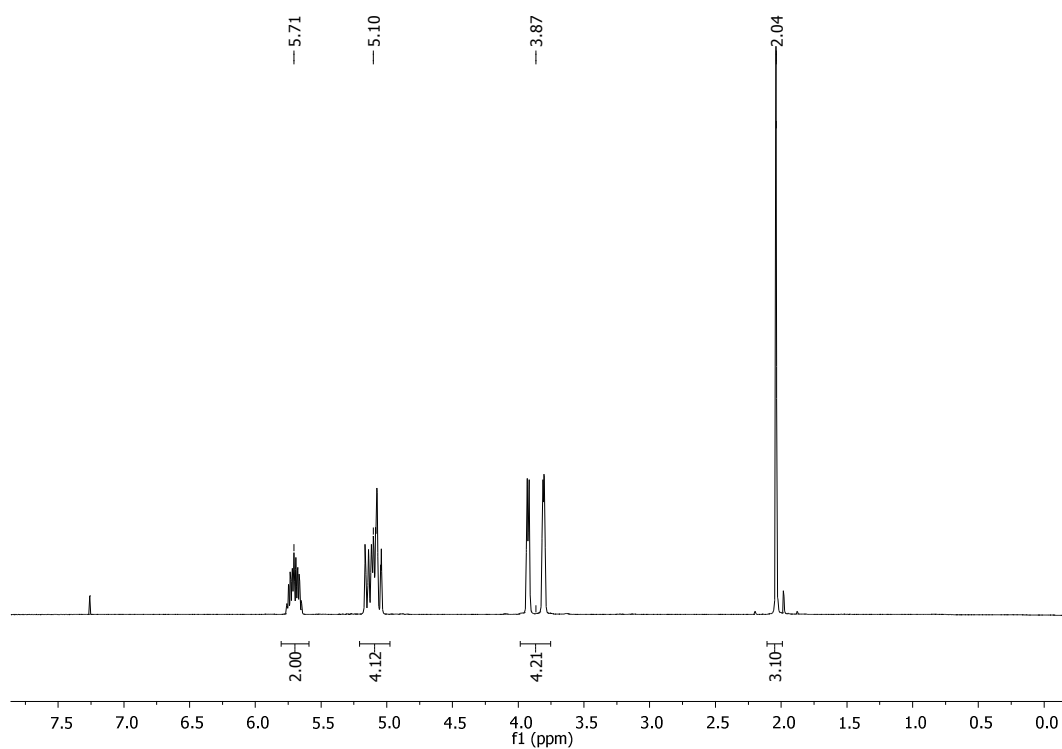
Figure S11. ^{1}H-NMR (CDCl$_3$) for *N,N*-diallylacetamide.
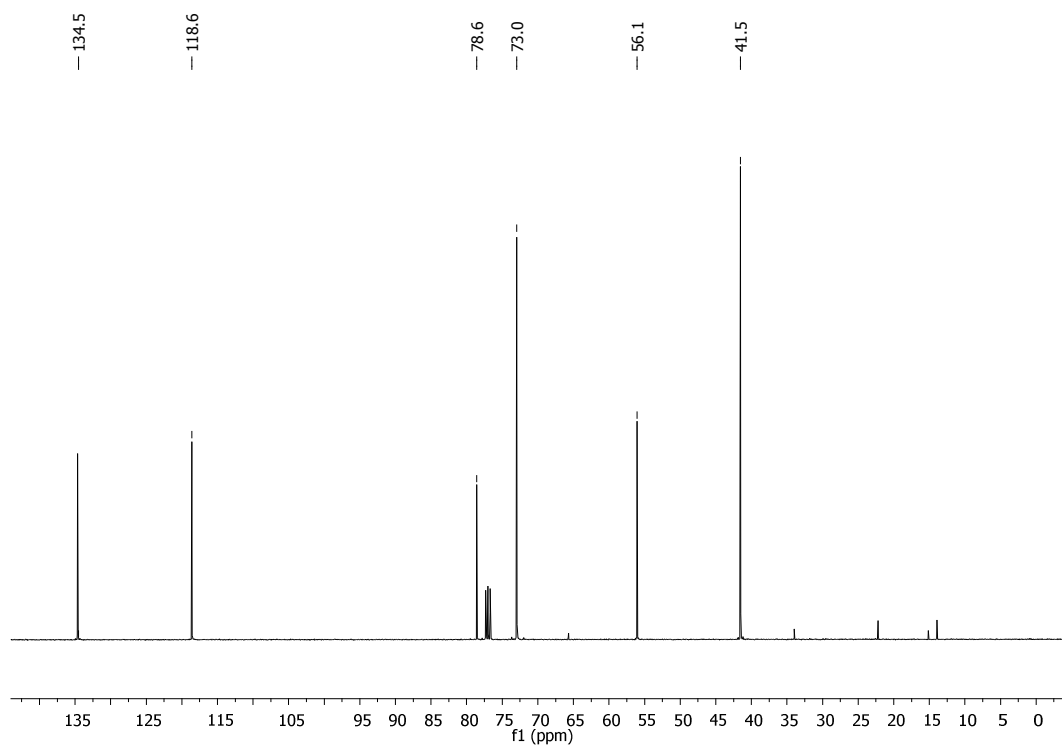
Figure S12. ^{13}C-NMR (CDCl$_3$) for *N*-allyl-*N,N*-dipropargylamine.

118

5.80
5.22
3.41
3.14
2.21

0.99
2.00
3.84
1.94
1.81

7.5 7.0 6.5 6.0 5.5 5.0 4.5 4.0 3.5 3.0 2.5 2.0 1.5 1.0 0.5 0.0
f1 (ppm)
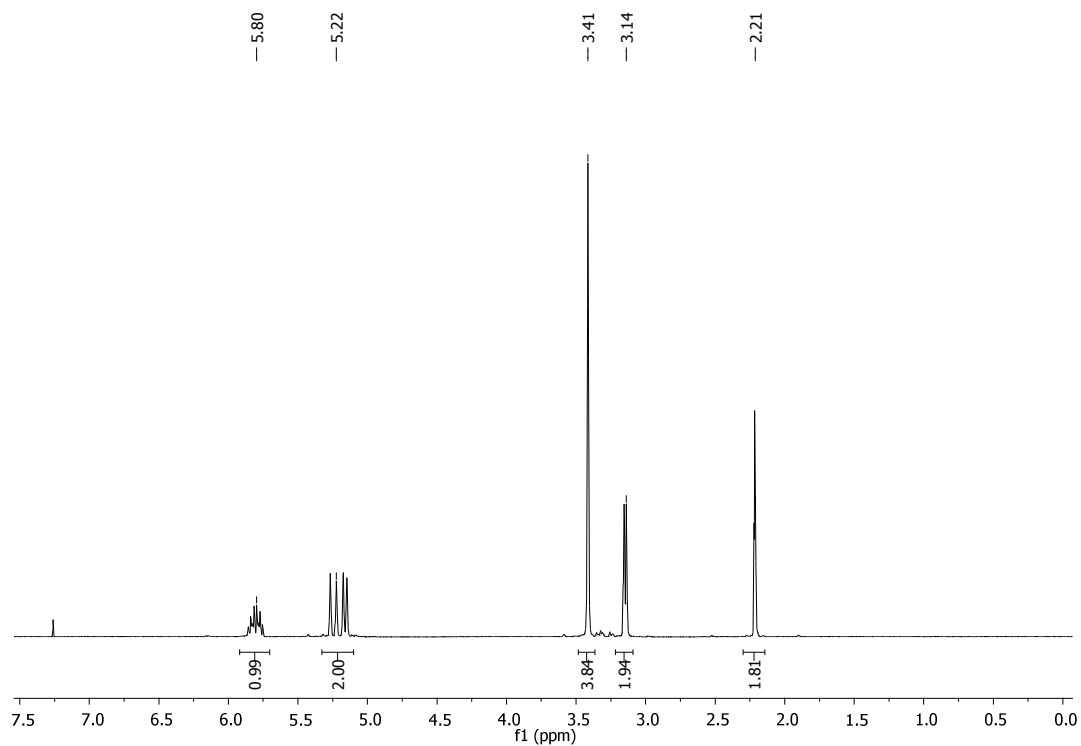
Figure S13. ^{1}H-NMR (CDCl$_3$) for *N*-allyl-*N*,*N*-dipropargylamine.

135.9
116.6
81.9
71.3
50.8
37.2

160 150 140 130 120 110 100 90 80 70 60 50 40 30 20 10 0
f1 (ppm)
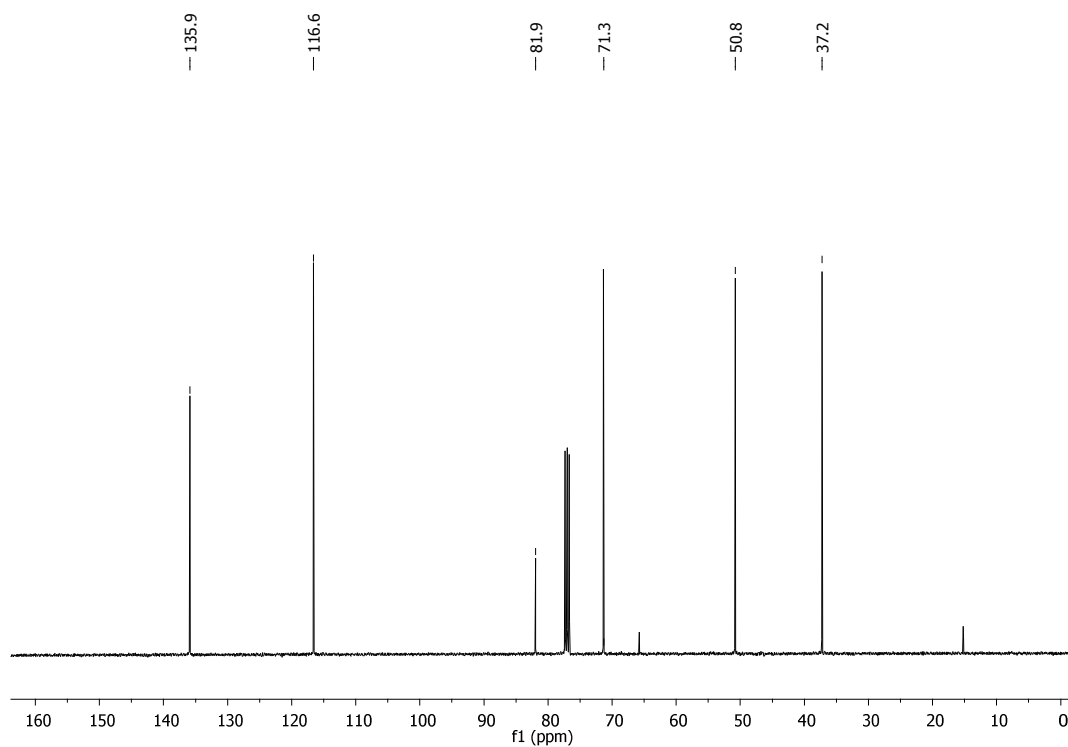
Figure S14. ^{13}C-NMR (CDCl$_3$) for *N*-allyl-*N*-propargyl trifluoroacetamide.

119
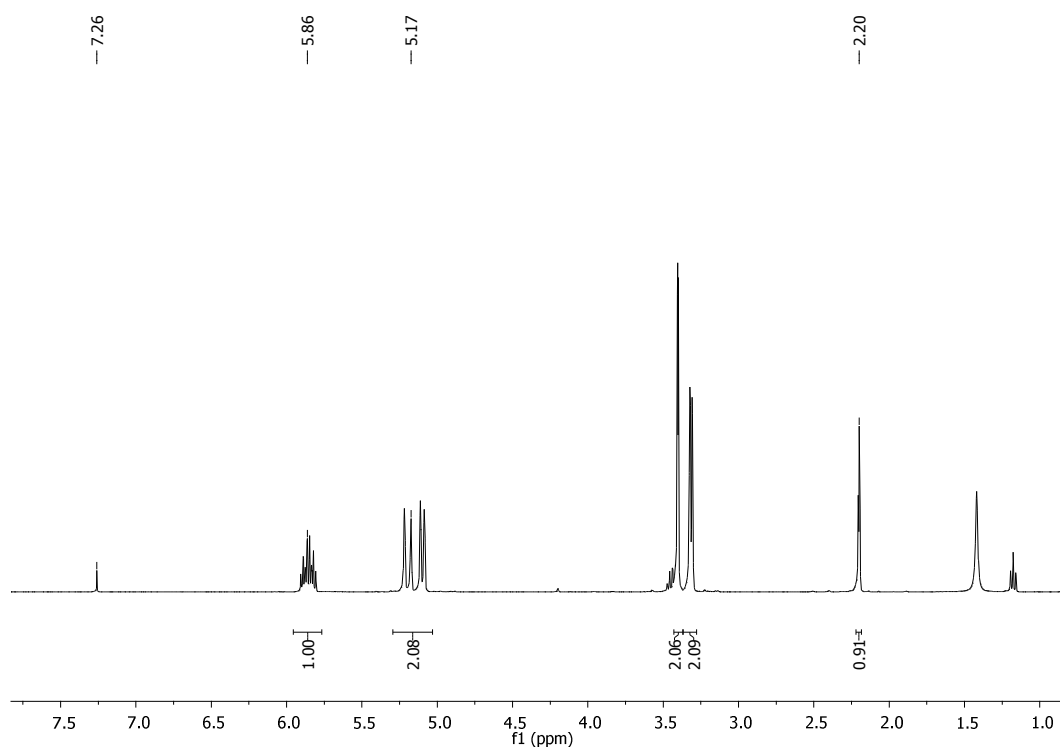
Figure S15. ^{1}H-NMR (CDCl$_3$) for *N*-allyl-*N*-propargyl trifluoroacetamide.
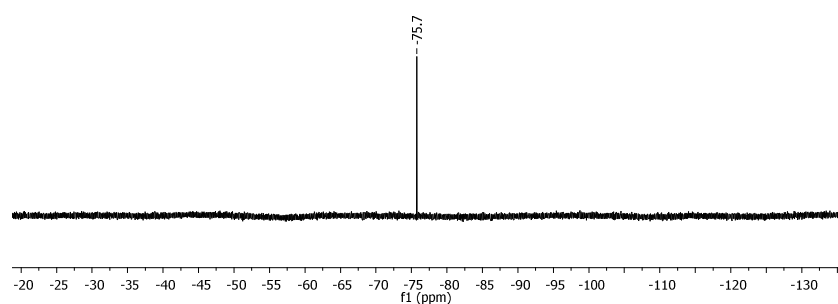
Figure S16. ^{19}F-NMR (CDCl$_3$) for *N*-allyl-*N*-propargyl trifluoroacetamide.
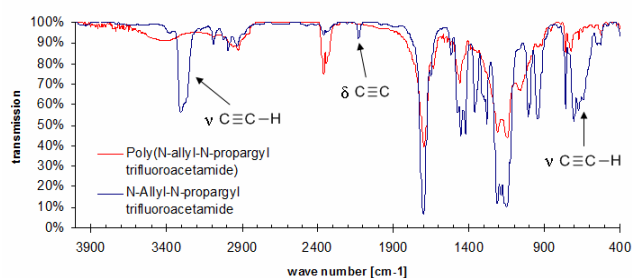
Figure S17. FT-IR of *N*-allyl-*N*-propargyl trifluoroacetamide and of the polymeric product resulting from 1-alkyne polymerization promoted by **1** at elevated temperature (100°C, toluene).
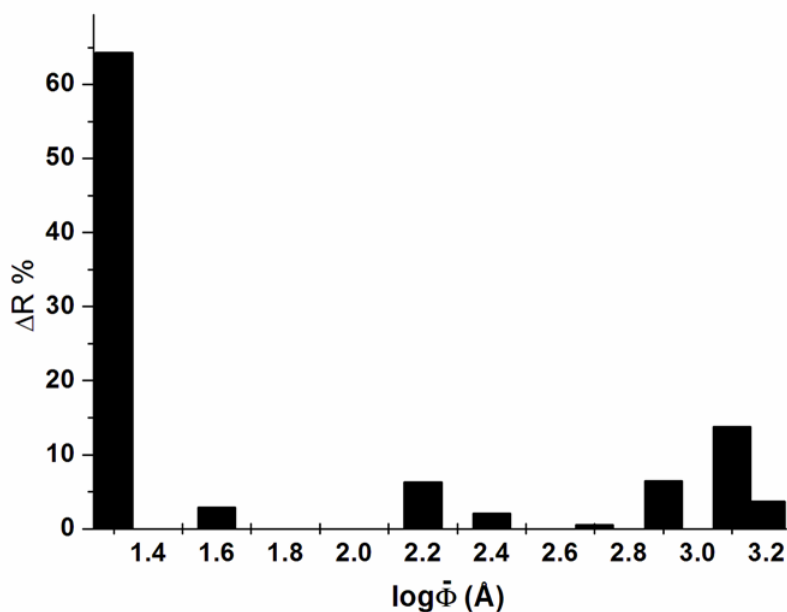
Figure S18. Pore-size distribution of the surface-functionalized monolith **B**.
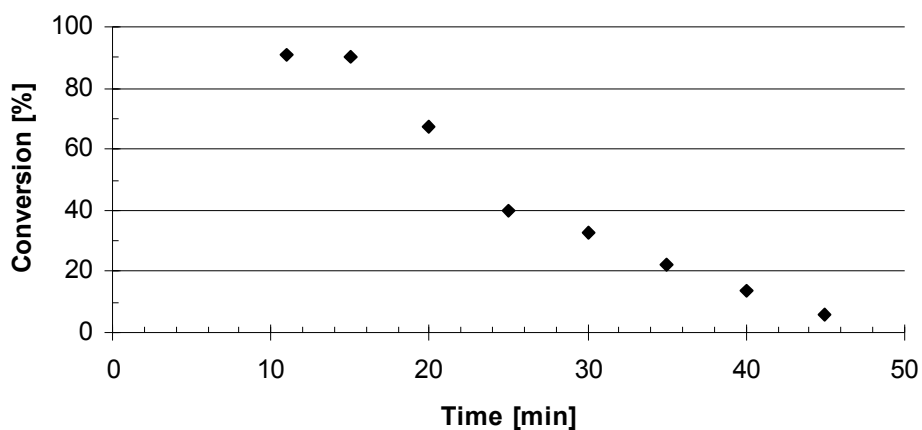
Figure S19. Plot of conversion *versus* time for the continuous biphasic RCM of DAFA. Conditions: Entry 1, Table S1: 3 g heptane, 0.1 mL/min, final TON: 800.
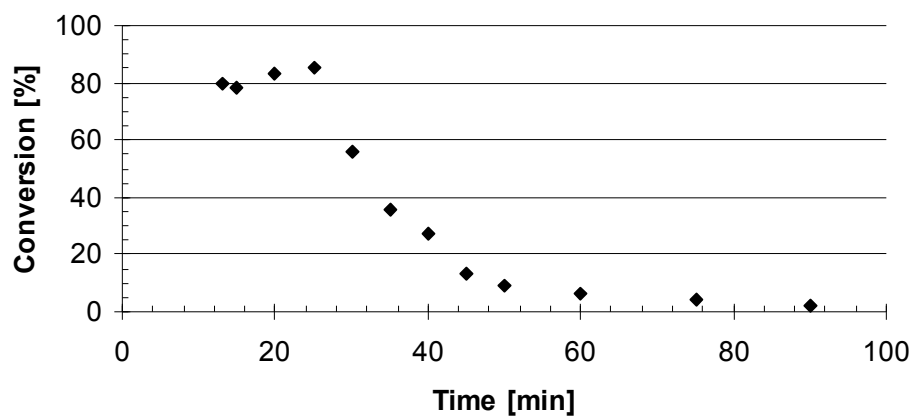
Figure S20. Plot of conversion *versus* time for the continuous biphasic RCM of DAFA. Conditions: Entry 4, Table S1: 7 g heptane, 0.1 mL/min, final TON: 550.

7.2 "Reactivity of 1 in Ring-Opening Metathesis and Cyclopolymerization"

Table S2. NMR-Shifts of alkylidene H and C in pseudohalide-derivatives of *Grubbs-Hoveyda* type catalysts

Compound	Color	^{1}H	^{13}C	Reference
[Ru(DMF)$_3$(IMesH$_2$)(=CH-2-(2-PrO)-C$_6$H$_4$)]$^{2+}$(BF$_4^-$)$_2$]	green	19.28 ppm (400.13 MHz, CD$_2$Cl$_2$, 25°C)	317.7 ppm (100.61 MHz, CD$_2$Cl$_2$, 25°C)	*Chem. Eur. J.* 2012, *18*, *14069.*
[Ru(CF$_3$CO$_2$)$_2$(=CH-2-(2-PrO)-C$_6$H$_4$)(ImesH$_2$)]	lilac	17.38 ppm (300.13 MHz, CDCl$_3$, 25°C)	314.7 ppm (75.47 MHz, CDCl$_3$, 25°C)	*Chem. Eur. J.* **2004**, *10*, 777.
[Ru(CF$_3$CF$_2$CO$_2$)$_2$(=CH-2-(2-PrO)-C$_6$H$_4$)(ImesH$_2$)]	lilac	17.59 ppm (300.13 MHz, CDCl$_3$, 25°C)	316.3 ppm (75.47 MHz, CDCl$_3$, 25°C)	*Chem. Eur. J.* **2004**, *10*, 2029.
[RuCl(CF$_3$SO$_3$)(=CH-2-(2-PrO)-C$_6$H$_4$)(ImesH$_2$)]	green	17.49 ppm (300.13 MHz, CDCl$_3$, 25°C)	313.8 ppm (75.47 MHz, CDCl$_3$, 25°C)	*Chem. Eur. J.* **2004**, *10*, 777.
[Ru(CF$_3$SO$_3$)$_2$(=CH-2-(2-PrO)-C$_6$H$_4$)(ImesH$_2$)]	green	18.48 ppm (300.13 MHz, CDCl$_3$, 25°C)	332.4 ppm (75.47 MHz, CDCl$_3$, 25°C)	*Chem. Eur. J.* **2004**, *10*, 777.
[Ru(C$_6$F$_5$CO$_2$)$_2$(=CH-2-(2-PrO)-C$_6$H$_4$)(ImesH$_2$)]	lilac	17.41 ppm (300.13 MHz, CDCl$_3$, 25°C)	313.3 ppm (75.47 MHz, CDCl$_3$, 25°C)	*J. Am. Chem. Soc.* **2009**, *131*, 387.
[Ru(N=C=O)$_2$(=CH-2-(2-PrO)-C$_6$H$_4$)(ImesH$_2$)]	green	16.37 ppm (600.25 MHz, CDCl$_3$, 25°C)	299.7 ppm (150.95 MHz, CDCl$_3$, 25°C)	*Chem. Asian J.* **2009**, *4*, 1275.
[Ru(N=C=S)$_2$(=CH-2-(2-PrO)-C$_6$H$_4$)(ImesH$_2$)]	yellow-green	16.40 ppm (600.25 MHz, CDCl$_3$, 25°C)	311.8 ppm (150.95 MHz, CDCl$_3$, 25°C)	*Chem. Asian J.* **2009**, *4*, 1275.
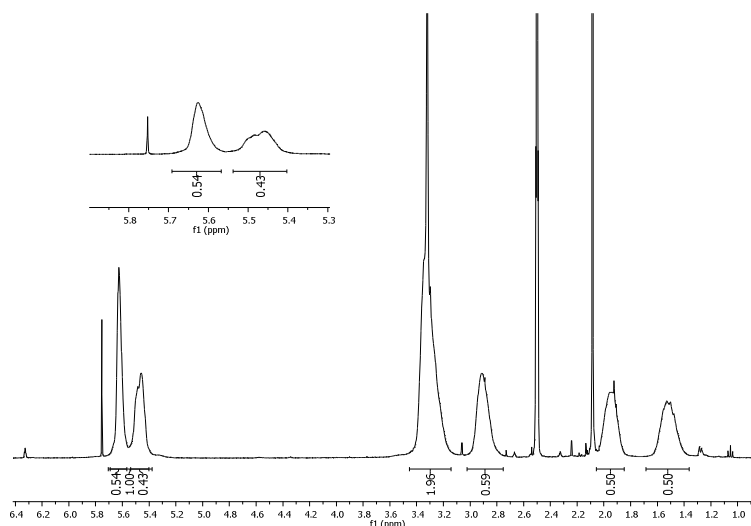
Figure S21. ^{1}H-NMR (DMSO-d_6) spectrum of poly-**M9** as an example for the determination of *cis/trans* ratio by integration of the olefinic signals.
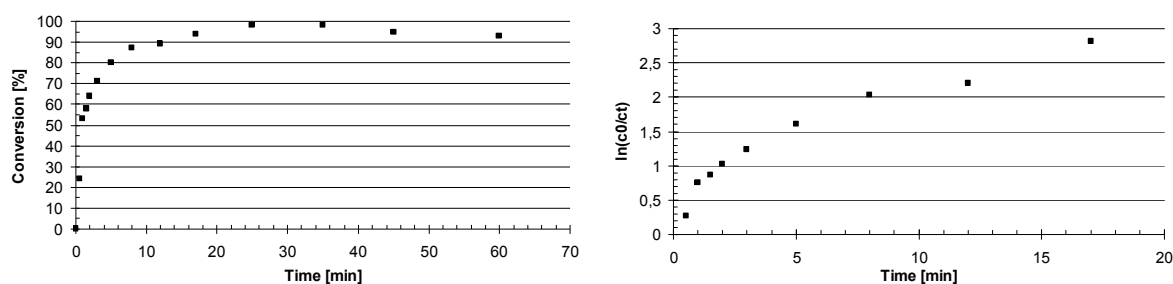
Figure S22. ROMP of **M6** promoted by **1** at 20°C, substrate:1=200:1 (left). 1st-order plot for the ROMP of **M6** at 20°C (right).
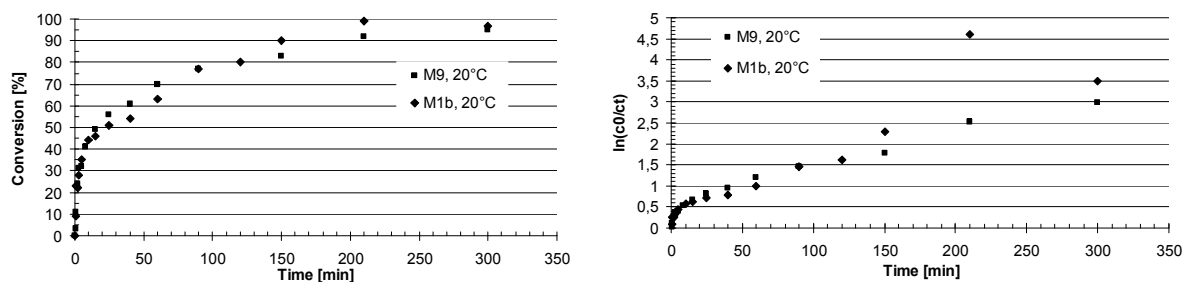
Figure S23. ROMP of **M9** and **M1b** promoted by **1** at 20°C, substrate:**1**=200:1 (left). 1st-order plot for the ROMP of **M9** and **M1b** at 20°C (right).
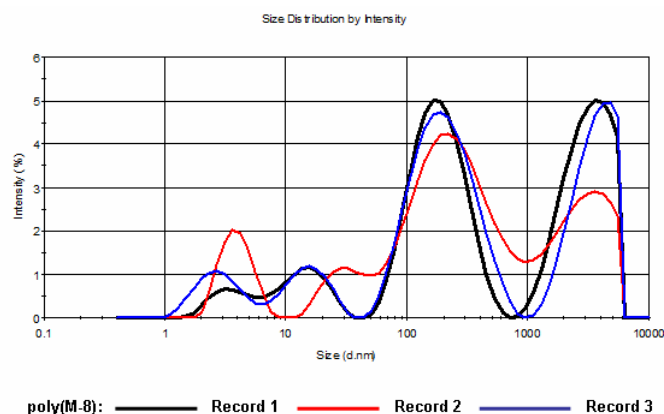
Figure S24. Size distribution of poly-**M1b** determined by DLS-measurements in DMF at 20°C. 3 total measurements which are an average of 15 scans each, 3 minutes to equilibrate. Peak 1 (16 nm diameter, 9% intensity) indicates polymer chain. Peak 2 (230 nm diameter, 50% intensity) and peak 3 (3630 nm diameter, 34% intensity) indicate aggregates.
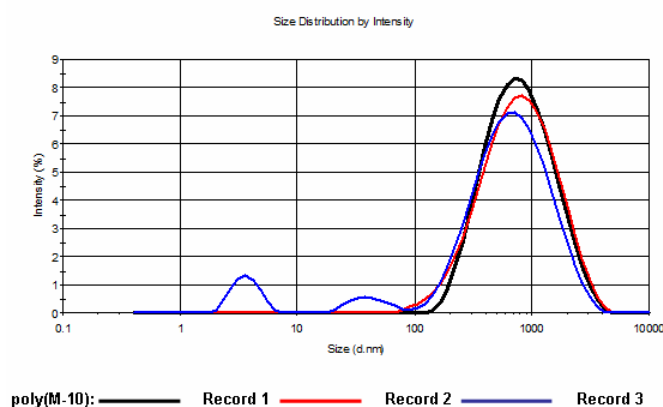
Figure S25. Size distribution of poly-**M2** determined by DLS-measurements in DMF at 20°C. 3 total measurements which are an average of 15 scans each, 3 minutes to equilibrate. Peak 1 (4 nm diameter, 7% intensity) indicates polymer chain. Peak 2 (834 nm diameter, 89% intensity) indicates aggregates.
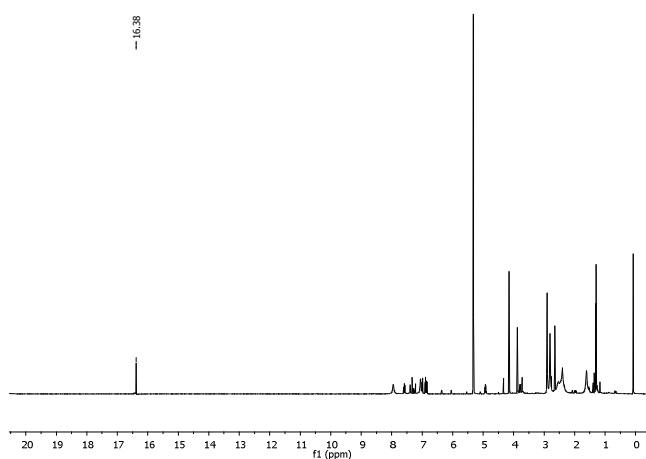
Figure S26. ^{1}H-NMR (CD$_2$Cl$_2$) for the ROMP of **M1b-Br** (Br$^-$ as counter ion). **1**:monomer = 1:5. The alkylidene signal of the parent complex (δ=19.28 ppm) completely vanished, a new signal at δ=16.38 ppm (indicative for the formation of [RuBr$_2$(IMesH$_2$)(=CH-2-(2-PrO)-C$_6$H$_4$)]), is observed.
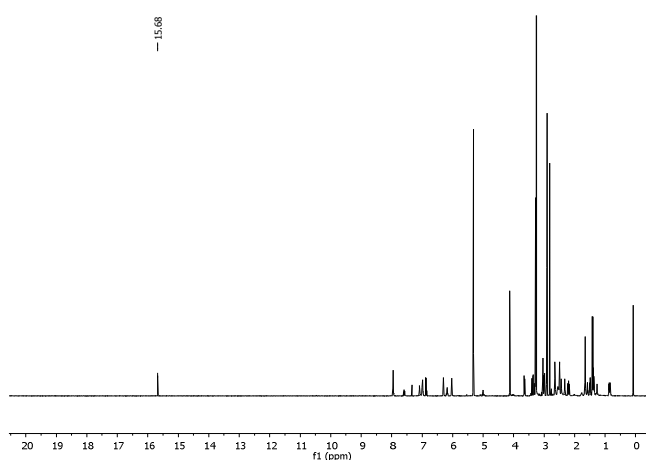
Figure S27. ^{1}H-NMR (CD$_2$Cl$_2$) for the ROMP of **M2-I** (I$^-$ as counter ion). **1**:monomer = 1:5. The alkylidene signal of the parent complex (δ=19.28 ppm) completely vanished, instead, a new signal at δ=15.68 ppm (indicative for [RuI$_2$(IMesH$_2$)(=CH-2-(2-PrO)-C$_6$H$_4$)]), is observed.

126
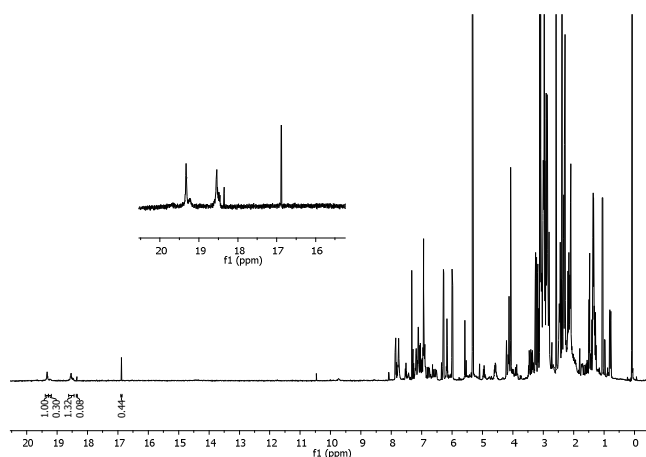
Figure S28. ^{1}H-NMR (CD$_2$Cl$_2$) for the ROMP of **M2** (BF$_4^-$ as counter ion). **1**:monomer = 1:5. The alkylidene signal of the parent complex (δ=19.28 ppm) is still present, in addition, several new downfield shifted alkylidene signals formed.
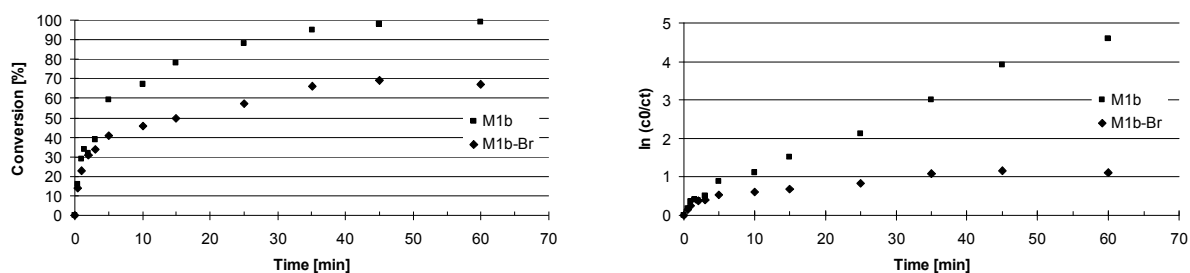
Figure S29. ROMP of **M1b** (BF$_4^-$ as counter ion) and **M1b-Br** (Br$^-$ as counter ion) promoted by **1** at 20°C, substrate:**1**=200:1.
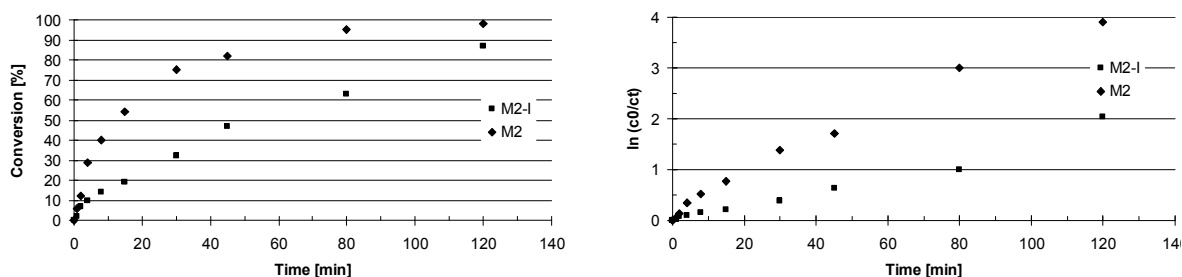
Figure S30. ROMP of **M2** (BF$_4^-$ as counter ion) and **M2-I** (I$^-$ as counter ion) promoted by **1** at 20°C, substrate:**1**=200:1.
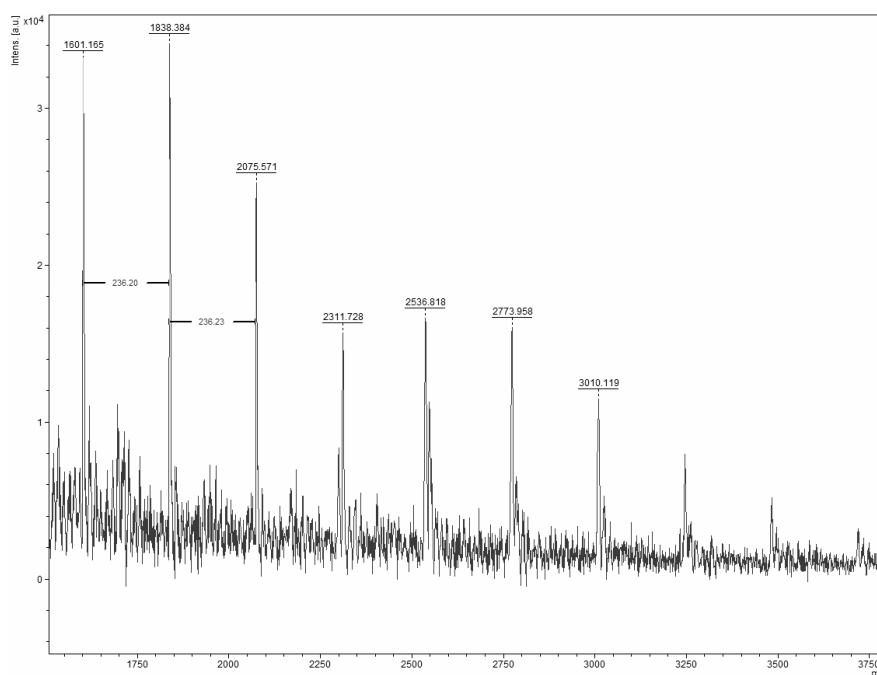
n	rep. unit	resid.	end 1	end 2	cation	M_n	M_w	pd	DP	% Int.
1	236.105	-0.50573	148.090	14.0100	22.9898	1690	1730	1.02	7	13.8
2	236.105	0.54263	148.090	14.0100	22.9898	1810	1830	1.01	8	13.6
3	236.105	1.58347	148.090	14.0100	22.9898	1890	1920	1.02	8	16.7

Figure S31. MALDI –TOF spectrum and results for poly-**H1**, prepared by the action of **1**. **1**:monomer = 1:5. End group 1 (end 1) indicates =CH-2-(2-PrO)-C_6H_4, end group 2 (end 2) corresponds to =CH_2. The cation is Na^+.
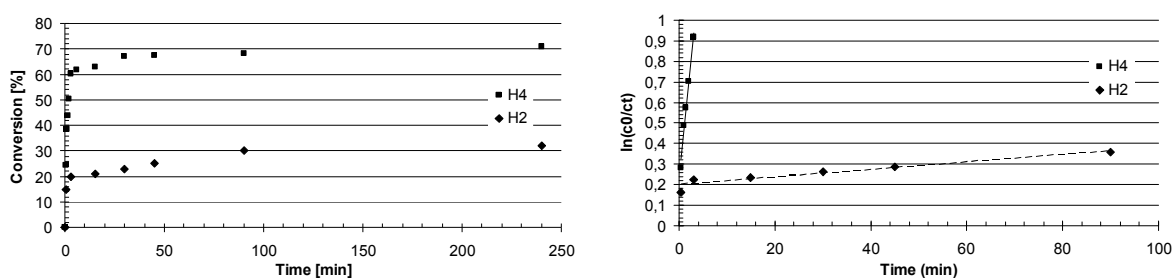
Figure S32. Cyclopolymerization of **H2** and **H4** promoted by **1** at 35°C, substrate:**1** = 80:1 (left). 1st-order plot for the cyclopolymerization of **H2** and **H4** at 35°C (right).
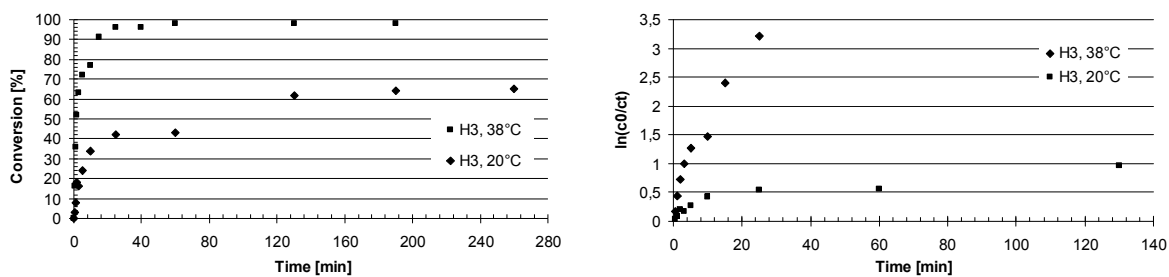
Figure S33. Cyclopolymerization of **H3** promoted by **1** at different temperatures (left). 1st-order plot for the cyclopolymerization of **H3** at different temperatures (right).
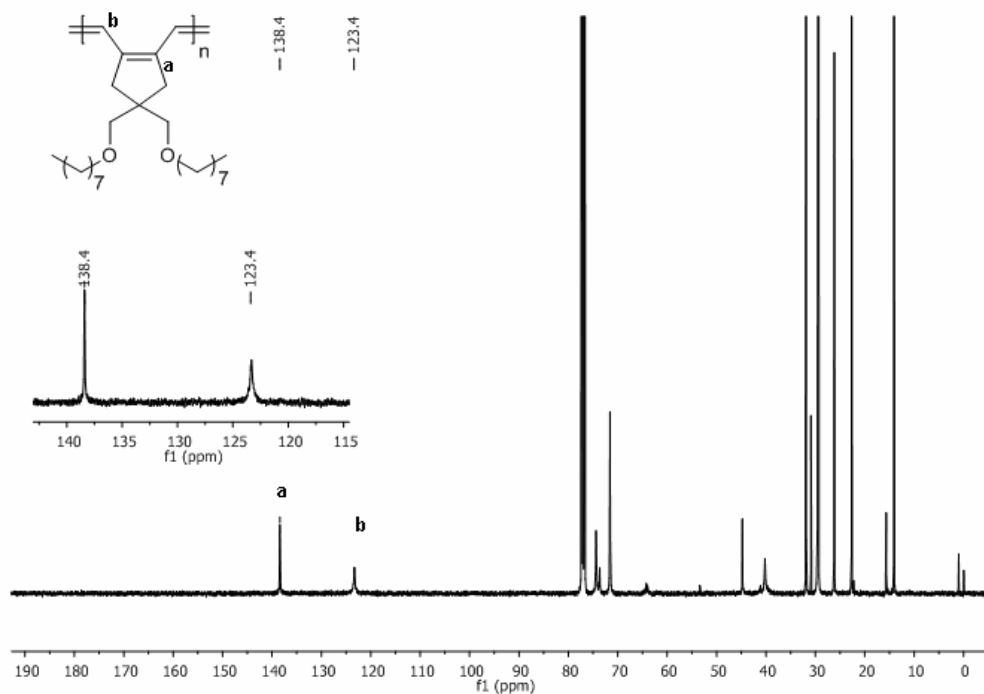
Figure S34. ^{13}C-NMR spectra (CDCl$_3$) of poly-**H3** prepared by the action of **1**.
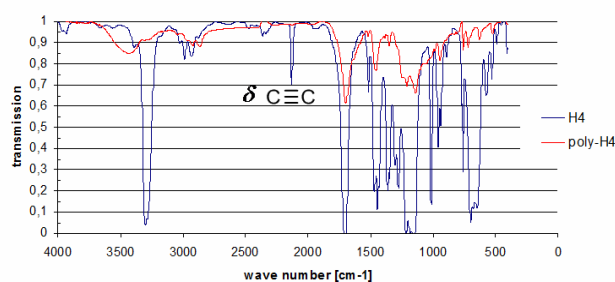
Figure S35. IR-spectra of **H4** and poly-**H4**.

129
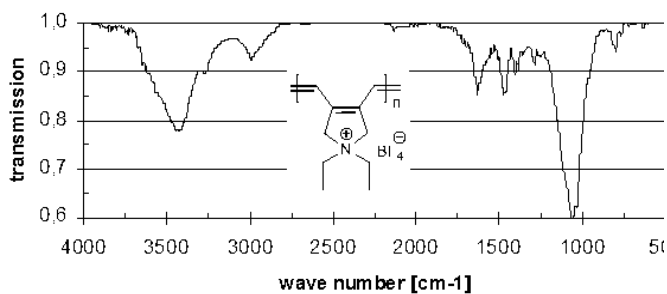
Figure S36. IR spectrum of poly-**H5**.
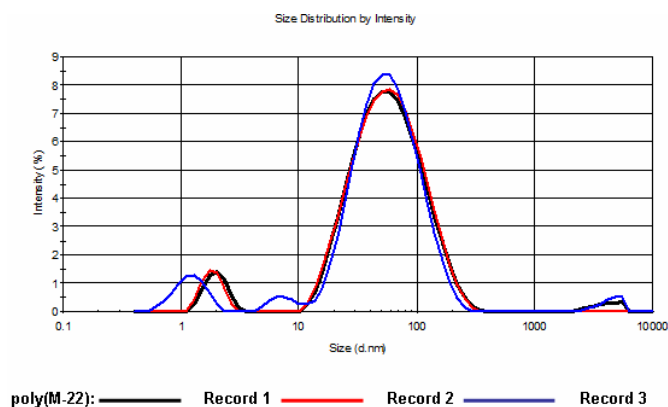
Figure S37. Size distribution of poly-**H4** determined by DLS-measurements in DMF at 20°C. 3 total measurements which are an average of 15 scans each, 3 minutes to equilibrate. Peak 1 (8 nm diameter, 2% intensity) indicates polymer chain. Peak 2 (70 nm diameter, 89% intensity) indicates aggregates.
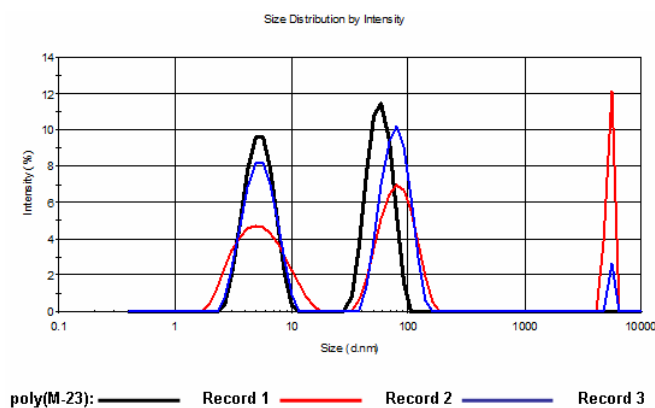
Figure S38. Size distribution of poly-**H5** determined by DLS-measurements in DMF at 20°C. 3 total measurements which are an average of 15 scans each, 3 minutes to equilibrate. Peak 1 (5 nm diameter, 47% intensity) indicates polymer chain. Peak 2 (80 nm diameter, 51% intensity) indicates aggregates.
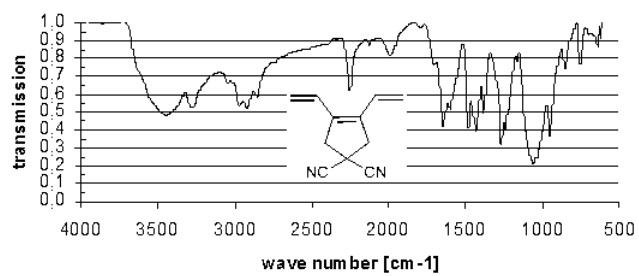
Figure S39. IR spectrum of poly-**H2**.

7.3 "Catalyst Optimization"
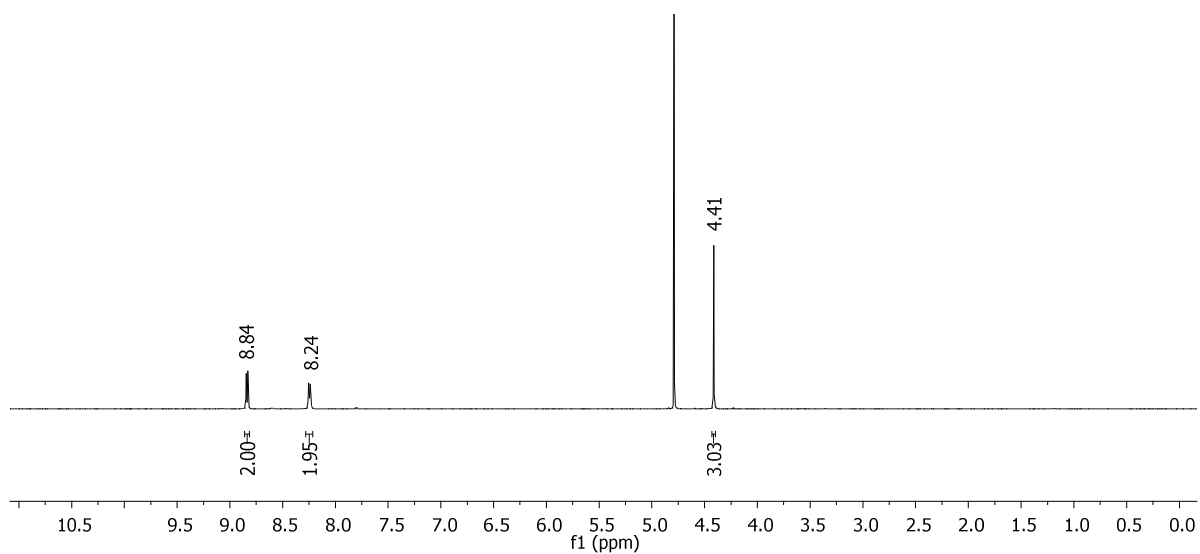
Figure S40. ^{1}H NMR spectrum (D$_2$O) of tetrafluoroborato *N*-methylpyridinium-4-potassium carboxylate.
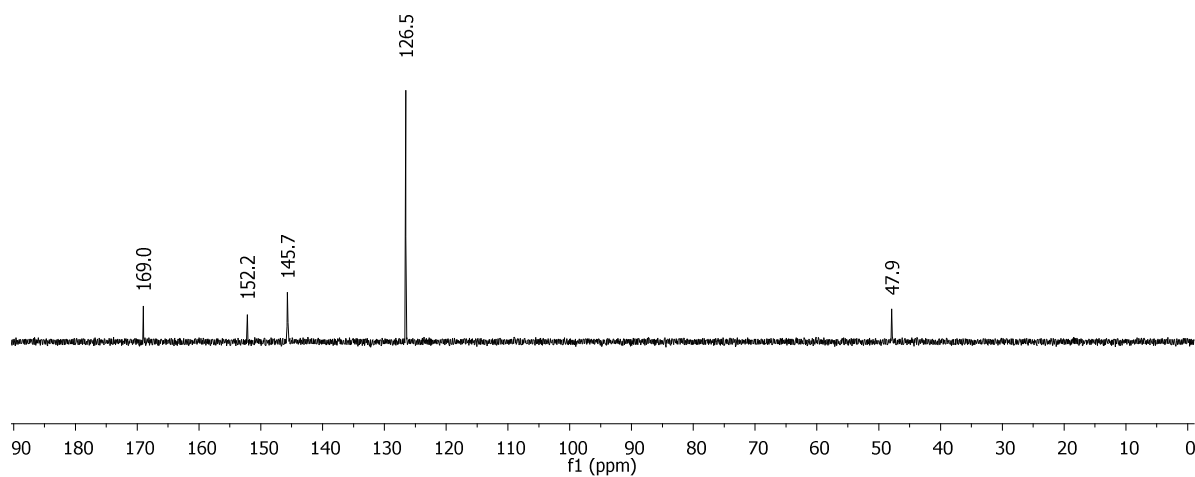
Figure S41. ^{13}C NMR spectrum (D$_2$O) of tetrafluoroborato *N*-methylpyridinium-4-potassium carboxylate.
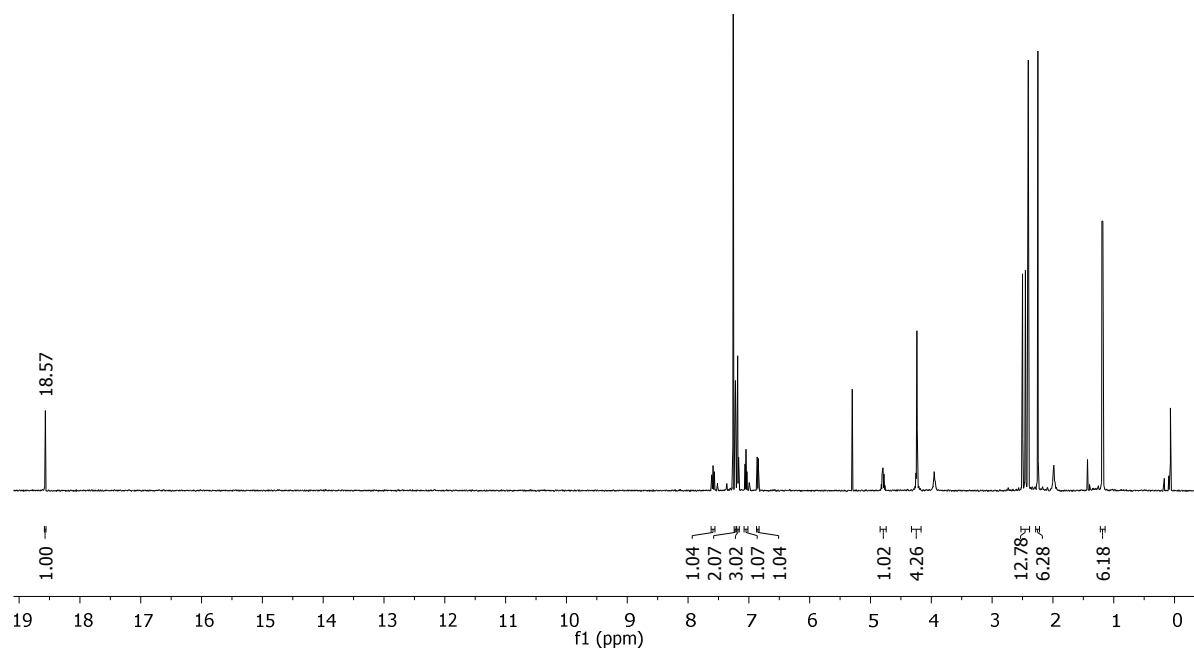
Figure S42. ^{1}H NMR spectrum (CDCl$_3$) of [Ru(CF$_3$SO$_3$)$_2$(IMesH$_2$)(=CH-2-(2-PrO)-C$_6$H$_4$)].
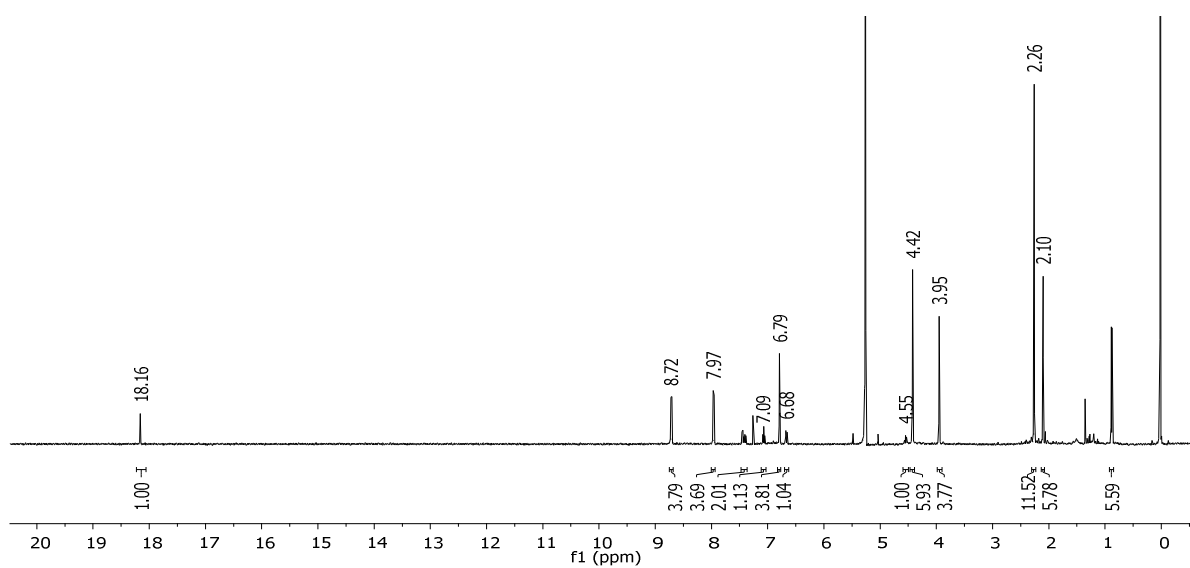
Figure S43. ^{1}H NMR spectrum (CD$_2$Cl$_2$) of [Ru[(4-CO$_2$)(1-CH$_3$)Py$^+$)]$_2$(IMesH$_2$)(=CH-2-(2-PrO)-C$_6$H$_4$)] [OTf $^-$]$_2$ (**2**).

133
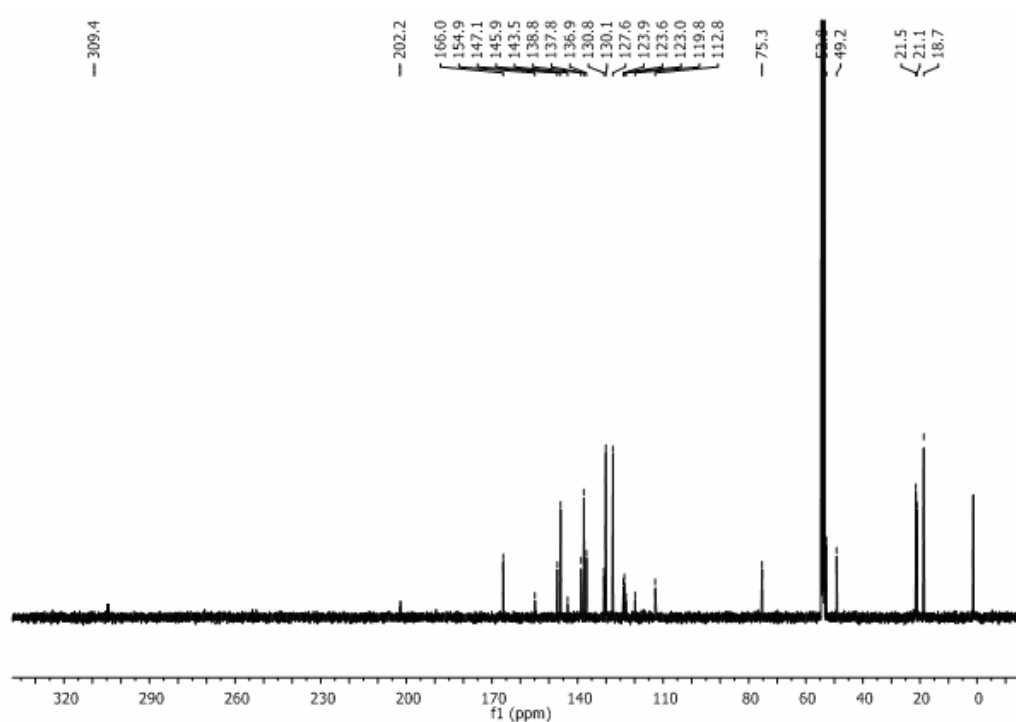
Figure S44. ^{13}C NMR spectrum (CD$_2$Cl$_2$) of [Ru[(4-CO$_2$)(1-CH$_3$)Py$^+$)]$_2$(IMesH$_2$)(=CH-2-(2-PrO)-C$_6$H$_4$)] [OTf $^-$]$_2$ (**2**).
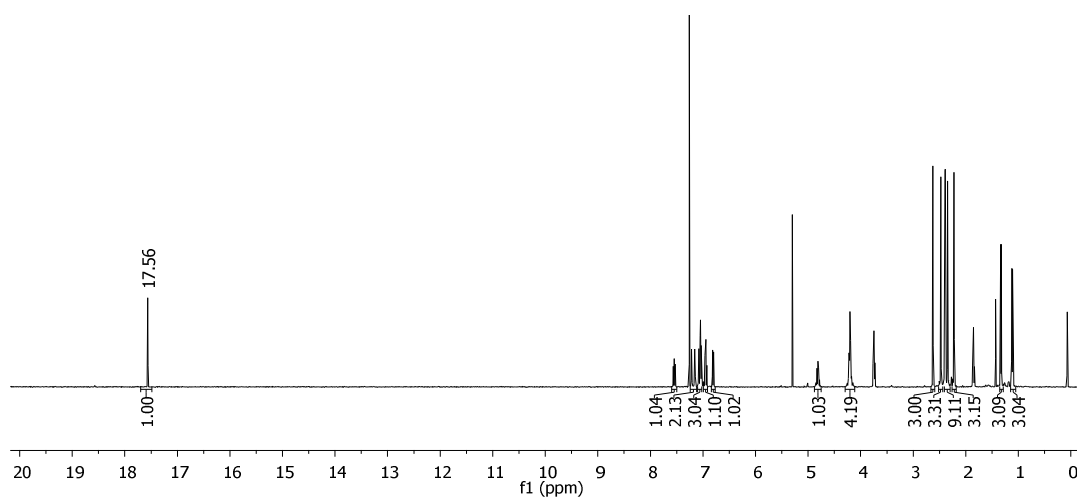
Figure S45. ^{1}H NMR spectrum (CDCl$_3$) of [RuCl(CF$_3$SO$_3$)(IMesH$_2$)(=CH-2-(2-PrO)-C$_6$H$_4$)].
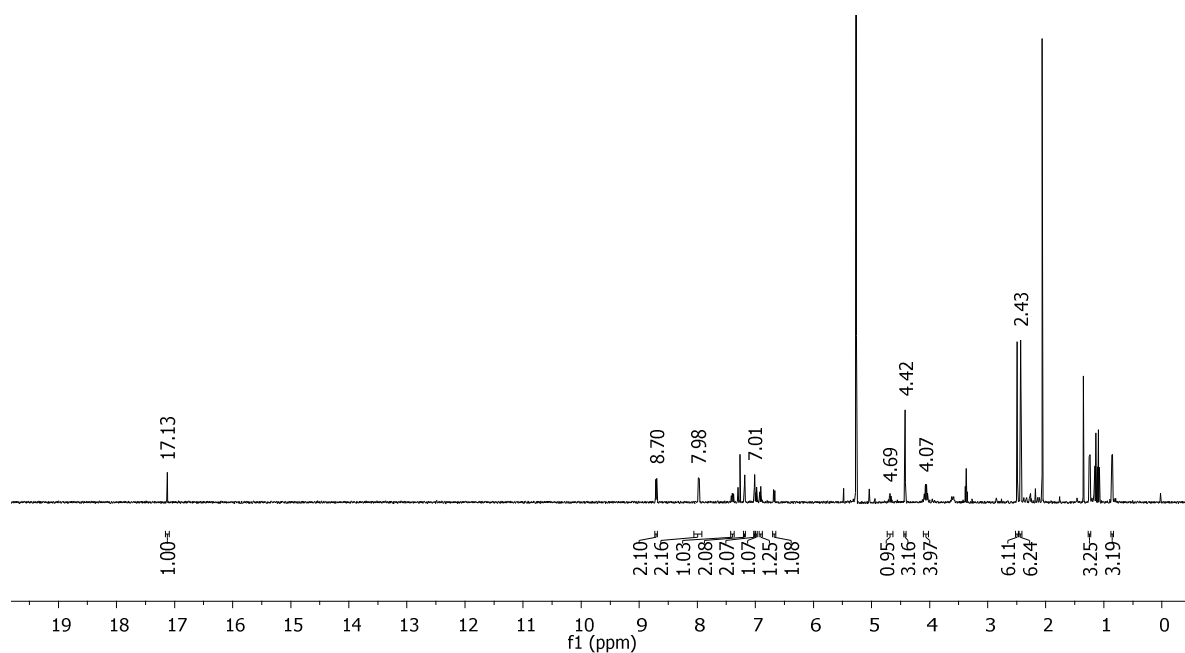
Figure S46. ^{1}H NMR spectrum (CD$_2$Cl$_2$) of [RuCl[(4-CO$_2$)(1-CH$_3$)Py$^+$)](IMesH$_2$)(=CH-2-(2-PrO)-C$_6$H$_4$)] [OTf $^-$] (**3**).
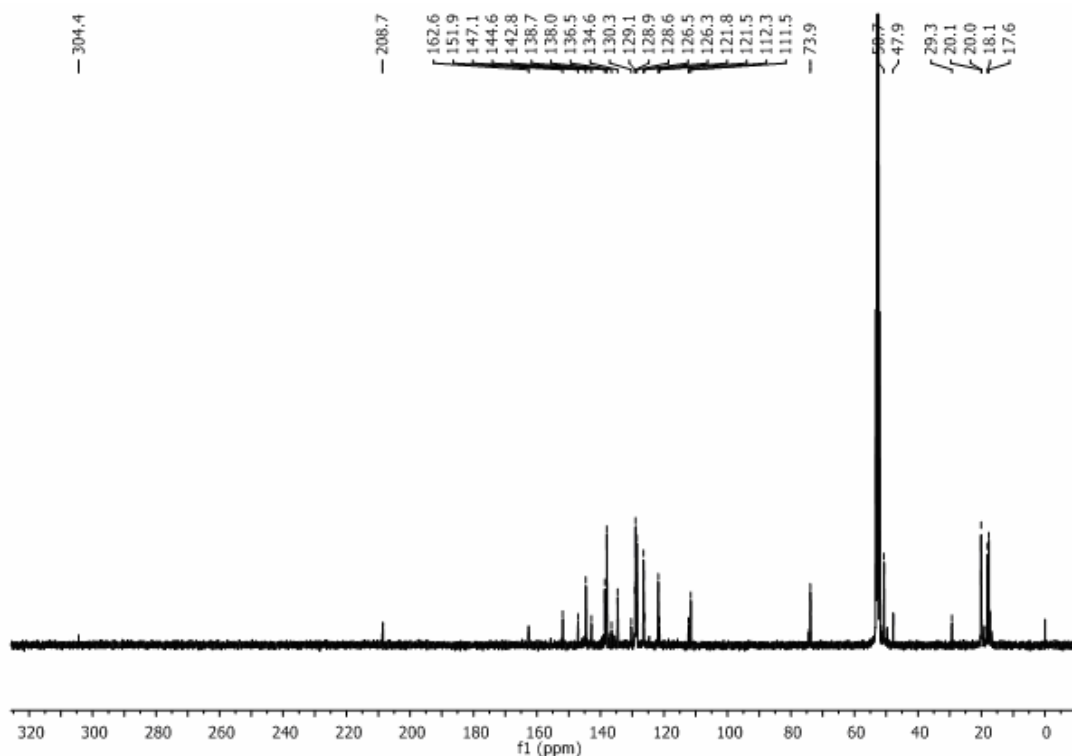
Figure S47. ^{13}C NMR spectrum (CD$_2$Cl$_2$) of [RuCl[(4-CO$_2$) (1-CH$_3$)Py$^+$)](IMesH$_2$)(=CH-2-(2-PrO)-C$_6$H$_4$)] [OTf $^-$] (**3**).
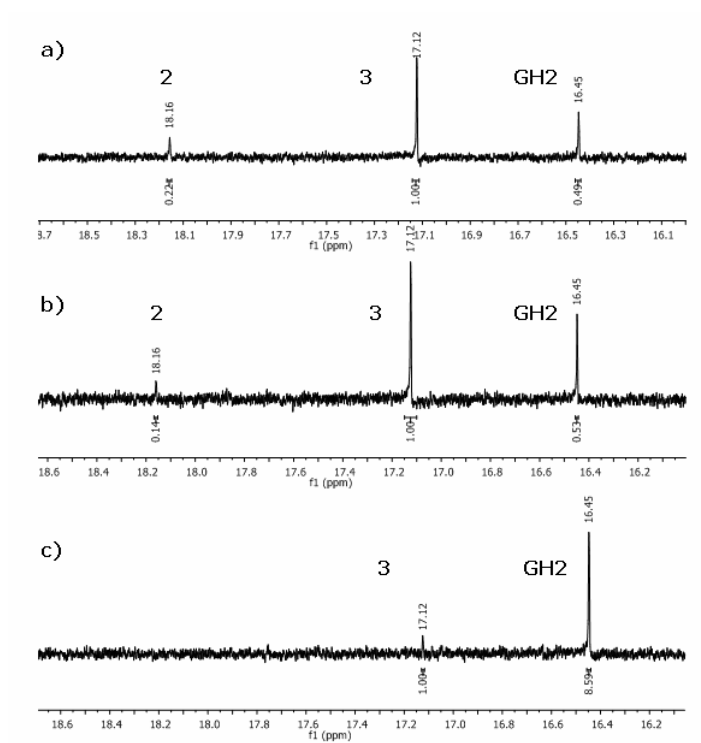
135

Figure S48. Disproportionation of **3** at 80°C in CD$_2$Cl$_2$. a): Complex **3** after 0.5 h in CD$_2$Cl$_2$ at 80°C. b): Complex **3** after 1 h in CD$_2$Cl$_2$ at 80°C. c): Complex **3** after 24 h in CD$_2$Cl$_2$ at 80°C.
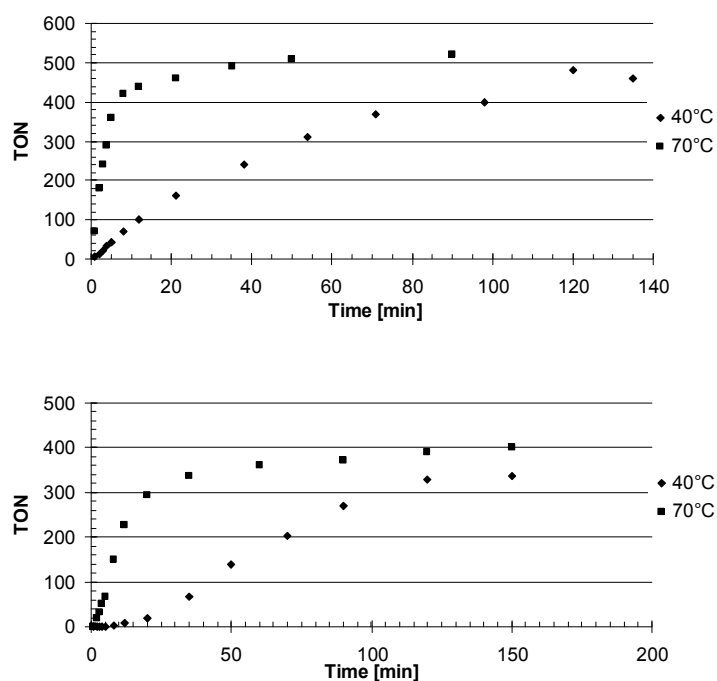

Figure S49. RCM of 1,7-octadiene (top) and *N,N*-diallyltrifluoroacetamide (DAFA, down) promoted by the ionic complex **2** at different temperatures.

7. Curriculum Vitae

Family name: Autenrieth
First name: Benjamin
Date of birth / Nationality: 11.02.1985 / German

Education

03.2010 – 05.2013   PhD-thesis:
                                    # "Continuous metathesis under biphasic liquid-liquid
                                       conditions using monolith-supported ionic liquids"
                                    # University of Stuttgart, Institute of Polymer Chemistry
                                    # Supervisior: Prof. Dr. Michael R. Buchmeiser

02.2009 – 08.2009   Diploma-thesis:
                                    # "Microreactor technology for miniemulsions and
                                       preparation of fluorescent polymer particles for cellular
                                       uptake *via* miniemulsion polymerization"
                                    # Max Planck Institute for Polymer Research, Mainz
                                    # Supervisior: Prof. Dr. Katharina Landfester

10.2004 – 01.2009   Studies of Chemistry at the University of Ulm, Germany

Publications

1. Ionic Grubbs–Hoveyda complexes for biphasic ring-opening metathesis
polymerization in ionic liquids: Access to low metal content polymers
C. P. Ferraz, B. Autenrieth, W. Frey, M. R. Buchmeiser, *ChemCatChem*, **2013**,
DOI:10.1002/cctc.201300751.

2. Ionically tagged Ru-alkylidenes for metathesis reactions under biphasic
liquid-liquid conditions
B. Autenrieth, F. Willig, D. Pursley, S. Naumann, M. R. Buchmeiser, *ChemCatChem*,
2013, *5*, 3033 - 3040.

3. Reactivity of the dicationic ruthenium-alkylidene complex [Ru(DMF)$_3$(IMesH$_2$)(=CH-2-(2-PrO)-C$_6$H$_4$)$^{2+}$][(BF$_4^-$)$_2$] in ring-opening metathesis and cyclopolymerization

B. Autenrieth, E. B. Anderson, D. Wang, M. R. Buchmeiser, *Macromol. Chem. Phys.*, **2013**, 214, 33 - 40.

Highlighted in *Materials Views*, Nov. 22, **2012** by Stefan Spiegel.

4. A dicationic ruthenium-alkylidene complex for continuous biphasic metathesis using monolith-supported ionic liquids

B. Autenrieth, W. Frey, M. R. Buchmeiser, *Chem. Eur. J.*, **2012**, *18*, 14069 – 14078.

5. Continuous metathesis within monolith-supported ionic liquids

B. Autenrieth, E. B. Anderson, M. R. Buchmeiser, *Stuttgarter Kunststoffkolloquium*, **2011**, 1V2, 1-7, ISBN 978-3-00034152-6.

6. The softer and more hydrophobic the better: Influence of the side chain of polymethacrylate nanoparticles for cellular uptake

S. Lorenz, C. P. Hauser, B. Autenrieth, C. K. Weiss, K. Landfester, V. Mailänder, *Macromol. Biosci.*, **2010**, 10, 1034-1042.

Posters

1. Cationic Ru-Alkylidene Complexes for Continuous Biphasic Metathesis Using Monolith-Supported Ionic Liquids

B. Autenrieth, W. Frey, M. R. Buchmeiser, *GDCh-Wissenschaftsforum CHEMIE 2013,* September 01-04, 2013, Darmstadt, Germany.

2. Continuous metathesis under liquid-liquid conditions using a dicationic Ru alkylidene in monolith-supported ionic liquids

B. Autenrieth, W. Frey, M. R. Buchmeiser, *4th EuCheMS Chemistry Congres*s, August 26 - 30, 2012, Prague, Czech Republic.

3. Continuous metathesis within monolith-supported ionic liquids

B. Autenrieth, M. R. Buchmeiser, *The 19th International Symposium on Olefin Metathesis and Related Chemistry* (ISOM XIX), July 10-15, 2011, Rennes, France.

Oral Presentations

1. **Continuous metathesis under liquid-liquid conditions using monolith-supported ionic liquids**
   17. Tag der Organischen Chemie - TOCUS, October 11, 2013, Stuttgart, Germany.

2. **Continuous metathesis under liquid-liquid conditions using monolith-supported ionic liquids**
   DWI/RWTH Aachen Summer School, June 24-25, 2013, Aachen, Germany.

3. **Continuous metathesis under liquid-liquid conditions using monolith-supported ionic liquids**
   46. Jahrestreffen deutscher Katalytiker, March 13-15, 2013, Weimar, Germany.

Erklärung über die Eigenständigkeit der Dissertation

Ich versichere, dass ich die vorliegende Arbeit mit dem Titel:

„Continuous Metathesis Under Biphasic Liquid-Liquid Conditions Using Monolith-Supported Ionic Liquids"

selbstständig verfasst und keine anderen als die angegebenen Quellen und Hilfsmittel benutzt habe; aus fremden Quellen entnommene Passagen und Gedanken sind als solche kenntlich gemacht.

Declaration of Authorship

I hereby certify that the dissertation entitled:

„Continuous Metathesis Under Biphasic Liquid-Liquid Conditions Using Monolith-Supported Ionic Liquids"

is entirely my own work except where otherwise indicated. Passages and ideas from other sources have been clearly indicated.

Name/Name: _____

Unterschrift/Signed: _____

Datum/Date: _____